Molecular targeting of prostate cancer invasion

Manuelli, Valeria

Awarding institution:
King's College London

Molecular Targeting of Prostate Cancer Invasion

Valeria Manuelli

2021

A thesis submitted to fulfil the requirements for the degree of Doctor of Philosophy

Division of Cancer and Pharmaceutical Science

King's College London

Declaration of Authorship

I declare that the work presented in this thesis is the work of the author. Contributions from others have been properly acknowledged and cited where included.

Valeria Manuelli

Acknowledgements

For four years London has been my home, and the people I have met there have been my family. Each and every one of them has enriched my life, gifting me with countless memories.

I would like to express my deepest gratitude to my primary supervisor, Dr. Claire Wells, for welcoming me in her lab and guiding me throughout the completion of this study. Dr. Wells' unwavering enthusiasm, profound knowledge and encouragement has taught me how to look at things from a positive angle, and she has supported me through the most challenging times with confidence and wisdom.

I would like to thank my second supervisor, Dr. Sarah Rudman, for the important role she has played in this project and for her valuable comments and suggestions. My appreciation also extends to my thesis committee: Tracey Mitchell, Magali Williamson and Claudia Linker, for their assistance and critical insights, and to Dr. James Arnold for his genuine kindness and help.

A massive thank goes to the people of the Wells' lab and the Cancer Division, past and present: Alex Rimmer, Christian Benzing, Paris Costi, Jamie Opzoomer, Dominika Sosnowska, Joanne Anstee, Lujain Kuwair, Alexandria Mitchell and Mahfuja Bulu. You have made my work more enjoyable and it wouldn't have been the same in the lab without your friendship. A special mention goes to Dr. Madeline Gale, the most colourful and disrespectful Brit I have met, the inappropriate napper Dr^2. Kiruthikah Thillai, and Dr. Peter Gordon, my "work husband" and personal back stretcher. Thank you for the endless mocking, the snack runs, the book clubs and most of all for introducing me to the garlic and herb dip on pizza. I'd like to thank my banana-coloured friends, Charly Brown and Marianne Best for their refreshing and sparkling wit that brightened my final year of PhD.

I owe my sincere appreciation to all my friends in Italy and abroad, who have put up with me all these years and have always been my rock back home. Dr. Giulia Raimondi, thanks for the endless wine, the whining, and the stalking – and the lucky seat.

To my wonderful flatmates in London, Annalisa Trecarichi and Davide Monaco, who have always backed me up in the most creative and funniest ways, even when I didn't ask for it. Davide, I will miss your under-appreciated humour. Annalisa, we have been on this rollercoaster together from day 1 and I couldn't have asked for a better partner in crime. Culo e camicia Annalì!

Finally, and above all, to my real family: Mum and Dad, you have raised me to be independent and follow my passions whatever they are (even if it's just about "mixing things in the lab"). Thank you for patiently watching me going back and forth, for feeding my friends, for taking care of the little furry one while I was away. I would have never made it this far without your unconditional love and support.

Abstract

Prostate cancer (PCa) is the most common cancer in men and the second most common cause of cancer death in the UK. Most of the prostate cancer-related deaths are due to metastasis formation, yet there are no efficient anti-metastatic drugs available, as most chemotherapeutics are directed against cancer proliferation, rather than invasion. Therefore, understanding the mechanisms underlying the metastatic process of PCa is crucial to develop novel therapeutics. It is widely believed that degradation of the extracellular matrix is required to navigate the tumour stroma and can be achieved by cancer cells via the extension of invadopodia, actin-rich structures that protrude from the ventral surface and release metalloproteases at the interface with extracellular matrix (ECM). Invadopodia formation has been observed *in-vitro* and *in-vivo* in metastatic cell lines derived from multiple tumour types, and invadopodia are considered important drivers of tumour invasion, although there is less evidence in the prostate setting. The p-21 activated kinases (PAKs) have previously been associated with invadopodia dynamics, and PAK4 was found to be found to be localized within invadopodia in melanoma where it is thought to regulate RhoA activity via PDZ-RhoGEF. However, the molecular mechanisms underlying invadopodia activity in prostate cancer (PCa) remain to be elucidated as the classic PCa cell lines have not been reported to form invadopodia without external stimulation. This study aims to identify if prostate cancer cell lines derived from primary adenocarcinoma can be used to study invadopodia and elucidate the precise mechanism by which PAK4 regulates invadopodia. Characterisation of invasiveness potential revealed that all PCa cell lines tested were capable of spontaneous invadopodia formation and produced significant visible metastasis in Zebrafish dissemination assay. Protein depletion experiments demonstrated that PAK4 is essential for invadopodia formation and invadopodia-mediated matrix degradation in PCa cells. Moreover, we found evidence that PAK4 can regulate both metalloproteases and RhoA activity, possibly via direct phosphorylation of PDZ-RhoGEF. These findings indicate that PAK4 could play multiple roles in invadopodia lifecycle by regulating different downstream pathways, and could therefore constitute an interesting therapeutic target for the prevention of metastasis.

Table of Contents

List of figures

List of tables

Abbreviations

2D	Two dimensional
3D	Three dimensional
ADT	Androgen deprivation therapy
AFMS	Anterior fibromuscular zone
AID	Auto inhibitory domain
AR	Androgen receptor
AREs	Androgen-response elements
Arp2/3	Actin-related proteins 2/3
ATP	Adenosine triphosphate
BAD	Bcl-2 antagonist of cell death
Bcl-2	B-cell lymphoma 2
BPE	Bovine pituitary extract
BPH	Benign prostatic hyperplasia
BSA	Bovine serum albumin
C. Elegans	Caernobitis Elegans
Cdc42	Cell division control protein 42
CDK	Cyclin-dependent kinase
CDKN1A	Cell cycle regulatory protein p21
CIP4	Cdc42-interacting protein 4
Co-IP	Co-immunoprecipitation
CRPC	Castration-resistant prostate cancer
CTCs	Circulating tumour cells
CZ	Central zone
DAPI	4,6-diamidino-2-phenylindole
DGCR6	DiGeorge critical region 6
DH	Dbl-homology
DHR	Dock-homology region-2
DMEM	Dulbecco's modified eagle's medium
DMSO	Dimethyl sulfoxide
DNA	Deoxyribonucleic acid
Dpf	Days post-fertilisation
DRE	Digital rectal exam
DTT	Dithiothreito
E.Coli	Escherichia Coli
ECL	Enhance chemiluminescence
ECM	Extracellular matrix
EGF	Epidermal growth factor

EGFR	Epidermal growth factor receptor
EMT	Epithelial-mesenchymal transition
ERK	Extracellular-signals regulated kinase
F-actin	Filamentous actin
FAK	Focal adhesion kinase
FBS	Foetal bovine serum
FRET	Fluorescence resonance energy transfer
Gab1	GRB2-assocaited-binding protein 1
GAPDH	Glyceraldehyde 3-phosphate dehydrogenase
GAPs	GTPase-activating proteins
GBD	GTPase binding domain
GDI	Guanine nucleotide dissociation inhibitor
GDP	Guanosine diphosphate
GEFs	Guanine nucleotide-exchange factors
GFP	Green fluorescent protein
GID	GEF-H1/Gab1-interacting domain
GTP	Guanosine triphosphate
H&E	Haematoxylin and eosin stain
HEPES	4-(2-hydroxyethyl)-1-piperazineethanesulfonic acid
HGF	Hepatocyte growth factor
HRP	Horseradish peroxidase
HSPs	Heat shock proteins
IQGAP1	IQ motif containing GTPase activating protein 1
KDa	Kilodaltons
KSFM	Keratinocyte serum free media
LB	Luria-Bertani
LIMK	LIM kinase
LPA	Lysophosphatidic acid
LUTs	Lower urinary tract symptoms
MAPK	Mitogen-activated protein kinase
mDia	Diaphanous-related formin
MET	Mesenchymal-epithelial transition
Met	Reactive oxygen species
MLC	Myosin light chain
MMP	Matrix metalloprotease
MRI	Magnetic Resonance Imaging
MTT	3-(4,5-Dimethylthiazol-2-yl)-2,5-Diphenyltetrazolium Bromide
Nck1	Noncatalytic region of tyrosine kinase adaptor protein 2
NMR	Nuclear magnetic resonance
N-WASP	Neural Wiskott–Aldrich syndrome protein
PAKs	p21-activated kinases

PAP	Prostatic acid phosphatase
PBS	Phosphate buffer saline
PCa	Prostate cancer
PCR	Polymerase chain reaction
PDGF	platelet derived growth factor
PFA	Paraformaldehyde
PH	Pleckstrin homology
PI3K	Phosphatidylinositol-3 kinase
PIN	Prostatic intraepithelial neoplasia
PIP 5-kinase	phosphatidylinositol-4-phosphate 5-kinase
PIP2	phosphatidylinositol-4,5-bisphosphate
PMSF	Phenylmethylsulfonylfluoride
PSA	Prostate specific antigen
PTU	N-phenylthiourea
PZ	Peripheral zone
Rac1	Ras-related C3 botulinum toxin substrate 1
Raf	Rapidly Accelerated Fibrosarcoma
RNA	Ribonucleic acid interference
ROCK	Rho-associated, coiled-coil containing protein kinase 1
RPMI-1640	Roswell Park Memorial Institute-1640
SD	Standard deviation
SDS-PAG	Sodium dodecyl sulphate polyacrylamide gel electrophoresis
SEM	Standard error of the mean
Ser	Serine
SH3	SRC Homology 3
shRNA	Shot hairpin ribonucleic acid
siRNA	Short interfering ribonucleic acid
SSH-1L	Sling-Shot phosphatase
TBST	Tris-buffered saline with Tween20
TGFβ	Transforming growth factor beta
Thr	Threonin
TNM	Tumour, node and metastasis
TZ	Transition zone
WASP	Wiskott-Aldrich Syndrome Protein
WAVE	WASP-family verprolin homologue

Chapter 1

Introduction

Chapter 1. Introduction

1.1. The prostate and prostate cancer

1.1.1. Anatomy and physiology of the prostate gland

The prostate is a tubuloalveolar exocrine gland about the size of a walnut, which is part of the male reproductive system. The prostate is conical in shape and comprises of a base and a lateral and an apex surface in the upper segment. A normal healthy adult prostate weighs approximately 20 grams and is located in the pelvis, positioned just below the neck of the bladder, anterior to the rectum and surrounds the prostatic urethra that exits from the bladder (Bhavsar and Verma 2014). Prostatic tissue can be sub-divided into four different zones based on their anatomical position and histological characteristics: the peripheral zone (PZ), the transition one (TZ), the central zone (CZ), and the anterior fibromuscular zone (AFM) (Figure 1.1) (McNeal et al. 1991).

The PZ extends posteriorly and laterally from the base to the apex of the gland body and is the largest of the zones, accounting for approximately 70% of the glandular tissue. The central zone is a cone-shaped area that surrounds the ejaculatory ducts running from the seminal vesicles to the urethra, and forms about the 20% of the entire prostate gland. The transition zone is constituted of two lobes that surround the proximal section of urethra and lie anterior to the central zone. The transition zone comprises only 5% of the total prostate volume, however, this structure typically undergoes tissue enlargement as men age, a condition called benign prostatic hyperplasia (BPH). The anterior fibromuscular zone is situated on the anterior surface of the gland. This area is devoid of glandular elements and enriched in fibrous and muscular components, which gradually blend into the bladder neck at the base, and into the thin layer of the capsule which surrounds the prostate (Hammerich, Ayala, and Wheeler 2008; Bhavsar and Verma 2014).

The histological architecture of prostatic tissue consists of branched tubulo-alveolar glands with lumina lined by simple or pseudostratified epithelium, composed of luminal secretory columnar cells and basal epithelial cells. Luminal cells play an exocrine role, producing and secreting into the gland lumen important components of the seminal fluid such as human PSA (prostate-specific antigen), prostatic acid phosphatase (PAP), and human kallikrein-2 (Maitland 2008). Luminal cells express high levels of androgen receptor (AR) as their survival is androgen-dependent (D. Zhang et al. 2018). The basal layer, consisting of flattened and

cuboidal cells not expressing AR, separates the luminal epithelium from the basement membrane (Maitland 2008). A progenitor stem cell population is thought to reside within the basal compartment, constituting the proliferative compartment which ensures the renewal of the prostate epithelium (Bonkhoff, Stein, and Remberger 1994). AR-negative neuroendocrine cells are also present in the basal cell layer (Bonkhoff, Stein, and Remberger 1995).

The human prostate has multiple functions. One of them is the production and secretion of a fluid that is present in the seminal fluid, consisting of proteolytic enzymes, citrate and zinc. By controlling the alkaline pH of the seminal liquid, the prostate sustains and protects sperm for successful fertilization. Moreover, the AFM is important in controlling both voluntary and involuntary sphincters.

1.1.2. Prostate Cancer epidemiology

Prostate cancer (PCa) is the most commonly diagnosed cancer in males with there being 57,192 new cases in 2018, and it being the 2nd most common cause of cancer death in the UK. It has been estimated that 1 in 8 men across the UK will be diagnosed with prostate cancer at some point during their lifetime (Prostate Cancer UK). Prostate cancer incidence rates have increased overall since 1990, and is projected to rise by 12% before the end of 2035. The five-year relative survival is higher for patients diagnosed with localized cancer, but the rate dramatically drops in cases of metastatic cancer, with only 49% of men predicted to survive 5 years after diagnosis.

The causes of PCa development have not yet been identified, although different heritable and environmental factors such as age, ethnic origin, obesity, and previous family history of PCa seem to be associated (Bostwick et al. 2004). Early detection of prostate cancer mostly relies on the digital rectal exam (DRE) and the detection of the blood PSA. PSA detection however, often leads to over-diagnosis and over-treatment of diseases that might remain clinically silent and are not expected to cause any health problems or symptoms. PSA level can also be high in presence of benign prostatic hyperplasia (BPH), a well-known condition consisting in a non-malignant enlargement of the prostate organ that is very common in ageing men. In BPH, proliferation of both epithelial and stromal components of the transition zone is often due to a hormonal imbalance between testosterone and oestrogen

levels which in turn increase the production of soluble growth factors (Maitland 2008). The condition can remain asymptomatic or become clinically relevant when associated to manifested symptoms, the most common and bothersome being lower urinary tract symptoms (LUTS). Interestingly, BPH and prostate cancer display many similarities: both conditions are age-related, androgen dependent, and share analogous genetic alterations (Schenk et al. 2011). BPH is traditionally not considered to be a risk factor for prostate cancer, although the two conditions coexist in a high proportion of patients (Chang, Kirby, and Challacombe 2012). It is not possible to discriminate between BPH and prostate cancer solely on the base of clinical symptoms, as there is not a specific pattern of LUTS associated to prostate cancer. Moreover, detection of elevated blood levels of PSA cannot distinguish between these two pathologies without the aid of additional clinical parameters, such as PSA threshold, prostate volume, and free vs total PSA ratio (Chang, Kirby, and Challacombe 2012). For these reasons, PSA has not been approved as screening test for prostate cancer in the UK (Wilt and Ahmed 2013). Therefore, despite extensive efforts have been made in the last years toward the prevention and early diagnosis of prostate cancer, between 17% and 34% of prostate cancer patients exhibit metastatic dissemination at the time of diagnosis (Prostate Cancer UK). Hence, there is an urgent need for more accurate diagnostic tools and therapeutic strategies for the prevention and treatment of advanced prostate cancer.

A

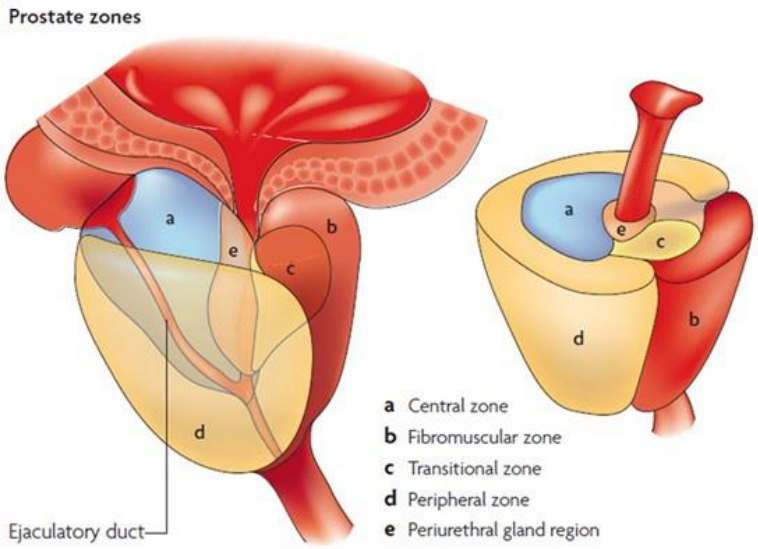

B

	Peripheral	Transition	Central
Benigh prostatic hyperplasia			
High-grade PIN			
Carcinoma			

Figure 1. 1: Zonal occurrence of prostate cancer.
Graphical representation of the anatomical subdivision of the prostate gland in different zones (A). The table shows the occurrence pattern of benign prostatic hyperplasia, high-grade PIN and prostate carcinoma based on their zonal predisposition. Red=high prevalence, orange=medium prevalence, yellow=low prevalence, white=none (B). Image adapted from (De Marzo et al. 2007).

1.1.3. Prostate carcinogenesis

Prostate cancer is a heterogeneous disease: 95% of prostate cancer cases are adenocarcinomas, while only 4% are characterised by neuroendocrine or transitional morphological features (Maitland 2008). Moreover, prostate cancer has a multifocal nature, with distinctive and individual tumour foci originating the same organ. More than 75% of prostate cancer cases occur in the peripheral zone, followed by the transition zone (15-20%) and a minority of cases in the central zone (5-10%) (Maitland 2008) (Figure 1.1). Inflammation is thought to be one of the determining factors in prostate cancer development. Indeed, epidemiological studies have shown a positive correlation and a significant increase in the risk of prostate cancer in men affected by, or with a history of prostatitis (Nakai and Nonomura 2013).

Pre-malignant focal inflammatory lesions have been found to occur mainly in the peripheral zone. Prostatic intraepithelial neoplasia (PIN) is a premalignant condition characterised by the abnormal growth of epithelial cells confined within a pre-existing prostatic acinus or duct, with no invasion of the surrounding stroma (A. G. Ayala and Ro 2007). PIN can be classified as low-grade or high-grade, depending on the extent of the tissue disorganisation. In high-grade PIN (HGPIN), cytological features are very similar to those of invasive prostate cancer, with most of the epithelial cells exhibiting nuclear enlargement, irregular cell size and shape, hyperchromasia, multiple nucleoli often surrounded by clearer halos (A. G. Ayala and Ro 2007). Other similarities include the increased prevalence of HGPIN with age, alterations of genetic and molecular markers, and the zonal predilection of incidence, as 75-80% of HGPIN cases are found in the peripheral zone and can be multifocal (A. G. Ayala and Ro 2007). Moreover, studies conducted on radical prostatectomy specimens showed a topographical association between HGPIN and prostate carcinoma: frequent morphologic transition areas were detected in which HGPIN merged with adenocarcinoma lesions (McNeal et al. 1991; Putzi and De Marzo 2000). Currently, HGPIN is widely recognized as a prostate cancer initiator, and possibly the intermediate step in the transformation path that leads to prostate adenocarcinoma (Bostwick, Pacelli, and Lopez-Beltran 1996; De Marzo et al. 2007). HGPIN is undoubtedly an important risk factor and a predictive marker of prostate cancer development (A. G. Ayala and Ro 2007).

1.1.4. Prostate cancer progression

More than 60% of prostate cancer patients in England are diagnosed at early stage with localised carcinoma, confined within the prostate organ (Prostate Cancer UK). Multiple options exist for the management of clinically localised prostate cancer, including active surveillance, radical prostatectomy, cryoablation and radiotherapy (Wilt and Ahmed 2013). Unfortunately, 20-30% of patients treated primarily with radiotherapy or local surgery relapse, possibly advancing to a later stage of prostate cancer (Afshar et al. 2015). For patients with recurring cancers or those presenting with locally invasive or metastatic disease androgen deprivation therapy (ADT) is the preferred strategy, as these cells require androgen to proliferate (Lonergan and Tindall 2011).

Androgens, functioning via the Androgen Receptor (AR), are essential for the normal development and function of the prostate gland, and to regulate the overall male fertility. AR is variably expressed in prostate cancer tissue, and up to 90% of diagnosed prostate cancer are androgen-dependant at diagnosis (Heinlein and Chang 2004). In absence of available androgens, the AR is found primarily in the cytoplasm, associated to heat shock proteins (HSPs) and other proteins involved in the cytoskeletal regulation (Lonergan and Tindall 2011). Binding of the AR to androgens lead to a conformational change that results in the dissociation from HSPs and dimerization of the AR. After associating with co-regulator proteins, AR translocates to the nucleus of the cell where it binds androgen-response elements (AREs) in the promoter region of target genes required for survival and proliferation of prostate cells (Lonergan and Tindall 2011). Hormonal therapies targeting the AR function via androgen deprivation and/or AR blockade proved to be effective in 80-90% of patients with metastatic cancer, who experienced remission of the disease and decrease of PSA levels (Harris et al. 2009). After a median of 2-3 years, however, patients undergoing ADT eventually experience progression of the disease due to hormone refractory. This type of cancer is known as castration-resistant prostate cancer (CRPC) (Harris et al. 2009). Eventually, 90% of patients with CRPC will develop metastasis, preferentially to the bones. Patients with metastatic CRPC are left with a very poor prognosis and a life-expectancy of only 16-18 months (Karantanos, Corn, and Thompson 2013). Because the AR is thought to remain active in CRPC, novel hormonal drugs based on AR inhibition such as abiraterone acetate can be employed (Karantanos, Corn, and Thompson 2013). These therapies, however, do not provide an effective cure for metastatic CRPC and produce only modest

effects, increasing the patient's survival by approximately 4-5 months, and are therefore considered to be mainly palliative drugs. The systemic nature of metastasis and their resistance to therapeutic agents make metastatic CRPC incurable.

1.1.5. Prostate cancer grading and staging

Diagnosis of prostatic carcinoma is based on the histological assessment of prostate tissue samples obtained via radical prostatectomy or needle biopsy. The H&E stained tissue specimens are evaluated by a pathologist who subsequently assign a Gleason score depending on the microscopic cell appearance and tissue architecture. The Gleason classification was developed in 1966 by Dr Donald Gleason, and remains the preferred and the most reliable grading system (Peter A. Humphrey 2004). Moreover, it represents a strong prognostic indicator for prostate cancer progression and clinical outcome. The Gleason score is based on five different grade patterns that can be identified by observing the differentiation degree of glandular components and the growth pattern of the tumour in the prostatic stroma at relatively low magnification (10X-40X) (Peter A. Humphrey 2004) (Figure 1.2). Gleason pattern 1 is the lowest and it's characterised by well-differentiated, closely packed, rounded and uniform acini which resembles the normal prostatic epithelium. Progression to higher Gleason grades implicates increased variability in cells size and shape, with presence of angular and more elongated components, possibly infiltrating in the stroma via thin protrusions. Gleason pattern 5 is the highest grade which typically includes a central area of necrosis, minimal or no glandular differentiation, and solid carcinoma sheets infiltrating the surrounding stroma (Peter A. Humphrey 2004).

Given the heterogeneity and multi-focal nature of PCa, two or more different patterns can be found within the same prostate. Therefore, the two predominant basic patterns are added together to generate a final histological score ranging from 2 to 10. The primary pattern represents 50% or more of the tissue architecture, while the secondary pattern represents less than 50% of the total pattern. If the secondary pattern is less than 5%, it is ignored and the primary pattern is doubled to give the final score (N. Chen and Zhou 2016). If a tertiary component of highest grade but less prevalence is identified, it is added to the final grade replacing the secondary pattern. Following the International Society of Urological Pathology (ISUP) recommendations made in 2005, Gleason score 1+1=2 is not being

diagnosed as it is impossible to discern it by needle biopsy, and only Gleason score of 6 or above should be reported (N. Chen and Zhou 2016).

In addition to the Gleason grading, PCa can be defined using the tumour, node and metastasis (TNM) staging system, in agreement to the classification of malignant tumour by the American Joint Committee on Cancer (AJCC) (Cheng et al. 2012). Each category of the TNM is accompanied by a number representing a sublevel which provide more in-depth information about the tumour characteristics. The size and extent of the tumour (T) can be determined prior to treatment by needle biopsy, clinical examination (DRE) or imaging techniques such as MRI. T1 means the carcinoma is clinically unapparent and can't be detected by simple examination of the prostate. T2 tumours are confined within the prostate gland, possibly involving one or both lobes, while T3 tumours have broken outside the prostate and it's therefore considered to be locally advanced. T4 denotes the spreading of the cancer to the nearby tissues such as seminal vesicles, bladder or pelvic floor (Cheng et al. 2012). Similarly, N0-N1 is utilised to indicate whether cancer cells have disseminated into lymph nodes. Lymph nodes involvement is an important prognostic factor for prostate cancer patients (Cheng et al. 2012). M0-1 describes whether metastasis are found in other parts of the body. Two additional annotations can be added before the letters TNM: "c" indicates whether the tumour has been clinically assessed, while "p" indicates whether the tumour is confined within the prostate. Both Gleason grading and TNM staging are important components of the risk stratifications of prostate cancer patients, which is widely used to determine the appropriate therapeutic approach (Table 1.1).

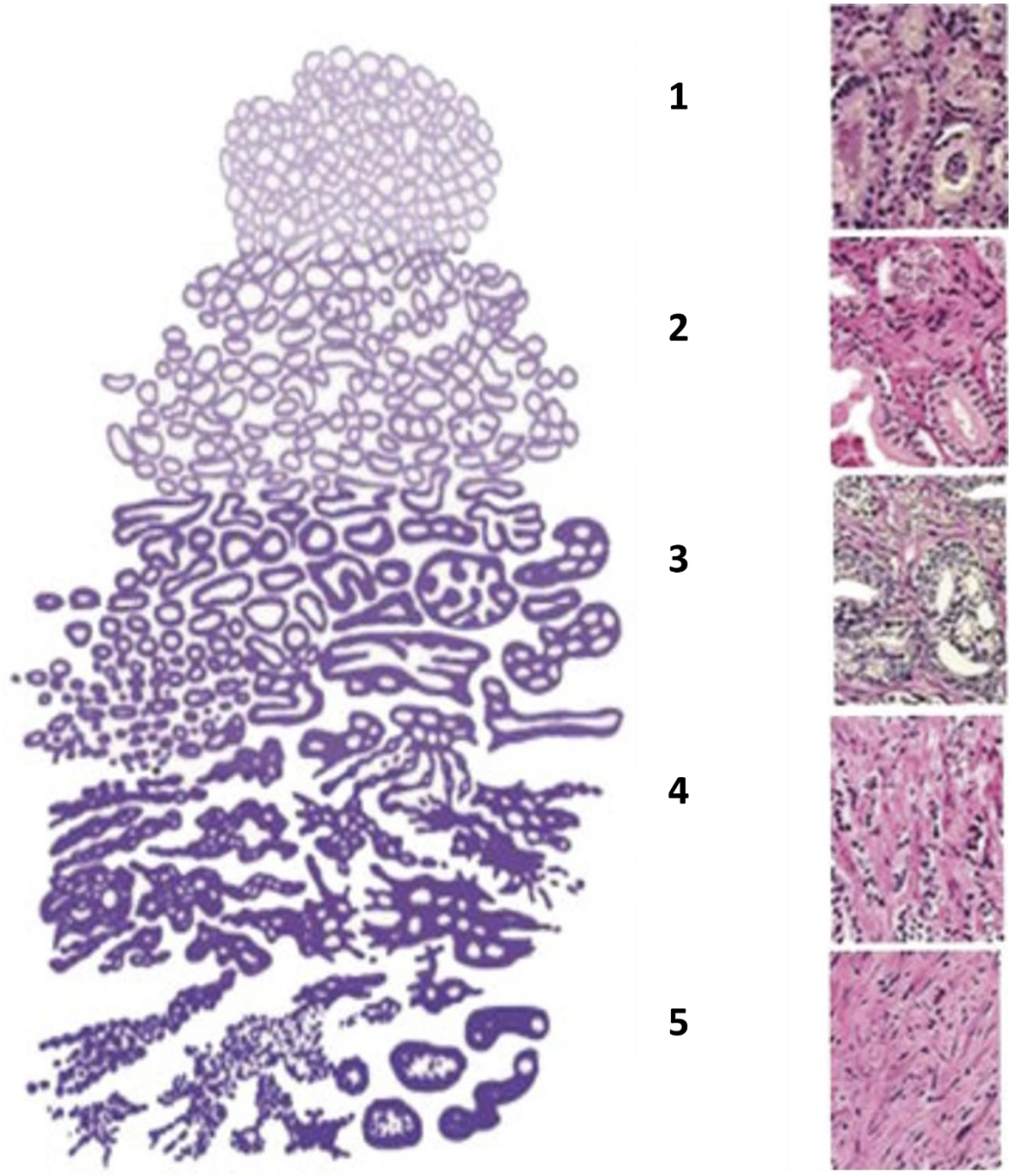

Figure 1. 2: Gleason grading of the histological patterns of prostatic carcinoma
Gleason grading depends on the histological architecture of the prostatic tissue examined at low magnification (10X-40X). Gleason pattern 1 is virtually undistinguishable from non-cancerous tissues. The Gleason score increases proportionally with the increased level of architectural and structural disruption of the prostatic epithelium. Gleason 5 represents the most undifferentiated grade, where no glandular structures are distinguishable. Figure adapted from (Harnden et al. 2007).

T score	N score	M score	PSA	GRADE	STAGE
cT1a-c, cT2a	N0	M0	<10 ng/mL	1	I
pT2	N0	M0	<10 ng/mL	1	I
cT1a-c, cT2a	N0	M0	≥10, <20 ng/mL	1	IIA
pT2	N0	M0	≥10, <20 ng/mL	1	IIA
cT2b-c	N0	M0	<20 ng/mL	1	IIA
T1-2	N0	M0	<20 ng/mL	2	IIB
T1-2	N0	M0	<20 ng/mL	3	IIC
T1-2	N0	M0	<20 ng/mL	4	IIC
T1-2	N0	M0	≥20 ng/mL	1-4	IIIA
T3-4	N0	M0	Any	1-4	IIIB
Any	N0	M0	Any	5	IIIC
Any	N1	M0	Any	Any	IVA
Any	Any	M1	Any	Any	IVB

Table 1. 1: Definitions of the American Joint Committee on Cancer TNM criteria for prostate cancer

1.2. Metastasis and cancer invasion

1.2.1. The Metastatic Cascade

Metastatic disease is the spread of cancerous cells from the primary tumour towards secondary malignant sites in distant parts of the body. More than 90% of cancer-related deaths are due to metastasis formation, rather than the primary carcinoma. Hence, metastasis represent the primary life-threatening aspect of cancer (Valastyan and Weinberg 2011). However, available chemotherapeutics are mainly directed against cell proliferation, rather than invasiveness. To efficiently target disseminating cancer cells, the identification of migration regulators and their pathways is crucial.

Metastasis formation is a complex multistep process that requires a sequence of biological events collectively named as “metastatic cascade” (Figure 1.3).

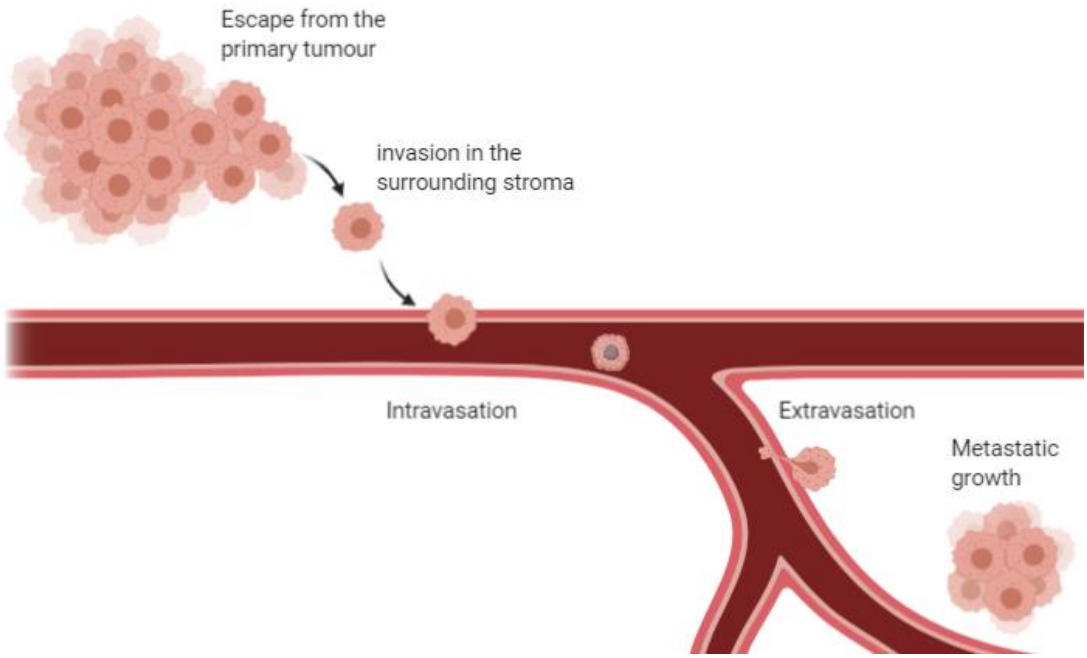

Figure 1. 3: Schematic representation of the events occurring in the metastatic cascade
In order to colonise distant sites, cells must detach from the primary tumour and invade through the extracellular stroma. Subsequently, cells enter the circulation (intravasation) and are transported in secondary districts of the body, where they exit the vasculature (extravasation) and establish a secondary tumour.

Tumour spread starts with the local invasion of adjacent tissues throughout the surrounding extracellular matrix (ECM) and stromal cell layers. Locally invasive tumour cells subsequently enter the vasculature and the lymphatic vessel system. Secretion of angiogenic factors by cancer cells facilitate intravasation by promoting neoangiogensis and new blood vessels formation. Once inside the local vasculature, disseminating cells can reach distant sites by traveling in the bloodstream. At a given point, cells lodge in the microvasculature of distant organs, and breach through the endothelial barrier in a process called extravasation, to colonise the parenchyma of the secondary organ (Valastyan and Weinberg 2011).

The successful establishment and growth of metastatic colonies is actually a rare event. It has been estimated that less than 0.01% of circulating tumour cells present in the vasculature will eventually develop into metastases (Fidler 1970). Cell survival in the bloodstream and metastatic colonization are the major limiting steps of the metastatic cascade, as they need to survive in foreign and inhospitable microenvironments. A tight coordination of molecular pathways involved in cell motility, invasion, proliferation and adhesion is required in order for cancer cells to efficiently progress throughout all the steps of the metastatic cascade, offering numerous potential therapeutic targets and valuable opportunities for pharmacological intervention.

1.2.2. Mechanisms of cell invasion

Cancer cell spreading within surrounding tissues is achieved throughout similar mechanisms of migration adopted by normal, non-neoplastic cells, during physiological processes such as immune response, wound healing, tissue morphogenic and homeostasis. The acquisition of motile behaviour in the cancer cell involves the activation of molecular pathways regulating cytoskeletal dynamics, cell-cell junctions and cell-matrix adhesion turnover (Friedl and Alexander 2011). To migrate, the cell body undergoes morphological changes, becomes more polarised and extend characteristic plasma membrane protrusion at the leading edge. These protrusions can be large and broad (lamellipodia) or finger-like (filopodia), and by anchoring the extracellular matrix (ECM) they provide the traction force necessary for the movement of the cell body (Friedl and Alexander 2011). Dissolution of cell adhesions at the cell rear allows the cell to detach and continue moving forward.

Depending on cell type and microenvironment, cancer cells can infiltrate through the ECM in two major different patterns: individually, referred to as “single cell migration”, or as multicellular groups, named “collective migration” (Figure 1.4). The two modes of migration can co-exist in the same tumour (Friedl and Alexander 2011; Sanz-Moreno and Marshall 2010). When migrating individually, cancer cells can utilise two interchangeable mechanisms: mesenchymal- or amoeboid-like migration (Sanz-Moreno and Marshall 2010; Krakhmal et al. 2015). Mesenchymal migrating cells are characterised by a fibroblast-like elongated and polarised morphology and their movement follows the multistep process and protrusive machinery similar of that of non-tumorigenic cells (Friedl and Alexander 2011). Differently from normal cells, however, mesenchymal cells rely on the secretion of proteases to degrade the extracellular matrix and enable invasion. Release of specific metalloproteases at cell-ECM interface can be achieved by the employment of ventral dynamic protrusions named invadopodia (Murphy and Courtneidge 2011). The mesenchymal type of migration is associated to tumours of the connective tissue, but it can also originate from epithelial cancers following progressive dedifferentiation and loss of cellular junctions (Friedl and Alexander 2011). Epithelial cancer cell can lose their characteristic phenotype in favour of a more mesenchymal morphology through the epithelial to mesenchymal transition (EMT). EMT encompasses a wide range of molecular and cellular changes that collectively are thought to facilitate cancer progression and invasion in multiple cancer types, including breast, ovary, colon, and lung and also prostate (Nieto and Cano 2012). One of the most recognized markers of EMT is the loss of E-cadherin, an important mediator of intercellular junctions which has been is associated with prostate cancer chemoresistance and poor prognosis (Puhr et al. 2012). E-cadherin is replaced by other markers representative of a mesenchymal phenotype, such as N-cadherin and vimentin, both involved in promoting cell invasiveness and survival (Nauseef and Henry 2011; Heerboth et al. 2015; Khan et al. 2015). SNAIL, TWIST, TGFβ and many other signalling pathways are important inducers of EMT as they trigger early events and regulates the expression levels of epithelial and mesenchymal proteins involved in the transition (Khan et al. 2015).

However, EMT role in cancer and as driver of cell metastasis is still matter of debate, as recent works indicates that EMT is not a binary switch but rather a series of transitionary states (Nieto et al. 2016). There is considerable data suggesting EMT is relevant in prostate cancer, as the expression of EMT related molecules is found to be well correlated with

aggressive tumours and could potentially hold a prognostic value (Nauseef and Henry 2011; Khan et al. 2015). Prostate cancer PC3 cells, for example, are known to have lost E-cadherin expression and increased vimentin expression, and do not form appreciable cellular junctions when cultured in a 2D monolayer (Christiansen and Rajasekaran 2006). Other findings indicate that EMT is dispensable for cancer invasion. When embedded in 3D Matrigel, PC3 cells generate polarized spheroids characterised by expression of prostate-specific markers, reduced vimentin and prominent cellular junctions (Christiansen and Rajasekaran 2006). Prostate cancer metastasis are reported to express both epithelial and mesenchymal markers, consistent with the idea of a partial EMT (Chao et al. 2012; Armstrong et al. 2011). Different to the mesenchymal migration, amoeboid migrating cells are characterised by a rounded morphology, lower adhesion force, and increased actomyosin contractility (Friedl and Alexander 2011). Amoeboid-like cells are able to easily adapt their shape thanks to rapid deformability, which allows them to "squeeze" throughout the narrow spaces contained within the ECM in a protease-independent manner. Rapid expansion and contraction of the cells body leads to the generation of a propulsive force that drives the cell forward. Additionally, the internal hydrostatic pressure can generate membranes protrusion named "blebs" that sense the surrounding ECM (Friedl and Wolf 2003; Pandya, Orgaz, and Sanz-Moreno 2017). Amoeboid and mesenchymal cell migration are interconvertible and cancer cells can transition between the two different motility styles depending on the properties of the surrounding ECM, such as pore size and fibrillar density. For example, high network density and/or abolishment of pericellular proteolysis promotes the shifting to an amoeboid type of tumour-cell movement (Friedl and Wolf 2003; A. G. Clark and Vignjevic 2015). Prostate carcinoma cell lines PC3 and DU145 have previously been reported to be capable of both amoeboid and mesenchymal migratory phenotypes (Taddei et al. 2011; Morley et al. 2014).

Collective cell migration consists of the movement of independent aggregates of cells retaining their intercellular junctions (mediated by cadherins) and cell-matrix adhesions (mediated by integrins) (Friedl and Alexander 2011). Collective migration can occur in different forms, depending on the cell type, the architecture of the invaded tissue, the number of invading cells that are joined together. Thus, invading cells can organize in sheets, clusters or streaming (Friedl and Alexander 2011). In most cases, collective migration is accompanied by a front–rear asymmetry. A "leader" cell at the tip of the group with a

mesenchymal-like morphology typically extends actin-rich protrusions that sense the extracellular matrix and generate forward traction. Leading cells are usually polarized and lack of tight junctions that are present in the rear cells, which, instead, are well-organised and packed together (Friedl and Alexander 2011). Collective migration is one of the predominant modes of invasion in epithelial cancers, and it is frequently seen in invasive carcinomas of prostate both in *in-vivo* and *in-vitro* settings (Brandt et al. 1996; Cui and Yamada 2013; Friedl and Wolf 2003). Clusters were isolated from the peripheral blood of prostate cancer patients (Brandt et al. 1996), while 3D Matrigel invasion assays experiments showed that PC3 prostate cancer cells collectively migrate in multicellular clusters, which are impaired by depletion of N-cadherin (Cui and Yamada 2013).

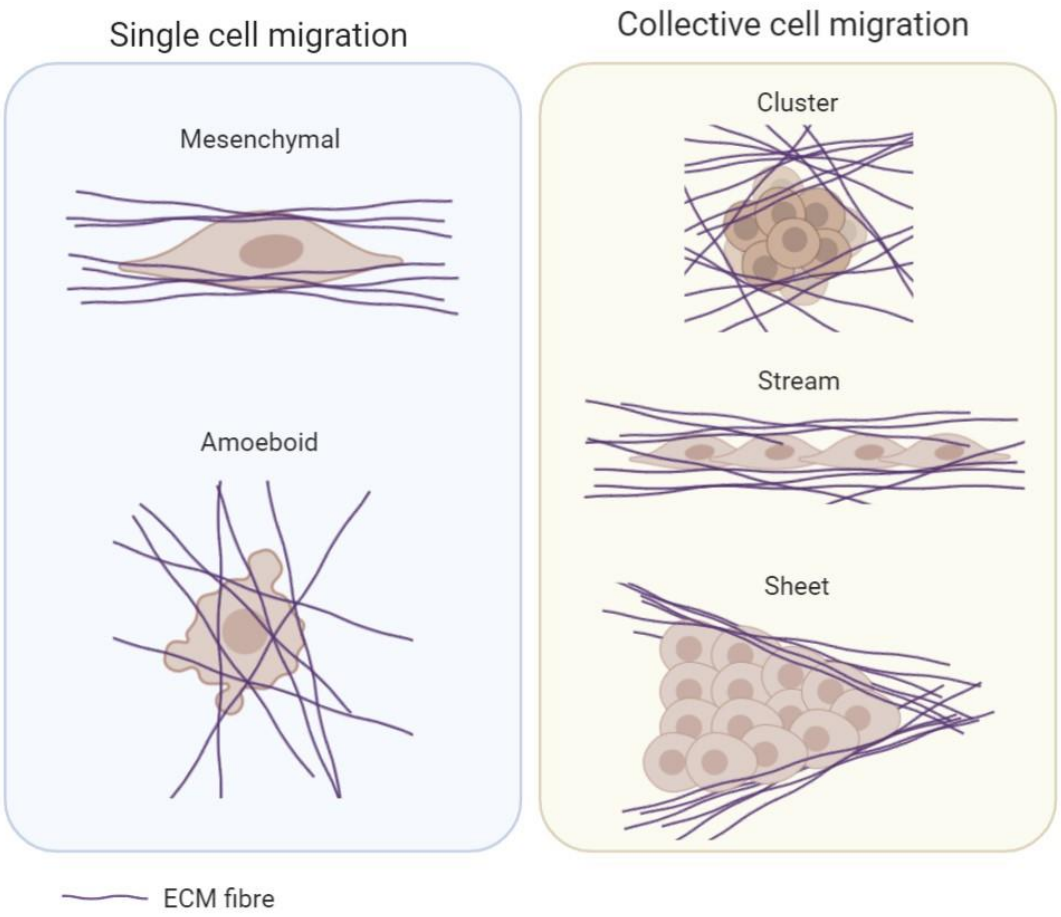

Figure 1. 4: Schematic representation of different modes of cell migration.
Cell can migrate as single cells or as a group of cells, termed collective migration. Single cells can navigate through the stroma by acquiring an elongate, mesenchymal phenotype that relies on the secretion of metalloproteases, or as more rounded, amoeboid cells, which squeeze through the pores and fibres of the stroma. Collective migration requires the retention of intercellular adhesions, and cells can migrate as clusters, streams or sheets.

1.3. Invadopodia

1.3.1. Invadopodia relevance in cancer

Degradation of ECM is a key step in the metastasis development process (when amoeboid migration is not used) and it is required for successful penetration into blood or lymphatic vessels (Valastyan and Weinberg 2011). One way the ECM barrier can be overcome by cancer cells is through the formation of specialized structures named invadopodia. Invadopodia consist of actin-rich structures of the plasma membrane that provide a link between the actin cytoskeleton and the extracellular matrix, facilitating the invasion and degradation of the ECM through the local release of metalloproteases (Buccione, Caldieri, and Ayala 2009; Linder, Wiesner, and Himmel 2011). Invadopodia are closely related to another type of membrane protrusion: the podosome. Together, these two types of structures are named invadosomes (Linder, Wiesner, and Himmel 2011). Invadopodia and podosomes display important molecular and structural similarities, thus, there is still uncertainty as to whether they represent two distinct structures, or they have evolved from a common ancestor structure. It has been speculated that podosome could be precursor of invadopodia, hence by extension particularly relevant for cancer studies (Flynn et al. 2008). One of the main differences between these two types of protrusions, however, is the cell types in which they are primarily identified. Podosomes are associated with myeloid cells, such as monocytes, megakaryocytes, osteoclasts, macrophages and dendritic cells that migrate to exert their physiological functions in response to environmental stimuli. Additionally, podosomes formation can be induced in endothelial and vascular smooth muscle cells upon stimulation with growth factors such as platelet derived growth factor (PDGF), transforming growth factor-beta (TGF-β) and epidermal growth factor (EGF) (Murphy and Courtneidge 2011). Invadopodia, by contrast, are thought to be restricted to carcinoma cells and are thought to play a key role in cancer invasion. Moreover, invadosome structures exhibit other relevant distinctions: invadopodia can have a life-span of several hours, much longer than podosome, characterised by a turnover of few minutes. Invadopodia have a diameter of approximately 8 µm and extend into the matrix 2-5 µm. In contrast, podosomes are relatively smaller: 1µm in diameter and can reach a length up to 0.5 µm (Buccione, Caldieri, and Ayala 2009; Flynn et al. 2008). Additionally, invadopodia

exhibit a higher degradative capacity, consistently with the high invasive and metastatic potential of cancer cells (Artym et al. 2011; Enderling et al. 2017).

The precise ultrastructural components of the invadopodial architecture are still not fully elucidated. Invadopodia were first identified by Chen et al. in chicken embryo fibroblasts that were Src-transformed by Rous sarcoma virus (W. T. Chen 1989). They were described as circular-shaped clusters (rosette) that exhibited adhesive and degradative capacity (W. T. Chen 1989). Structurally, invadopodia consists of a F-actin core enriched in actin-nucleator molecules, such as Arp2/3, Cortactin or WASP, and their upstream regulators, such as Nck1 and Cdc42. Microtubules and intermediate filaments are also thought to engage with the invadopodia core, which is surrounded by a ring of adhesion and scaffolding proteins, as signalling molecules and membrane-associated proteases (Figure 1.5) (Linder 2007).

Since their discovery, invadopodia have been detected in *in-vitro* in several different cell lines of tumour, such as bladder (Yamamoto et al. 2011), breast (W. T. Chen et al. 1994; Coopman et al. 1998), melanoma (Aoyama and Chen 1990; Mueller et al. 1999), squamous carcinoma (Takkunen et al. 2010), colon cancer (Schoumacher et al. 2010). Despite considerable effort has been made, it is yet not clear whether invadopodia play a physiological role in prostate cancer. PC3 cells were reported to form unique adhesive and migratory structures capable of degrading the matrix in an *in-vitro* matrix degradation assay (Desai, Ma, and Chellaiah 2008). However, the structures identified in prostate cancer cell lines have never been confirmed for unique invadopodia markers and they have been considered to be invadopodia solely on the base of the differential degradation pattern exhibited by PC3 cells when compared to osteoclasts (Desai, Ma, and Chellaiah 2008). In comparison to osteoclasts, which are thought to utilise podosome for the physiological bone resorption (Georgess et al. 2014), the degradative ability exhibited by PC3 cells appeared to be relatively small and increased only upon stimulation of the osteopontin/αvβ3 pathway (Desai, Ma, and Chellaiah 2008). Another study analysed the relationship between clinical prostate cancer tissues and the expression levels of Cortactin (Ma et al. 2016), an actin regulator which is localized to invadopodia and is thought to be critical for invadopodia functions (E. S. Clark et al. 2007). Cortactin expression was found to be increased in tissue samples derived from more advanced stages of prostate cancer, and was remarkably higher in lymph node metastasis sample (Ma et al. 2016). These findings indicate that invadopodia

might play a crucial role in promoting prostate cancer progression, but the lack of efficient models to study invadopodia and the difficult experimental characterisation of invadopodia structures have been hindering progresses in invadopodia research in the prostate cancer setting.

Invadopodia can be visualized in a 2D environment by seeding the cells on a planar surface coated with a layer of ECM proteins, which can be native proteins such as fibronectin, or denatured collagen proteins forming gelatin. Active invadopodia forming on the ventral surface of the cells will degrade the underneath matrix, which is fluorescently labelled. Thus, digestion of matrix by invadopodia activity results in dark areas lacking fluorescent signal colocalizing with dot-like accumulation of F-actin, and is easily detected by fluorescence microscopy (Artym, Yamada, and Mueller 2009). Invadopodia have been reported also in a three-dimensional (3D) setting. Human melanoma, fibrosarcoma and breast cancer cells surrounded by a dense gel-based matrix, which allows the formation of integrin-ECM site of contacts along the entire cell surface, have been reported to extend invadopodia-like structures with degrading activity (Hotary et al. 2000; Tolde et al. 2010; Wolf and Friedl 2009; Schoumacher et al. 2010).

The characterisation of invadopodia *in-vivo* is notably challenging, as current technologies do not allow an adequate visualization of the cell:matrix interface during cell migration in vertebrate models. The invasive process, furthermore, is highly dynamic and difficult to predict. Nevertheless, considerable efforts have been dedicated to the identification of invadopodia structures and their importance within the *in-vivo* setting. Intravital imaging experiments and mammary adenocarcinoma xenograft tumours in rats identified cortactin-positive protrusions characterised by proteolytic activities required for tumour cell intravasation. The knockdown of neural Wiskott–Aldrich syndrome protein (N-WASP), which regulates reorganization of the actin cytoskeleton, led to an impaired ability of mammary adenocarcinoma cells to form invadopodia, resulting in suppression of cell invasion, intravasation and lung metastasis (Gligorijevic et al. 2012). High resolution time-lapse intravital microscopy was also utilised for visualisation of human tumour growth and migration in ex-ovo chicken embryo models. Here, the silencing of cortactin, SH3-domain-rich proteins Tks4 and Tks5, that are a known structural and functional requirement of invadopodia, reduced the metastatic efficiency, and provided clear evidence supporting

requirement of invadopodia for the early phase of cancer cell extravasation (Leong et al. 2014). Experiments in zebrafish and C. Elegans confirmed the existence of invadopodia breaching through the basement membrane barrier and their Src- and Tsk5-dependent formation *in-vivo* (Seiler et al. 2012; Hagedorn et al. 2013).

Taken together, these studies led to the identification of approximately 100 different proteins that have been associated with different stages of assembling and activity, and suggested that invadopodia might play a key role in cell invasion *in-vivo*. Therefore, therapeutic agents targeting the mechanisms involved in invadopodia development and activity may represent a novel strategy to inhibit or prevent tumour dissemination and metastasis.

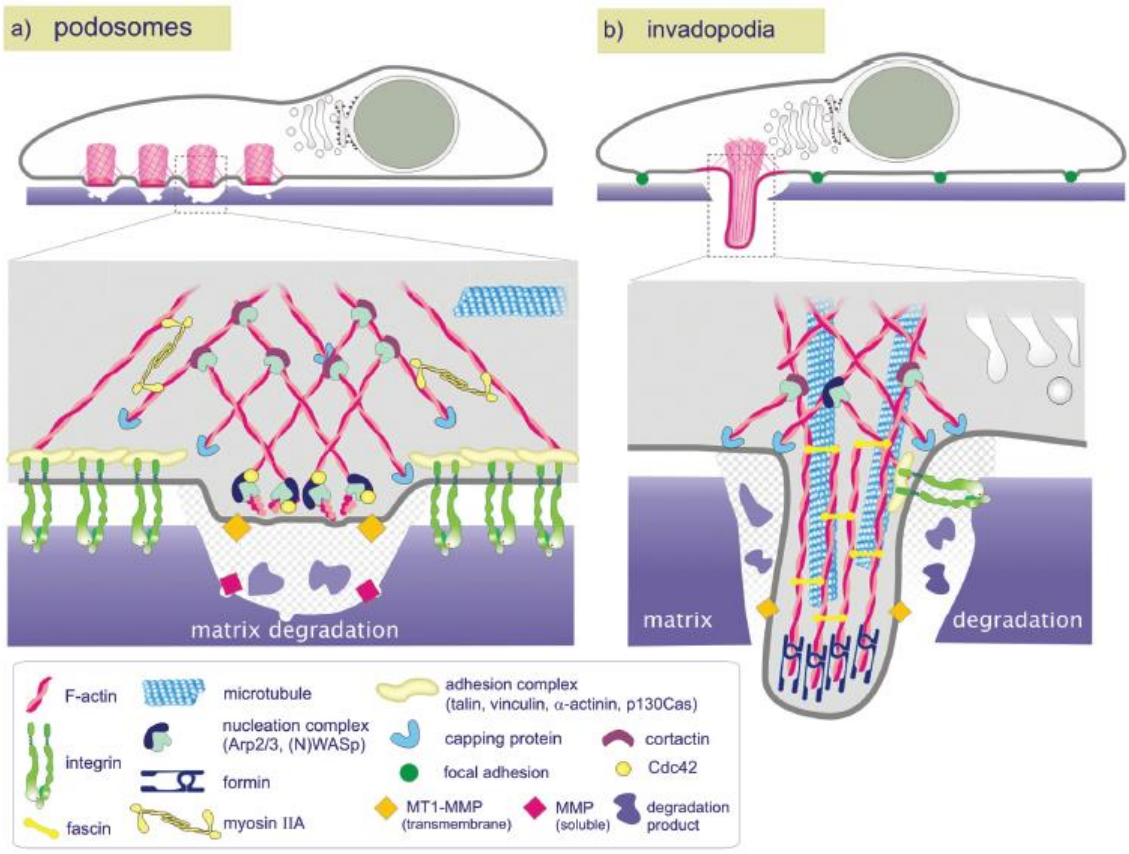

Figure 1. 5; Schematic representation of podosomes and invadopodia.
The architectural structure of podosomes and invadopodia consists of a core of actin filaments that protrude from the ventral surface of the cell and secrete metalloproteases to degrade the ECM. WASP and Arp2/3 complex promoted actin nucleation and thus filaments elongation downstream of Cdc42, allowing the podosome elongation. A network of scaffold proteins and adhesion complexes link the podosome core to the extracellular matrix (A). Invadopodia elongates longer into the surrounding ECM compared to podosome. WASP and Arp2/3 complex are localised at the base of the invadopodia core, which contains also microtubules. Formins drive the linear elongation of actin filaments (B). Image taken from (Spuul et al. 2014).

1.3.2. Invadopodia lifecycle

Invadopodia lifecycle is a very dynamic and complex process that encompasses different successive stages, each of them associated with a wide range of structural proteins and specific molecular regulators. These phases have been defined as invadopodium initiation, invadopodium precursor stabilization, and invadopodium maturation (Figure 1.6) (Beaty and Condeelis 2014).

Formation of invadopodia is triggered by extracellular signals which bind to plasma membranes receptors and elicit intracellular signalling cascades involved with invadopodia dynamics (Hoshino, Branch, and Weaver 2013). These stimuli can be of different natures: growth factors, integrins, cytokines, ECM components, reactive oxygen species (ROS), and micro RNAs, calcium (Murphy and Courtneidge 2011). EGF, Met, PDGF and TGFβ receptors have been reported to promote invadopodia formation in different cancer cell types (Díaz et al. 2013; Eckert et al. 2011; Pignatelli et al. 2012; Rajadurai et al. 2012; Yamaguchi et al. 2005a). These receptors act as serine/threonine or tyrosine kinases, and their stimulation activates a set of kinases, such as Src, ERK and PAK, which, in turn, phosphorylates several downstream effectors involved in cytoskeletal regulation (Foxall et al. 2016). An initial complex of actin and cortactin is formed, where cortactin binds and inhibit the actin-binding protein cofilin, which normally promotes the generation of free actin barbed ends used for actin polymerization (E T Bowden et al. 1999). The actin-related protein (Arp2/3) complex, formins and N-WASP are recruited around the initial core (Beaty and Condeelis 2014). It has been suggested that phosphorylation of cortactin releases cofilin from inhibition, activating formins and the Arp2/3 complex to drive linear and branched actin polymerization, resulting in the elongation of actin barbed ends the formation of the precursor (Oser et al. 2009). The precursor is further stabilised via the formation of tightly packed bundles of actin filaments which are anchored to the plasma membrane via the adaptor protein Tks5 (Beaty and Condeelis 2014). Other actin bundle proteins, such as Fascin and Filamin-A have been reported to stabilize the protrusion (Takkunen et al. 2010; A. Li et al. 2010).

Maturation of the invadopodium involves inactivation of cofilin activity upon de-phosphorylation of cortactin, which is therefore able to bind and sequester cofilin again (Oser et al. 2009). A microtubule network and vimentin filaments extend at the base of the structure, possibly participating in the elongation of invadopodium and in the transport of

several proteases towards the tip (Schoumacher et al. 2010). The predominant proteolytic enzymes utilised by mature invadopodia to degrade the surrounding ECM are metalloproteases (MMPs), amongst there, membrane type 1 MMP (MT1-MMP), MMP2 and MMP9 have been reported to be particularly enriched to invadopodia (Jacob and Prekeris 2015). MT1-MMP is a transmembrane protein that directly cleaves many different components of ECM, including collagen type I, II and III, gelatin, fibronectin, vitronectin and fibrin (Poincloux, Lizárraga, and Chavrier 2009). MMP2 and MMP9 are soluble proteins that recognise collagen type IV, one of the most abundant components of basement membranes, and denatured collagen (gelatin). MMP2 and MMP9 are secreted into the extracellular space as proenzymes, which can be activated via proteolytic cleavage by the transmembrane MT1-MMP (Poincloux, Lizárraga, and Chavrier 2009). MT1-MMP is thought to play a crucial role in invadopodia function, as inhibition or depletion of this protease significantly impairs invadopodia formation and matrix degradation (E. S. Clark et al. 2007; Sakurai-Yageta et al. 2008). MT1-MMP is normally present in the cells in an inactive state, sequestered within intracellular storage compartments. Activation of the Rho-GTPases RhoA and Cdc42 triggers the association between the exocyst complex and the IQ motif containing GTPase activating protein 1 (IQGAP1). This interaction results in the fusion of the vesicle containing MT1-MMP to the target site on the plasma membrane of the invadopodium, with subsequent release of MT1-MMP (Jacob and Prekeris 2015). Studies conducted by Clark et al. indicate that MT1-MMP trafficking and surface expression is regulated by cortactin, which can positively influence also MMP2 and MMP9 secretion (E. S. Clark et al. 2007).

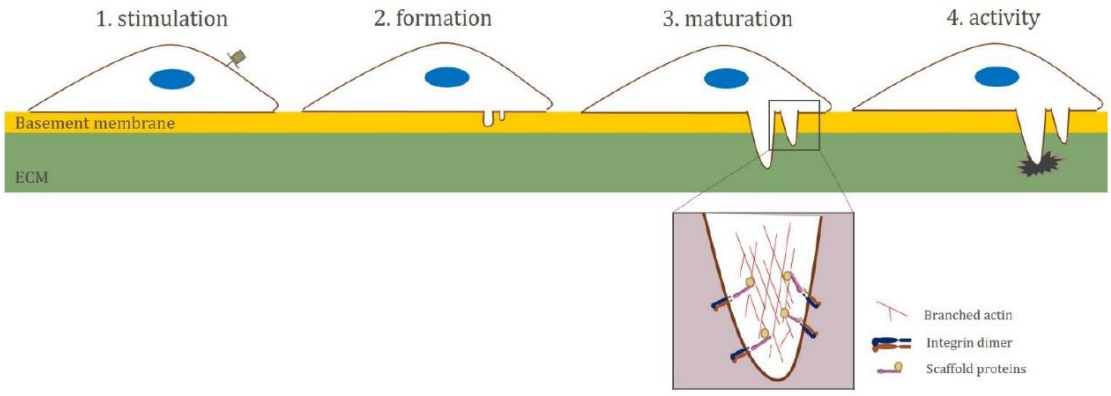

Figure 1. 6: Different phases of invadopodia lifecycle
An extracellular signal (i.e. growth factors, cytokines, ECM proteins, micro RNAs) induces invadopodia formation (1). Subsequently, short cells protrusions invade the basement membrane (2) and further elongate across the ECM (3). Mature invadopodia are characterised by adhesion proteins connected to a ring structure of scaffold proteins and other regulatory factors, which surround the actin core. Mature invadopodia degrade the ECM through secretion of metalloproteases (4).

1.4. Rho GTPases in cell migration and invasion

1.4.1. Rho-GTPases are important regulators of cell motility

Multiple processes involved in cell migration are coordinated by the members of the Rho family GTPases. More than 20 distinct Rho-GTPases have been identified, involved in the regulation of a wide range of cellular functions including cell protrusions, cell adhesion, cell polarization and transduction of several receptor signalling pathways (Guan et al. 2020; Hall 2012). Rho-GTPases can act as molecular switches by cycling between an active GTP-bound state and an inactive GDP-bound state. In their active GTP-bound state, Rho-GTPases can interact with over 50 different downstream effectors, including serine/threonine kinases, lipid kinases, scaffold proteins, oxidases and lipases (Phuyal and Farhan 2019). The transition between GTP- and GDP-bound conformations is regulated via the alternate activity of Rho guanine nucleotide exchange factors (RhoGEFs) and Rho GTPase activating proteins (RhoGAPs). RhoGEFs promote the activation of Rho-GTPases by catalysing the exchange of GTP to GDP. It has been shown that the same Rho-GTPase can be activated by multiple RhoGEFs, which act downstream of extracellular signals and allows a dynamic regulation of Rho-GTPases depending on the tissue and molecular context. The RhoGEFs family comprises more than 70 proteins, mainly belonging to the Dbl family (Cook, Rossman, and Der 2014). These GEFs share a catalytic Dbl-homology domain (DH), which engage with the Rho-GTPase and promote the nucleotide exchange and it's adjacent to a regulatory C-terminal pleckstrin homology (PH) domain (Cook, Rossman, and Der 2014). Other GEFs have been identified belonging to the DOCK family, where the catalytic domain is represented by a conserved Dock-homology region-2 (DHR) (Goicoechea, Awadia, and Garcia-Mata 2014). RhoGAPs, on the contrary, facilitate the hydrolysis of GTP to GDP, causing the inactivation of Rho-GTPases (Bos, Rehmann, and Wittinghofer 2007). A third mechanism of regulation involve the binding of the Rho guanine-nucleotide-dissociation inhibitors (GDIs) to the GDP-bound form of Rho GTPase protein, blocking the protein and impeding its interaction with its regulatory factors and downstream effectors (Leonard et al. 1992) (Figure 1.7).

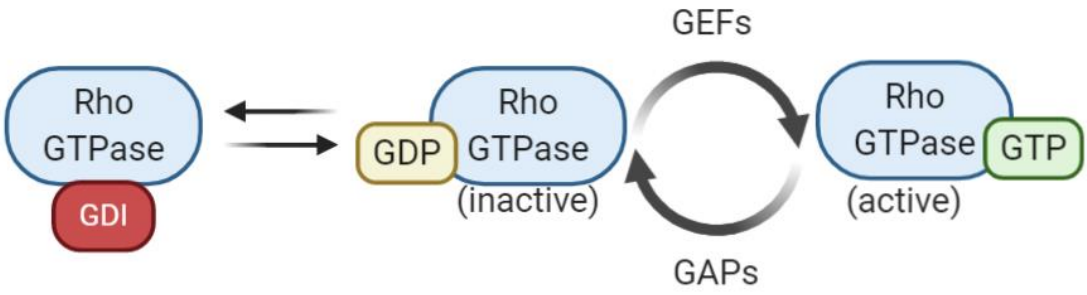

Figure 1. 7: Schematic representation of the mechanisms of Rho-GTPases regulation
GDI binds to Rho-GTPases, preventing its activation and thus it's downstream signaling. Inactive GDP-bound Rho-GTPases is activated by RhoGEF that promotes the exchange of GDP to GTP. Active Rho-GTPase is inactivated by Rho-GAPs that promote the hydrolysis of GTP to GDP.

The most studied Rho GTPases proteins involved in the regulation of actin dynamics are Ras homolog gene family member A (RhoA), Ras-related C3 botulinum toxin substrate 1 (Rac1) and cell division control protein 42 (Cdc42). The activation of these Rho-GTPases has been associated with the formation of distinctive actin-based structures responsible for cell motility. Rac1 protein intervenes in the initial step of the migration process by promoting the formation of lamellipodia protrusions at the leading edge of the cell. Rac1 interaction with the members of the WASP-family verprolin homologue (WAVE) family lead to the activation of the actin-related proteins 2/3 (Arp2/3) complex, which initiates the formation of a new branched actin filaments network (Miki, Suetsugu, and Takenawa 1998; Machesky and Insall 1998). Another mechanism by which Rac1 promotes the polymerization of actin filaments is via the removal of capping proteins that prevents actin nucleation at barbed ends (+) in resting cells. Rac1 binding to phosphatidylinositol-4-phosphate 5-kinase (PIP 5-kinase) triggers the synthesis of phosphatidylinositol-4,5-bisphosphate (PIP2), which then inhibits capping proteins activity (Tolias et al. 2000). Rac1 has also been implicated in formation of focal adhesion, which can be found mainly in lamellipodia in migrating cells and mediates the cell-substrate attachments necessary to generate the traction force for cell movement (Nobes and Hall 1995; Ridley and Hall 1992). Activation of Rac1 promotes the acquisition of an elongate shape and drives mesenchymal invasion via the adaptor protein NEDD9 or through the exchange factor DOCK3 (Sanz-Moreno et al. 2008). Moreover, reduction of Rac1 levels significantly decreased cell invasion (Chan et al. 2005).

Cdc42 is responsible for the maintainment of cell polarity and for the initiation of filopodium extension through activation of Arp2/3. However, differently from Rac1, activation of the

Arp2/3 complex is achieved via interaction with the Wiskott-Aldrich syndrome protein (WASP) family. Importantly, filopodia protrusions can provide guidance during cell migration by acting as chemosensors of the surrounding environment which detect and transmit extracellular signals (Ridley 2001; Mattila and Lappalainen 2008).

RhoA is a well-known inducer of actin stress fibres formation through the activation of the downstream effectors mDia and ROCK (Le Clainche and Carlier 2008). Activation of ROCK also results in the regulation myosin II activity via inhibition of the myosin light chain (MLC) phosphatase. This leads to enhanced phosphorylation of MLC, which results in the formation cross-link of actin filaments and enhanced cellular contractility (Nobes and Hall 1995). It has been shown that increased RhoA/ROCK activity is a key driver of amoeboid invasion in cancer cells (Sahai and Marshall 2003; Sanz-Moreno et al. 2008). A different study has suggested that active RhoA is present at the leading edge where it plays a role in the formation of membrane ruffles (Pertz et al. 2006). Importantly, RhoA is implicated in the maturation and disassembly of focal adhesion at the rear of the cells, an essential process for ensuring an efficient cell invasion (Rottner, Hall, and Small 1999; Huttenlocher and Horwitz 2011).

The regulation of the many processes that are controlled by Rho-GTPases activity is complex, and the resulting effect is dependent on the tight control of Rho-GTPases activation and localisation. A significant cross-talk amongst Rho-GTPases can contribute to the maintainment of this balance. For example, RhoA and Rac1 have been reported to be mutually antagonists, as increase in one of them results in the inhibition of the other (Sander et al. 1999).

1.4.2. Rho-GTPases in invadopodia

The activity of Rho-GTPases to regulate the architectural dynamics of cytoskeletal structures is also required in invadopodia, and different Rho-GTPases might function in different phases of invadopodia lifecycle. Cdc42 is crucial to initiate the assembly of invadopodia precursors by promoting the actin polymerization via N-WASP. Both N-WASP and Arp2/3 have both been localised at invadopodia, with N-WASP found predominantly at the base of the protrusion (Lorenz et al. 2004; Yamaguchi et al. 2005a). Reduction of Cdc42 activity by siRNA or dominant-negative Cdc42 in rat mammary carcinoma cells resulted in decreased

invadopodia formation (Yamaguchi et al. 2005a). Similarly, in pancreatic cancer Cdc42 activity was necessary for the assembly of the actin core precursor (Razidlo et al. 2014). Additional experiments have shown that Cdc42 associates with the scaffold protein CIP4 (Cdc42-interacting protein 4), which is localized to invadopodia where it is thought to generate the plasma membrane curvature of invadopodia (Pichot et al. 2010). Cdc42, together with RhoA, has also been reported to participate in the final phases of invadopodia maturation by stimulating MMPs delivery to the invadopodial membrane that is necessary for the ECM degradation (Sakurai-Yageta et al. 2008). The activity of Cdc42 in promoting invadopodia formation is tightly regulated by a number of Rho GEFs, such as Fgd1 (I. Ayala et al. 2009), β-PIX, induced under hypoxic conditions (Md Hashim et al. 2013) and Vav1, which is activated downstream of the Src kinase (Razidlo et al. 2014).

The exact role of Rac1 in invadopodia is much less understood, as studies on Rac1 have generated conflicting results. Constitutive activation of Rac1 in melanoma cells via active mutants enhanced matrix degradation (Nakahara et al. 2003), while Rac1 knockdown of expression dramatically decreased invadopodia formation and matrix degradation in glioma cells (Chuang et al. 2004). Oppositely, more recent studies employing Rac1 biosensor in breast cancer have reported that Rac1 is inactivated in invadopodia precursors, but it's transiently activated during invadopodia disassembly (Moshfegh et al. 2014). These findings suggest that Rac1 mainly functions in the dissolution and turnover of invadopodia rather than during the formation and maturation phases (Moshfegh et al. 2014).

The role of RhoA in invadopodia is controversial. Activation of RhoA by the Rho-GTPase Arghef5 was required for Src-induced invadosome formation and maturation (Kuroiwa et al. 2011), while depletion of RhoA decreased invadopodia activity (Bravo-Cordero et al. 2011) Moreover, RhoA participates in the delivery of MT1-MMP by regulating the interaction of IQGAP with the exocyst complex, and depletion of RhoA significantly inhibited matrix degradation (Sakurai-Yageta et al. 2008). Other studies have shown that expression of dominant-active or dominant-negative mutants of RhoA did not affect invadopodia-mediated degradation (Nakahara et al. 2003), and blocking RhoA signalling increased formation of invadopodia (Sedgwick et al. 2015). Bravo-Cordero and colleagues reported that in breast cancer cell lines RhoA is not required for invadopodia formation, but rather it intervenes in invadopodia maturation (Bravo-Cordero et al. 2011). By using a FRET-based RhoA biosensor, they have showed that RhoA is active both inside and outside the invadopodial core, with no evident differences in the pattern of RhoA activation. RhoC, in

contrast, exhibited a more defined spatial restriction, with RhoC-GTP accumulating to a ring area surrounding the invadopodium core. The differential activation of RhoC in the invadopodial structures is governed by the localisation of p190-RhoGEF, which is confined outside the invadopodia where it promotes the exchange of GDP to GTP, and p190-RhoGAP, which is enriched within the core where it inactivates RhoC (Bravo-Cordero et al. 2011). As a result, outside the invadopodia RhoC -GTP activates LIMK, which, in turn, phosphorylates and inactivates the actin-binding protein Cofilin. Cofilin remains active inside the invadopodia core, where it stimulates actin polymerization and invadopodial extension (Bravo-Cordero et al. 2011). Thus, it seems that RhoA and RhoC plays differential roles in the invadopodia lifecycle. However, more recent studies conducted on melanoma suggested that RhoA might function earlier in the invadosome lifecycle, and it's inhibited later during matrix degradation, possibly via different spatiotemporal mechanisms (Nicholas et al. 2016). These observations further highlight the highly complex regulation of Rho-GTPases activity and their different roles in invadopodia dynamics.

1.5. P-21 activated kinases (PAKs)

The importance of kinases in driving invadopodia activity has been clear since their discovery, as these structures were first characterised as Src-enriched protrusion. Amongst these kinases are the members of p21-activated kinases (PAKs) family. PAKs are Serine/Threonine kinases that act as downstream effectors of Rho GTPases Rac and Cdc42 to elicit a wide range of biological functions, including regulation of cell proliferation, cell survival, motility and cytoskeletal dynamics, gene transcription (King, Nicholas, and Wells 2014). PAKs proteins are highly conserved in several organisms, including Drosophila and C. Elegans (Bokoch 2003). In mammals, there are six members of the family that can be classified into two subgroups based on their chemical and structural properties: group I includes PAK1-PAK3, while group II PAKs includes PAK4-PAK6 (King, Nicholas, and Wells 2014) (Figure 1.8).

Normal tissue distribution of individual PAKs vary according to the isoform considered, most likely because of different substrates recognition. All group I PAKs are widely expressed in neuronal tissues, with PAK3 being the predominant isoform expressed in the brain (Arias-Romero and Chernoff 2008). Accordingly, PAK3-null mice displayed defective learning, memory and synaptic plasticity (Kelly and Chernoff 2012). PAK2 is ubiquitously expressed, and PAK2 gene is required for embryonic development, as loss of this gene is lethal for mice embryos (Kelly and Chernoff 2012). PAK1 is highly present in brain, muscle and spleen, and although PAK1 knockout mice are viable and fertile, they display defective glucose homeostasis and immune deficiencies of bone marrow-derived immune cells (Kelly and Chernoff 2012). PAK4 was the first PAK isoform identified in group II, and the most studied. PAK4 is ubiquitously expressed, with notably highly levels in prostate, testis and colon (Arias-Romero and Chernoff 2008). PAK4 activity has been reported to be particularly important in development. Mice lacking PAK4 gene display embryonic lethality at 11 days post fertilization, possibly due to genetic disorders affecting blood vessel formation and neuronal development (Jian Qu et al. 2003; Kelly and Chernoff 2012). The expression of both PAK5 and PAK6 increases later in development. Similarly to PAK3, PAK5 is highly expressed in the brain, while PAK6 can be found in the testis, prostate, brain, kidney and placenta. Mice null for either one or both PAK5 and PAK6 are healthy and do not display visible defects (Kelly and Chernoff 2012).

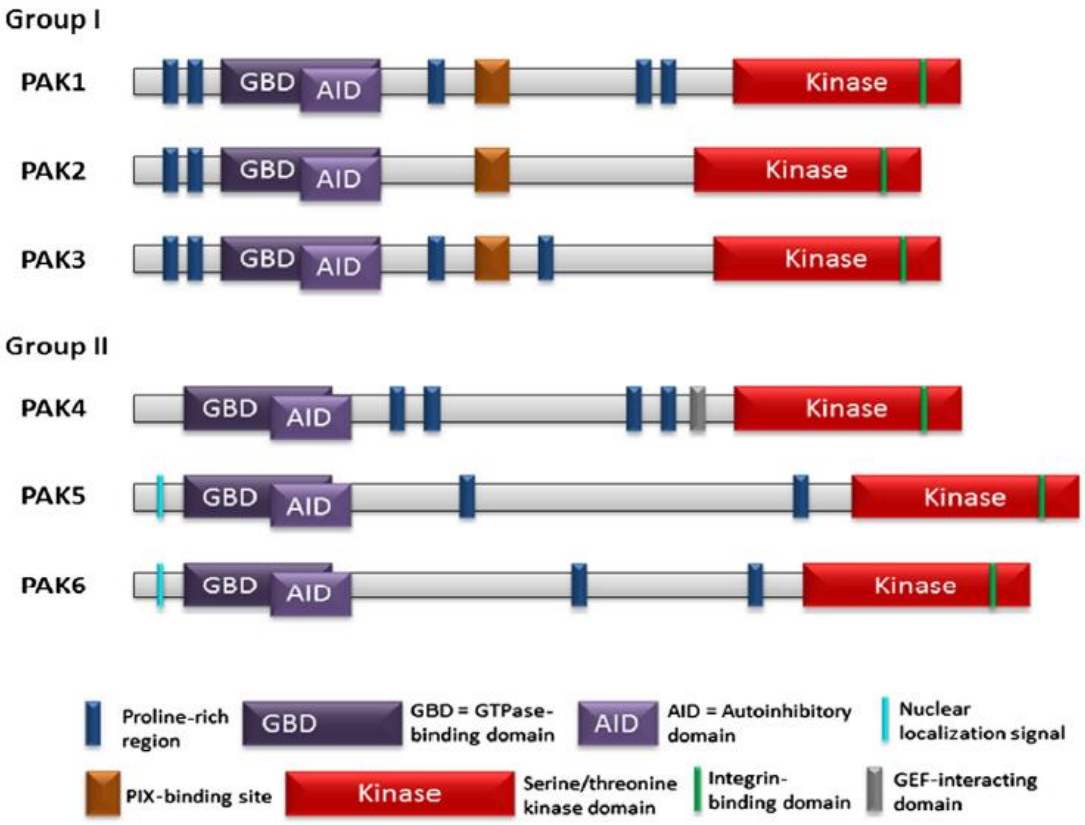

Figure 1. 8: Structures of the p21-activated kinase family members.
PAK family members are divided into two subgroups: group I (PAK1-3) and group II (PAK4-6), according to their structural and sequence homology. All PAKs possess a N-terminal p21-GTPase binding domain (GBD) and a catalytic C-terminal kinase domain. Figure adapted from (King, Nicholas, and Wells 2014).

1.5.1. Structure and regulation

All PAK isoforms exhibit a N-terminal GTPase binding domain (GBD), and a C-terminal kinase domain (Arias-Romero and Chernoff 2008). Group I PAKs share a high degree of sequence identity and structural similarities. The GBD domain recruits important regulators such as Cdc42 and Rac, and it overlaps with an auto inhibitory domain (AID). Additionally, the regulatory domain includes several proline-rich sites characterised by SH3 (Src homology 3)-binding motifs (Arias-Romero and Chernoff 2008). Group I PAKs are maintained in an inactive state by forming homodimers in a trans-inhibitory mechanism via AID. AID binds to the kinase domain of another PAK acting as pseudosubstrate to block protein activation (Lei et al. 2000; Parrini et al. 2002). Even in an inhibitory state, group I PAKs are characterised by low basal kinase activity, which is enhanced upon binding to GTPases. Binding of the GTP-bound Cdc42 or Rac determines a conformational change that release the pseudosubstrate

from its binding site, allowing the activating autophosphorylation at Thr-423, Thr-402 and Thr-421 for PAK1, PAK2 and PAK3 respectively (F T Zenke et al. 1999; Arias-Romero and Chernoff 2008). Other proteins can indirectly lead to PAK activation by modulating PAK's localisation: binding of the adaptor protein Nck to the N-terminal of PAK1 results in PAK1 shuttling from the cytoplasm to the plasma membrane where it can be activated by Rho-GTPases (Wange Lu and Mayer 1999). Alternative Cdc42/Rac independent mechanisms of activation have been described for group I PAKs, including phosphorylation by upstream kinases, proteolytic cleavage, binding of sphingosine or SH3-containing proteins (Knapp 2013). Interestingly, different isoforms of PAK3 display dissimilarities in the GIB/AID domain, which result in constitutive kinase activity in one of the four variants. Moreover, another spliced variant has been reported to form heterodimers with PAK1 (Kreis et al. 2008; Combeau et al. 2012).

The structure of group II PAKs also comprises an N-terminal GBD and C-terminal kinase domain, but they lack several structural motifs found within PAK1–3, thus, they can be considered as a distinct set of kinases. One notably difference is that the basal catalytic activity of group II proteins is higher compared to PAK1-3, but it does not appreciably increase upon binding to Rho-GTPases (Abo et al. 1998). Moreover, the level of structural and sequence similarity amongst proteins of group II PAKs is significantly lower compared to that of group I (Arias-Romero and Chernoff 2008). A specific feature to PAK4, which has never been reported in other PAKs, is the presence of a GEF-H1/Gab1-interacting domain (GID), which binds to the RhoGEF PDZ-RhoGEF (Barac et al. 2004), and a binding site for αvβ5 integrin in the C-terminal region (H. Zhang et al. 2002). The mechanisms by which group II PAKs activity is regulated is still a subject of debate, and findings on this matter mainly focused on PAK4, the most studied isoform of the family (King, Nicholas, and Wells 2014). Following initial evidence that PAK4 binding with Cdc42 and Rac did not have a significant impact on PAK4 activity (Abo et al. 1998), different regulatory routes for Group II PAKs have been suggested that varies from that of Group I PAKs. It has been suggested that activation of PAK4 was dependent on phosphorylation of activation loop Ser 474, however this site was found to be constitutively phosphorylated (Baskaran et al. 2012; Ha et al. 2012). More recently, new data has uncovered evidence that Cdc42 could participate to PAK4 activation, and two possible mechanisms that might be able to turn PAK4 activity on or off have been proposed. The first study hints that PAK4 is held in an inactive state due to the presence of

an autoinhibitory domain in the N-terminal region similar to that identified in group I PAK. Binding of GTP-Cdc42 results in a conformational change that can revert this autoinhibited state (Baskaran et al. 2012). The second mechanism identified a pseudosubstrate containing a key proline residue in the N-terminal motif (R49PKPLV) that, following the binding of kinase domain, would lead to constitutive autoinhibition. PAK4 is then activated upon binding with a protein having a SH3 domain which release the inhibition (Ha et al. 2012). Subsequent evidence from nuclear magnetic resonance (NMR) studies identified the presence of an autoinhibitory pseudosubstrate motif occupying the entire cleft region between the two kinase lobes (W. Wang et al. 2013). It has been demonstrated that group II PAKs can additionally be activated via the PI3K signalling pathway (Wells, Abo, and Ridley 2002). Stimulation with hepatocyte growth factor (HGF), which is independent from Cdc42, resulted in PAK4 autophosphorylation and increased PAK4 kinase activity in MDCK cells downstream of the PI3K signalling, triggering cytoskeletal reorganization and cell rounding (Wells, Abo, and Ridley 2002). Interestingly, the addition of specific PI3K inhibitors prevented morphological changes in presence of the whole PAK4, but it did not seem to affect cellular response when the isolated C-terminal kinase domain of PAK4 was utilised. These findings suggest that the N-terminal region of PAK4 might negatively regulate PAK4 (Wells, Abo, and Ridley 2002).

1.5.2. The importance of PAKs in cancer

Accumulating evidence link PAKs aberrant expression or activation to tumour growth, survival and motility (King, Nicholas, and Wells 2014). Amongst group I, PAK1 kinase represents the most frequently overexpressed in a wide variety of cancers, such as breast (Holm et al. 2006; Ong et al. 2011), liver (Ching et al. 2007) lung (Ong et al. 2011), colorectal (Carter et al. 2004) and also in a subset of melanoma (Ong et al. 2013). PAK1 phosphorylation of β-catenin at Ser675 results in increased proliferation of colon cancer cells (Xiang Li et al. 2011). Works on transgenic mouse models demonstrated that constitutive activation of PAK1 drives the development of mammary gland tumours alongside a variety of breast lesions (R.-A. Wang et al. 2006). Phosphorylated form of PAK1 stimulates MAPK and MET signalling, facilitating the formation of anchorage-independent colonies from breast cancer cells (Vadlamudi et al. 2000). Additionally, PAK1 as well as PAK5, are thought to stimulate cellular proliferation through an upregulation of various cell cycle

regulators including CDK2, CDC25A, and cyclin (Jun et al. 2012; Balasenthil et al. 2004). Hyperactivation of PAK4 results in the activation of the proliferative MEK1/2 and p38-MAPK signalling pathways (R.-A. Wang et al. 2006). PAKs play also a role in inhibition and resistance to apoptosis via regulation of the BAD/Bcl-2 pathway. PAK1 and PAK5 phosphorylation of Raf1 at Ser-338 stimulates its translocation to the mitochondria, where Raf1 binds the proto-oncogene Bcl-2 and phosphorylates the protein BAD, preventing the formation of the proapoptotic BAD-Bcl-2 complex (Jin et al. 2005; Wu et al. 2008; Cotteret et al. 2003). Similarly, PAK2 phosphorylation of caspase 7 can inhibit the apoptosis by in breast cancer cells (Xiang Li et al. 2011). Because many of PAK substrates control different aspects of cytoskeletal organisation and morphology, they are likely to promote the invasiveness and metastasis formation. For example, PAK5 promotes breast cancer cell migration and invasion via the PAK5-MMP2 signalling pathway (X.-X. Wang et al. 2013), while PAK1 can induce lamellipodia and filopodia formation (Sells et al. 1997).

1.5.3. PAK4 plays different roles in cancer

PAK4 was found to be overexpressed at either mRNA or protein levels in several types of cancers, such as breast (Callow et al. 2001; Yingying Liu et al. 2008; Y Liu et al. 2010), ovarian (Siu et al. 2010), prostate (Ahmed et al. 2008; Wells et al. 2010; Whale et al. 2013), gastric (Ahn et al. 2011; J. Zhang et al. 2012) and gallbladder cancer (Kim et al. 2008). Alteration of PAK4 level through genomic amplification of the PAK4 gene, which is located on chromosome 19 (19q13.2), has been detected in in ovarian (Davis et al. 2013), pancreatic (S. Chen et al. 2008; Mahlamäki et al. 2004), colon (Parsons et al. 2005), breast (W. Yu et al. 2009) and squamous cell carcinoma (Begum et al. 2009). High PAK4 activity has been often associated with poor prognosis, and several studies investigating the clinical significance of PAK4 overexpression in cancer suggested that PAK4 might represent an independent prognostic factor in some cancer (Siu et al. 2010; He et al. 2017). For example, in patients with breast carcinoma and ovarian cancer high PAK4 expression has been linked to more advanced stage and poor survival (Siu et al. 2010; He et al. 2017). Similarly, metastatic gastric tumours exhibited higher PAK4 expression when compared to primary tumours (Guo et al., 2014), and increased levels of PAK4 in gastric cancer patients was associated to a poorer survival (Ahn et al. 2011).

Cancer Type	Alteration	References
Breast	Protein overexpression Genomic Amplification	Callow et al., 2001; Liu et al., 2008; 2010; Minden 2012; Rafn et al., 2012; Yu et al., 2009
Gallbladder	Protein overexpression	Kim et al., 2008
Gastric	Protein overexpression	Ahn et al., 2011; Zhang et al., 2012
Glioma	Protein overexpression	Kesanakurti et al., 2012
Lung	Protein overexpression	Callow et al., 2002
Ovarian	Protein overexpression Genomic amplification	Siu et al., 2010b; Davis et al., 2013
Pancreatic	Genomic amplification	Chen et al 2008; Kimmelman et al., 2008; Mahlamaki et al., 2004
Prostate	**Protein overexpression**	**Ahmed et al., 2008; Park et al., 2012; Wells et al., 2010; Whale et al., 2013**
Squamous cell carcinoma (SCS)	Genomic amplification	Begum et al., 2009 ; Zanivan et al., 2013

Table 1. 2: PAK4 alteration in different types of cancer.

PAK4 is involved in controlling different crucial processes participating in oncogenesis. Notably, expression of a constitutively active PAK4 mutant in fibroblast was sufficient to acquire a transformed morphology and induced tumorigenesis (J Qu et al. 2001; Callow et al. 2001). Another study conducted on breast cancer cell line growth in a 3D culture system revealed that PAK4 depletion was able to revert the transformant tissue to a normal acinar architecture, similar to that of normal breast epithelium (Wong et al. 2013). These findings indicate that PAK4 might play a key role in promoting tumorigenesis. Moreover, increased PAK4 expression or PAK4 phosphorylation has been reported to induce resistance to anoikis in glioma, whereas PAK4 depletion led to increase cell death (Kesanakurti et al. 2012). Constitutive activation of PAK4 conferred protection against several proapoptotic stimuli such as tumour necrosis factor α stimulation, UV irradiation, and serum starvation (Gnesutta, Qu, and Minden 2001). It has been suggested that PAK4 promotes cell survival and protects from apoptosis throughout two different mechanisms. PAK4 either phosphorylates the Bcl-2 antagonist of cell death (BAD), preventing its interaction with Bcl family members and the consequential release of cytochrome C from mitochondria (Gnesutta, Qu, and Minden 2001; Gnesutta and Minden 2003). Alternatively, PAK4 can act by inhibiting the binding of caspase-8t death domain receptors in a kinase-independent mechanism (Gnesutta and Minden 2003). In addition to apoptosis, PAK4 has been reported to play a key role in the regulation of proliferation and cell-cycle progression through downregulation of the cell cycle regulatory protein p21 (CDKN1A), thus preventing recruitment of cyclin D1 to the CDK4 complex (Tanya and Audrey 2011). Additionally, PAK4 directly regulates the expression of cyclin D1 and CDC25A at both mRNA and protein levels in ovarian cancer cells. Here, PAK4 constitutive expression significantly enhanced cellular proliferation, whereas PAK4 depletion impaired cell growth (Siu et al. 2010). Similarly, choriocarcinoma cell lines with depleted PAK4 expression displayed a lower proliferation rate accompanied by downregulation of CDK6 when compared to control cells and PAK4 overexpressing cells (H.-J. Zhang et al. 2011).

One of the most studied PAK4 functions is the regulation of actin dynamics and cytoskeletal organisation in cancerous and non-cancerous cells. PAK4 has been reported to induce localized actin polymerization and filopodia formation downstream of Cdc42 (Abo et al. 1998). In fibroblasts and MDCK cells, activation of PAK4 led to dissolution of actin stress fibres and inhibition of new stress fibres formation via activation of the phosphoinositide 3-

kinase (PI3K) pathway (Wells, Abo, and Ridley 2002; Callow et al. 2005; J Qu et al. 2001). PAK4 can phosphorylate the serine/threonine kinase LIMK1, which, in turns phosphorylates and inactivates cofilin (Dan et al. 2001; Ahmed et al. 2008). In myoblast, phosphorylation of LIMK by PAK4 enhanced its inhibitory effect on cofilin, impairing cofilin's ability to bind and depolymerize actin filaments and thus suppressing actin disassembly (Dan et al. 2001). Alternatively, PAK4 negatively regulates cofilin activity via a different mechanism involving the formation of a multiprotein complex comprising LIMK1, Sling-Shot phosphatase (SSH-1L) and the scaffold protein 14-3-3ζ (Soosairajah et al. 2005). A more recent work identified PAK4 as downstream target of the protein kinase D (PKD), a serine-threonine kinase that phosphorylates PAK4 in the autophosphorylation site Ser-474, which results in the increased activation of LIMK (Spratley et al. 2011). Moreover, in human gastric cancer cells PAK4 directly binds the DiGeorge critical region 6 (DGCR6) protein via its C-terminal domain (Xiaodong Li et al. 2010). This interaction induced an upregulation of the phosphorylation level of LIMK1 and increased the migratory potential of cancer cells (Xiaodong Li et al. 2010). Thus, PAK4 orchestrates cofilin activity via multiple mechanisms that involve several different molecules and regulatory pathways. PAK4 is also known to regulate the ability of cells to adhere to their substrate, by influencing focal adhesions turnover, another aspect of the cystoskeletal dynamics that intervenes in cell migration and cancer invasion. Stable expression of activated PAK4 resulted in reduction in focal adhesions and promoted anchorage-independent growth (J Qu et al. 2001; Wells, Abo, and Ridley 2002). PAK4-mediated turnover of focal adhesion is thought to be achieved through phosphorylation of β5 integrin 5 cytoplasmic domain at Ser-759 and Ser-762 (Z. Li et al. 2010). Additionally, PAK4 was found involved in promoting focal adhesion turnover via phosphorylation of paxillin Ser-272 (Wells et al. 2010), which in breast cancer might be achieved downstream of a PAK4–RhoU complex (Dart et al. 2015). Indeed, breast cancer cell lines overexpressing PAK4 showed increased cell motility, which was impaired when a β5 integrin mutated in the PAK4 target residues was used (Z. Li et al. 2010; H. Zhang et al. 2002).

Considering the important role of PAK4 in regulating cell proliferation, cytoskeleton reorganisation and cell:substrate adhesion, it is not surprising that PAK4 can influence tumour cell invasion and metastasis. Therefore, PAK4 and its downstream substrates constitute potential targets for development of novel therapeutic opportunities to target metastasis in several tumours.

1.5.4. Linking PAK4 to prostate cancer

Several works demonstrated that PAK4 is a key regulator of prostate cancer cell migration and invasion. Immunohistochemistry analysis of prostate cancer tissues revealed that the levels of phosphorylated PAK4, mostly found in the nucleus, strongly correlated with high-risk prostate cancer having a Gleason score of 8 or more (J.-J. Park et al. 2018). In the same study, PAK4 depletion reduced EMT, invasion, and *in-vivo* metastasis of prostate cancer cells (J.-J. Park et al. 2018). Activation of PAK4 downstream of the HGF/c-Met signalling has been reported to be required for efficient prostate cancer cell scattering and migration (Ahmed et al. 2008; Whale et al. 2013). Here, HGF stimulation of PC3 cells was sufficient to increase PAK4 interaction with LIMK1, and the subsequent phosphorylation levels of LIMK1 and cofilin, resulting in increased migratory speed (Ahmed et al. 2008). Likewise, PAK4 depletion in DU145 human prostate cancer cells negatively affected cell migration in response to HGF (Wells et al. 2010). Moreover, in DU145 cells PAK4 was found to be localised at focal adhesion involved in the regulation of cellular adhesion turnover via paxillin phosphorylation at Ser-272 (Wells et al. 2010).

It has been suggested that PAK4 regulation of F-actin structures is driven by the interaction between PAK4 and GEF-H1, a microtubule-associated Rho GEF that activates Rho GTPases (Wells, Abo, and Ridley 2002; Callow et al. 2005). PAK4 has been reported to phosphorylate GEF-H1 at Ser-885 *in-vitro* (Callow et al., 2005), and experiments in PCa showed that PAK4-depleted cells exhibited a reduction in cell invasiveness, but increased RhoA levels (Wells et al. 2010). Thus, in prostate cancer cell lines, the GEF-H1:PAK4 interaction resulted in inhibition of the GEF-H1 exchange activity and consequent decrease in RhoA activation level (Wells et al. 2010).

1.5.5. PAK4 in invadopodia

Initial studies investigating the involvement of PAK4 in invadosome have shown that PAK4 localises in podosome in primary human macrophages (Gringel et al. 2006; Wells and Jones 2010). Gringel et al. demonstrated that in this cell type PAK4 is a physiological regulator of podosome and is specifically required for podosome formation, possibly in cooperation with its regulator αPIX (PAK-interacting exchange factor). Indeed, PAK4 depletion or mutation reduced the number and the size of podosome (Gringel et al. 2006). These observations

were further confirmed in macrophages, where high resolution imaging experiments identified PAK4 localized to the podosome ring, rather than the core (Foxall et al. 2019).

PAK4 has been reported to localize also to invadopodia in melanoma cell lines (Nicholas et al. 2016). Interestingly, PDZ-RhoGEF, a regulator of RhoA that coordinate actin stress fibres and focal adhesions formation, was found to be co-localised with PAK4 to invadopodia in melanoma cells (Nicholas et al. 2016). PDZ-RhoGEF binds and activates RhoA, and it is negatively regulated by PAK4, which prevents the accumulation of Rho-GTP (Barac et al. 2004). While RhoA inactivation seems to be required to successfully reach the invadopodia maturation, other data suggest RhoA may play a role in other phases of invadopodia lifecycle, and that its expression levels are subjected to a fine special-temporal regulation (Berdeaux et al. 2004). This hypothesis aligns with the observation that PAK1, associated with the early phase of invadopodia formation, rather than maturation, do not bind PDZ-RhoGEF, and PAK1 depleted cells don't increase levels of RhoA (Nicholas et al. 2017). These studies suggest that different isoforms of PAKs might intervene in regulation of different phases of invadopodia lifecycle, and a balance between RhoA activity and inhibition is important for their formation and functions.

However, despite the recent advancements in understanding molecular pathways involved in invadopodia dynamics, PAK4 role and the precise mechanism by which the PAK4:PDZRhoGEF:RhoA pathway regulates invadopodia remains unclear.

1.6. Project aims

This PhD project seeks to investigate whether PAK4 mediates invadopodia formation and function in prostate cancer, and identify its molecular regulators/interactors that could represent potential therapeutic targets, paying special attention to RhoA signalling.

More specifically, the research questions aimed to:

• Investigate the invasive potential of CT-1532, -1535, -1542 cell lines and evaluate whether they represent a valid model system for normal vs cancer comparative studies or a valid model as cancer cells alone.

• Investigate whether PAK4 is required for efficient invadopodia formation in prostate cancer cells.

• Understand if PAK4 acts as a regulator of RhoA activity in prostate cancer and explore the spatial/temporal regulation of RhoA, paying special attention to its role within invadopodia.

Chapter 2

Materials and Methods

Chapter 2. Materials and methods

2.1. Materials

2.1.1. General Reagents

Materials	Company
3-(4,5-Dimethylthiazol-2-yl)-2,5-Diphenyltetrazolium Bromide (MTT)	Sigma-Aldrich, UK
4-(2-hydroxyethyl)-1-piperazineethanesulfonic acid (HEPES)	A&E scientific
4',6-diamidino-2-phenylindole (DAPI)	Sigma-Aldrich, UK
Acetic acid	Sigma-Aldrich, UK
Acrylamide (30%)	Severn Biotech Ltd, UK
Agarose	Invitrogen, UK
Ammonium persulfate (APS)	Sigma-Aldrich, UK
Aprotinin	Sigma-Aldrich, UK
Beta (β)- mercaptoethanol	Sigma-Aldrich, UK
Bovine pituitary extract (BPE)	ThermoFisher Scientific, USA
Bovine serum albumin (BSA)	VWR International, UK
Bromophenol blue	Bio-Rad
Calcium phosphate transfection kit	Invitrogen, UK
Cell dissociation buffer	Sigma-Aldrich, UK
Coverslips 13mm	Scientific Laboratories Supplies
Dimethyl sulfoxide (DMSO)	Sigma-Aldrich, UK
Dithiothreitol (DTT)	Sigma-Aldrich, UK
DMEM	Sigma-Aldrich, UK
Dulbecco's phosphate-buffered saline without calcium and magnesium **(**DMEM)	Gibco, Invitrogen, UK
Ethanol	BDH Laboratory Supplies, UK
Ethyl 3-aminobenzoate methanesulfonate (MS222)	Sigma-Aldrich, UK
Ethylenediaminetetraacetic acid (EDTA)	Sigma-Aldrich, UK
FluorSave™ Reagent	Calbiochem, UK
Foetal bovine serum (FBS)	Gibco, Invitrogen, UK
Gel Cassettes	Invitrogen, UK
GFP-TRAP	ChromoTek, Germany
Glycerol	Sigma-Aldrich, UK
Glycine	Sigma-Aldrich, UK
Hydrochloric acid (HCl)	VWR International, UK
Kanamycin	Invitrogen, UK
Keratinocyte Serum-free (KSFM)	ThermoFisher Scientific, USA
Leupeptin	Sigma-Aldrich, UK

Lipofectamine 3000	Invitrogen, UK
Low melting point agarose	Invitrogen, UK
Luria-Bertani (LB) Agar	Sigma-Aldrich, UK
Luria-Bertani (LB) broth tablets	Sigma-Aldrich, UK
Magnesium acetate	Sigma-Aldrich, UK
Magnesium chloride ($MgCl_2$)	Sigma-Aldrich, UK
Methanol	VWR International, UK
Methylene blue	ThermoFisher Scientific, USA
Milk powder	Marvel, UK
NEB®-10 beta competent E.coli cells (high efficiency)	New England Biolabs, UK
Nitrocellulose membrane	PerkinElmer, UK
Nonidet P-40	Sigma-Aldrich, UK
N-Phenylthiourea (PTU)	Sigma-Aldrich, UK
Oleoyl-L-α-lysophosphatidic acid sodium salt (LPA)	Sigma-Aldrich, UK
OptiMEM	Invitrogen, UK
P3000	Invitrogen, UK
PAK4 Kinase	Abcam, UK
Paraformaldehyde (PFA)	Sigma-Aldrich, UK
Penicillin-streptomycin	Sigma-Aldrich, UK
PepSpots™ Peptides on Cellulose	JPT Peptide Technologies
Phenylmethylsulfonyl fluoride (PMSF)	Sigma-Aldrich, UK
Phosphate buffered solution (PBS) tablets	Oxoid Limited, UK
Pierce™ ECL Western blotting substrate	ThermoFisher Scientific, USA
Polyvinylpyrrolidone solution (PVP)	Sigma-Aldrich, UK
Precision Plus Protein™ dual color standards	Bio-Rad, UK
Protein A Agarose beads	Invitrogen, UK
PureLink® HiPure plasmid maxiprep kit	Invitrogen, UK
Puromycin	Sigma-Aldrich, UK
QCM™ Gelatin Invadopodia Assay	Merck, USA
Rhotekin-RBD beads	Cytoskeleton, Inc., USA
Roswell Park Memorial Institute (RPMI)-1640 medium	Sigma-Aldrich, UK
Sodium Chloride (NaCl)	Sigma-Aldrich, UK
Sodium dodecyl sulfate (SDS)	Sigma-Aldrich, UK
Sodium fluoride (NaF)	Alfa Aesar, UK
Sodium Hydroxide (NaOH)	Sigma-Aldrich, UK
Sodium orthovanadate (Na_3VO_4)	New England Biolabs, UK
Tris-base	Sigma-Aldrich, UK
Triton X-100	VWR International, UK
Trypsin	Gibco, Invitrogen, UK
Tween® 20	VWR International, UK
ViaFect™ transfection reagent	Promega, UK
Virkon Powder Disinfectant	DuPont, USA
X-ray film	Scientific Laboratories Supplies

Table 2. 1. General Materials.

2.1.2. Buffers

Buffer/solution	Composition
Blocking solution	5% w/v milk powder or 5% w/m BSA in tris buffered saline (TBS)-tween (TBST)
CoIP lysis buffer	0.5% NP-40, 10mM Tris-HCl pH7.6, 150mM NaCl, 0.5mM EDTA, 1mM DTT, 10µg/ml leupeptin, 1µg/ml aprotinin, 10mM PMSF, 10mM NaF, 1mM NA_3VO_4
CoIP dilution/wash buffer	10mM Tris-HCl pH7.6, 150mM NaCl, 0.5mM EDTA, 1mM DTT, 10µg/ml leupeptin, 1µg/ml aprotinin, 10mM PMSF, 10mM NaF, 1mM NA_3VO_4
Rho-GTP pulldown washing buffer	250mM Tris-HCl pH7.6, 40mM NaCl, 30mM $MgCl_2$, 1mM DTT, 10µg/ml leupeptin, 1µg/ml aprotinin, 10mM PMSF, 10mM NaF, 1mM NA_3VO_4
Gel sample buffer (6x)	375mM Tris-HCl pH 6.8, 10% w/v SDS, 30% v/v glycerol, 6% β-mercaptoethanol, 0.2% w/v bromophenol blue
Stripping buffer	25mM Glycine pH2, 1% w/v SDS
Protease inhibitor cocktail:	50mM NaF, 1mM Na3VO4, 1mM PMSF, 10µg/ml leupeptin, 1µg/ml aprotinin and 1mM DTT
SDS-PAGE running buffer (10x)	250mM tris-base, 1.92M glycine, 1% w/v SDS
SDS-PAGE transfer buffer (10x)	250mM tris-base. 1.92M glycine
TBST	25mM tris-HCl pH7.6, 50mM NaCl, 0.1% v/v tween 20
E3 Media	5mM NaCl, 0.17mM KCl, 0.44mM CaCl2, 0.68mM MgSO4 in H2O
Phospho-array stripping buffer A	1% SDS, 8M urea, 0.5% beta-mercaptoethanol
Phospho-array stripping buffer B	50% ethanol, 10% glacial acetic acid
Kinase cocktail solution	2.5 mM Hepes pH 7.4, 50 mM magnesium acetate, 0.5 mM ATP
Kinase assay reaction buffer (5x)	40 mM MOPs pH 7, 1 mM EDTA

Table 2. 2. Buffers and solutions.

2.1.3. Primers

Primer	Sequence
PAK4 shRNA rescue deltaPxxP-FW	GTTCACGGGGTACCTCGACAATTTCATTAAGATTGGCGAGGGC
PAK4 shRNA rescue deltaPxxP-REV	GCCCTCGCCAATCTTAATGAAATTGTCGAGGTACCCCGTGAAC

Table 2. 3. Primers used.

2.1.4. Plasmids

Plasmid	Resistance
pEGFP-RhoA Biosensor	Kanamycin
Myc-PDZ-RhoGEF	Ampicillin
Myc-PAK4	Ampicillin
Myc-PAK4 iRNA rescue	Ampicillin
Myc-PAK4 iRNA rescue - H19,22L	Ampicillin
Myc-PAK4 iRNA rescue - K350,351M	Ampicillin
Myc-PAK4 iRNA rescue -deltaPxxP7	Ampicillin
Myc-RhoC	Ampicillin
FLAG-RhoA	Ampicillin
pDEST-myc	Ampicillin
pENTRY-PAK4 rescue	Gentamicin
pENTRY-PAK4 rescue H19,22L	Gentamicin
pENTRY-PAK4 rescue K350,351M	Gentamicin

Table 2. 4: Plasmids used

2.1.5. Antibodies

	Antibody	Species	Company	WB dilution	IF dilution
Primary	C-Met	Mouse	Santa Cruz Biotechnology	1:1000	
	C-Myc	Mouse	Bio Legend	1:1000	1:100
	Cortactin	Mouse	Merck		1:50
	E-cadherin	Mouse	Abcam	1:1000	1:50
	EGFR	Rabbit	Cell Signalling Technology	1:1000	
	FLAG	Mouse	Merck	1:1000	
	GAPDH	Mouse	Santa Cruz Biotechnology	1:2000	
	GFP	Mouse	Roche	1:2000	
	HA	Rabbit	Santa Cruz Biotechnology	1:1000	
	HSP90	Mouse	Santa Cruz Biotechnology	1:2000	
	MT1-MMP	Mouse	Merck	1:1000	1:50
	N-cadherin	Mouse	BD Bioscience	1:1000	
	PAK1	Rabbit	Cell Signalling Technology	1:1000	

	PAK4	Rabbit	In-house	1:1000	
	PAK6	Rabbit	Genetex	1:1000	
	PDZ-RhoGEF	Mouse	Santa Cruz Biotechnology	1:500	
	RhoA	Rabbit	Cell Signalling Technology	1:1000	
	RhoC	Rabbit	Cell Signalling Technology	1:500	
	IgG	Rabbit	Santa Cruz Biotechnology		
	CD45 Alexa Fluor647	Mouse	Biolegend		1:200

Table 2. 5. Primary antibodies used.

	Antibody	Species	Company	WB dilution	IF dilution
Secondary	Anti-rabbit IgG-HRP	Goat	DAKO	1:2000	
	Anti-mouse IgG-HRP	Goat	DAKO	1:2000	
	Anti-mouse Alexa Fluor 488	Goat	Invitrogen		1:200
	Anti-mouse Alexa Fluor 647	Goat	Invitrogen		1:200

Table 2. 6. Secondary antibodies used.

		Brand	IF Dilution
Phalloidin	Alexa Fluor Rhodamin	Invitrogen	1:400
	Alexa Fluor 488	Invitrogen	1:400
	Alexa Fluor 647	Invitrogen	1:500

Table 2. 7: Type of fluorescently labelled phalloidin used.

2.2. Methods

2.2.1. Cell lines culture

The primary human prostate matched pairs NP/CT-1532, -1535, -1542 (obtained from John Master, University College London) cell lines and normal prostate cell line RWPE-1 (obtained from Charlotte Bevan, Hammersmith Hospital, London) were cultured in Keratinocyte serum-free medium (KSFM) supplemented with 10% heat-inactivated fetal bovine serum (HI-FBS), 1 mM penicillin-streptomycin, 25 µg/ml bovine pituitary extract (BPE), 5 ng/ml human EGF. Human pancreatic tumour cells AsPC-1 and prostate cancer cells PC3 (obtained

from Claire Wells, King's College London) were cultured in Roswell Park Memorial Institute-1640 (RPMI-1640) media supplemented with 10% v/v HI-FBS and 1 mM penicillin-streptomycin. Human embryonic kidney HEK-293 cells and mouse fibroblast NIH/3T3 cells (obtained from Claire Wells, King's College London) were cultured in Dulbecco's modified Eagle's media (DMEM) supplemented with 10% HI-FBS and 1 mM penicillin-streptomycin. All cell lines were passaged at 70-80% confluency by washing the flask with 1x phosphate buffered saline (PBS) followed by the addition of appropriate volume of trypsin/EDTA or non-enzymatic dissociation buffer. The flasks were incubated until detachment at 37°C and 5% CO2. Media was added to neutralise the trypsin and cells were centrifuged for 4 minutes at 600xg. The supernatant was discarded and pellet was resuspended in the appropriate volume of media.

2.2.2. Cell lysis

Cells were seeded at appropriate density in 6-well plates and let adhere for 24 hours. Wells were washed twice with PBS before adding 100 µl of 2x gel sample buffer to each well. Cells were immediately scraped and transferred into Eppendorf tubes. Eppendorf tubes were boiled for 4 minutes at 95°C and lysates were stored at -20°C until use.

2.2.3. Cell treatment with C3-transferase

Cells were seeded at appropriate density in 6-well plates and let adhere for 24 hours in 1 ml of media without FBS. On the following day 0.5 µg/ml of either C3 or DMSO was added to the each well, according to the manufacturer's protocol. Cells were incubated for 4 hours, then washed three times with PBS and detached via dissociation buffer. Dissociated cells were plated onto coverslips in 1 ml of complete media and incubated 24 hours before being fixed for immunostaining.

2.2.4. Cell treatment with Compound C31

Cells were seeded at appropriate density in a 6-well plate on glass coverslips and let adhere for 24 hours in 1 ml of media. On the following day either 1 µl of DMSO or 1 µl Compound

C31 was taken from the 1mM stock and added to the wells in order to achieve 1 µM/ml concentration. Cells were incubated 24 hours, then fixed and stained.

2.2.5. Cell treatment with lysophosphatidic acid (LPA)

LPA sodium salt was dissolved in the appropriate volume of PBS to achieve 10mM stock, which was stored at 4°C. The day prior the experiment cells were seeded at appropriate density in 6-well plates on glass coverslips and let adhere for 24 hours in 1 ml of media without FBS. 10 µl/ml of LPA were then added to each well and the plate was transferred back into the incubator. After 1 hour incubation, coverslips were washed three times with PBS and the fixed and stained.

2.2.6. Transient transfection with the Calcium Phosphate kit

HEK293 cells were transfected with the calcium phosphate transfection kit. Cells were plated at a density of $1x10^5$ in a 6-wells plate and incubated overnight at 37°C. On the following day, media was replaced 3-4 hours prior transfection. The reaction mix was prepared according to the following conditions:

	2 cm culture dish (2ml)	**10 cm culture dish (10ml)**
Tube A	6µl of 2.5M $CaCl_2$ 4µg DNA Make up to 60µl with sterile water	30µl of 2.5M $CaCl_2$ 20µg DNA Make up to 300µl with sterile water
Tube B	60 µl 2x Hepes buffered saline	300µl 2x Hepes buffered saline

Table 2. 8. Calcium phosphate kit transfection mix.

Mixture A was slowly added to mixture B in presence of aeration and incubated for 30 minutes at room temperature. The transfection mix was added to the plate dropwise and cells were incubated overnight at 37°C. On the following day, fresh media was replenished, and cells were incubated for additional 24 hours before lysis.

2.2.7. Transient transfection with the Lipofectamine 3000

For simple immunostaining experiments, cells were seeded at appropriate density on glass coverslips in a 6-wells plate in 1 ml of complete media. On the following day, media was changed with fresh media without antibiotics. The reaction mixture was prepared as follow: 3 µl of Lipofectamine 3000, 3 µl of P3000 and 250 µl optiMEM were incubated for 30 minutes at RT as per manufacturer's protocol, and then were added drop wise to the cells. After 24 hours of incubation, coverslips were washed three times in PBS, subsequently fixed and stained.

For the shPAK4 rescue experiments, the reaction performed was a reverse transfection: the reaction mixture was incubated in a 6-wells plate together with gelatin-coated coverslips for 30 minutes at RT. Meanwhile, cells were detached from flasks using the appropriate volume of cell dissociation buffer and centrifuged at 2.500xg for four minutes. The resulting pellet was resuspended in complete media and $1x10^5$ cells were seeded onto the coverslips in 2 ml of media without antibiotics. The following day media was replenished, and coverslips were incubated for additional 24 hours before being fixed and stained.

2.2.8. RNA interfering (RNAi)

Transient silencing of PAK4 and RhoA was achieved via siRNA using RNAiMAX transfection reagent. CT-1532 and CT-1535 cells were seeded to a density of $1x10^5$/ml in 6-well plates one day before transfection. On the day of transfection, media was aspirated and replaced with 2 ml/well of P/S free media. The transfection mixture containing 60nM of either control siRNA (Santa Cruz Biotechnology, sc-44230) or working siRNA (30nM/ml), 7.5 µl of RNAiMAX and 90 µl optiMEM was incubated for 30 minutes at RT before being added drop wise to the cells. Cells were then incubated for 72 hours at 37°C before cells were lysed or used for further experiments.

Stable knockdown expression of PAK4 was achieved via shRNA using Lipofectamine 3000 transfection reagent. CT-1532 cells were seeded in a T25 flask in media without antibiotics. On the day of transfection cells were at 80% confluency, media was aspirated and replaced with 5ml of KSFM without P/S. The transfection mixture containing 8 µg of either control shRNA or working shRNA, 12 µl of Lipofectamine 3000, 12 µl of Lipofectamine 3000, 12 µl

of P3000 and 500 µl optiMEM was incubated for 30 minutes at RT before being added drop wise to the cells. 48 hours post transfection cells were washed three times with PBS and detached with the appropriate volume of dissociation buffers. Dissociated cells were sent to the Flow Cytometry Facility at King's College for FACS sorting of GFP-expressing cells, in order to obtain a population of cells actively expressing the transfected GFP-tagged vector. Isolated cells were then transferred in a T25 with fresh media. Puromycin selection antibiotic, at a concentration of 0.5 µg/ml, was added to the media 3 days post-sorting and kept over the duration of two cell passaging with the intent of removing all non-transfected cells that had been accidentally eluted alongside the target cells.

Oligo Name	Oligo Sequence (5'-3')	Company
PAK4 siRNA #3	GGATAATGGTGATTGGAT	Ambion
PAK4 siRNA #5	GGGTGAAGCTGTCAGACTT	Dharmacon
RhoA siRNA #1	AUGGAAAGCAGGUAGAGUU	Dharmacon
RhoA siRNA #2	GAACUAUGUGGCAGAUAUC	Dharmacon
PAK4 shRNA #1 (pGIPz)	CTGGACAACTTCATCAAGA	Open Biosystems
Control shRNA (pGIPz)	CTCTCGCTTGGGCGAGAGTAAG	Open Biosystems

Table 2. 9. iRNA oligos used.

2.2.9. Immunostaining

Fixed cells on coverslips were permeabilised in 0,2% Triton X-100 for 5 minutes at RT and incubated 30 minutes with PBS 5% BSA to prevent non-specific binding. Coverslips were then incubated with primary antibodies against the target protein in PBS 5% BSA for 1 hour at RT and subsequently incubated with secondary antibody for 1 hour at RT. DAPI (1:5000) and TRITC-phalloidin or 488-phalloidin (1:400) were added to allow visualization of nucleus and F-actin, respectively. Finally, coverslips were washed twice with PBS and once with water and mounted onto glass slides with FluorSave solution. Cells were visualized at 40X objective magnification with an Olympus IX71 inverted microscope. Images of at least 90 cells/coverslip from three different experiments were taken.

2.2.10. Analysis of cell morphology

Analysis of cell morphology was conducted using ImageJ software. F-actin–stained fluorescence images were inverted into binary (black and white) images and the threshold adjusted to fully highlight one cell. Using the Wand Tool, the cell form was selected and the cell area and roundness was measured. 90 cells from at least three different experiments were analysed. The roundness is calculated as $4A/(\pi \text{ major axis}^2)$ where A = area. Values equal to 1 are closer to the representation of a perfect circle, whereas values tending to 0 are more elongated.

2.2.11. MTT proliferation assay

The cell viability was assessed by evaluating the [3-(4,5-dimethylthiazol-2-yl)-2,5-diphenyl-tetrazolium bromide] (MTT) reduction to formazan. Cells were seeded in triplicate in four 96-well plates at a density of $6x10^3$ per well. On the day of the experiment, the media was removed and cells were incubated 4 hours in presence of 50 µl of MTT solution (2mg/ml). The MTT was subsequently removed and formazan crystals dissolved by adding 50 µl of DMSO to each well, then absorbance was measured at 570 nm and subtracted for the blank, consisting in media only. The assay was repeated for 4 consecutive days to evaluate differences in the metabolic rate throughout the time. The growth rate for each cell line was calculated through a non-linear regression curve analysis.

2.2.12. Invadopodia assay

Coverslips were coated with a thin layer of 488- or Cy3- conjugated gelatin (EMD Millipore's QCM Gelatin) according to the manufacturer protocol. Briefly, each coverslip was first covered with poly-L-lysine diluted in deionized water for 20 minutes at room temperature (RT). Coverslips were then rinsed three times in PBS and incubated 15 minutes with diluted glutaraldehyde to stimulate the poly-L-lysine surface for further gelatin attachment. Each coverslips was again washed three times and finally coated with a 1:5 ratio of fluorescently-labeled:unlabeled gelatin. Meanwhile, cells were detached from the culture flask using dissociation buffer, and $2x10^4$ cells were seeded onto each coverslip in 1ml of complete medium. After 24 hours, cells were fixed in 4% paraformaldehyde (PFA) for 20 minutes at room

temperature and stored at 4°C until staining. The ratio between total degradation area underneath cells surface and total cell area (n=90 from at least three independent experiments) was calculated by using ImageJ. For invadopodia diameter analysis, a line was drawn in ImageJ from two opposite points at the periphery of the biggest active invadopodia per cell, and the distance between the two edges of the line was measured. Moreover, to minimise differences in staining intensity, cell images were taken from the central area of the coverslip using the same exposure time

2.2.13. Gel electrophoresis and immunoblotting

Cell lysates were loaded into 7.5%, 10% or 12% acrylamide gels and proteins were separated by electrophoresis at 125 V. The proteins were then transferred onto a nitrocellulose membrane for 1 hour at 100V in Transfer Buffer. Membranes were then blocked 30 minutes in TBST 5% milk or TBST 5% BSA, followed by overnight incubation at 4°C with the primary antibody in the same solution as used for blocking. On the following day, the membrane was washed three times in TBST and incubated 1 hour at RT with the respective HRP-conjugated secondary antibody diluted in the same dilution buffer utilised for the primary antibody. The membranes were then washed three times in TBST. Proteins were visualised using Pierce enhance chemiluminescence (ECL) Western blotting substrate.

2.2.14. Densitometry analysis

Protein expression was quantified by densitometric analysis using ImageJ software. A mean grey value was assigned to each protein band of interest based on its density. Resulting values were normalised to the background noise and to the loading control utilised for the experiment, detected on the same membrane as the target protein. Where appropriate, values were made relative to the control condition.

2.2.15. Construction of myc-PAK4 shRNA resistant constructs

In order to generate myc-tagged PAK4 shRNA resistant expression constructs, the Gateway LR Technology system was employed. The PAK4 shRNA resistant entry clones of interest

were already available in the Wells lab. Each clone was transferred into the pDEST-Myc vector containing the attR sites via LR reaction, according to the manufacturer's instructions. Briefly, each purified entry clone was incubated at 25°C for 1h with the destination vector in TE buffer in presence of 2 µl of LR Clonase enzyme II mixture. The reaction was then incubated with 1 µl of Proteinase K at 37°C for 10 min to terminate the reaction. The reaction mixtures were used to transform chemically competent *E. coli.* Each expression clone was selected according to its antibiotic resistance and the plasmid DNA was purified. The resulting products were subsequently sent for sanger sequencing to Source BioScience prior to any further use. This procedure led to the generation of Myc-PAK4 shRNA-rescue; Myc-PAK4 shRNA-rescue H19,22L; Myc-PAK4 shRNA-rescue K350,351M.

2.2.16. Site directed mutagenesis

To produce myc-tagged PAK4-ΔPxxP shRNA resistant plasmid, point mutations were introduced into the original myc-PAK4-ΔPxxP construct via site-directed mutagenesis using QuikChange II XL kit from Agilent. Primers for PAK4 shRNA resistance were designed according to the manufacturer's instructions and are listed in table 2.4. The PCR reaction was set up as follows:

Segment	Cycles	Temperature	Time
1	1	95°C	1 minute
2	18	95°C	50 seconds
		60°C	50 seconds
		68°C	1 minute/kb of plasmid length
3	1	68°C	7 minutes

Table 2. 10: Cycling Parameters for the QuikChange XL Method

The nonmutated, methylated parental DNA template was digested by adding 1 µl of the Dpn I restriction enzyme (10U/µl) to the reaction product, allowing for the select for mutation-containing synthesized DNA. The resulting DNA was subsequently sent for sanger sequencing to Source BioScience to assess the effectiveness of the mutagenesis and the presence of the desired mutations.

2.2.17. Transformation of E.Coli cells

Ultracompetent NEB-10 beta E.coli bacteria cells were gently thaw on ice and transformed with 2 µl of DNA. The reaction mix was incubated on ice for 30 minutes, followed by a heat-shock in a 42°C water bath for 30 seconds. The tube was immediately transferred back on ice for 2 minutes. A 500 µl volume of L-broth was then added to the transformed bacteria and incubated at 37°C for 1 hour with shaking. The transformed bacteria were then spread onto pre-warmed agar plates enriched with the appropriate antibiotic for plasmid selection and incubated at 37°C overnight.

2.2.18. DNA plasmid purification

One single colony per plate was picked and plasmid DNA was purified using the Purelink® HiPure Plasmid Filter Maxi-prep kit, according to the manufacturer's protocol. Resulting DNA was resuspended in TE buffer and the DNA concentration was measured in ng/µl using a nano-drop.

2.2.19. Endogenous immunoprecipitation

On the day before the experiment, 1.2 x 10^6cells were seeded on a 10-cm dish in 10 ml of complete media and let adhere overnight. On the following day, dishes were placed on ice, cells were washed three times with ice-cold PBS and 1 ml of cold lysis buffer was added. After 10 minutes of incubation, cells were scraped off the dish and centrifuged at 13.000 x g for 10 min at 4°C. The supernatant was transferred to fresh tubes while the cell pellet was discarded. Approximately 50 µl of supernatant was saved for immunoblot analysis of the inputs and stored at -20°C, while the remaining sample was incubated overnight on a rotating wheel at 4˚C with 3 µl of antibody. On the following day, 30 µl of Protein A beads was added to each tube, and samples were further incubated for 2 additional hours. Protein A beads were washed three times with ice-cold dilution buffer (2.500x g for 2 min at 4°C). After the final wash, the supernatant was removed and the beads were resuspended in 25 µl of 2x gel sample buffer, boiled for 3 mins 95˚C and stored at -20°C until use.

2.2.20. Immunoprecipitation with GFP-TRAP

Transfected HEK293 cells were scraped off the dish and washed three times at 500x g for 3 minutes at 4°C. Cell pellet was then resuspended in co-IP lysis buffer completed with the protease inhibitors and kept in ice for 30 minutes. Cell lysate was then centrifuged at 20.000x g for 10 min at 4°C, the supernatant was transferred to a pre-cooled tube and diluted with co-IP dilution buffer. Approximately 50 µl of supernatant was saved for immunoblot analysis of protein expression before proceeding with the GFP beads. To equilibrate GFP trap beads, they were washed three times with ice-cold dilution buffer (2.500x g for 2 min at +4°C). Diluted lysate was added to the trap beads and incubated on the rotor for 1h at 4°C. The beads were washed 3 times with the dilution buffer. Finally, pellet was resuspended with 100 µl of 2x gel sample buffer and the sample was boiled at 95°C for 10 min.

2.2.21. Immunoprecipitation of Rho-GTP

Rhotekin-RBD beads were reconstitute in 600ul of distilled water to have a 3.3 mg/ml solution, which was aliquoted and stored at -80°C until use. $1.5x10^6$ CT-1532 cells were seeded on a 10 cm dish the day before the experiment and let adhere overnight. On the day of the experiment, cells were washed twice in cold PBS and lysed in 1ml cold lysis buffer. Cell lysates were transferred into 1.5ml tubes and centrifuged at 13.000xg for 10 mins at 4°C. Approximately 50 µl of supernatant was saved for input immunoblot analysis, while 16 µl Rhotekin-RBD beads were added to the remaining lysates beads and incubated on the rotor for 1h at 4°C. Rhotekin-RBD beads were washed three times with ice-cold wash buffer (2.500x g for 2 min at 4°C). After the final wash, the supernatant was removed and the beads were resuspended in 25 µl of 2x gel sample buffer, boiled for 3 mins 95˚C and stored at -20°C until use.

2.2.22. Peptide array

For the preparation of the protein array, the oligopeptides were designed based on the amino acidic sequence corresponding to the C-terminal domain of PDZ-RhoGEF protein. Each peptide sequence includes at least one Serine on the central region and has a length

of at least 10 amino acids, according to the manufacturer's instructions. Oligopeptides were immobilized by JPT Peptides on a PDVF membrane supports by their C-terminus and have an acetylated N-terminus which confers a higher resistance to degradation and is more representative of the native protein. Prior the experiment start, the membrane was activated by 5 minutes wash in Ethanol, and then washed three times in TBST for 3 minutes at RT. The membrane was then incubated mix at 30°C for 30 minutes in 2.5 ml of the reaction mix composed by 750 µl of the kinase cocktail solution, 740 µl of 5x reaction buffer, 10 µg of purified PAK4 kinase and 25 µCi/mL of [γ32P]ATP. After four washes in the phospho-array stripping buffer A, the membrane was additionally washed three times in stripping buffer B, followed by three final wash in ethanol. The membrane was let to dry at room temperature for 15 minutes. The membrane was then exposed to a phosphor-screen and kept one week in the dark, inside a film cassette appropriately labelled for radioactive substances.

2.2.23. Circulating tumour cells (CTCs) isolation

Blood samples for circulating tumour cells (CTC) isolation were drawn from 17 patients diagnosed with prostate cancer with a Gleason score equal to 7 or more. For each patient, 7.5 ml of blood was collected in a 10 ml vacutainer EDTA tube, maintained at room temperature and processed within 4 hours of collection. The study was conducted upon the obtainment of written informed consent and under the King's Health Partners' Prostate Cancer Biobank (KHP PCaBB) blinding protocols for the protection of patients' identities and sensitive data. The isolation of CTCs was achieved through Parsortix Cell Separation System, which separates CTCs from hematopoietic cells normally present in blood based on their different size and deformability. Eluted CTCs were suspended in 200 µl of cold PBS. The isolated CTCs were immediately plated on Cy3-gelatin overnight in 1 ml of KSFM media. On the following day, coverslips were washed three times with PBS and incubated with anti-human CD45 Alexa Fluor647 Antibody in PBS 5% BSA for 30 minutes at RT before proceeding to normal staining with DAPI and Phalloidin-488.

2.2.24. Zebrafish embryo maintenance

Zebrafish experiments were conducted under the UK Home Office project licence PPL 70/7912 and had been approved by the King's College Ethical Review Committee prior the experiment start. Zebrafish embryos were collected from the King's College Fish Facility and separated into multiple 10cm dishes at the appropriate density. Zebrafish embryos were maintained into 1X E3 media with 0.0002% methylene blue at 28°C. At 1 day post-fertilization (dpf), the chorions (acellular envelopes that encloses the embryos) were opened and removed using a pair of handheld tweezers in order to prevent curling of the fish body during development. Dechorionated embryos were subsequently placed in new dishes at 28°C in fresh E3 medium and exposed to 3.5mM of Ethyl 3-aminobenzoate methanesulfonate (MS222) and 1% penicillin-streptomycin. At the completion of the experiment or at maximum 5 days post fertilisation all embryos were humanely killed via exposure to an anaesthetic overdose of 15mM MS222.

2.2.25. Zebrafish yolk-sac injection and imaging

Injection needles were prepared by pulling a borosilicate glass capillary at both ends away from a central heating element until the glass has stretched out to create two fine needs. Cells for injection were dissociated from a T75 flask using the appropriate volume of dissociation buffer. Detached cells were collected and. The resulting cell pellet was then resuspended in 1 ml of PBS-/- and incubated with 0.5 µl of Green CMFDA Dye CellTracker for 30 minutes at RT in order to fluorescently label the cells. Cells were subsequently centrifuged for four minutes at 2.500xg and resuspended at a final density of 2 x 10^4cells/µl in 50 µl of media. On the day of injection (1.5 dpf), zebrafish were placed in E3 media containing 3.5mM of MS222 and 1% penicillin-streptomycin. Approximately 500 GFP-tagged PCa cells or AsPC-1 cells were injected into the yolk sac using a Nikon SMZ-U zoom 1:10 Picospritzer II microinjection station. Injected embryos were placed in fresh E3 media and incubated 1 hour at 28°C in order to recover, then transferred to 33°C for the remains of the experiment. 12 hours after injection embryos were screened for the presence of a GFP-positive tumour mass in the yolk sac. All embryos exhibiting lack of a defined xenograft or diffuse dissemination in other regions of the body were excluded from further analysis and

humanely killed using 15mM MS222. The percentage of embryos with cancer cell tail invasion was calculated 3 days post-injection.

2.2.26. Statistical analysis

Statistical analysis was performed using Graphpad Prism software on datasets obtained by at least three independent experiments. When possible, One-way Anova with Multiple Comparison test was performed. Alternatively, Student t-test was used. A P value of ≤0.05 (95% confidence interval), ≤0.01 (99% confidence interval) and ≤0.001 (99.9% confidence interval) are indicated by *, ** and *** respectively. The error bars show Mean ± SEM.

Chapter 3

Characterisation of Prostate Cancer cell lines

Chapter 3. Characterisation of Prostate Cancer cell lines

3.1. Introduction

Previous work has identified a role for PAK4 in melanoma cell invasion via invadopodia activity and *in-vivo* dissemination (Nicholas et al. 2016). This project aims to understand if PAK4 plays a similar role in prostate cancer invasion. To test this, it was hoped to use two different techniques that reproduce the ability of cancer cells to degrade and navigate through the ECM to metastasize: *in-vitro* invadopodia assay and *in-vivo* Zebrafish yolk invasion assay (Teng et al. 2013; Yamaguchi 2012), in the prostate setting. However, there is little data in the literature establishing the use of invadopodia during prostate cancer progression. The "classical" PCa cell lines, although obtained directly by metastasis, are not reported to efficiently form invadopodia *in-vitro*. PC3 cells have been reported to form some actin-enriched invadopodia-like structures with a degraded area underneath the cells, however there remains limited evidence demonstrating the presence of specific invadopodia markers. Moreover, to reach a detectable degradative activity, PC3 cells required hyperactivated osteopontin/αvβ3 signalling (Desai, Ma, and Chellaiah 2008). This necessity is not reflective of the prostate cancer tumour environment, but rather the bone tissue they were isolated from. Thus, a PCa cell line that can be routinely used to study invadopodia has not been established. Moreover, conventional PCa cell lines (PC3, DU-145 and LNCaP) have been derived from advanced metastatic lesions and are poorly differentiated; therefore, they do not constitute an ideal model for studying the early phases of prostate adenocarcinoma progression and metastasis.

A promising tool comes from cell lines generated through viral-mediated immortalization of primary human tumour prostate epithelium. Three different benign (NP-) and malignant (CT-) matched pair sets of cells, designated as 1532, 1535 and 1542 were isolated from radical prostatectomy specimens obtained from patients with intermediate risk T2 stage prostate cancer and subjected to microscopic inspection (Bright et al. 1997). Tumour specimens containing a mixture of benign and malignant cells were subsequently divided into smaller tissue fragments until at least 95% of neoplastic cells were present in a single specimen. Cell lines derived from these specimens were cultured in 1-2% FBS and/or cholera toxin to selectively eliminate fibroblasts contamination, and transformed with a

recombinant retrovirus encoding E6 and E7 proteins of human papillomavirus 16 (HPV-16) to induce long-term proliferation (Bright et al. 1997). All cell lines obtained were tested for the presence of prostatic markers (PSA, PAP), and high and low molecular weight cytokeratin proteins, confirming their epithelial origin. Interestingly, the different benign or malignant nature of the resulting cells was not apparent on simple morphological ground, and therefore the characterization of the freshly established cultures was done based on the pattern of loss of heterozygosity on chromosome 8p, a feature associated with prostate cancer (Bright et al. 1997; Emmert-Buck et al. 1995). While normal epithelium did not exhibited evidence of LOH, tumour samples were positive for LOH on chromosome 8p (Bright et al. 1997).

Given their origin, these cell lines might constitute a valid experimental model to enhance our understanding of the early phase of PCa development and metastatic progression arising from primary localized adenocarcinoma. Promisingly, CT-1542 cell line was shown to express c-Met and have a migratory response to HGF (De Piano et al. 2020), a well-known inductor of cancer cell proliferation and invasion (P A Humphrey et al. 1995; Kasai et al. 1996). However, these cell lines have yet to be characterised, and little data are available regarding their potential as *in-vitro* model for invadopodia research.

The aim of the work presented in this chapter is to characterise the matched pairs proliferative and invasive capability, whilst also determining if any of the cancer cell lines efficiently make invadopodia. Based on the results gathered from this initial characterisation, two cell lines were chosen as the most suitable for use through the course of this project.

3.2. Results

3.2.1. No significant difference in growth curves were observed for any of the cell lines

Characterisation of the matched pairs was two-fold in aim. It was designed to test if the "normal" cell lines and "cancer" cell lines could be used for comparative studies whilst also screening the cancer cells invasive behaviour.

One of the essential hallmarks of cancer is the ability to sustain chronic proliferation, as defined by Hanahan and Weinberg (Hanahan and Weinberg 2011). Abnormal growth of cancer cells can be achieved in a number of ways, mainly by deregulation of production and release of proliferating factors that remain tightly controlled in normal cells (Hanahan and Weinberg 2011).

Therefore, phenotypical differences in cell proliferation in all the matched pairs were evaluated. Differences in growth ability between normal and malignant cells across all the cell lines were assessed by evaluating the ability of the cells to reduce MTT to formazan, a well-established measure of cell proliferation by measuring the number of viable cells in a population over time (Stockert et al. 2018). Initially, the same number of cells were seeded on day 0 and the optical density (OD) was measured up to day 4. From this measurement the following observations were made: in 1532 cell line there was no significant difference in the absorbance reading between cancer and normal cells. Both absorbance increased over the time, showing a comparable proliferating ability (Figure 3.1A). In the 1535 cell line there was a divergence in the absorbance reading between cancer and normal cells, with a significant decrease in proliferation of CT-1535 compared to the normal counterpart (Figure 3.1B). In the 1542 cell line there was a divergence in the absorbance reading between cancer and normal cells starting from day 1, suggesting that the observed difference could be due to a proliferation gap reached within the first 24 hours of incubation, when no measurement is performed (Figure 3.1C).

After observing such abnormalities, the growth rate for each cell line was calculated and compared to an established cell line representative of the normal prostate epithelium: RWPE-1.Thus, the experiment was repeated for the evaluation of RWPE-1 proliferation (Figure 3.2).

Each curve was modelled according to the typical growth curve for cultured cells that follows a sigmoid pattern of proliferation, characterised by an initial Lag Phase during which cells do not divide, followed by a Logarithmic Growth Phase, characterised by an active proliferation that lasts until the Stationary Phase is reached. At the starting time of observation, cells are most likely entering in the log phase, which terminates after few days, probably due to lack of nutrients and full confluency that inhibits further proliferation. For the calculation of growth rate, only the OD values between day 1 and day 3 in which cells were visibly in log phase were considered.

No significant differences in growth rates between normal and malignant cells were observed in any of the matched pairs assessed, as well as when compared to the non-malignant prostate cells RWPE-1 (Table 3.1).

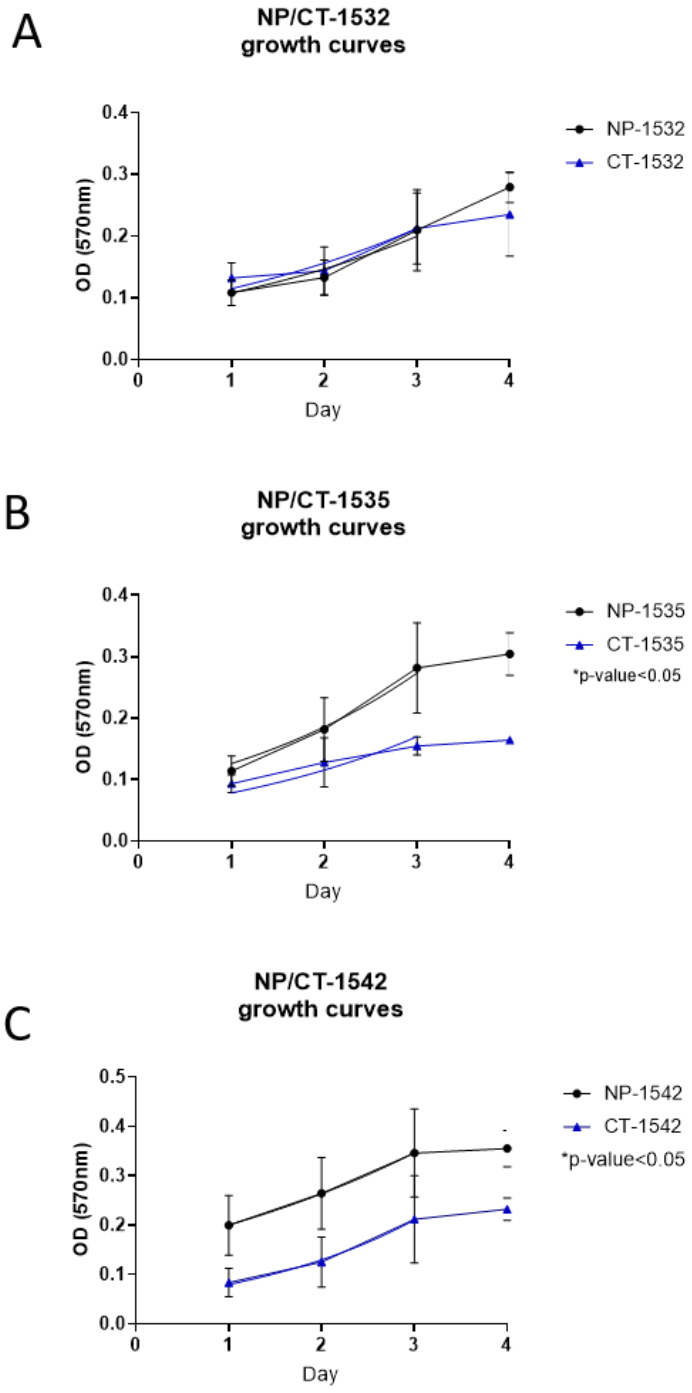

Figure 3. 1: Cell proliferation analysis reveals differences in cell growth curves between normal and cancer cells.

Cell growth curve analysis for each matched pair obtained through MTT assay repeated over four consecutive days. Data are presented as mean ± SEM, over 3 independent experiments. Statistical significance between normal and cancer cells for each matched pair was calculated with Two-way Anova followed by Sidak's multiple comparison test.

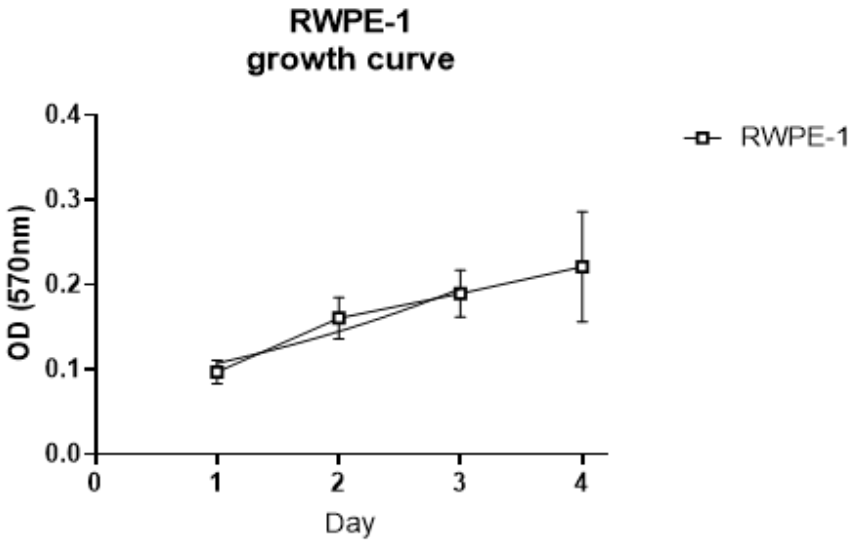

Figure 3. 2: Cell proliferation analysis of RWPE-1 cell line.
Cell growth curve for RWPE-1 cell line. The curve was obtained through MTT assay repeated over four consecutive days. Data are presented as mean ± SEM, over 3 independent experiments.

Cell line	Growth rate	Doubling time (days)	p-value NP vs CT	p-value vs RWPE-1
NP-1532	0.36	1.93	ns	ns
CT-1532	0.26	2.65	ns	ns
NP-1535	0.45	1.55	ns	ns
CT-1535	0.24	2.88	ns	ns
NP-1542	0.27	2.53	ns	ns
CT-1542	0.49	1.43	ns	ns
RWPE-1	0.23	3.00	na	na

Table 3. 1: No differences between the growth rates of matched pairs and RWPE-1
Analysis of the cell viability through MTT assay repeated over four consecutive days. Data for each dataset is derived from three independent experiments (n=3). Growth rate and doubling time for each cell line was calculated through the best-fit exponential growth curve between day 1 and 3. Statistical significance was calculated to the RWPE-1 cell line (One-way Anova) or between normal and cancer all cell lines (student t-test). No significant differences were observed between different growth rates.

3.2.2. 1532 and 1535 cancer cells exhibit decreased intracellular E-cadherin expression

Proliferation studies did not distinguish between cancer cell lines and the normal prostate epithelium cell line. Cancer progression can also be characterised by a progressive loss of epithelial phenotype and the acquisition of mesenchymal traits, termed epithelial to mesenchymal transition (EMT). During classical EMT cancer cells transition from E-cadherin to N-cadherin expression, often referred to as "cadherins switch" (Hazan et al. 2004). However, EMT and its reverse process MET have been reported more recently not to be binary events, with cells exhibiting a hybrid epithelial/mesenchymal phenotype (Jolly et al. 2015). There is considerable data suggesting the existence of EMT in PCa, indicating its possible role in PCa progression and metastasis (Nauseef and Henry 2011). For these reasons, the matched pairs were further characterised for the presence of EMT markers that are known to contribute to metastatic dissemination. To evaluate the epithelial characteristics of the matched pairs cell lines, intracellular expression of E-cadherin was assessed. Western blot analysis demonstrated that in 1532 and 1535 cell lines the level of E-cadherin was consistently lower in cancer cells compared to normal cells (Figure 3.3A-D), suggesting a shift towards a more mesenchymal phenotype. Thus, matched pairs cell lines were also tested for N-cadherin expression levels (Figure 3.4). Interestingly, reduction of E-cadherin expression was not followed by gain of N-cadherin in CT-1532 (Figure 3.4A-B) and CT-1535 (Figure 3.4C-D). Instead, N-cadherin expression was lower in CT-1535 when compared to NP-1535 (Figure 3.4C-D). No differences were observed in N-cadherin expression between CT-1542 and NP-1542 cell lines (Figure 3.4E-F).

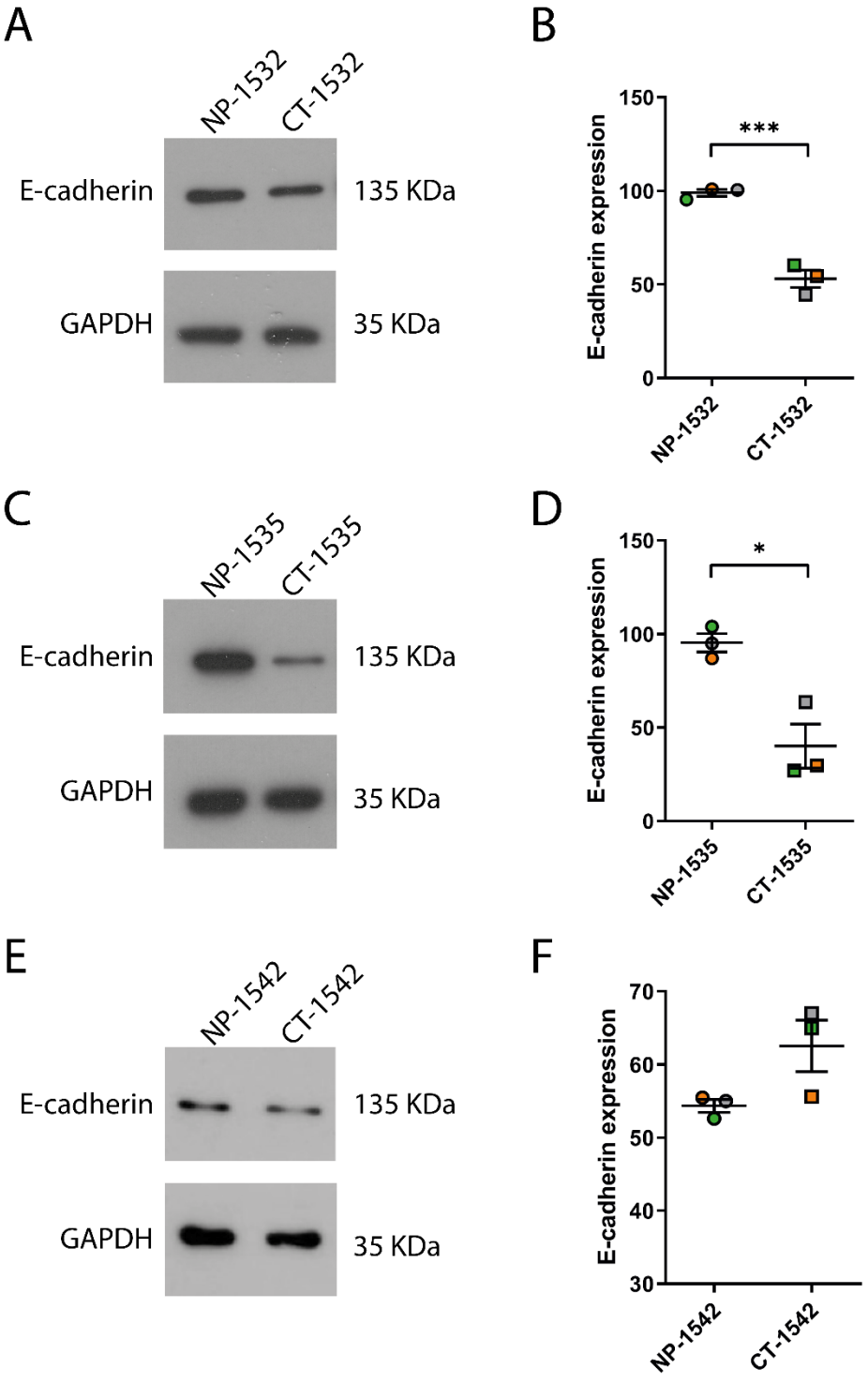

Figure 3. 3: CT-1532 and CT-1535 show downregulation of E-cadherin by Western blot.
Western blot analysis of the expression levels of E-cadherin in 1532 cells (A-B), 1535 cells (C-D) and 1542 cells (E-F). Intensity of bands related to the protein of interest were corrected for the loading control (GAPDH) and plotted as relative ratio mean ± SEM. Experiment was repeated with three independent cell lysates (n=3). Statistical significance was calculated with unpaired student's t-test, *p<0.05, ***p<0.001.

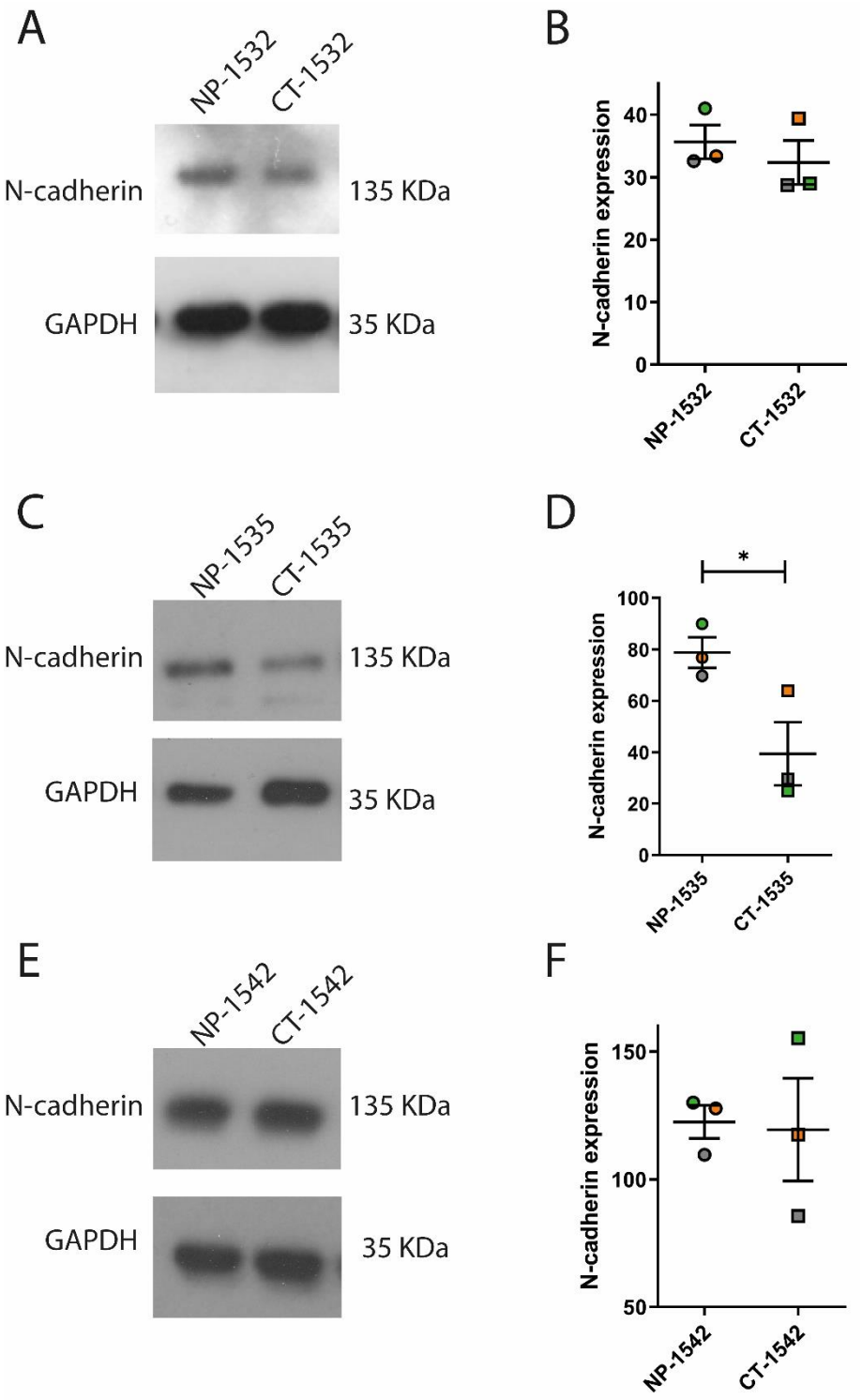

Figure 3. 4: N-cadherin expression is downregulated in CT-1535 cells.
Western blot analysis of the expression levels of N-cadherin in 1532 cells (A-B), 1535 cells (C-D) and 1542 cells (E-F). Intensity of bands related to the protein of interest were corrected for the loading control (GAPDH) and plotted as relative ratio mean ± SEM. Experiment was repeated with three independent cell lysates (n=3). Statistical significance was calculated with unpaired student's t-test, *p<0.05.

Western blot analysis suggested that CT-1532 and CT-1535 cells express reduced level of E-cadherin (Figure 3.3). However, reduced E-cadherin expression does not necessarily correlate with a decrease in cell junction formation. To assess whether the drop in total E-cadherin levels observed by Western blot (figure 3.3) correlates with decreased protein expression specifically at cellular junctions, cells were seeded on coverslips and stained for E-cadherin. All cell lines were able express E-cadherin, which was more concentrated at cell-cell junctions (Figure 3.5A).

To further explore possible phenotypic differences between cell lines, each cell line was scored for the level of colony formation. Cells forming adhesions with at least two other neighbouring cells were considered as colony-forming cells and further scored for their absence or presence of E-cadherin at the junction sites. On the contrary, single cells and those establishing contact with only one adjacent cell were excluded from the analysis. Unexpectedly, quantification of cells expressing E-cadherin at junctions did not show any significant difference between normal and malignant cells for all the matched pairs assessed, as a comparable number of cancer and normal cells exhibited E-cadherin at their adhesion sites (Figure 3.6A-C). This suggests a down-regulation of E-cadherin in CT-1532 and CT-1535 cells, which is restricted to the intracellular compartment.

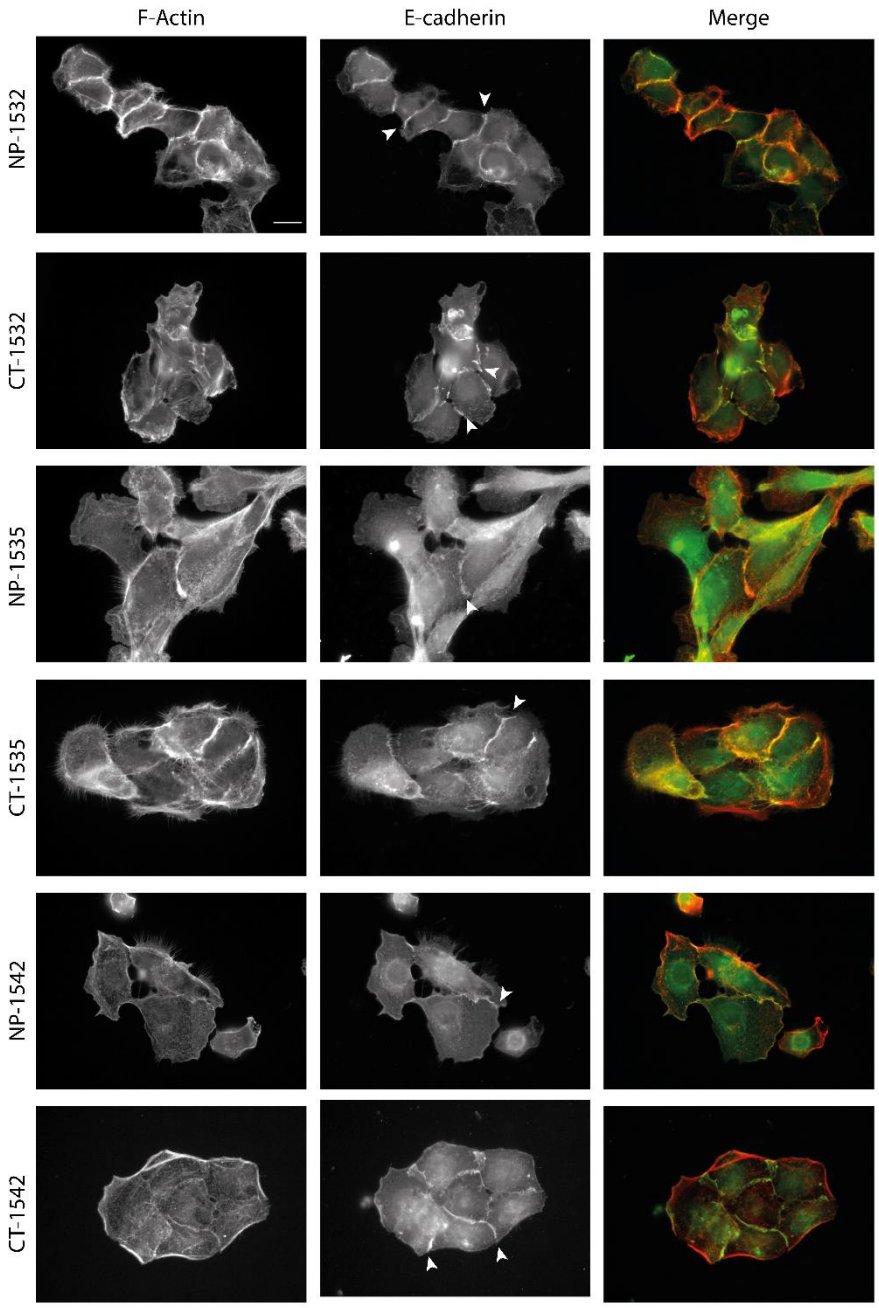

Figure 3. 5: Representative images of E-cadherin staining in matched pair cell lines.
Representative images of matched pair cell lines subjected to immunofluorescent staining to observe the expression of E-cadherin (green), in combination with actin (red). All cell lines tested appear to express E-cadherin at cell to cell junctions. Scale bar = 10µm

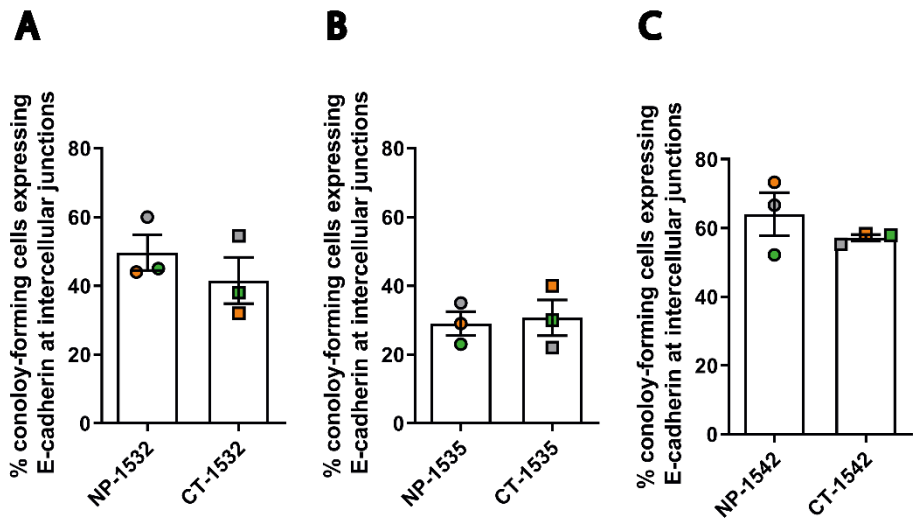

Figure 3. 6: Quantification of the percentage of cells expressing E-cadherin at junctional sites across matched pairs.

The percentage of cells was forming colonies and exhibiting E-cadherin signal at cell:cell junctions was quantified, revealing no differences between normal and cancer cells for 1532 (A), 1535 (B) and 1542 cell line (C). Graphs shown are representative of 3 independent experiments. Statistical significance was calculated with unpaired student's t-test.

3.2.3. EGFR and c-Met are expressed in all matched pairs cell lines.

CT-1542 cells have been previously reported to have upregulated surface EGFR expression (Hastie et al. 2005), while CT-1532 and CT-1535 have not been tested. EGFR has been reported to activate the Arp2/3 complex with Cdc42 being an upstream regulator of N-WASP, leading to invadopodia formation in rat mammary adenocarcinoma cells (Yamaguchi et al. 2005b). Indeed, EGFR is a potent mitogen in several types of solid tumours and has been found expressed in both primary and metastatic prostate cancer specimens (Schlomm et al. 2007; Guérin et al. 2010). Therefore, matched pairs cell lines were tested for EGFR expression. All cell lines expressed endogenous EGFR with no significant differences between normal and cancer cells in 1532 and 1535 cell lines (Figure 3.7A-D). CT-1542 exhibited an increase in EGFR levels, suggesting a hyper-activation of the EGFR pathway that may lead to increased stromal invasion ability (Figure 3.7E-F), consistent with previous studies.

Similarly to EGFR, Changes in c-Met activity and/or expression are implicated in invadopodia regulation and prostate cancer progression (Rajadurai et al. 2012; Knudsen et al. 2002). HGF was found able to stimulate PAK4 through PI3K, determining changes in actin organisation and cell migration ability (Wells, Abo, and Ridley 2002). Interestingly, CT-1542 cells were reported to express c-Met and have a migratory response to HGF (De Piano et al. 2020). Western blot analysis revealed that total c-Met expression levels were unchanged in 1532 and 1542 cell lines, whilst appeared to be decreased in the CT-1535 cell line compared to the normal counterpart (Figure 3.8).

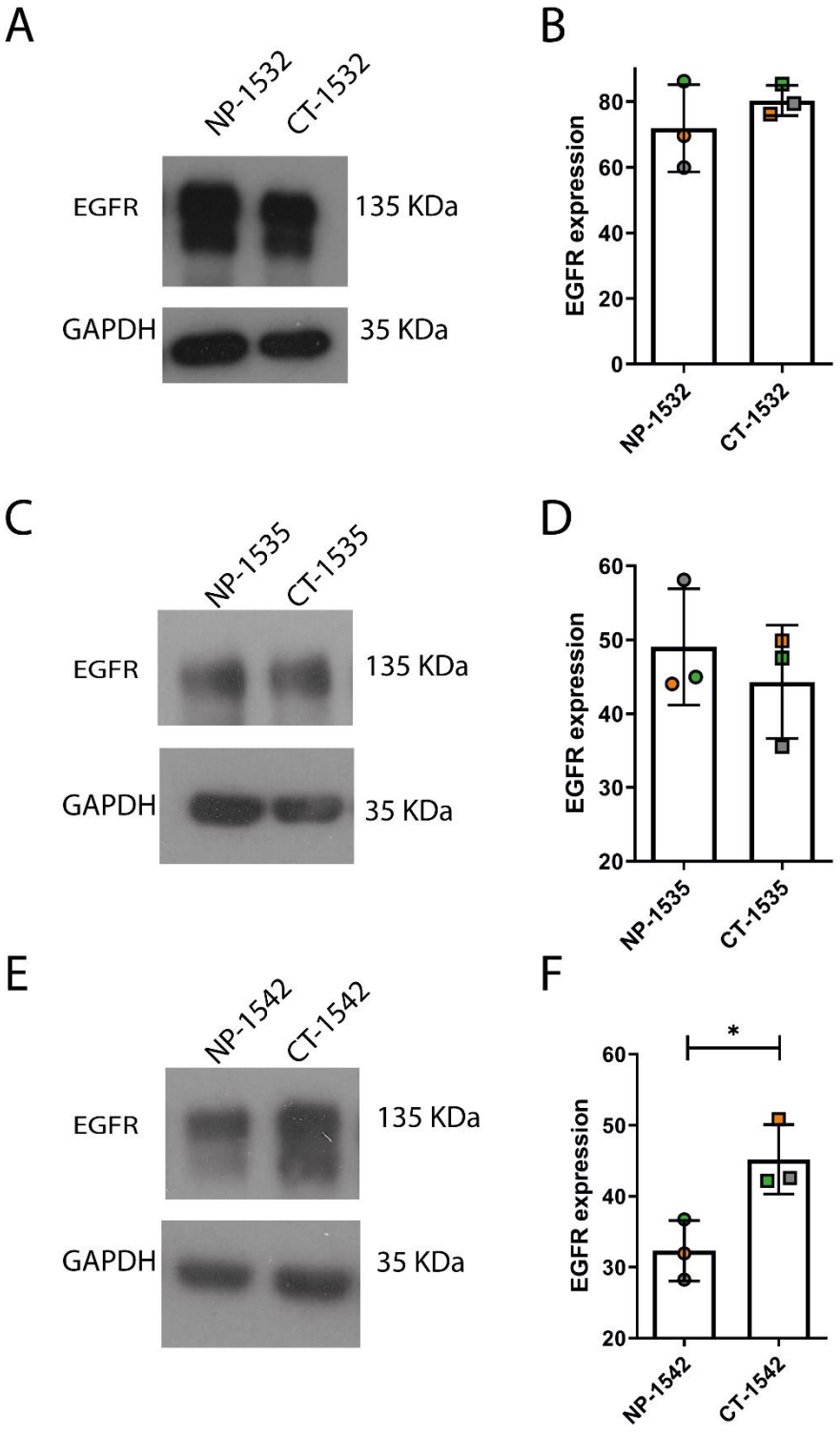

Figure 3. 7: EGF receptor expression is upregulated in CT-1542 cell line.
Western blot analysis of the expression levels of EGFR in 1532 cells (A-B), 1535 cells (C-D) and 1542 cells (E-F). Intensity of bands related to the protein of interest were corrected for the loading control (GAPDH) and plotted as relative ratio mean ± SEM. Experiment was repeated with three independent cell lysates (n=3). Statistical significance was calculated with unpaired student's t-test, *p<0.05.

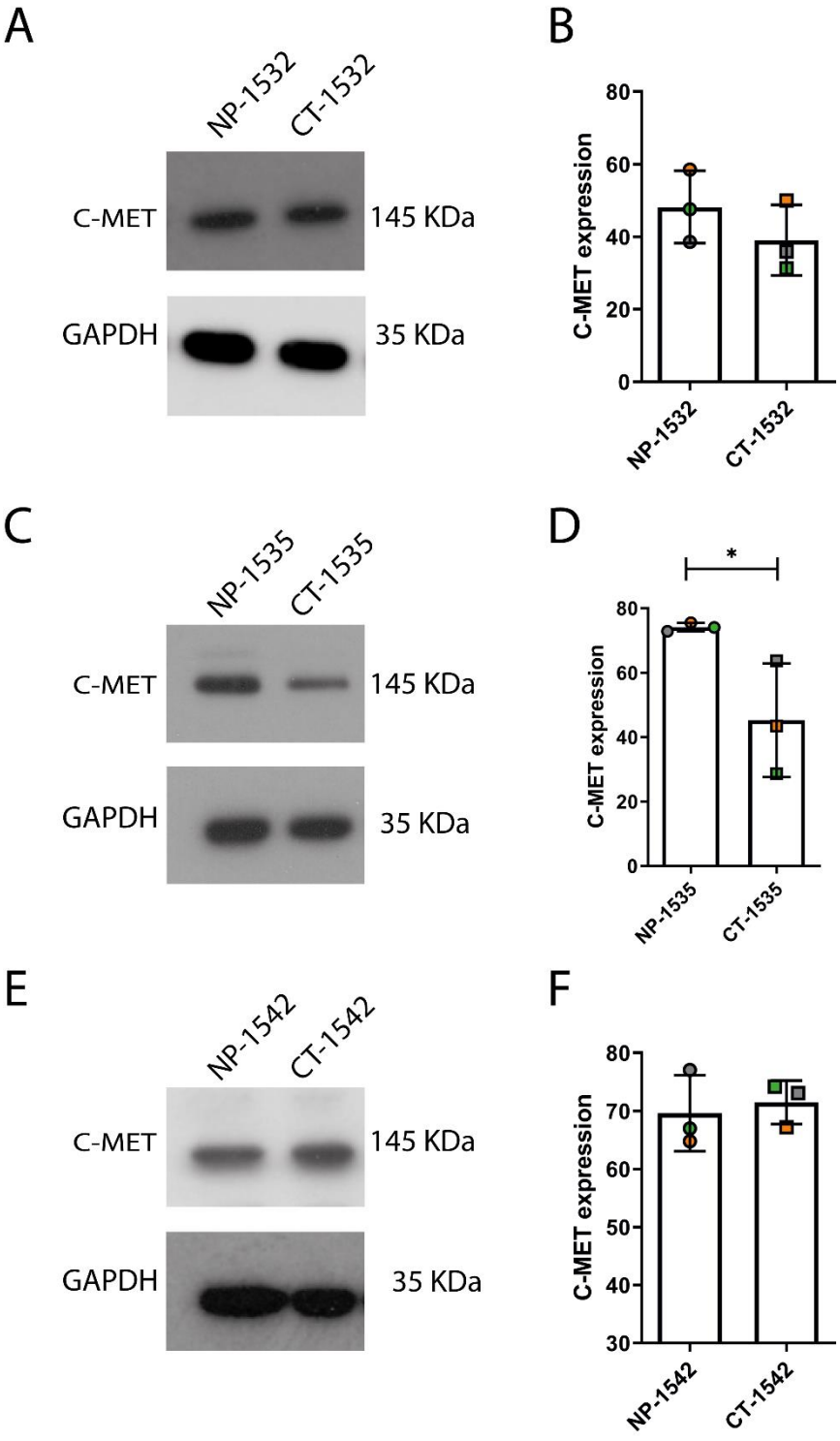

Figure 3. 8: C-Met expression is downregulated in CT-1553 cell line
Western blot analysis of the expression levels of EGFR in c-Met in 1532 cells (A-B), 1535 cells (C-D) and 1542 cells (E-F). Intensity of bands related to the protein of interest were corrected for the loading control (GAPDH) and plotted as relative ratio mean ± SEM. Experiment was repeated with three independent cell lysates (n=3). Statistical significance was calculated with unpaired student's t-test, *p<0.05.

3.2.4. All matched pairs cell lines are able to form invadopodia

Characterisation of the matched pairs had not consistently identified the cancer cell from the normal counterpart. One defining feature often seen in cancer cells is the ability to degrade matrix using invadopodia. The ability of cells to form invadopodia and degrade the matrix is thought to correlate with their invasive and metastatic capacity *in-vitro* and *in-vivo* (Yamaguchi 2012). Whilst many of the cell lines that are widely used in cancer research for a variety of tumour models display invadopodia-like structures and are able to degrade the extracellular matrix, this is not true in the case of prostate cancer. There is currently no strong evidence in the literature of prostate cancer cell lines that spontaneously and efficiently make invadopodia, hampering the study of early cancer progression and invasion in prostate cancer.

For the purpose of this study, it was therefore crucial to establish whether our cancer cell lines were able to form invadopodia. Cells were incubated for 24 hours on glass coverslips coated with a thin layer of Cy3-labelled gelatin, and subsequently stained with Phalloidin-488. Invadopodia were visualized as actin-enriched puncta colocalizing with dark spots on the matrix, corresponding to degraded area of the matrix devoid of fluorescent signal (Figure 3.9). To confirm that the observed structures were truly invadopodia, cells were additionally stained for cortactin, a well-known component and a specific marker of invadopodia that colocalizes with F-actin (E. S. Clark et al. 2007). PC3 cell lines, established from bone metastasis, was used as a negative control due to its lack of remarkable degradative activity without prior stimulation (Desai, Ma, and Chellaiah 2008).

All the cancer cell lines screened but PC3 showed a degree of invadopodia formation and activity (Figure 3.9A). The colocalization of F-actin enriched puncta with matrix degradation and cortactin signal was further confirmed by fluorescence intensity plot measured along an arbitrary line crossing throughout an invadopodia structure (Figure 3.9B).

On the contrary, in this study PC3 cells did not exhibit invadopodia making capacity: even though some sparse matrix degradation spots were observed. On closer inspection, they were rarely confined within the cell boundary, and no colocalization of cortactin with actin puncta was detected (Figure 3.9A).

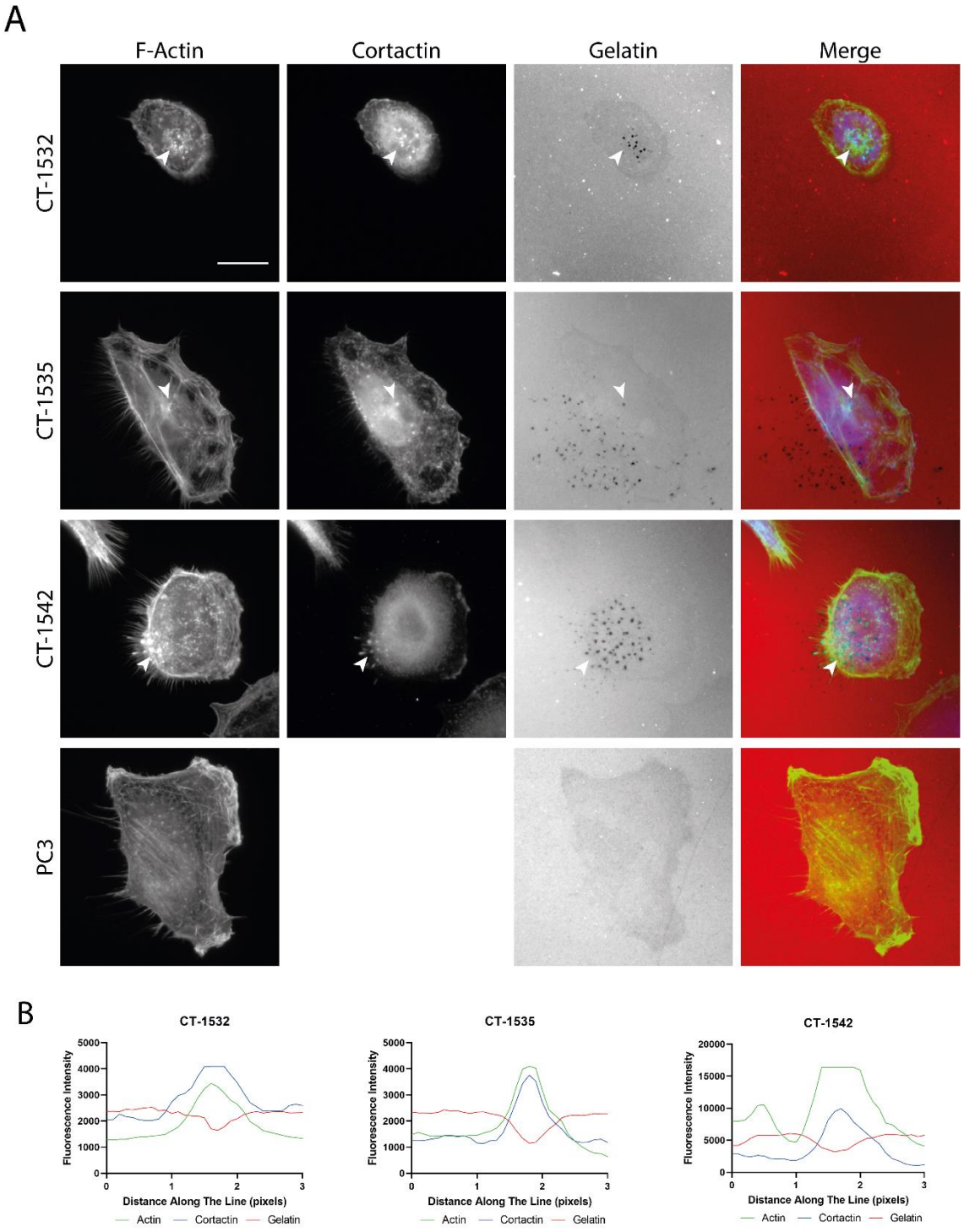

Figure 3. 9: Level of invadopodia activity in PCa cell lines.
Invadopodia assay images of malignant cell lines representative of three independent experiments. Cells were seeded on Cy3-conjugated gelatin for 24 hrs and stained for F-actin and Cortactin. All cell lines tested but PC3 are able to make invadopodia. Arrows indicate invadopodia and the area of degradation on the gelatin underneath cells' surface (A). Representative co-localization analysis for each cell line. Representative fluorescence intensity plot for each cell line showing co-localisation of cortactin, F-actin and gelatin degradation. Fluorescence intensity for F-Actin, Cortactin and Cy3-gelatin was measured an arbitrary line crossing through an invadopodia structure and the plot profile was calculated though ImageJ (B). Scale bars = 10µm

Surprisingly, some low level of invadopodia activity was also observed in the normal cell lines using the same criteria (Fig. 3.10A). Furthermore, RWPE-1 cells (routinely used as a normal control (Bello et al. 1997)) also exhibited some low level of invadopodia activity (Figure 3.10A-B). The structures detected in normal cells were also positive for cortactin staining, which coincided with the peak in F-actin signal and a reduction in gelatin intensity (Figure 3.10B).

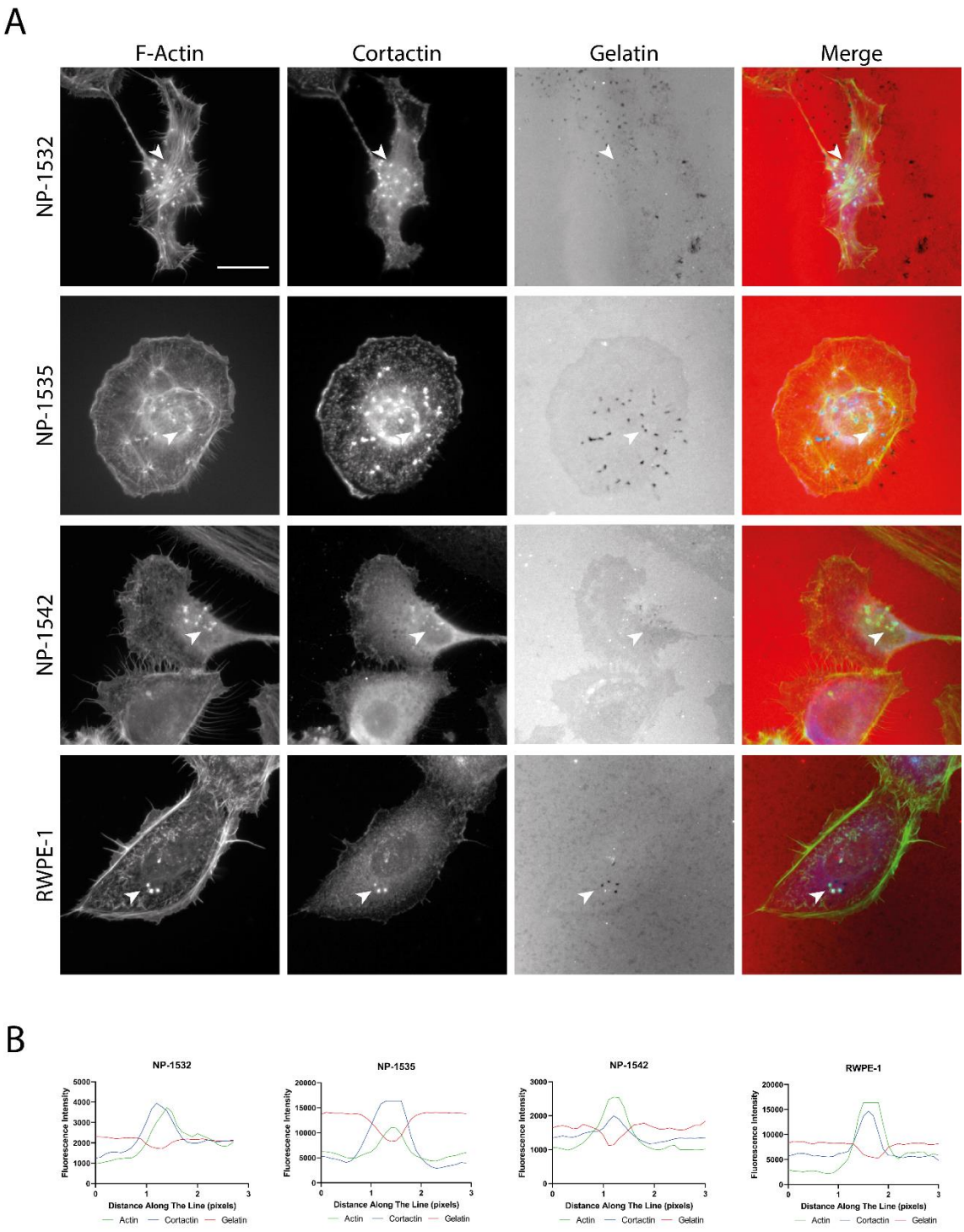

Figure 3. 10: Levels of invadopodia activity in normal prostate cell lines.
Invadopodia assay images of normal cell lines representative of three independent experiments. Cells were seeded on Cy3-conjugated gelatin for 24 hrs and stained for F-actin and Cortactin. All cell lines tested are able to make invadopodia. Arrows indicate invadopodia and the area of degradation on the gelatin underneath cells' surface (A). Representative co-localization analysis for each cell line. Representative fluorescence intensity plot for each cell line showing co-localisation of cortactin, F-actin and gelatin degradation. Fluorescence intensity for F-Actin, Cortactin and Cy3-gelatin was measured an arbitrary line crossing through an invadopodia structure and the plot profile was calculated though ImageJ (B). Scale bars = 10µm

3.2.5. Matched pair cell lines show different degradative ability

Although invadopodia activity was detected across all cell lines, there appeared to be a large differential in the extent of matrix degradation. Thus, a comparative analysis of the degradative ability was performed. There are multiple ways to quantify invadopodia, such as scoring the percentage of cells showing active invadopodia or quantify the average number of active invadopodia per cell (Eckert et al. 2011). However, it was noted that CT-1542 cells tended to form tight clusters and to adhere together when seeded on gelatin, making it difficult to distinguish the exact individual cell margins within a cluster. Moreover, CT-1542 cells exhibit a high level of heterogeneity in puncta size and a high concentration of puncta in actin dense regions that would affect the ability to determine the number of invadopodia precisely. Therefore, the method of analysis chosen suitable for all cell lines screened, was to quantify the percent degradation area underneath total cells area (Figure 3.11).

Results from the degradation analysis clearly identified significant differences in invadopodia activity across the cell lines. The 1532 and 1535 cancer cell lines were characterised by robust invadopodia activity (Figure 3.12). Only the 1535 matched pair exhibited a significant difference between normal and cancer cells, while no significant differences were observed between cancer and normal cells for both 1532 and 1542 paired cell lines (Figure 3.12). As expected, RWPE-1 cells exhibited an extremely low level of activity (Figure 3.12). All prostate cancer cell lines but CT-1542 were characterised by an increased invadopodia activity when compared to normal RWPE-1 cell line. NP-1535 cell line, was characterised by the lowest level of degradation of gelatin and comparable to RWPE-1, becoming the most promising candidate as possible representative of normal prostate epithelium cell line (Figure 3.12).

Previous data in the Wells lab suggested a positive correlation between cells spread area and invadopodia activity in breast cancer cells, with invadopodia competent cells exhibiting greater cell area than cells which did not form invadopodia (unpublished data). Thus, the average cell spread was examined to ascertain if differences in cell area correlates with differences in degradative ability in prostate cancer. In contrast to that observed with matrix degradation, no significant differences were observed in the average cell spread across all cell lines tested, with only CT-1542 cell line showing an increased cell area when

compared to RWPE-1 (Figure 3.13). This result suggests that invadopodia activity in prostate cancer is not influenced by cell spread area.

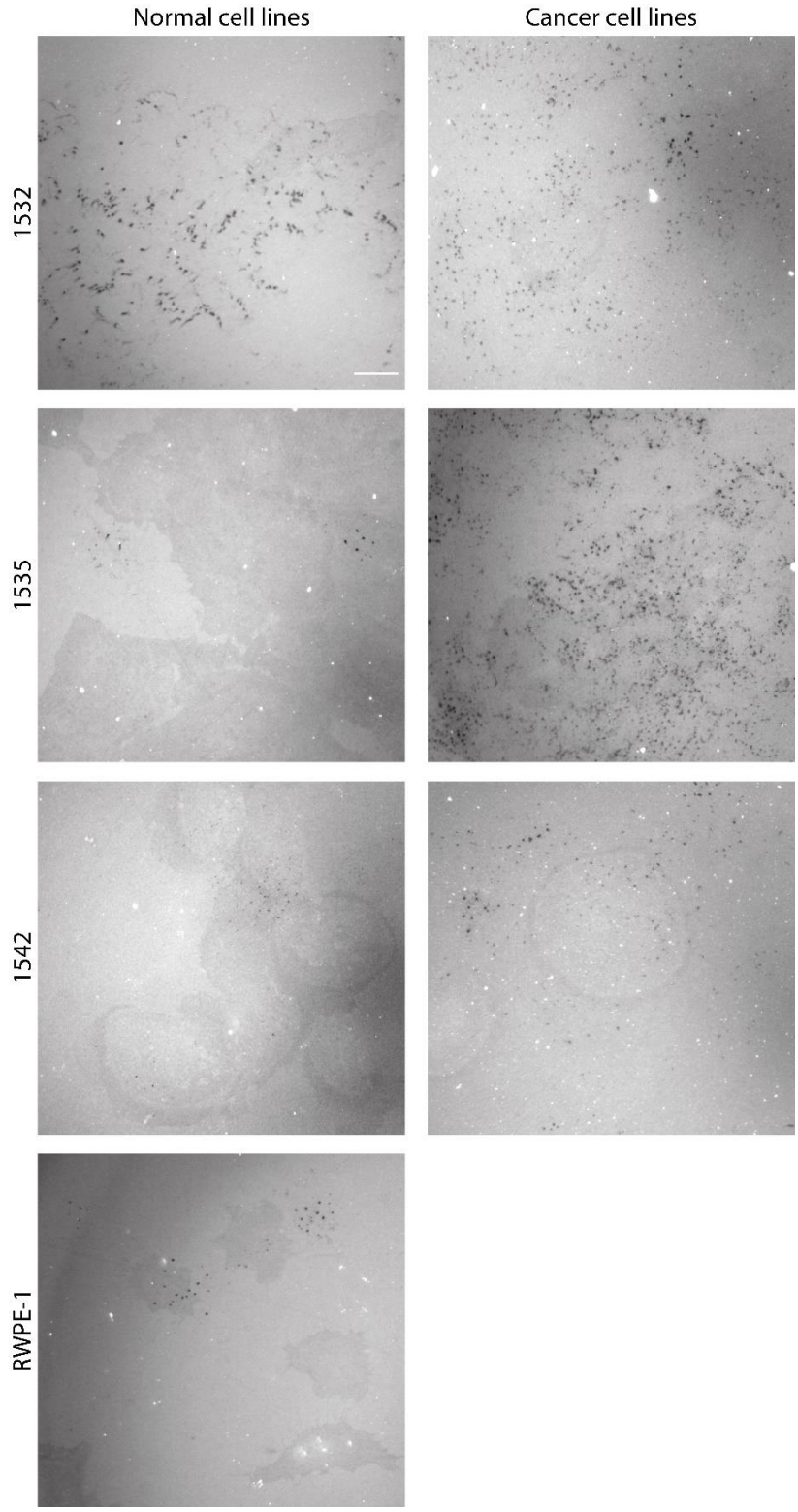

Figure 3. 11: Representative images of matrix degradation in invadopodia assay.
Images of gelatin degradation reflecting the different extent of degradative ability of each cell line tested. Cells were seeded on TRITC- conjugated gelatin for 24 hrs and stained for F-actin and DAPI. Images are representative of three independent experiments. Degradative ability was calculated as percentage of degraded area of the gelatin underneath total cells surface area corresponding to 90 cells over 3 independent experiments (n=3). Scale bars = 10µm

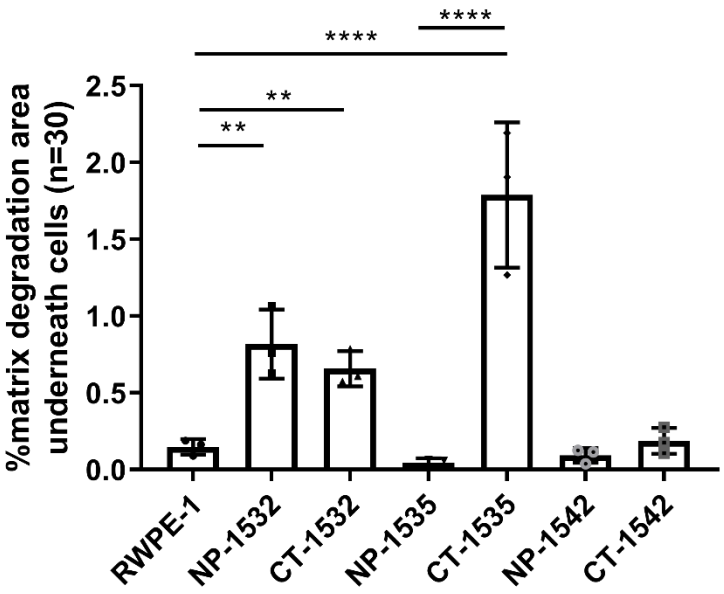

Figure 3. 12: Quantitative analysis of the matrix degradation in invadopodia assay.
Measurement of the degraded area underneath cells surface revealed CT-1535 cells to be the most invasive amongst all cell lines and exhibited a remarkable increase in cell degradative activity when compared to either its normal counterpart (NP-1535) or normal prostate RWPE-1 cells. Significance was calculated with One-way Anova followed by Tukey's test, **p<0.005, ****p<0.0001. Data are presented as mean values ± S.E.M.

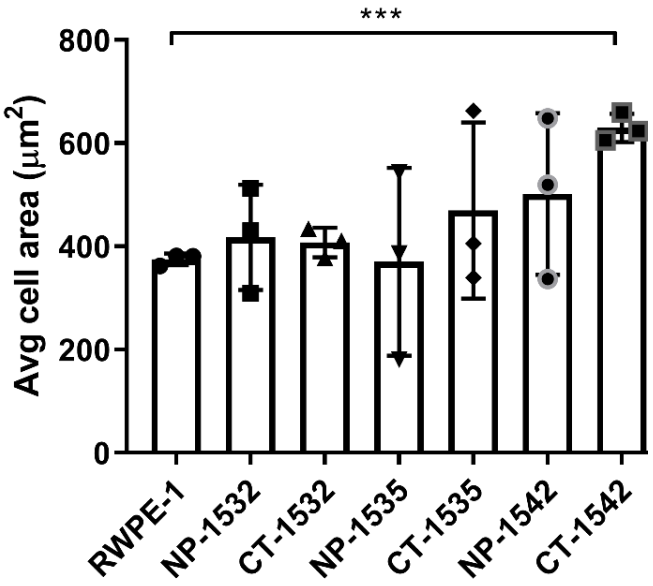

Figure 3. 13: Degradative ability was not influenced by cell area.
The cell area was calculated for 90 cells, over 3 independent experiments and found to not correlate with the different degradative ability. Significance was calculated with One-way Anova followed by Tukey's test, ***p<0.001. Data are presented as mean values ± S.E.M

3.2.6. All cancer cell lines are able to disseminate *in-vivo*

Having evaluated the ability of our prostate cancer cell lines to degrade *in-vitro*, their invasive potential *in-vivo* was assessed through using the Zebrafish yolk invasion assay, which constitutes a second robust and validated assay to evaluate the metastatic ability of cancer cells (Teng et al. 2013).

AsPC-1 cell line, derived from pancreatic adenocarcinoma, is well known for being characterized by an aggressive and metastatic phenotype (Deer et al. 2010), and it has been reported to function particularly well in this assay (Teng et al. 2013). Hence, AsPC-1 cells were used as positive control. On the contrary, the non-tumorigenic mouse fibroblast NIH/3T3 cell line served as negative control. Fluorescently labelled cells were injected into the distal half of Zebrafish yolk sac to avoid direct injection within the cardiovascular system. After 16-20 hours embryos were screened for the presence of a compact and spherical deposit of cells resembling a tumour mass in the yolk sac, while embryos exhibiting scattered and non-specific fluorescence were excluded from the experiment (Figure 3.14A).

All cancer cell lines tested were able to form a compact xenograft in the yolk-sac space of Zebrafish embryos (Figure 3.14B). NIH/3T3 cells failed to form a compact and well-defined mass (Figure 3.14B), confirming that the ability to form a xenograft is associated to the tumorgenicity of the cell lines tested as it is impaired in a non-invasive cell line. As a result of the lack of tumour formation into injected fish, NIH/3T3 cell line was excluded from further analysis. Three days post injection, embryos with fluorescent deposit in the tail (Figure 3.15A), were recorded as positive for metastasis. All cancer cell lines exhibited metastatic deposits in the distal tail compartment, demonstrating their ability to navigate the tissue architecture, disseminating distantly possibly utilising the vascular network (Figure 3.15B). All the PCa cell lines were able to disseminate to the tail; with CT-1542 cell line exhibiting significantly increased incidence of dissemination compared to the AsPC-1 cell line (Figure 3.16). Taken together, these findings indicate a potentially metastatic behaviour in all cell lines tested.

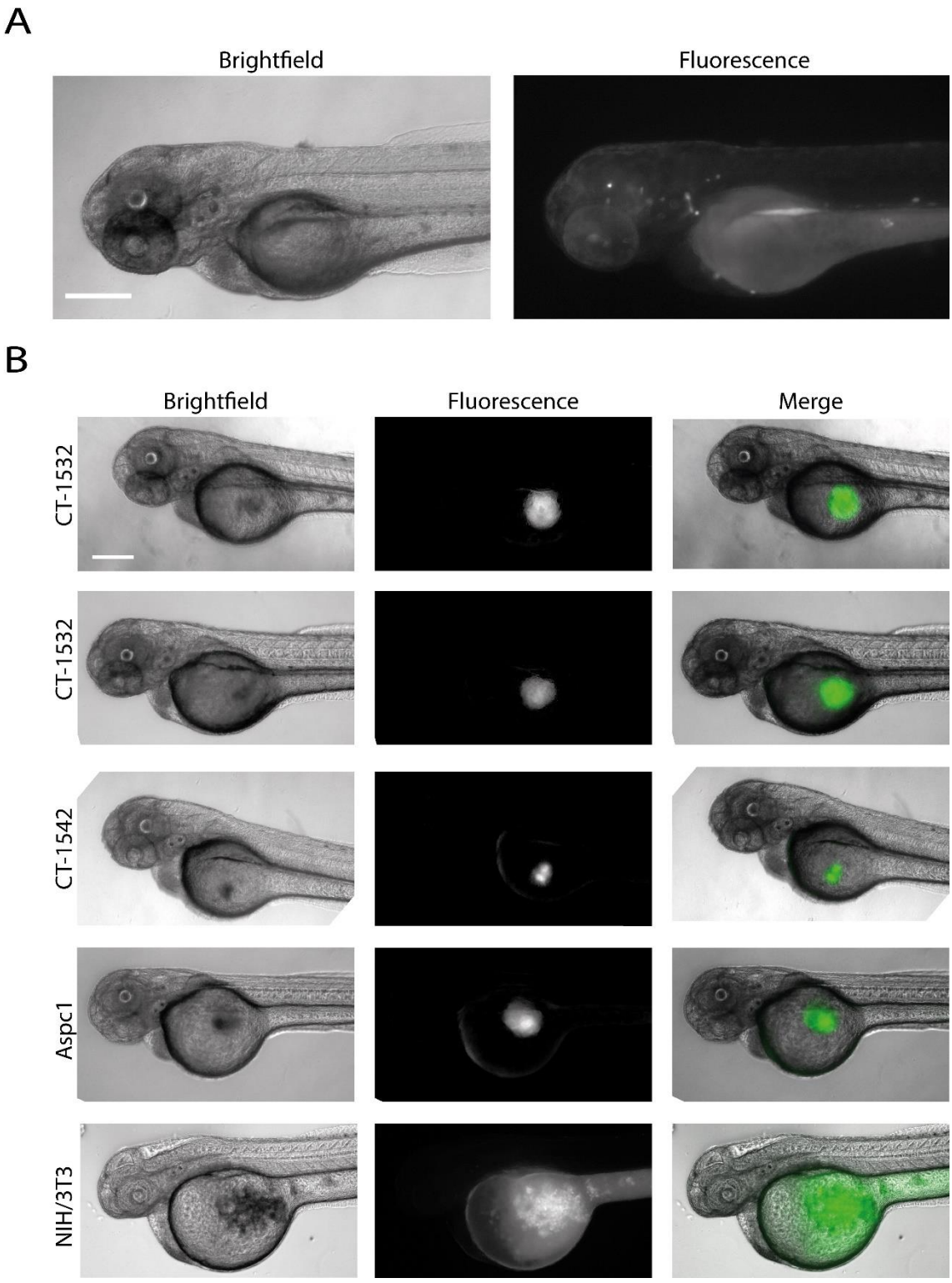

Figure 3. 14: Representative images of xenograft formation in zebrafish yolk-sac invasion assay. GFP-labelled cancer cell lines were injected into 1dpf zebrafish embryos and screened for the presence of tumour mass into the yolk-sac. Embryos with aspecific and disperse signals were excluded from the analysis (A). All cancer cell lines were able to form a compact xenograft, whilst non-metastatic NIH/3T3 fibroblast failed to produce a defined mass (B)

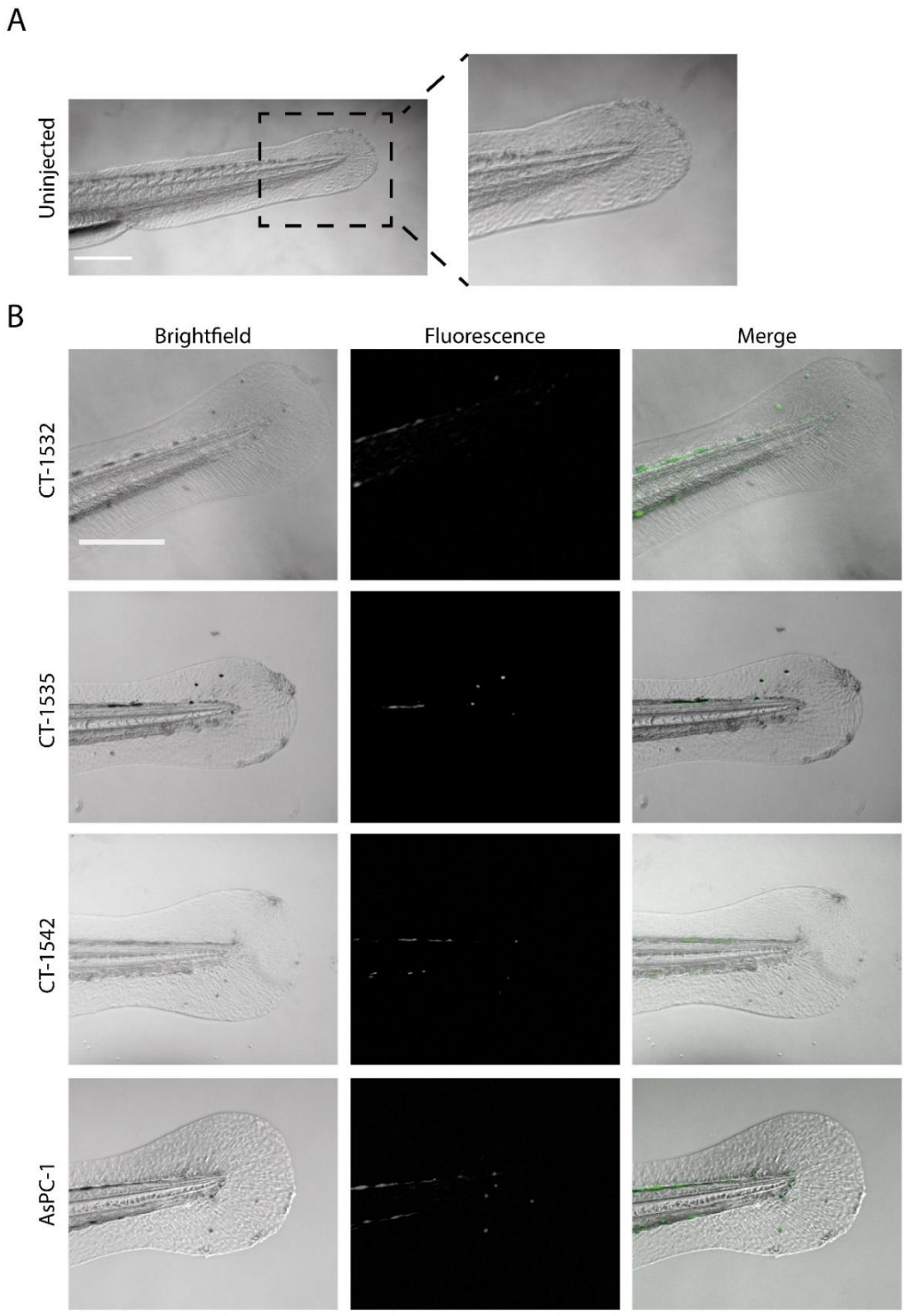

Figure 3. 15: Representative images of cancer cell lines tail disseminating in zebrafish invasion assay. Representative image of the optical transparent and pigment free tail compartment of an uninjected embryo at 4dpf (A). Representative phase contrast and fluorescent images of a zebrafish tail (lateral view) and 4 days post injection with cancer cells (B). All prostate cancer cell lines were able to disseminate and lodge in the tail of zebrafish embryos. Scale bar = 200µm.

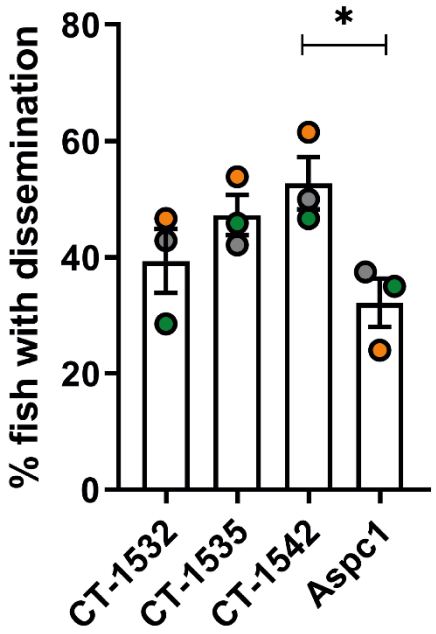

Figure 3. 16: Incidence of tail dissemination in zebrafish invasion assay.
Graphical representation of the percentage of embryos with dissemination. Data are representative of three independent experiment, with at least 15 embryos screened for metastasis at the end of each experiment. Significance was calculated with One-way Anova followed by Tukey's test, *p<0.05. Data are presented as mean values ± S.E.M.

3.2.7. Circulating prostate tumour cells exhibit degradative ability in 2D

Following the discovery that prostate cancer cell lines isolated from primary tumour were able to form invadopodia *in-vitro* and disseminate *in-vivo*, it was decided to extend our study and investigate whether these findings would apply in a more clinical setting.

Circulating tumour cells (CTCs) represent an intermediate stage of the metastatic process and are considered to be a prognostic marker and an indicator of the clinical outcome in many types of metastatic cancers, including prostate (de Bono et al. 2008). Despite extensive studies conducted on CTCs in prostate cancer (Pantel, Hille, and Scher 2019), little progresses have been made regarding their molecular characterisation, and there is no evidence linking prostate CTCs to invadopodia formation.

CTCs were isolated from the peripheral blood of 17 prostate cancer patients (Table 3.1) using the Parsortix Cell Separation System, which separates CTCs from haematopoietic cells normally present in blood based on their different size and deformability. Isolated CTCs were immediately plated onto Cy3-conjugated gelatin overnight and subsequently fixed and stained for F-Actin and CD45. CD45 is a lineage-restricted glycoprotein that is expressed on all haematopoietic cells except for erythrocytes and exclude white blood cells from the analysis. One coverslip per each patient was obtained through this methodology.

Coverslips were manually screened for CD45-negative cells. Out of a total of 17 samples, it was possible to successfully identify F-Actin-positive and CD45-negative CTCs seeded on fluorescent coverslips in 16 samples (figure 3.17A), indicating the experimental protocol was able to deliver viable cells. The CTCs count greatly varied across the patients, with patient 15 exhibiting the largest number of CT cells detected (Figure 3.17B).

All CD45-negative cells were screened for the presence of actin puncta and gelatin degradation that might be a sign of invadopodia activity (Figure 3.18A). Over 60% of the cells exhibited actin puncta, whilst approximately 20% of cells showed puncta being colocalised with matrix degradation spots (figure 3.18B). Almost 40% of CTCs displayed actin puncta and general matrix degradation underneath cell's surface, possibly indicating invadopodia formation and degradative activity that was not in place at the time of fixation due to the rapid turnover of the process. Furthermore, cortactin-positive puncta co-localised with actin dots were observed in cells isolated from patient 17, which was additionally stained for Cortactin (figure 3.18B). Overall, almost 80% of patient samples displayed clear evidence of matrix degradation, while 40% were positive for invadopodia activity (figure 3.18C), thus

strongly suggesting human prostate cancer cells could utilise invadopodia *in-vivo* during dissemination.

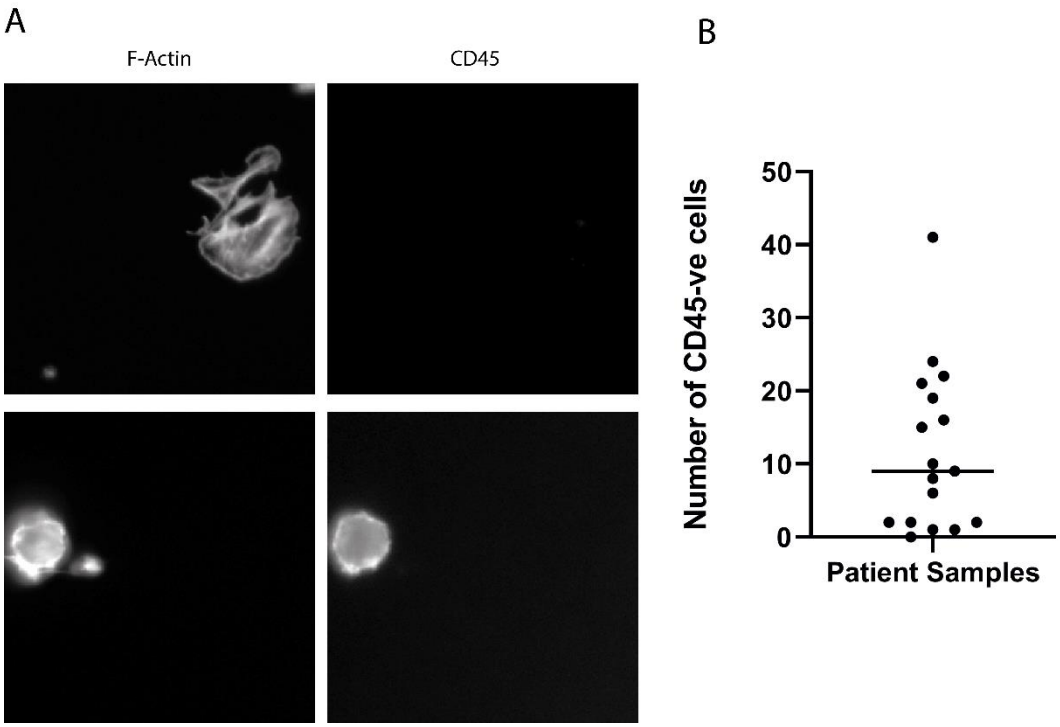

Figure 3. 17: Representative image of prostate CTC cells isolated from blood samples.
Representative images of circulating tumour cells (top) and hematopoietic cells (bottom) isolated via Parsortix System from PCa blood samples and stained for the surface antigen CD45 (A). Graphical representation of the number of CD45-negative cells that were isolated from each sample and manually screened following invadopodia assay (B).

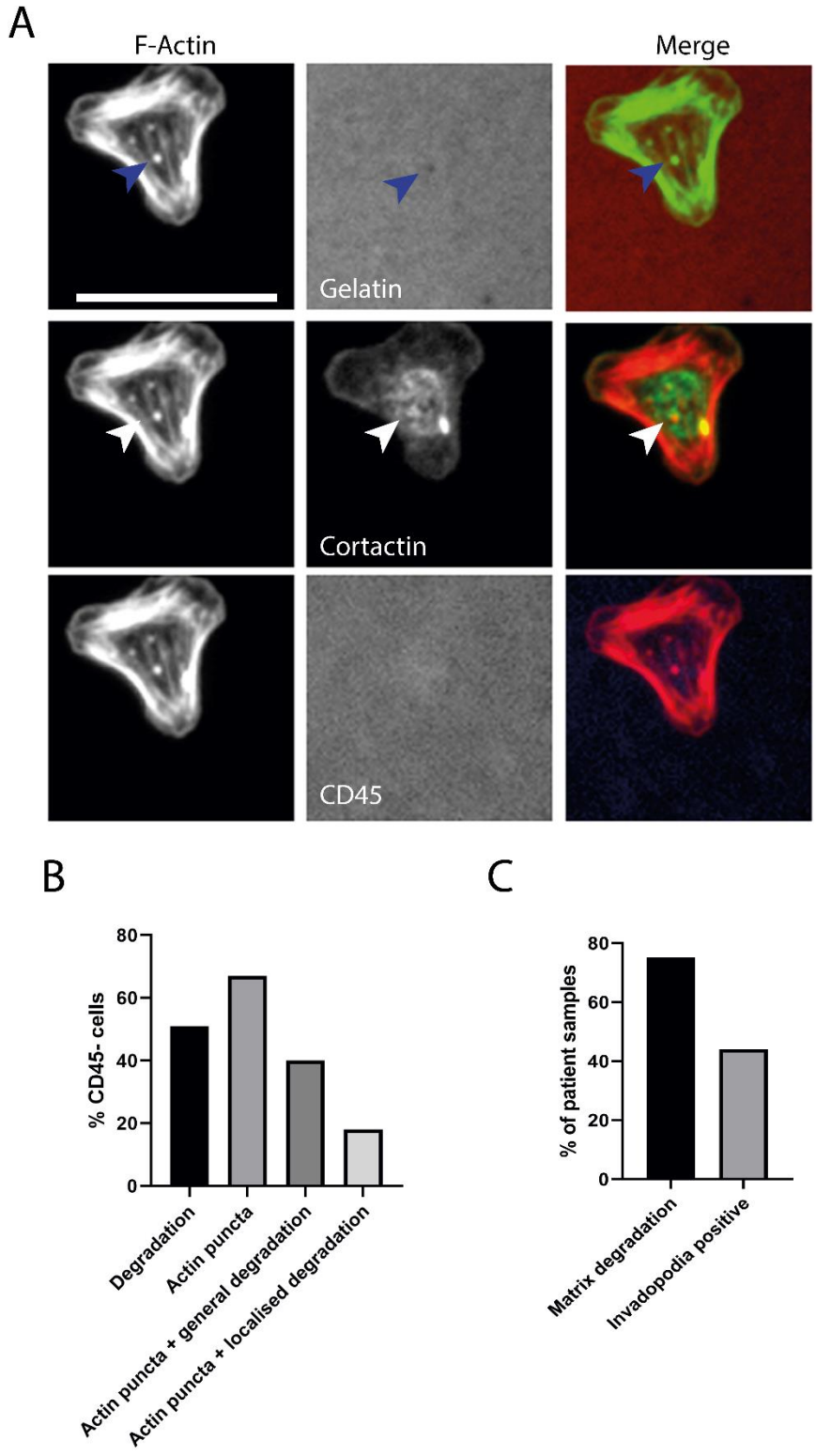

Figure 3. 18: Prostate CTCs ehibit localised gelating degradative ability and puncta formation.
Representative images of prostate CTCs subjected to invadopodia assay and stained for F-Actin and Cortactin after 24 hours incubation. Cells exhibited localised matrix degradation overlapping with actin puncta (blue arrow) and cortactin puncta co-localising with actin-rich dots (white arrow) (A). Graphical representations of the percentage of CD45-negative cells displaying puncta and/or degradation (B), and the overall percentage of the blood samples that showed evidences of matrix degradation and invadopodia when subjected to invadopodia assay (C). Scale bar=10µm.

CTCs					
Patient	**Gleason score**	**# of isolated CTC**	**Actin puncta**	**Degradation under cell**	**Puncta aligned with degradation**
1	4+5	1	0	0	0
2	Unknown (Diagnosed Radiologically)	2	0	0	0
3	4+5	24	15	12	**12**
4	5+5	0	0	0	0
5	4+5	2	1	1	**1**
6	5+4	9	6	6	0
7	4+4	10	1	8	0
8	Unknown (Diagnosed Radiologically)	1	0	0	0
9	4+5	8	5	6	0
10	4+5	22	19	9	**9**
11	3+4	16	12	9	**1**
12	4+5	21	15	8	0
13	3+4	6	3	1	0
14	4+3	15	9	3	**1**
15	3+4 at diagnosis, later upgraded to 4+5	41	31	21	**4**
16	4+5	2	1	0	0
17	4+5	19	15	12	**7**

Table 3. 2: Gleason score and invadopodia assay data of human blood samples analysed.

3.3. Discussion

Given the high heterogeneity of PCa, obtaining a single model that successfully recapitulates all the malignant features of the disease is hard to achieve. Primary tumour derived cell lines constitute a valid experimental model to enhance our understanding of PCa development and metastatic progression, but there are no *in-vivo* models that spontaneously develop this type of cancer, and establishing long-term cell cultures is difficult. In this study, we aim to characterise the human prostate autologous matched pairs 1532, 1535 and 1542 cell lines, focusing on their invasiveness potentiality, to understand whether they can be used as valid models for normal versus cancer comparative studies and the cancer cells can be utilised for invadopodia studies.

Results described here suggest that the matched pairs cell lines are characterised by an elevated degree of heterogeneity in terms of behaviour and protein expression.

While no significant differences were observed for 1532 and 1542 cell lines, CT-1535 cell line proliferation appeared to be strongly delayed compared to its normal counterpart, producing a lower and flattener growth curve (Figure 3.1). The impaired growth of CT-1535 cells might be explained by a higher sensitivity of this cell line to the lack of nutrient and growth factors present in the plate after 5 days of continuous growth without media change. However, the same slower growth was observed upon standard culturing and cell line maintenance, when media is routinely replaced.

These data align with emerging observations that challenge the long-held belief of cancer cells dividing more rapidly than normal cells. Despite the hyper-proliferative nature of many tumours, in fact, the link between malignancy and growth speed is still unclear and filled with contradictory data. The escape of cancer from molecular pathways regulating cell proliferation does not necessarily translate in an increase in the cell division rate, as most people believe, but rather in a continuous growth, regardless of the speed. Several studies, in fact, reported that tumour cells from primary cultures grow slower than their normal counterparts *in-vitro* (Buehring and Williams 1976), highlighting the relevance of tumour individuality. Studies on prostate cancer growth kinetics found that prostate cancer cells within the prostate are characterised by a remarkably slow growth that is comparable to that of early stage high-grade PIN, considered as precursor of prostatic cancer (Berges et al.

1995; Schmid, McNeal, and Stamey 1993). Reduced expression of a multi-gene proliferation signature was found associated with enhanced invasiveness in two independent cohorts of colon cancer patients (Anjomshoaa et al. 2008). Several works have already highlighted the existence of this unusual relationship in different types of cancer, both *in-vivo* and *in-vitro*, hinting that invasion occurs mainly during the G1/G0 phase of the cell cycle, when cells are in a quiescent state (Kohrman and Matus 2017). Thus, a switch from a proliferative to a more invasive status may be occurring in the CT-1535 cell line.

Analysis of E-cadherin and N-cadherin expression suggests an incomplete cadherin switch occurring in 1532 and 1535 cancer cells, in which downregulation of E-cadherin is not followed by upregulation of N-cadherin (Figure 3.3, 3.4). Cadherin switching is one aspect of EMT, and the shift from different isoforms of the cadherin transmembrane proteins is thought to be associated to an increased aggressive behaviour (Hazan et al. 2004). However, E-cadherin is found to be differently regulated in many types of cancer independently of EMT, and it has been reported to often be replaced by alternative cadherins different from N-cadherins. For example, high grade prostate cancer cells showed a *de novo* expression of cadherin-11 in comparison with normal prostate (Tomita et al. 2000; Bussemakers et al. 2000). Analysis of these alternative cadherins status might provide important information about the correlation between mesenchymal phenotype expression and invadopodia in prostate cancer. Moreover, E-cadherin expression was found necessary for metastasis in multiple models of breast cancer (Padmanaban et al. 2019). In case of prostate cancer, loss of E-cadherin led to the development of neoplastic lesions in prostatic epithelium but prevented cells to progress to tumour cells by inducing apoptosis and disruption of epithelial structures (Olson et al. 2019). Recent studies established a crucial significance for the co-expression of epithelial and mesenchymal markers and partial EMT in cancer metastasis (Jolly et al. 2015). Thus, the maintenance of epithelial integrity to some extent by E-cadherin expression seems to be required during the course of tumour progression.

The E-cadherin loss observed by Western blot was not confirmed by E-cadherin immunostaining (Figure 3.5, 3.6). This may suggest a downregulation of E-cadherin restricted to the intracellular compartment only, where it regulates other important cell signallings, rather than at cell:cell junctions (Klezovitch and Vasioukhin 2015).

All the primary adenocarcinoma cell lines were found to have invadopodia present, and efficiently degraded the matrix (Figure 3.9). Invadopodia formation is not a common feature of the other classic metastatic prostate cancer cell lines. In fact, although more than 200 prostate cancer cell lines and sublines are currently used in prostate cancer research, there are consistent difficulties in achieving a reliable prostate cancer cell line that efficiently invades *in-vitro* spontaneously, without prior stimulation. Nicholas et al. noticed that the melanoma cell lines best at generating degradative invasions were derived from a primary tumour (Nicholas et al. 2016).

This may suggest that primary tumour cells are expressing proteins associated with invasion while cells derived from a metastatic site have already down regulated such proteins. This might explain why previous attempts to identify invadopodia in prostate cancer cells have been limited in success as they relied on cell lines taken from distant sites.

Indeed, it has been reported that tumour cells deposited at metastatic sites seem to undergo phenotypic changes, possibly due to deprivation of appropriate adhesive and signalling interactions, or in response to inhibitory signals originating in the parenchyma of target organs (Giancotti 2013). It has been proposed a reversible EMT metastasis model in which primary epithelial tumour cells activate EMT to invade and disseminate throughout the body, while, upon arriving at distant sites, disseminated tumour cells undergo a reversion process, or MET, to form epithelial metastases (Thiery 2002). Thus, perhaps invadopodia formation and activity in prostate cancer is subjected to a similar temporal/spatial regulation.

The different extent of degradative ability exhibited by the cancer cell lines tested might be reflective of the complexity and individuality of the primary tumour specimens they were isolated from. This could be translated in differential genetic regulation of those factors involved in invadopodia activity. CT-1542 showed increased invasion compared to NP-1542 (Figure 3.11, 3.12), possibly due to upregulation of the surface receptor EGFR (Figure 3.7). On the contrary, the 1532 and 1535 cell lines are most likely relying on other molecular pathways unrelated to EGFR and c-Met expression, such as TGF-β (Mandal, Johnson, and Wheelock 2008). It is interesting to note that amongst all cancer cell lines, CT-1535 cell line exhibited the highest degradative ability and at the same time the slowest proliferation rate (Figure 3.1), suggesting an inverse relation between invasiveness potential and proliferative activity (Kohrman and Matus 2017).

Unexpectedly, normal cells, including the RWPE-1, were found positive for the presence of invadopodia and matrix degradation, although conventional descriptions of invadopodia restrict this activity to cancerous cells (Paz, Pathak, and Yang 2014). However, the extent of matrix degradation for normal cells was considerably lower compared to cancer cells. This acquisition of malignant features in normal cells may be the result of a genomic instability occurring during the immortalization process (Kang and Park 2001). HPV-16 E6 and E7 proteins expression results in inactivation of the p53 protein, destabilization of the Rb protein and activation of telomerase (Huibregtse and Beaudenon 1996; Jones, Thompson, and Munger 1997; Steenbergen et al. 1996). Even though these viral oncogenes are not sufficient for a conversion to a fully tumorigenic cell population, their combined effect might lead to acquisition of some malignant features (Kang and Park 2001). Taken together, these results suggest the matched pairs cannot be confidently used for comparative studies, thus, the "normal" cell lines were not employed any further in this project.

The invasiveness ability of 1532, 1535 and 1542 cancer cell lines was further tested *in-vivo* through Zebrafish yolk-sack invasion assay. All cancer cell lines performed optimally, causing visible metastatic dissemination in tail in 40% of the fish or above (Figure 3.15, 3.16). Interestingly, CT-1542 cell lines, which was the least invasive as measured by the invadopodia assay, performed equally well to the other cell lines tested in Zebrafish. It is possible that migration of CT-1542 tumour cells in Zebrafish is governed by an invadopodia-independent pathway, which does not rely on matrix degradation, such as the rounded-amoeboid migration (Pandya, Orgaz, and Sanz-Moreno 2017). This hypothesis is additionally supported by the observation that CT-1542 cells lack of actin puncta formation *in-vitro*, suggesting that these cells are deficient of invadopodia precursor and therefore it's unlikely they utilise invadopodia degradation for dissemination *in-vivo*. Moreover, the prostate cancer PC-3 cells, which do not efficiently form invadopodia, have been reported to lodge and proliferate in the caudal hematopoietic tissue of the zebrafish tail following injection into the duct of Cuvier (Hill et al. 2018). Therefore, it is highly possible that non invadopodia-competent cells employ a different molecular process to invade *in-vivo*.

Alternatively, Wisdom et al. suggested an additional function of invadopodia that consists in the deformation of the surrounding ECM through the application of a protrusive and contractile force that is independent of degradation (Wisdom et al. 2018). This could explain

why the high invasive ability of CT-1542 cell line *in-vivo* did not correlate with the observed degradative ability *in-vitro*.

This study highlighted the importance of invadopodia in prostate cancer not only *in-vitro*, but also in a more clinical setting, by employing circulating tumour cells isolated from whole blood samples of prostate cancer patients. Circulating tumour cells represents the closest portrait of a cancer cell that has escaped the primary tumour and is circulating in the bloodstream, potentially offering a true "snapshot" of the molecular changes that lead to the acquisition of an invasive phenotype. As the majority of cancer related deaths is due to metastasis formation, their value as preclinical models for the characterisation of molecular profiles associated with cancer invasion and for future therapeutic developments is undisputed. Given both the induction of gelatin degradation and the formation of punctate structures with co-localized invadopodia markers (Figure 3.18), it was demonstrated here for the first time a novel link between invadopodia and prostate cancer CTCs. The discovery that CTCs present invadopodia-like structures and are capable of degrading the matrix provides interesting new insights into the relevance of invadopodia in prostate cancer progression, paving the way for a new series of studies that could corroborate and extend these findings. We speculate that prostate cancer cells detaching from the primary tumour could potentially employ invadopodia in order to degrade the extracellular matrix and reach the vasculature, where they intravasate.

The number of CTCs detected differ greatly across the analysed samples (Figure 3.17). This difference is most likely attributed to the variability in nature and disease progression of the patients that were selected for this study. Moreover, CTCs are indeed extremely rare population in the blood of cancer patients, especially considering that that 7.5 ml of blood per patient was provided. CTCs counts was significantly elevated in one sample, which exceed by far the overall mean CTC enumeration. It must be kept in mind, however, that the experimental model presented here exhibits some limitations, as circulating fibroblasts might be involuntarily eluted together with CTCs. Therefore, it would be ideal to perform additional immunostaining for prostate specific antigen, such as PSA expressed by prostate cells, or fibroblasts markers, such as vimentin or fibroblast surface protein (SFP), which is expressed by fibroblasts and macrophages but not epithelial cells (Singer et al. 1989).

Even though no correlation was observed between the number of CTCs isolated and number of invadopodia-forming cells from a single blood sample, it would be interesting to see

whether the samples presenting the highest rate of invadopodia are associated with a poor clinical outcome. Monitoring the disease progression in a wider and more heterogeneous population which includes multiple stages of prostate cancer the long-term could lead to inferring a prognostic value to invadopodia detection, although at present it's still too early to test the patients' survival outcome. In summary, these data undoubtedly demonstrate that invadopodia are physiologically relevant in prostate cancer.

The findings presented in this chapter reveal that the prostate cancer cell lines here characterised could offer a robust and valid model for studying the early phase of prostate cancer progression and invasion, on the basis of: being isolated from primary adenocarcinoma they are more representative of the tumour of origin; the invasive potential was confirmed both *in-vitro* and *in-vivo*; all cancer cell lines efficiently form invadopodia *in-vitro*.

The highest invasive ability was detected in CT-1532 and CT-1535 cells, combined with an efficient dissemination *in-vivo* this led to the selection of these cell lines for the rest of the project.

3.4. Future work

The work presented here established prostate cancer cell lines that can be utilised for invasion studies. It would be interesting to assess cells migration ability in 2D and 3D, such as wound healing assay and Boyden chamber assay. Additional *in-vivo* experiments to assess the tumorigenicity of these cell lines could be performed in animal models different from Zebrafish, i.e. mice. It could be noteworthy to assess the genetic traits that are conventionally associated with prostate cancer. Gene profiling and expression analysis using microarrays could be employed in these cell lines to uncover the early molecular changes that occur in localised adenocarcinoma and potentially trigger a transformation towards a more invasive phenotype.

Expression of alternative cadherin isoforms, such as R-cadherin, cadherin 11, T-cadherin and P-cadherin could be tested (Hazan et al. 2000; De Wever et al. 2004; Nieman et al. 1999).

The so-called "normal" cells were found able to form invadopodia, and there is uncertainty whether the expression of this malignant feature is due to viral-mediated immortalization. To better elucidate this finding, invadopodia assay could be performed with cells isolated from healthy prostate tissue retaining its original genetic and molecular characteristics. Fresh prostate tissue samples could be obtained from patents undergoing cystoprostatectomy surgery, which involves surgical removal of the urinary bladder and as part of the procedure the prostate gland is also removed.

Finally, an extraordinary amount of work could be done employing human prostate CTCs to better understand invadopodia dynamics in prostate cancer. First, in a long term prospective study, invadopodia ability could be correlated to high Gleason score, tumour stage, relapse and treatment response. Cells isolated form samples with the highest number of invadopodia-making CTCs could be also characterised by their androgen receptor status, PSA expression, and expression of invadopodia markers such as Tsk5 and Cortactin. Indeed, one main challenge would be the achievement of a greater number of CTCs necessary to conduct such of experiments and obtain statistically relevant data, which would require continuous blood drawn from each patient. Obtaining a molecular signature associated with invadopodia in a clinical setting that complements cell culture experiments would provide validated targets for novel

therapeutics directed against cell invasion, and invadopodia could be employed as biomarkers for better tailored anticancer treatments for individual patients.

Chapter 4

The role of PAK4 in invadopodia

Chapter 4. The role of PAK4 in invadopodia.

4.1. Introduction

Cancer invasion is a dynamic and adaptive process involving rearrangements of the cell actin cytoskeleton, which can be coordinated by the Rho GTPase signalling pathway (Spuul et al. 2014). Rho GTPases cycle between a GTP-bound active form and a GDP-bound inactive form, controlling signal transduction pathways by binding multiple effector molecules (Vega and Ridley 2008). Amongst the Rho GTPases effectors are members of the p21-activated kinases (PAKs) family. There are six members of the family that can be classified into two subgroups based on their chemical and structural properties: group I (PAK1-PAK3) and group II PAKs (PAK4-PAK6) (Arias-Romero and Chernoff 2008). Several studies have linked aberrant PAK expression or activation to tumour growth, survival and motility (King, Nicholas, and Wells 2014).

PAK4, the most studied member of Group II PAKs, contains a catalytic Serine/Threonine kinase domain in the C-terminal region, a p21-GTPase-binding domain (PBD) in the N-terminal, and eight proline-rich PxxP domains in the central region. PAK4 was found to be overexpressed or genetically amplified in several types of cancer lines, such as breast, prostate, colon and pancreatic, where it influences tumour proliferation, survival and progression (King, Nicholas, and Wells 2014). Considering the important role of PAKs in cell morphology and motility, it is not surprising that PAK4 can influence tumour cell invasion. PAK4 kinase activity promoted ovarian cancer cell proliferation and invasion, which was reduced in PAK4 depleted cells (Siu et al. 2010). PAK4 has been shown to localise to invadopodia in melanoma cell lines (Nicholas et al. 2016). Studies conducted in melanoma suggest that different isoforms of PAKs might influence the regulation of different phases of invadopodia dynamics, and that PAK4 activity might be focussed in later stages of the invadopodia lifecycle (Nicholas et al. 2017). PAK4 has been shown to localise in podosome, specialised actin-rich protrusions belonging to haematopoietic cells that coordinate ECM degradation in normal physiology (Murphy and Courtneidge 2011). PAK4 localisation into podosome was found in human macrophages (Gringel et al. 2006) and bone-marrow-derived mouse dendritic cells (Wells and Jones 2010). PAK4 can regulate cofilin activity, which is known to promote lamellipodia protrusion formation and actin filament

disassembly (Dan et al. 2001; Ahmed et al. 2008). Inhibition of cofilin activity by PAK4 leads to inhibition of actin disassembly and formation of plasma membrane protrusions in myoblast (Dan et al. 2001). Constitutive activation of PAK4 in pancreatic ductal cells increased cell migration and invasion(Kimmelman et al. 2008), possibly acting as downstream effector of the c-Met:HGF axis to regulate cancer cells motility (King et al. 2017). Indeed, HGF-stimulated MDCK cells led to PAK4 activation through PI3K, and resulted in reorganisation of cellular adhesions, which are essential for efficient migration (Wells, Abo, and Ridley 2002).

In prostate cancer, work has focused on prostate cancer cell proliferation and migration, rather than invasion. PAK4 involvement in PCa invasion remains unclear, and very little is known about PAK4 in invadopodia, especially in the prostate cancer setting. A study conducted on PC3 and DU145 cells identified PAK4 as substrate of PKA, able to promote tumorigenesis in athymic mice, possibly through the PAK4 CREB domain (M.-H. Park et al. 2013). In PC3 cells, PAK4 phosphorylates LIMK and is required for HGF-induced cancer cell migration (Ahmed et al. 2008). Activation of PAK4 downstream of HGF was also reported in DU145 cells (Wells et al. 2010). Here, PAK4 phosphorylation of the RhoGEF GEF-H1 promoted cell motility (Wells et al. 2010). Moreover, PAK4 depleted PC3 cells exhibited decreased LIMK1-driven cell migration in response to HGF (Whale et al. 2013)

Results obtained in Chapter 3 provide for the first time the opportunity to study the role of PAK4 in prostate cancer invadopodia activity. Therefore, in this chapter we aim to explore whether melanoma findings of PAK4 functionality in invadopodia (Nicholas et al. 2016, 2017) translate to the prostate setting. Moreover, these primary adenocarcinoma cells performed optimally in Zebrafish yolk sac invasion assay, thus allowing new *in-vivo* studies regarding PAK4 functions in prostate cancer dissemination.

4.2. Results

4.2.1. All matched pair cell lines express PAK4

PAK4 is reportedly overexpressed or genetically amplified in several types of cancer lines, including prostate (Callow et al. 2001; King, Nicholas, and Wells 2014). In order to investigate whether PAK4 levels correlate with the different invasive ability as reported in the previous chapter of this thesis (Figure 3.11), all primary adenocarcinoma cell lines were tested for PAK4 expression.

PAK4 was ubiquitously expressed by all cell lines tested by Western blot analysis (Figure 4.1A). Quantification of protein expression revealed that PAK4 expression was significantly higher in CT-1542 cell line compared to CT-1535 cell line (Figure 4.1B).

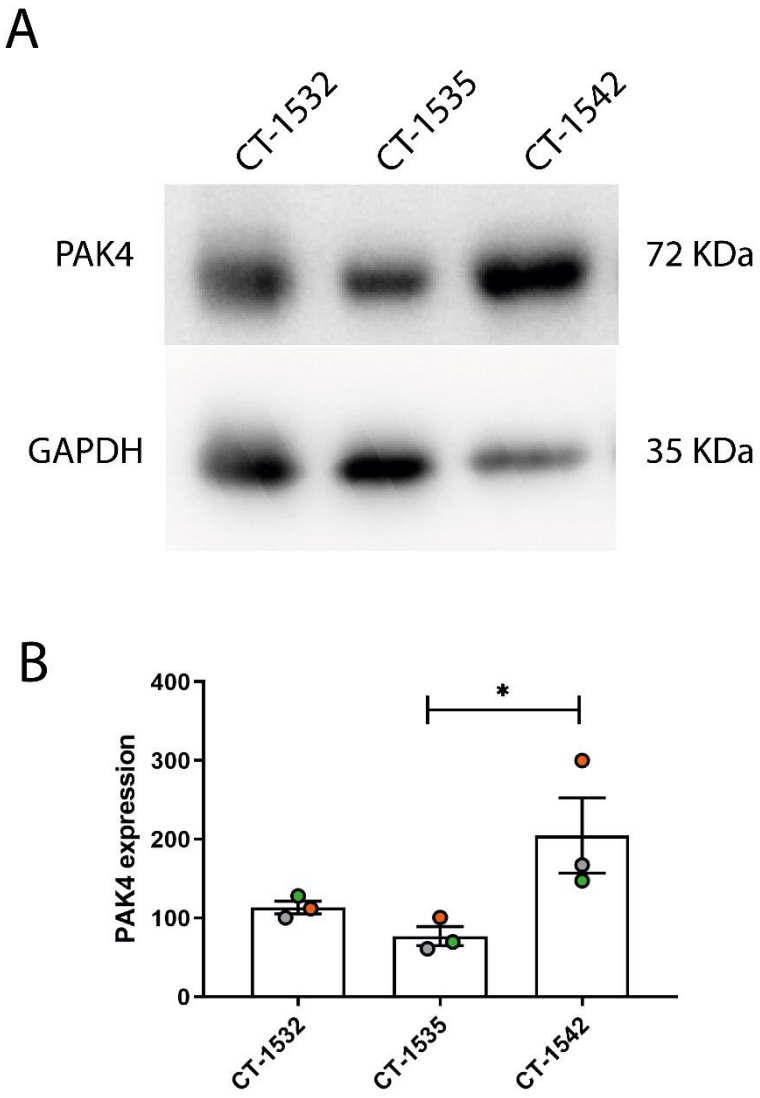

Figure 4. 1: PAK4 expression analysis in primary adenocarcinoma cell lines.
Western blot analysis of the expression levels of PAK4 PCa cell lines (A). Protein levels were analysed by densitometric analysis. Intensity of bands related to the protein of interest were corrected for the loading control (GAPDH) and plotted as relative ratio mean ± SEM (B). Experiments were repeated with three independent cell lysates (n=3). Statistical significance was calculated between each cell line with One-way Anova followed by Tukey's multiple comparison test, *$p<0.05$.

4.2.2. Transient PAK4 depletion reduces invadopodia formation and matrix degradation

PAK4 depletion has been shown to inhibit prostate cancer cells migration and to negatively regulate focal adhesion turnover (Ahmed et al. 2008; Wells et al. 2010). However, the role of PAK4 signalling in prostate cancer invasion, had not been previously evaluated. Thus, having confirmed PAK4 expression in all the prostate cancer cell lines tested, the effect of PAK4 reduction on invadopodia was tested. The CT-1532 cell line was selected as the most suitable for knockdown of expression experiments based on its efficient growth *in-vitro* and its high ability to form invadopodia, hence alterations in invadopodia activity be easily detected.

PAK4 knockdown was achieved via siRNA with two different oligos targeting the PAK4 RNA sequence alongside a non-targeting scramble siRNA that was used as a control. After 72 hours of incubation with siRNA, cells were detached and re-seeded for 24 hours in order to test whether PAK4 knockdown effects would be maintained for the entire time frame required for an invadopodia assay. Cells were subsequently lysed and probed for PAK4 expression. Western blot analysis of PAK4 levels confirmed that PAK4 expression was significantly reduced for both the oligos tested when compared to siRNA control cells, with a knockdown level of approximately 70% for oligo 3 and 85% for oligo 5. As expected, no difference in PAK4 expression was observed between untransfected cells and siControl cells (Figure 4.2).

CT-1532 cells with reduced PAK4 expression were then subjected to invadopodia assay (Figure 4.3A). These cells exhibited a significant decrease in the percentage of cells forming invadopodia (Figure 4.3B), which was reflected in a reduction of the degraded area underneath cells (Figure 4.3C).

In order to validate the effects of PAK4 depletion, it was decided to repeat the experiment in a second cell line. CT-1535 was chosen to corroborate PAK4 knockdown due to its high degradative ability. In CT-1535 cells, PAK4 expression was successfully reduced with both siRNA oligos (Figure 4.4).

Depletion of PAK4 expression in CT-1535 cells led to a significant reduction in the percentage of cells forming invadopodia, as well as in the amount of matrix degraded area (Figure 4.5), in agreement with that observed for CT-1532 cells (Figure 4.3).

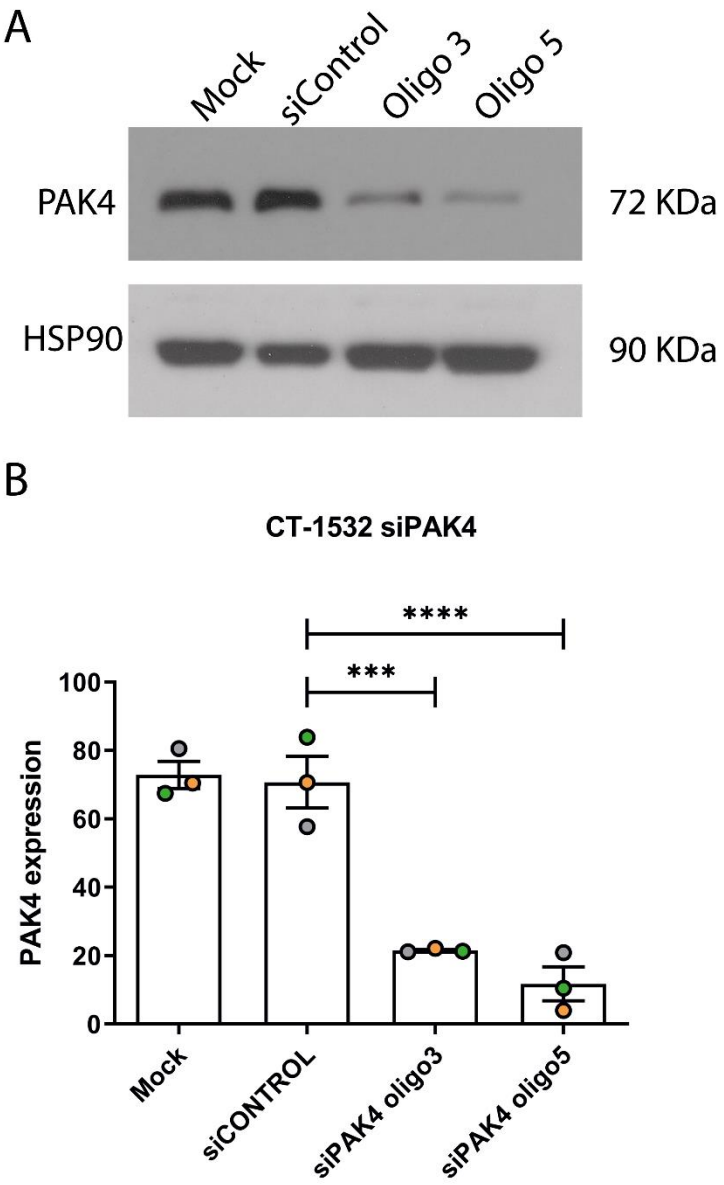

Figure 4. 2: Transient reduction of PAK4 expression in CT-1532 cell line by siRNA.
CT-1532 cells were transfected using two different PAK4 siRNA ooligonucleotides and RNAiMAX transfection reagent. Control cells were transfected with a control siRNA (siControl) or treated with transfection reagents in absence of oligos (Mock). PAK4 expression levels were analysed by Western blot 72 hours post-transfection (A). Protein levels were analysed by densitometric analysis. Intensity of bands related to the protein of interest were corrected for the loading control (GAPDH) and plotted as relative ratio mean±SEM (B). Experiment was repeated with three independent cell lysates (n=3). Statistical significance was calculated against the siControl with One-way Anova followed by Tukey's multiple cmparison test, ***p<0.001.

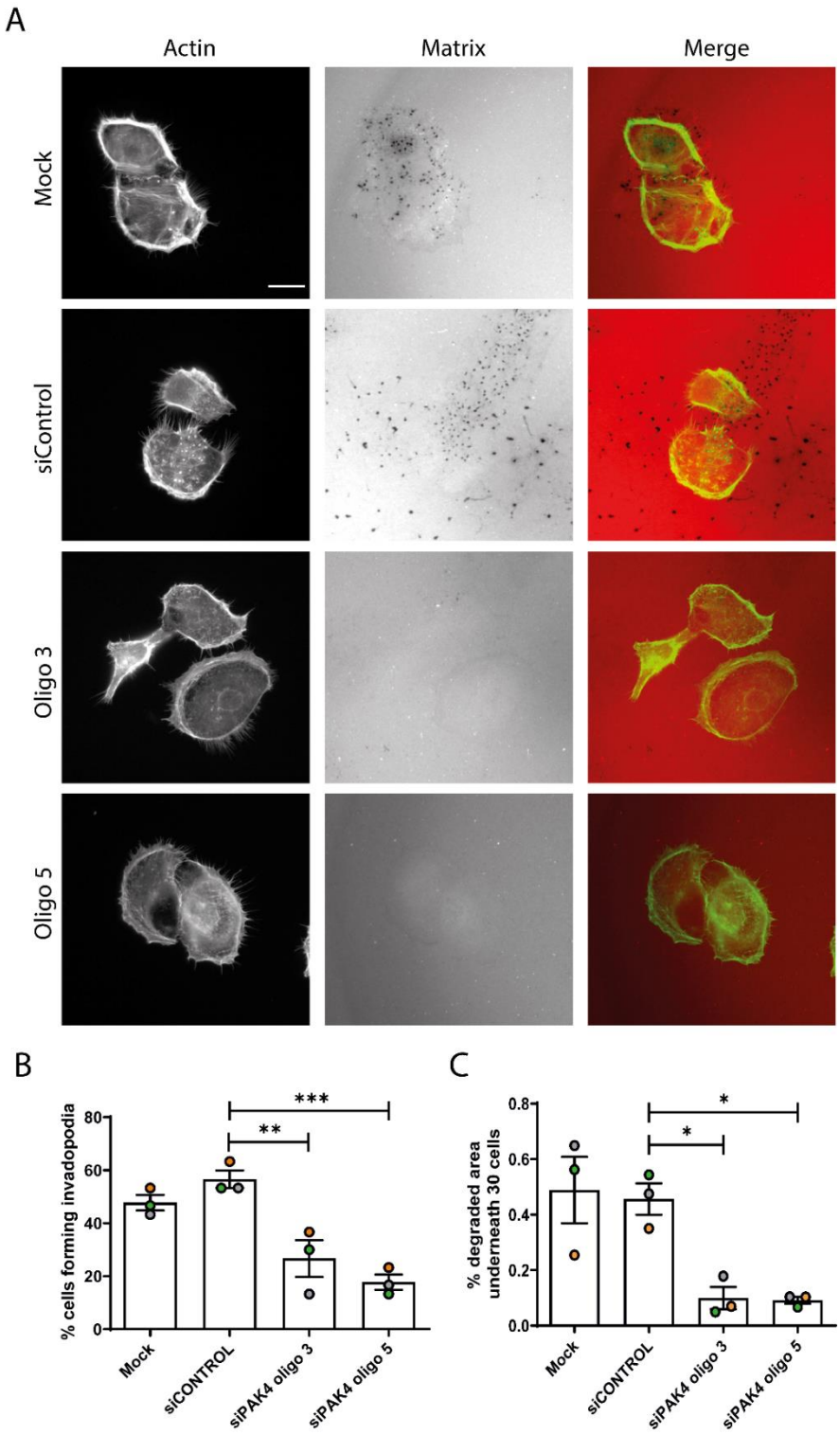

Figure 4. 3: Invadopodia assay of CT-1532 siPAK4 cells.
Representative invadopodia assay images of siPAK4 CT-1532 cell line. Cells were seeded on Cy3-conjugated gelatin for 24 hrs and stained for F-actin (A). Graphical representation of percentage of cells forming invadopodia (B). Measurement of the degraded area underneath cells surface (C). Significance was calculated against the siControl population with One-way Anova followed by Tukey's test. *p<0.05, **p<0.01, ***p<0.001. Data are presented as mean values ± S.E.M. Scale bar = 10µm.

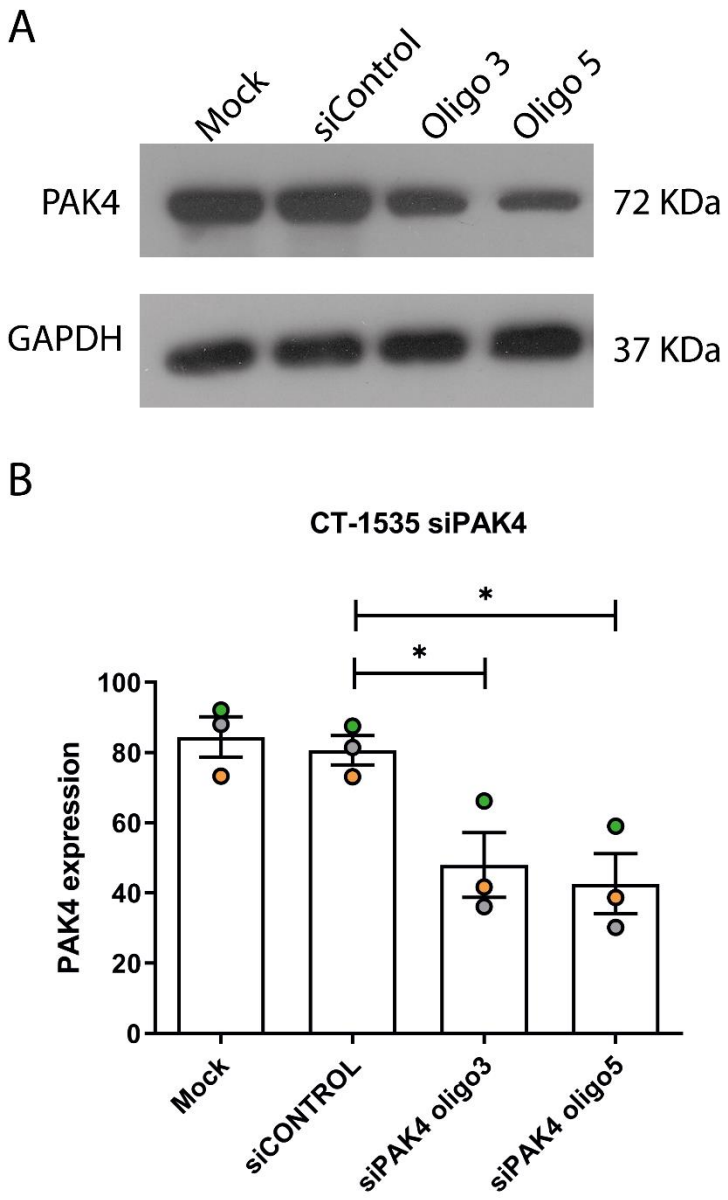

Figure 4. 4: Transient reduction of PAK4 expression in CT-1535 cell line by siRNA
CT-1535 cells were transfected using two different PAK4 siRNA oligonucleotides and RNAiMAX transfection reagent. Control cells were transfected with a control siRNA (siControl) or treated with transfection reagents in absence of oligos (Mock). PAK4 expression levels were analysed by Western blot 72 hours post-transfection (A). Protein levels were analysed by densitometric analysis. Intensity of bands related to the protein of interest were corrected for the loading control (GAPDH) and plotted as relative ratio mean±SEM (B). Experiment was repeated with three independent cell lysates (n=3). Statistical significance was calculated against the siControl with One-way Anova followed by Tukey's multiple comparison test, *p<0.05.

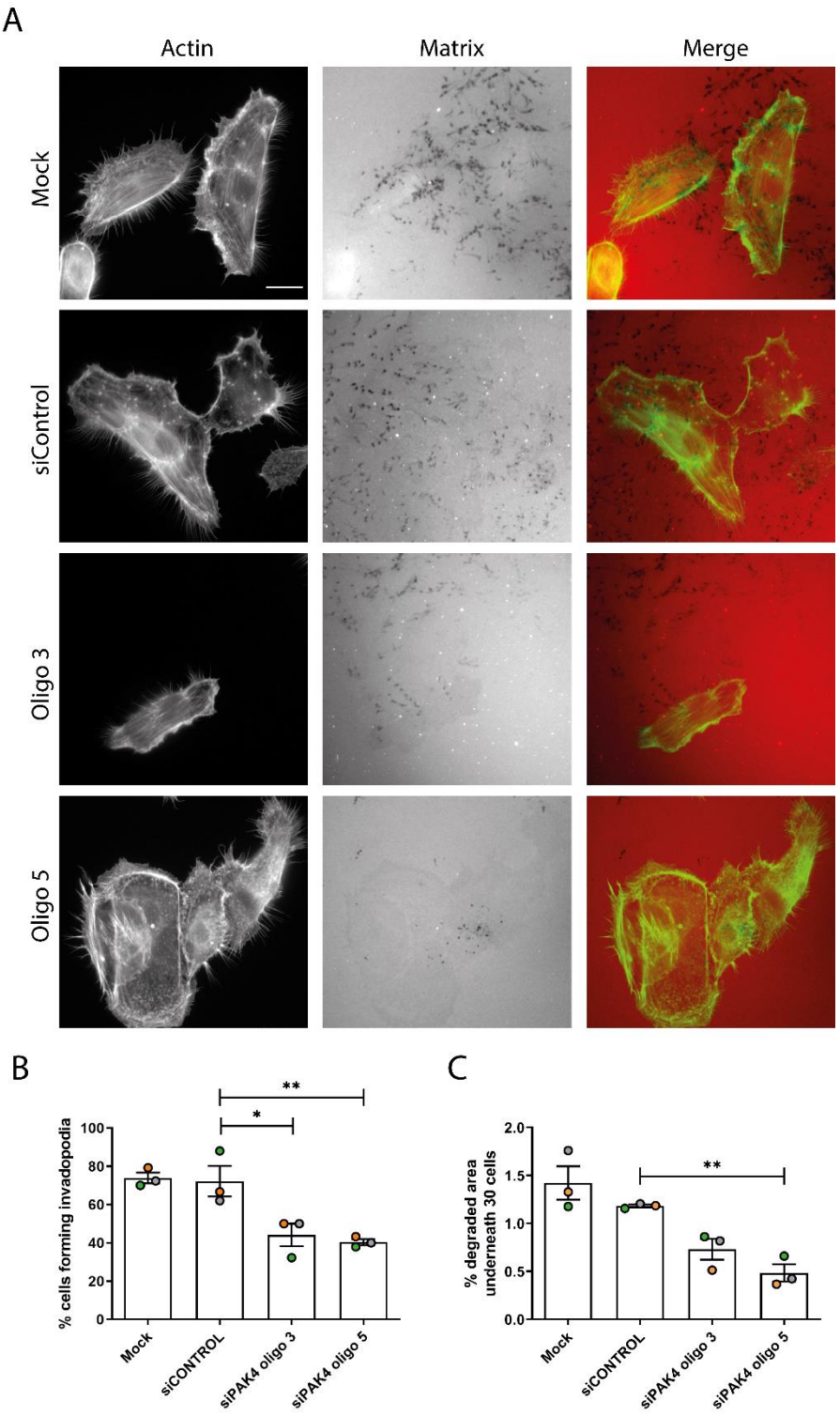

Figure 4. 5: Invadopodia assay of CT-1535 siPAK4 cell line.
Representative invadopodia assay images of siPAK4 CT-1535 cell line. Cells were seeded on Cy3-conjugated gelatin for 24 hrs and stained for F-actin (A). Graphical representation of percentage of cells forming invadopodia (B). Measurement of the degraded area underneath cells surface (C). Significance was calculated against the siControl population with One-way Anova followed by Tukey's test. *p<0.05, **p<0.01. Data are presented as mean values ± S.E.M. Scale bar = 10µm

4.2.3. Establishment and validation of the PAK4 stable knockdown in CT-1532 cell line

The siRNA experiments indicate that PAK4 might be relevant in invadopodia in prostate cancer, as transient reduction of PAK4 decreased invadopodia formation. However, protein depletion via siRNA technology could lead to variable transfection efficiency across different experiments, and experimental data reliability and reproducibility might be negatively affected by the involuntary selection of untransfected cells, which retain their native protein expression. Moreover, *in-vivo* Zebrafish injections require a much higher number of fluorescently labelled cells than those achieved by simple siRNA transfections. It was therefore decided to move to the shRNA technology to develop a stable cell line with reduced PAK4 expression, using a shPAK4 vector that has been already established in the lab (Figure4.6A) (Whale et al. 2013). The CT-1532 cells were successfully transfected with a GFP-tagged PAK4 targeting RNA or with a non-specific RNA to use as a control. The resulting pool of GFP-expressing were further selected by antibiotic resistance and PAK4 levels were analysed by Western blot. PAK4 levels were reduced by approximately 80% in shPAK4 cells when compared to wildtype and control shRNA cells (Figure 4.6B and C).

ShRNA experiments confirmed a successful achievement of stable PAK4 protein reduction. However, a poor transfection efficiency resulting from the shRNA control plasmid was noted, which might lead to the inadvertent selection of a subclonal population that is not representative of the wildtype CT-1532 cell line. Therefore, morphological properties of the shControl cells and those carrying the scramble shRNA were evaluated by analysing cell shape descriptors, which are indicators of possible changes in the major pathways involved in cytoskeletal organization following shRNA transfection. No differences were observed in the average cell area (Figure 4.7B). Similarly, there was no significant change in the cell elongation parameters, evaluated as average cell roundness (Figure 4.7C) and aspect ratio (ratio between major and minor axis, Figure 4.7D). Additionally, no obvious changes in the rate of growth between shControl and parental CT-1532 cells were observed upon *in-vitro* culturing.

It was concluded that shControl cells behaviour did not significantly deviate from the behaviour of wildtype cells, therefore all subsequent assays were performed using shRNA transfected cell populations only, and PAK4 depletion effects were compared against shControl.

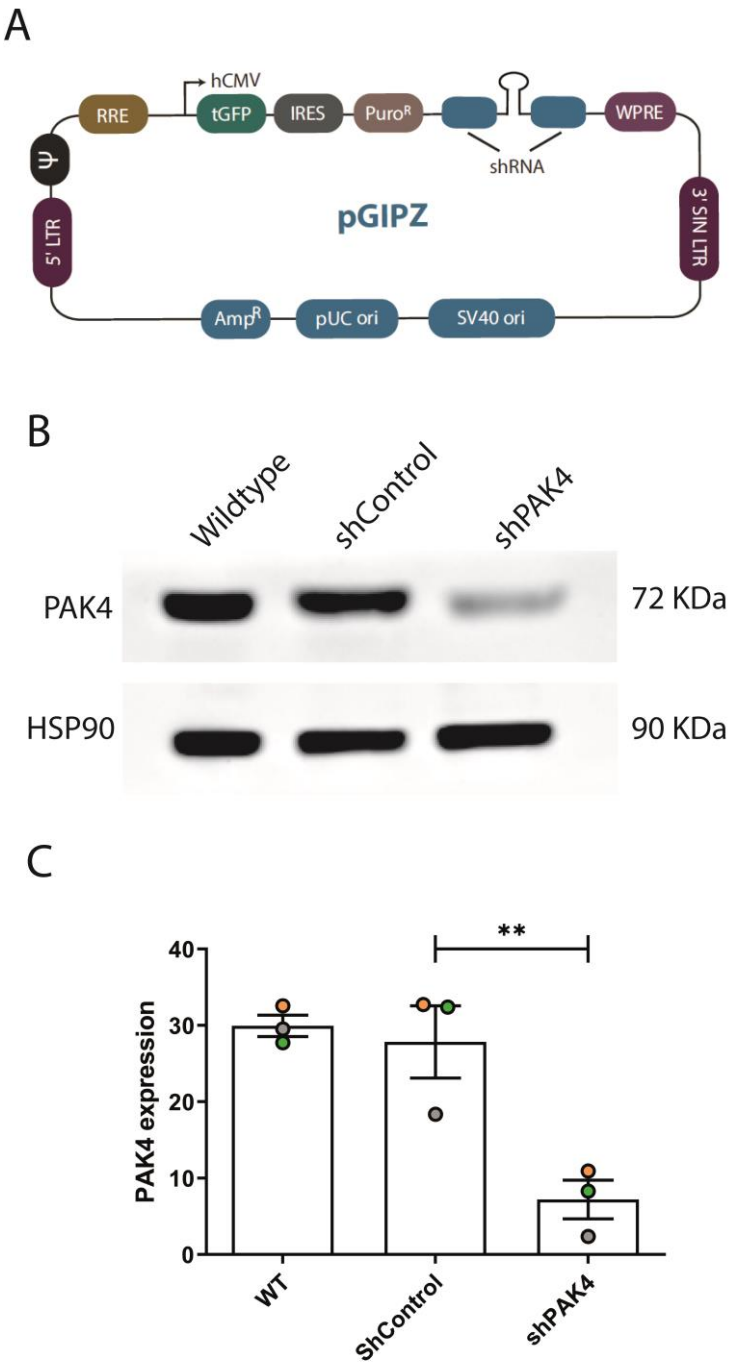

Figure 4. 6: stable reduction of PAK4 expression in CT-1532 cell line by shRNA.
Graphical representation of the bicistronic shRNA construct utilised to reduce PAK4 expression. Human cytomegalovirus promoter drives expression of the GFP reporter, puromycin resistance and the shRNA for gene knockdown. Image taken from Horizon Discovery (A). Western blot analysis of the expression levels of PAK4 in CT-1532 following stable transfection with PAK4 shRNA (B). Protein levels were analysed by densitometric analysis. Intensity of bands related to the protein of interest were corrected for the loading control (GAPDH) and plotted as relative ratio mean±SEM (C). Experiment was repeated with three independent cell lysates (n=3). Statistical significance was calculated against the shControl cell lines with One-way Anova followed by Tukey's multiple cmparison test, **p<0.01.

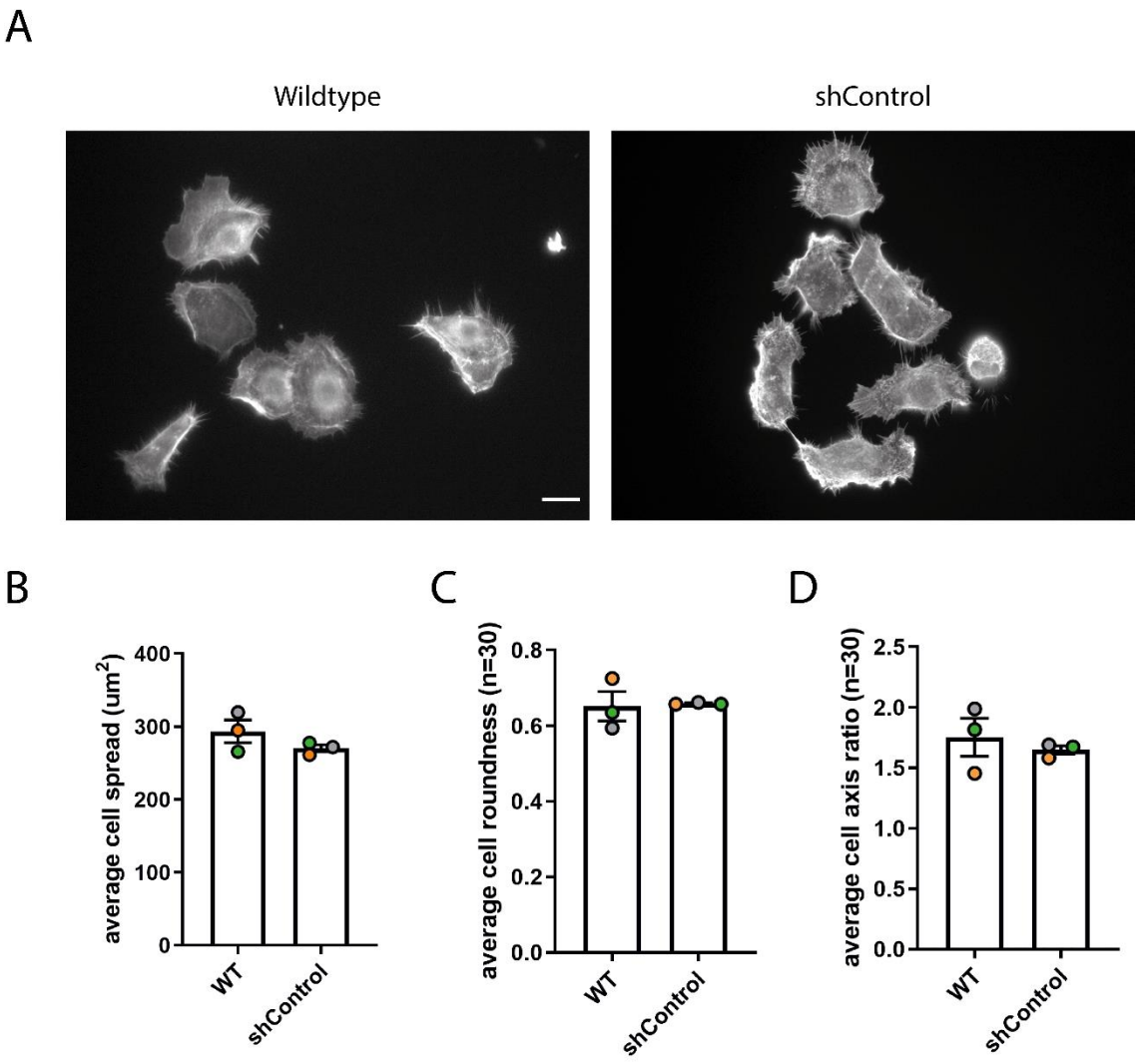

Figure 4. 7: Morphology analysis of parental CT-1532 cell lines and CT-1532 stably transfected with a OFF target shRNA.

Representative images of wild-type CT-1532 and shControl cell lines subjected to immunoflourescent F-actin staining to observe morphological differences (A). Graphical representation indicating the verage cell spread (B), roundness (C) and axis ratio (D). Morphological analysis was performed using ImageJ software. Graphs shown are representative of 3 independent experiments, at least 30 cells per experiment were scored. Statistical significance was calculated with unpaired student's t-test. Scale bar = 10µm.

4.2.4. PAK4 depletion does not affect protein expression of PAK1 and PAK6 in CT-1532 cells.

To ensure that the PAK4 depletion effects from subsequent shRNA experiments do not depend on the compensatory overexpression of other PAK isoforms, the expression levels of PAK family members that have been reported to play a role in cancer cells invasion and dissemination were assessed. PAK1 (the best characterised PAK isoform of group I), overexpression has been detected in highly invasive prostate cancer cells and is required for transendothelial migration *in-vitro* (Goc et al. 2013). Moreover, previous experiments in the Wells lab conducted in Zebrafish demonstrated that PAK1 is required for *in-vivo* cell migration of melanoma cancer cells (Nicholas et al. 2016). Accordingly, PAK6 (belonging to group II) was also found to be overexpressed in prostatic carcinoma tissues and linked to prostate cancer cell dissemination (Wen et al. 2009; Fram et al. 2014).

Western blot analysis of CT-1532 PAK4 depleted cells showed that the protein levels of both PAK1 and PAK6 were comparable between shControl and shPAK4 cell lines (Figure 4.8), excluding a possible compensatory effect in this cell line.

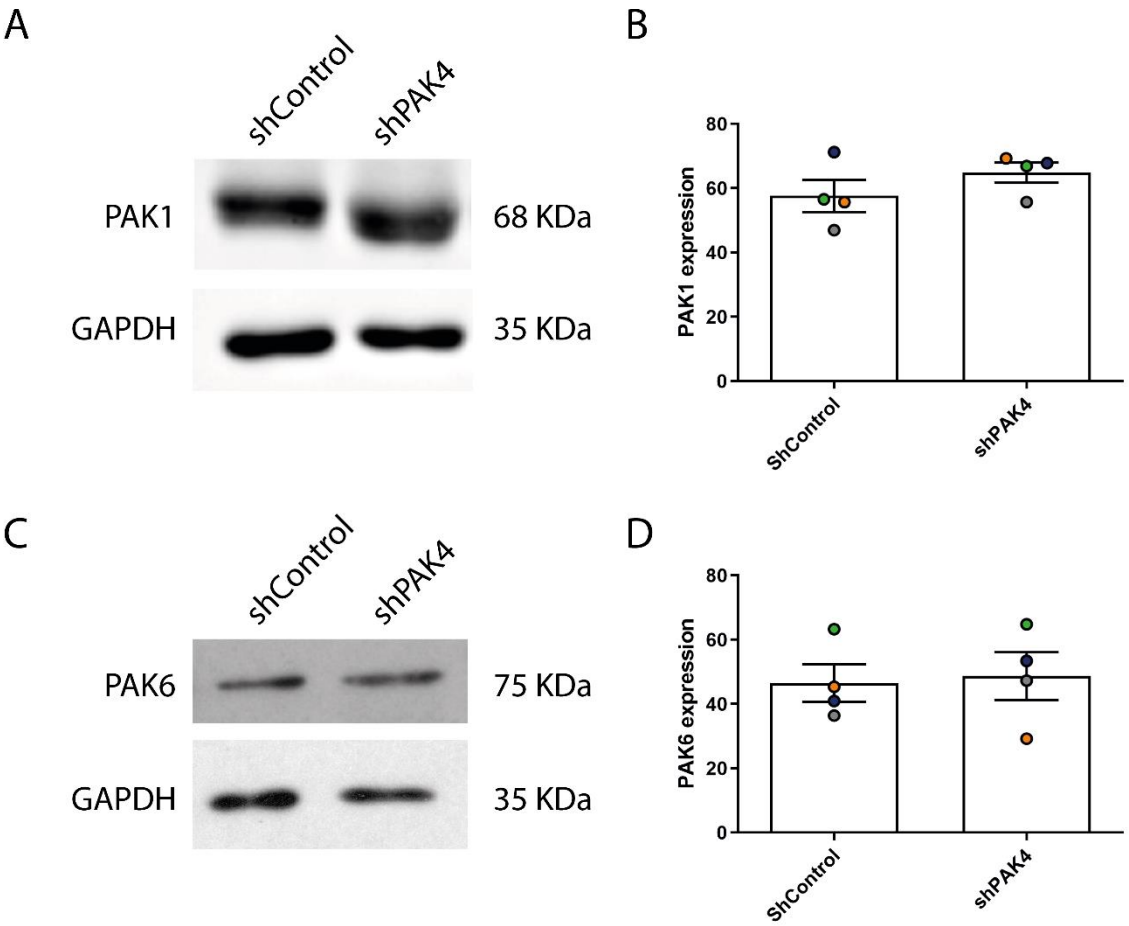

Figure 4. 8: PAK4 depletion does not affect PAK1 and PAK6 expression levels.
Western blot analysis of the expression levels of PAK1 (A-B) and PAK6 (C-D) in shPAK4 cell line compared to shControl cell line. Intensity of bands related to the protein of interest were corrected for the loading control (GAPDH) and plotted as relative ratio mean±SEM. Experiment was repeated with three independent cell lysates (n=3). Statistical significance was calculated with unpaired student's t-test, *p<0.05.

4.2.5. Stable PAK4 depletion reduces invadopodia formation and matrix degradation in CT-1532 cell line

The invasiveness ability of shPAK4 cells was tested *in-vitro* via the invadopodia assay. ShControl and shPAK4 cell lines were seeded on fluorescent gelatin and incubated for 24 hours before staining and screening for degradation.

Quantification of the gelatin degraded confirmed a reduction in the degradative capability of PAK4 depleted cells. Moreover, the number of invadopodia-forming cells in shPAK4 cell line significantly decreased when compared to the shControl cell line (Figure 4.9). These data are in agreement with the invadopodia phenotype exhibited after transient PAK4 silencing by siRNA, confirming that PAK4 plays a role in prostate cancer invadopodia.

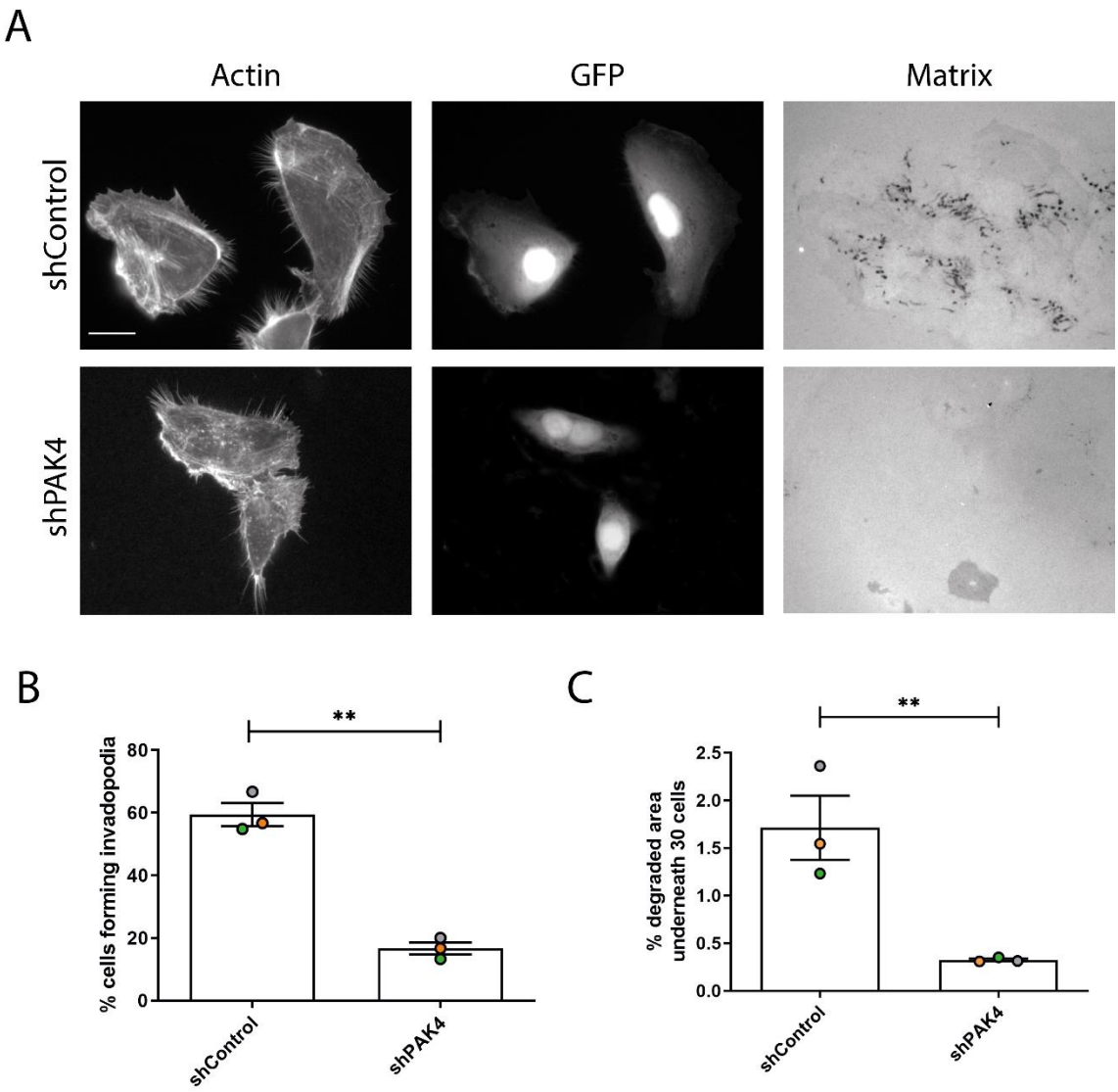

Figure 4. 9: Invadopodia assay of CT-1532 shPAK4 cells.
Representative invadopodia assay images of GFP-tagged shPAK4 cell line compared to shControl cell line. Cells were seeded on Cy3-conjugated gelatin for 24 hrs and stained for F-actin (A). Graphical representation of percentage of cells making invadopodia (B) Measurement of the degraded area underneath cells surface (C). Significance was calculated with student's t-test. **p<0.01. Data are presented as mean values ± S.E.M. Scale bar = 10µm.

4.2.6. PAK4 depletion decreases the percentage of cells with actin puncta

The data presented so far indicate that PAK4 might drive invadopodia activity in prostate cancer, corroborating previous observation in melanoma (Nicholas et al. 2016). Reduction of PAK4 in melanoma significantly decreased matrix degradation, but, interestingly, did not affect the formation of actin puncta, which are thought to represent invadopodia precursors (Nicholas et al. 2017). The retention of actin puncta in melanoma may suggest a late role for PAK4 in the invadopodia lifecycle, where PAK4 activity coordinates invadopodia-mediated degradation, rather than invadopodia formation.

However, in contrast to the melanoma studies, stable depletion of PAK4 expression in this prostate cancer cell line reduced the formation of actin puncta (Figure 4.10). Only 50% of PAK4 depleted cells exhibited actin puncta presence, as opposed to 80% of cells forming actin puncta in the shControl population (Figure 4.10).

To further validate this observation, the percentage of cells with actin puncta when plated on gelatin was calculated in CT-1532 subjected to transient PAK4 depletion via siRNA (Figure 4.11). Reduction of PAK4 with either oligo 3 or oligo 5 led to a significant in decrease in cells with actin puncta when compared to the siControl cells (Figure 4.11).

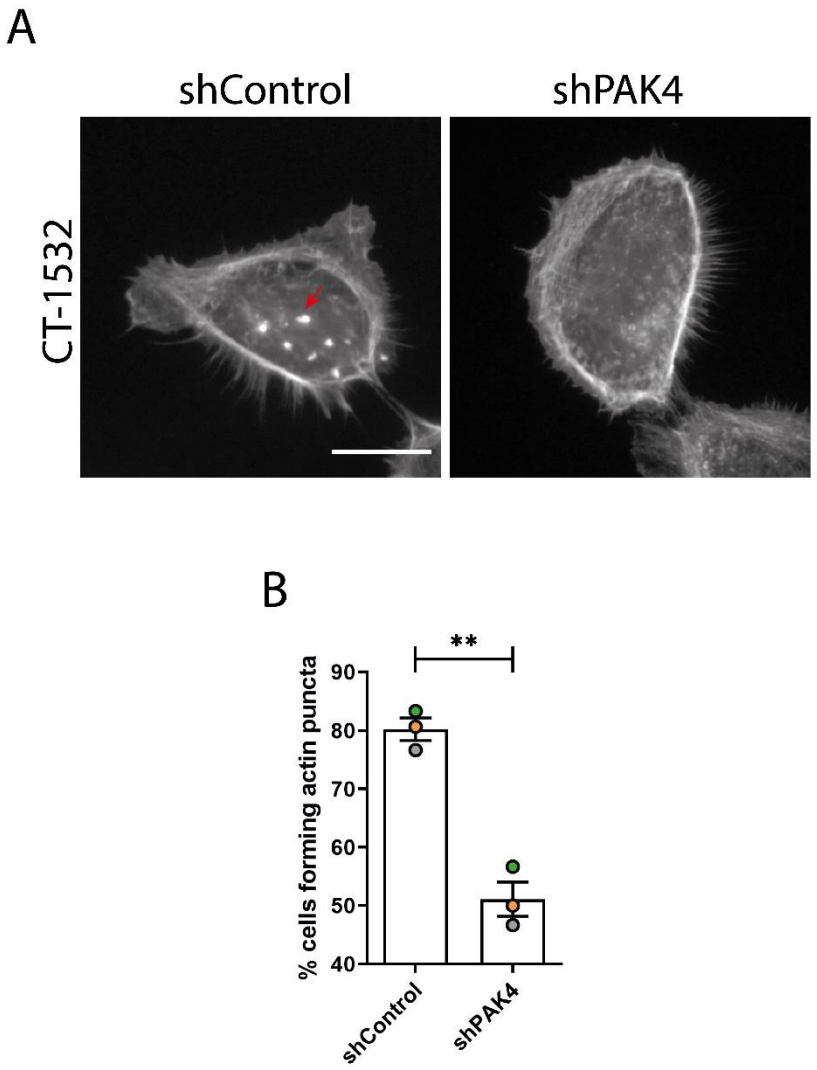

Figure 4. 10: Analysis of actin puncta formation in CT-1532 shPAK4 cell line.
Representative images of CT-1532 cell lines with reduced PAK4 expression via shRNA. Cells were seeded on Cy3-conjugated gelatin for 24 hrs and stained for F-actin. Actin puncta are indicated by red arrows (A). Graphical representation of percentage of cells forming prominent actin puncta in CT-1532 shPAK4 cell line (B). Significance was calculated with Student's t-test, **p<0.01. Data are presented as mean values ± S.E.M. Scale bar=10µm

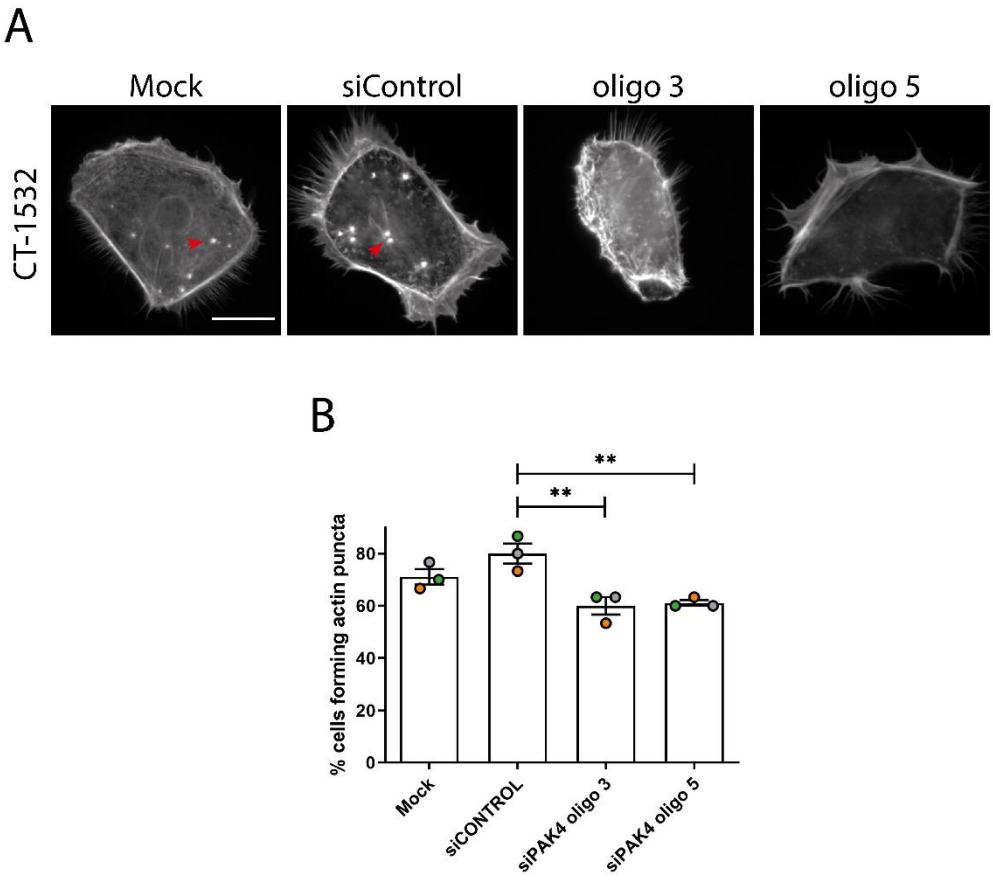

Figure 4. 11: Analysis of actin puncta formation in CT-1532 siPAK4 cell line.
Representative images of CT-1532 cell line with reduced PAK4 expression via siRNA. Cells were seeded on Cy3-conjugated gelatin for 24 hrs and stained for F-actin. Actin puncta are indicated by red arrows (A). Graphical representation of percentage of cells forming prominent actin puncta in CT-1532 siPAK4 cell line (B). Significance was calculated against the siControl population with One-way Anova followed by Tukey's test, **p<0.01. Data are presented as mean values ± S.E.M. Scale bar=10µm

4.2.7. PAK4 depletion does not affect xenograft formation and invasiveness *in-vivo*

PAK4 depletion in melanoma cells reduced metastatic dissemination *in-vivo* in zebrafish (Nicholas et al. 2016). However, the *in-vivo* migratory ability of primary prostate cancer cells in response to modulation of PAK4 expression has not been previously reported. Using the control and PAK4 stable knockdown CT-1532 cells, the impact of PAK4 depletion in prostate cancer invasion was investigated *in-vivo* using the Zebrafish yolk sac invasion assay. This represents a distinct assay for evaluation of the metastatic potential and had already proved to be successful with our cancer cell lines, as outlined in Chapter 3 (Figure 3.15).

CT-1532 shControl and shPAK4 cells were injected into the yolk-sac of Zebrafish embryos at 1dpf, and tail dissemination was evaluated 4dpf. Both cell lines tested were able to form a compact mass in the yolk-sac (Figure 4.12). No significant differences were observed in the percentage of fish exhibiting fluorescent deposits in the tail (Figure 4.13A-B). To better explore any differences in the extent of metastatic capability between the injected cell populations, the average number of metastasis throughout the tail of the fish was also counted. No significant differences were detected in the number of disseminated cells between shControl and shPAK4 fish (Figure 4.13C-D).

Therefore, reducing PAK4 expression did not inhibit the invasion of prostate cancer cells *in-vivo*, compared to the work performed *in-vitro*.

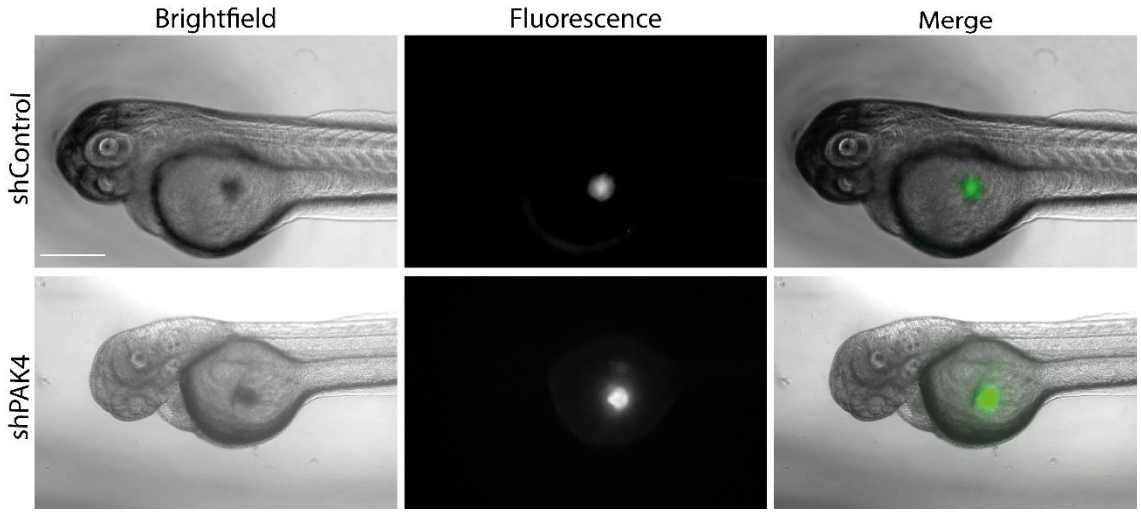

Figure 4. 12: Representative images of shPAK4 xenograft formation in Zebrafish yolk-sac invasion assay.

GFP-labelled shControl and shPAK4 CT-1532 cancer cell lines were injected into 1dpf zebrafish embryos and screened for the presence of tumour mass into the yolk-sac. Embryos with aspecific and disperse signals were excluded from the analysis. Both cell lines were able to form a compact xenograft. Scale bar 200um

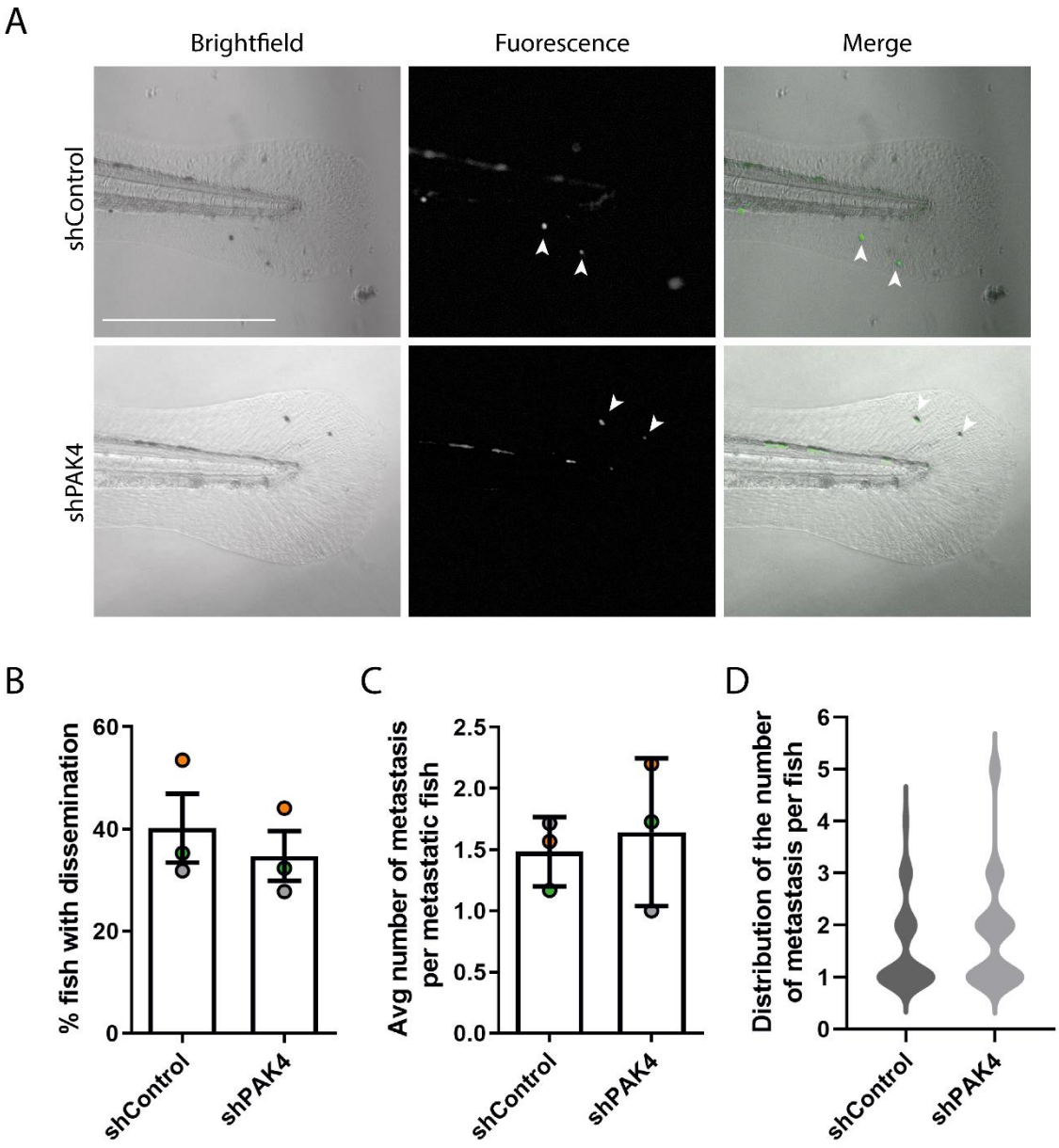

Figure 4. 13: Representative images of shControland shPAK4 cell lines disseminating in tail in zebrafish invasion assay.

Representative phase contrast and fluorescent images of a Zebrafish tail (lateral view) 4 days post injection with cancer cells. Both shPAK4 and shControl cell lines were able to disseminate and lodge in the tail of Zebrafish embryos (A). Graphical representation of the percentage of embryos with dissemination (B) and the average number of metastasis detected in the tail per fish. Fish without any apparent metastasis were excluded from this analysis (C). Graphical representation of the distribution of the number of metastasis per fish, showing the majority of fish exhibiting one deposit in the tail (D). Data are representative of three independent experiment, with at least 15 embryos screened for metastasis at the end of each experiment. Significance was calculated with student's t-test. Data are presented as mean values ± S.E.M. Scale bar = 200µm.

4.2.8. PAK4 depletion reduces invadopodia puncta size

Whilst it was not possible to detect any impact of PAK4depletion *in-vivo*, results presented here clearly demonstrate a role for PAK4 in prostate cancer invadopodia formation. As we have already demonstrated the potential clinical relevance of invadopodia in prostate cancer dissemination, attention was focussed on gaining a better understanding of the activity of PAK4 across the invadopodia lifecycle. In contrast to melanoma cells, loss of PAK4 in prostate cancer cells appeared to impact on actin puncta formation. It was noted that not only did less cells in the prostate cancer population have actin puncta but that those present were smaller in size.

In order to confirm the effect of PAK4 depletion on invadopodia size, the number of invadopodia-forming cells exhibiting at least one mature invadopodia (associated with matrix degradation) reaching a diameter of 0.5 μm or more was quantified. This arbitrary threshold for minimum invadopodia width was chosen according to the literature (Murphy and Courtneidge 2011). PAK4 knock-down led to a significant drop in invadopodia size, as only 20% of invadopodia competent cells exhibited at least one invadopodia equal or larger than 0.5 μm in diameter (Figure 4.14). These data suggest that PAK4 might be involved in regulation of actin puncta dynamics in prostate cancer.

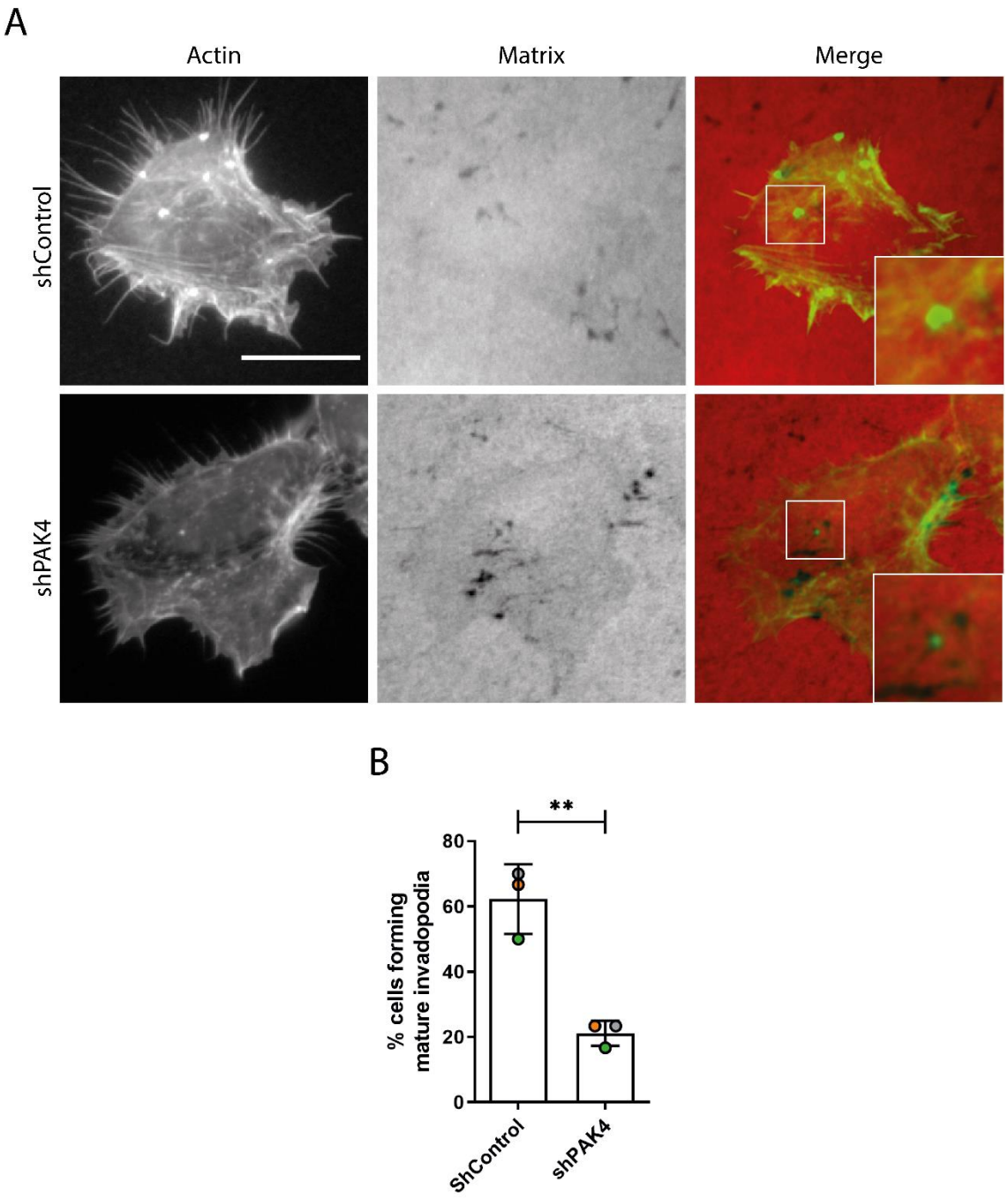

Figure 4. 14: Analysis of invadopodia maturation in CT-1532 shPAK4 cell line.
Representative invadopodia assay images of shPAK4 and shControl cell lines. Cells were seeded on Cy3-conjugated gelatin for 24 hrs and stained for F-actin. ShPAK4 cells with active invadopodia showed consistently smaller puncta when compared to shControl cells (A). Graphical representation of the percentage of cells forming at least one mature invadopodia, defined as one actin puncta of a diameter equal or superior to 0.5µm, overlapping with matrix degradation. The diameter of the actin puncta was measured via a line crossing through an invadopodia structure and analysed with ImageJ software. Only invadopodia-competent cells were considered for the analysis (B). Significance was calculated with Student's t-test, **p<0.01. Data are presented as mean values ± S.E.M. Scale bar=10µm.

4.2.9. Kinase dead PAK4 cannot rescue invadopodia formation and matrix degradation in CT-1532 cells with depleted PAK4

Reduced expression of PAK4 disrupted invadopodia activity and matrix degradation in CT-1532 cells. To confirm the phenotype observed upon knockdown was actually due to the specific PAK4 depletion and thus to exclude any off-target effect, CT-1532 shPAK4 cells were transfected with a Myc-PAK4 rescue construct. Transfection of Myc-PAK4 construct in shPAK4 cells was able to rescue PAK4 protein expression, as detected by Western blot analysis (Figure 4.15). Transfected cells were subsequently subjected to invadopodia assay, and only *myc*-positive cells were analysed (Figure 4.16). Expression of the whole length PAK4 rescue construct in shPAK4 cells was able to restore both the percentage of cells forming invadopodia and degraded matrix to levels comparable to the shControl population (Figure 4.17), further confirming the role of PAK4 in prostate cancer cells.

Having established that the loss of invadopodia activity was specific to PAK4 depletion, the functionality of PAK4 was explored in more detail. Myc-tagged PAK4 mutated rescue constructs were tested alongside the wild type PAK4. To investigate the relevance of PAK4 interaction to the Rho-GTPase Cdc42, PAK4 depleted cells were transfected with a PAK4 rescue plasmid mutated in conserved histidine residues within the N-terminal Cdc42 interactive binding (CRIB) region (H19,22L) (Whale et al. 2013). Analogous to that observed for PAK4 native, PAK4-H19,22L mutant rescued the invadopodia phenotype to levels comparable to the shControl cells (Figure 4.16 and 4.17). Expression of PAK4 rescue construct depleted in the amino acid motifs Pro-x-x-Pro enriched sequence, a region that includes both GEF-H1/Gab-1 and PI3K interaction domain (deltaPxxP) (Whale et al. 2013), was also able to rescue the invadopodia phenotype in shPAK4 cells (Figure 4.16 and 4.17). Finally, a kinase-inactive PAK4 rescue (K350,351M) (Callow et al. 2001; Whale et al. 2013) was employed to evaluate the role of PAK4-mediated phosphorylation on invadopodia (Figure 4.15). Interestingly, kinase dead PAK4-K350,351M failed to restore the number of cells forming invadopodia as well as the percentage of degraded matrix underneath cells (Figure 4.16 and 4.17). This finding indicates that while CRIB and PxxP domains are dispensable for invadopodia activity, the kinase domain might play a crucial role in PAK4-mediated invadopodia formation and gelatin degradation.

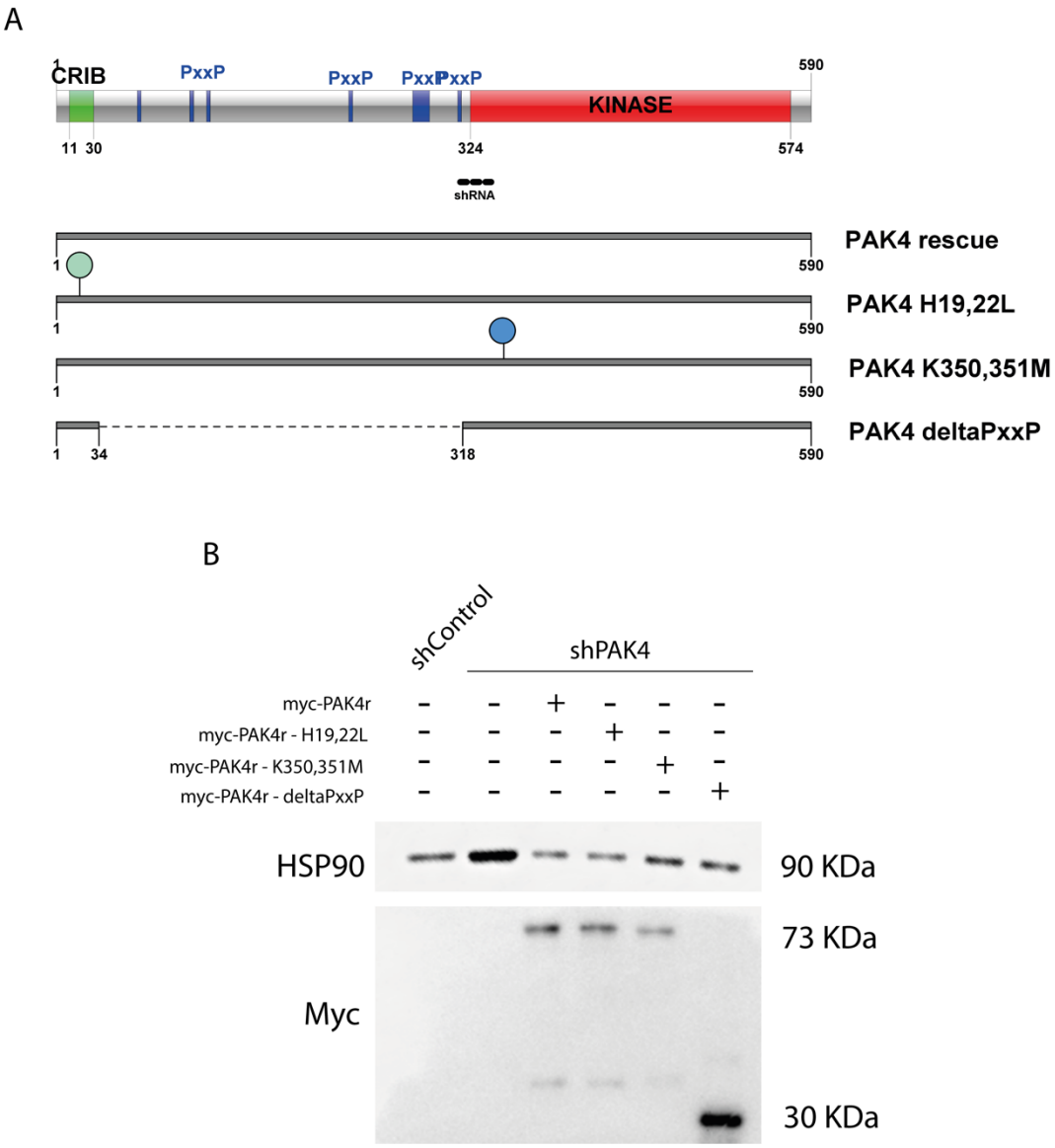

Figure 4. 15: Expression of myc-PAK4-shRNA resistant constructs in CT-1532 shPAK4 cell line.
Graphical representation of PAK4 domain structure and myc-PAK4-shRNA resistant constructs. CRIB: Cdc42 and Rac interactive binding motif; PxxP: Pro-x-x-Pro amino acid sequence motifs. Dotted line indicates a depleted region. The green pin indicates somatic mutations inactivating the CRIB domain (H19,22L), blue pin indicates somatic mutations inactivating the kinase domain (K350,351M) (A). Expression of the shRNA resistant constructs in shPAK4 cell by Western blot. Lysates were probed for Myc and HSP90 (B).

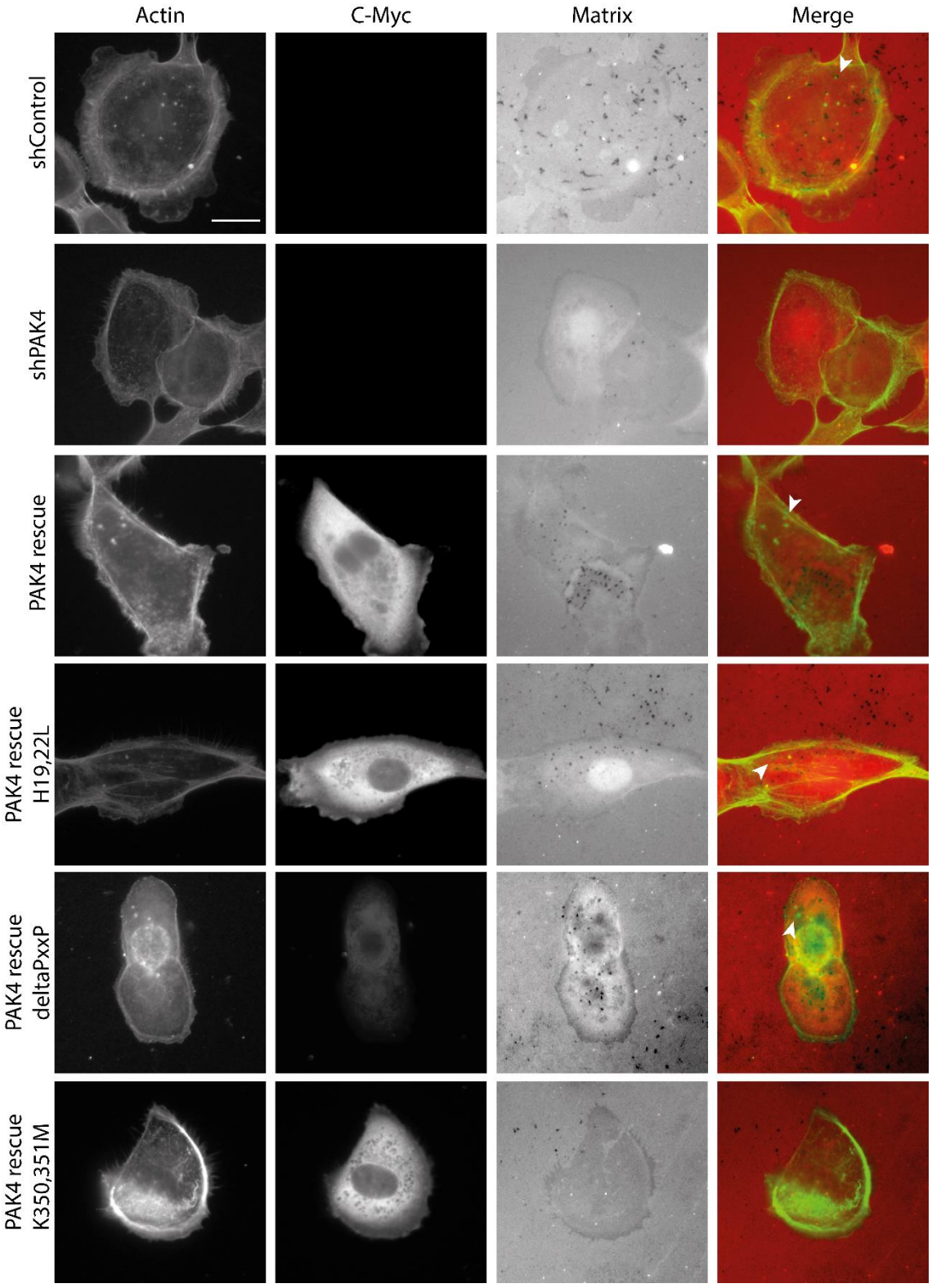

Figure 4. 16: Invadopodia assay of CT-1532 shPAK4 cells expressing myc-PAK4-shRNA resistant constructs.

Representative invadopodia assay images of shPAK4 cell line expressing myc-PAK4-shRNA resistant constructs. Cells were reversely transfected onto GFP-conjugated gelatin, after 24 hours media was replenished and cells were incubated additional 24 hours, then stained for F-actin. Only myc-positive cells were considered for the analysis. Scale bar = 10µm.

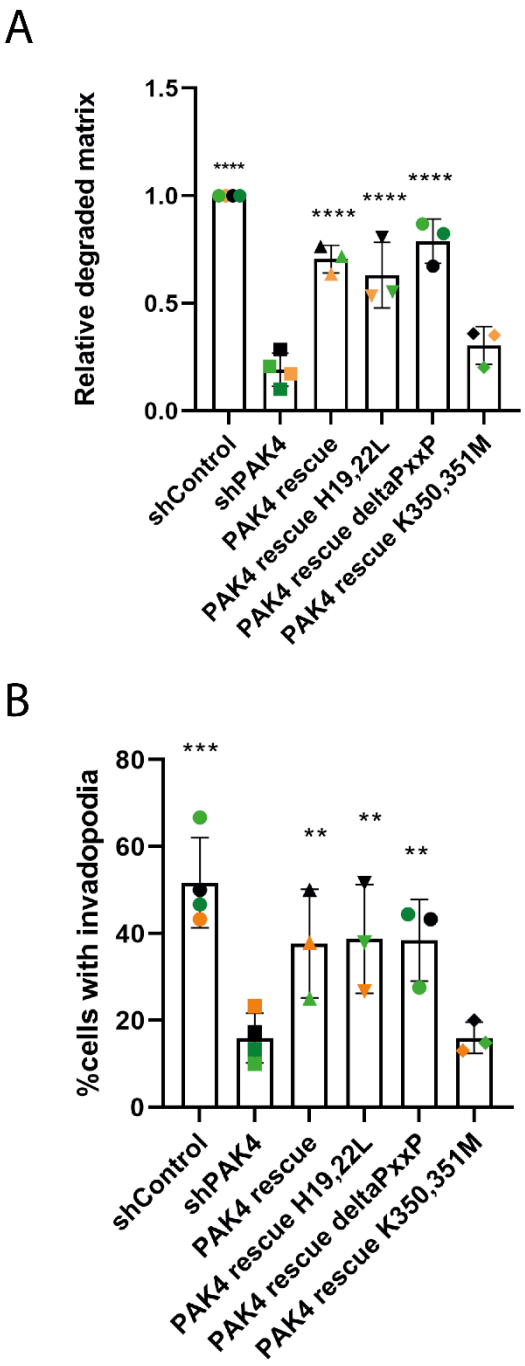

Figure 4. 17: Levels of invadopodia activity in CT-1532 shPAK4 cell line expressing myc-PAK4-shRNA resistant constructs.

Graphical representation of the relative degraded matrix (A) and the percentage of cells making invadopodia (B) Only myc-positive cells were considered for the analysis. At least 3 replicates per each condition were analysed over 4 independent experiments. Significance was calculated with One-way Anova against shPAK4 cell line followed by Dunnet's multiple comparison test. **p<0.01, ***p<0.001, ****p<0.0001. Data are presented as mean values ± S.E.M.

4.2.10. PAK4 regulates MMP2 and MT1-MMP levels in CT-1532 cells

Our PAK4 knockdown and rescue experiments, alongside the melanoma results (Nicholas et al. 2016), point to a potential role for PAK4 in matrix degradation stage. Degradation of the ECM by invadopodia is thought to be achieved via matrix metalloproteinases (MMPs). The soluble MMP2 and MMP9 and transmembrane MT1-MMP (also known as MMP14) are considered to be key regulators of invadopodia function (Jacob and Prekeris 2015). Different PAK isoforms has been shown to influence the expression and secretion of metalloproteases. PAK1 inhibition in prostate cancer PC3 cells led to reduction of MMP9 expression (Goc et al. 2013). Rider et al. showed that PAK1 can down-regulate the secretion of MMP2 in three-dimensional collagen IV in breast cancer, while induces MMP1 and MMP3 (Rider, Oladimeji, and Diakonova 2013). PAK4 depletion led to reduced activation and expression of MMP2 in ovarian and glioblastoma cancer cell lines (Franovic et al. 2015; Siu et al. 2010), and to a decreased detection of MT1-MMP delivery to invadopodia in melanoma cell line (Nicholas et al. 2016). Moreover, PAK4 and MMP2 has been reported to directly interact to regulate invasion of glioma (Kesanakurti et al. 2012). PAK4 influence on MMP2 was investigated using Compound 31 (C31), a potent PAK4 pharmacological inhibitor which has been shown to reduce MMP2 expression in lung cancer cells (Hao et al. 2018).

Thus, the expression level of MMPs were examined in PAK4 depleted cells. Unfortunately, immunoblotting of endogenous MMP9 and MMP2 failed to produce reliable data, as protein expression for these two MMPs seemed to be inconsistent across the different lysate sets analysed. However, it was possible to test the impact of Compound 31 in the prostate cancer cells. CT-1532 cells were incubated with 1μM of DMSO or C31 for 24 hours and then protein lysates were analysed by Western blot. MMP2 protein levels were reduced by approximately 20% following C31 treatment (Figure 4.18), in agreement with previous studies (Hao et al. 2018).

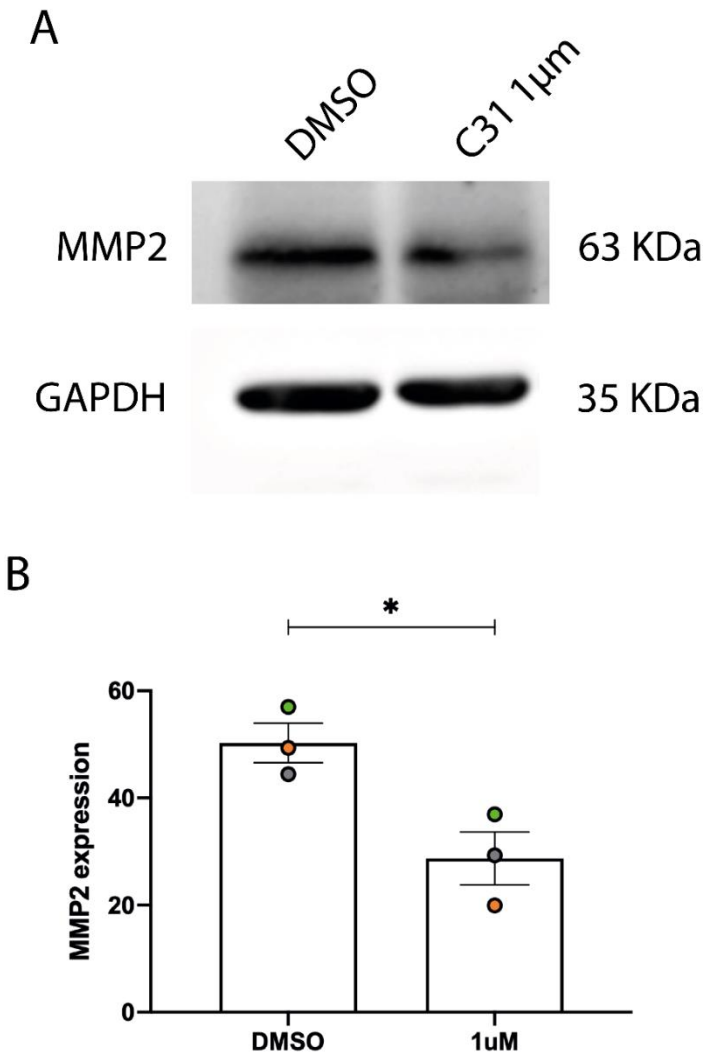

Figure 4. 18. Inhibition of PAK4 activity reduces total level of MMP2 expression in CT-1532 cell line. Western blot analysis of the expression levels of MMP2 in CT-1532 cells. Cells were treated with 1µm/ml of C31 for 24 hours prior lysis in 2x GSB (A). Protein levels were analysed by densitometric analysis. Intensity of bands related to the protein of interest were corrected for the loading control (GAPDH) and plotted as mean±SEM. (B) Experiment was repeated with three independent cell lysates (n=3). Statistical significance was calculated with unpaired student's t-test, *p<0.05.

4.2.11. PAK4 depletion leads to intracellular MT1-MMP accumulation

Having confirmed a link between PAK4 activity and MMP2 expression, we sought to examine the impact of PAK4 depletion on MT1-MMP expression. Interestingly and unexpectedly, Western blot analysis of shPAK4 cell lysates revealed a significant increase in the MT1-MMP levels when compared to shControl cells (Figure 4.19).

This finding was particularly surprising as MT1-MMP participates in invadopodia-dependent matrix degradation and invadopodia activity is heavily affected in shPAK4 cells. MT1-MMP is initially synthesized as a 64 KDa proenzyme that is activated by proteolytic cleavage in the trans-Golgi network (TGN) and subsequently delivered to the plasma membrane (Yana and Weiss 2000). MT1-MMP proteolytic activity at the cell surface is regulated by a balance between exocytosis and caveola/clathrin-mediated endocytosis, which also controls the levels of intracellular MT1-MMP (Remacle, Murphy, and Roghi 2003). It is possible that PAK4 depletion influences intracellular levels of MT1-MMP by affecting its molecular trafficking on the cell surface. To further investigate if PAK4 plays a role in the regulation of MT1-MMP intracellular trafficking, shPAK4 cells were seeded onto coverslips and stained for MT1-MMP.

ShControl showed no evident pattern of MT1-MMP expression, with the protein being sparsely diffused within the cytoplasm of the cell (Figure 4.20A). Interestingly, PAK4 depleted cells exhibited a localised accumulation of MT1-MMP in the perinuclear region of the cell (Figure 4.19A). 53% shPAK4 were characterised by this MT1-MMP deposit compared to 27% shControl cells (Figure 4.20B).

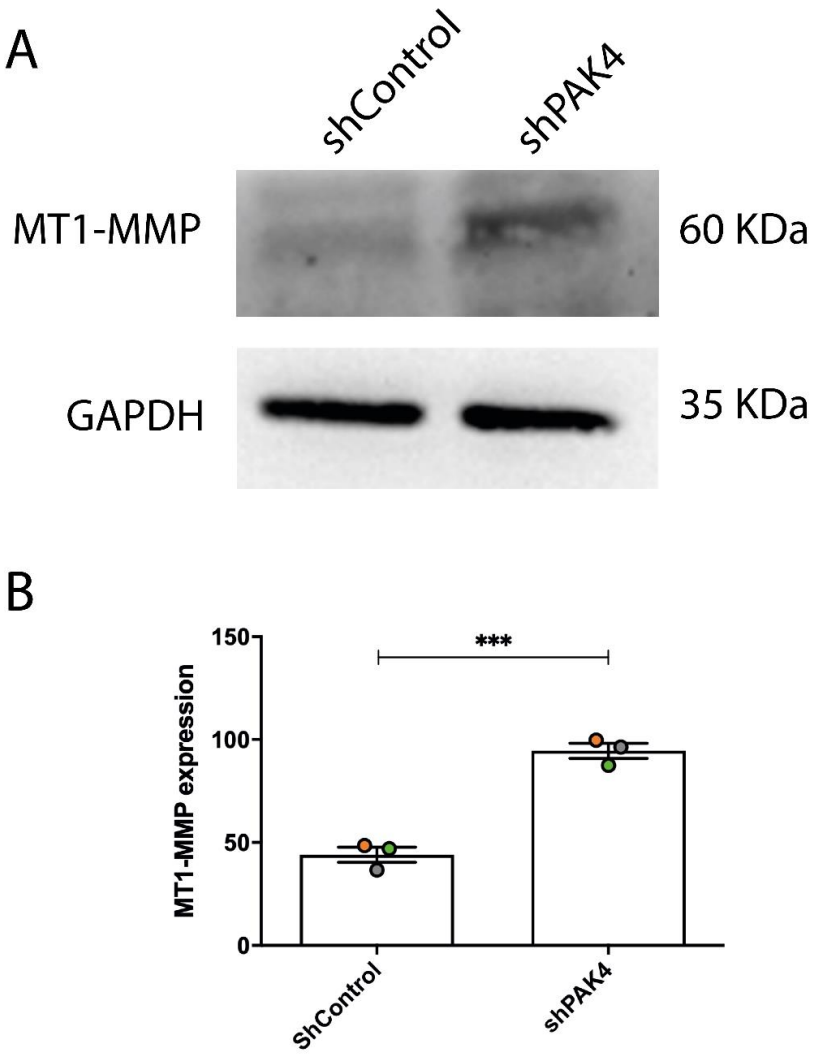

Figure 4. 19: PAK4 depletion increases total level of MT1-MMP expression in CT-1532 cell line.
Western blot analysis of the expression levels of MT1-MMP in CT-1532 shPAK4 cells (A). Protein levels were analysed by densitometric analysis. Intensity of bands related to the protein of interest were corrected for the loading control (GAPDH) and plotted as mean±SEM (B). Experiment was repeated with three independent cell lysates (n=3). Statistical significance was calculated with unpaired student's t-test, *p<0.05.

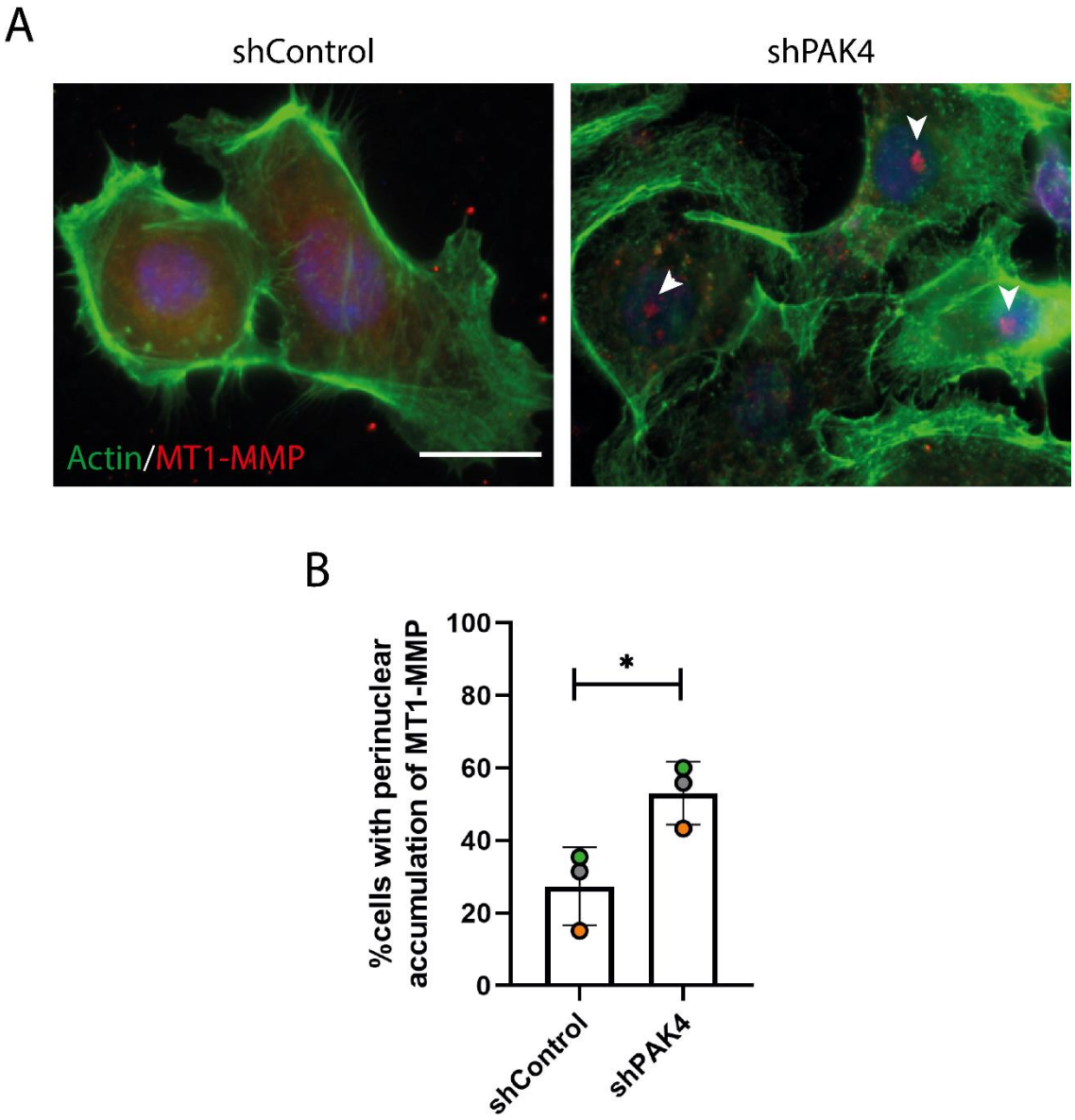

Figure 4. 20: MT1-MMP immunostaining assay in CT-1532 shPAK4 cell line.
Representative images of CT-1532 shPAK4 cell line subjected to immunofluorescent staining to observe the expression of MT1-MMP (red), in combination with actin (green). PAK4 depletion leads to perinuclear accumulation of MT1-MMP, while MT1-MMP is diffused in the cytoplasm in shControl cells (A). Graphical representation indicating the percentage of cells exhibiting perinuclear accumulation of MT1-MMP. Analysis was performed on 90 cells per condition over three independent experiments. Data are presented as mean±SEM. Statistical significance was calculated with unpaired student's t-test, *p<0.05. Scale bar = 10µm.

4.3. Discussion

This chapter investigated the role of PAK4 in prostate cancer invasion. Previous studies have demonstrated overexpression of PAK4 in many type of malignancies including prostate (Callow et al. 2001), and that PAK4 upregulation enhances cancer cell migration (Siu et al. 2010; Whale et al. 2013). PAK4 depletion inhibited cell migration and invasion in non-small cell lung cancer (Cai et al. 2015), choriocarcinoma (H.-J. Zhang et al. 2011) and endometrial cancer (W Lu et al. 2013) in Matrigel transwell invasion assays. To date, however, there have been no studies in primary prostate cancer cell lines regarding their invasive potential in response to PAK4 depletion, and invadopodia development in the context of PAK4 in PCa remains unexplored. To elucidate the role of PAK4 in prostate cancer invasion, PAK4 expression was reduced via siRNA technology in CT-1532 and CT-1535 cell lines, and the effect on cell invasiveness was evaluated by invadopodia assay. Reduction of PAK4 expression by either siRNA or shRNA resulted in a significantly decreased cell invasion in 2D invadopodia assay, confirming that reported in melanoma studies (Nicholas et al. 2016) and highlighting the importance of PAK4 in invadopodia in prostate cancer. Although the same oligos were utilised for the PAK4 transient depletion, the extent of the RNA silencing varied across the cell lines tested. This difference can be explained by the fact that knockdown efficiency is largely dependent on the cell lines used, and it is possible that RNA oligos are subject to a faster degradation in CT-1535 cells than CT-1532 cells. Interestingly, the ability of cells to form invadopodia and degrade the matrix appeared to correlate with the level of PAK4 reduction, as the cells lines characterised by the highest knockdown efficiency exhibited the lowest level of invadopodia activity. Thus, PAK4 is required for invadopodia activity and PAK4 depletion potentially affects invadopodia activity in a dose-dependent manner.

Although siRNA-mediated PAK4 depletion had already been established in the Wells lab and proved to be satisfactory for the time frame required by invadopodia experiment, this technique presents some important limitations. SiRNA molecules often requires high concentrations to achieve an effective knockdown of protein expression due to their rapid degradation and turnover, and thus increasing the possibility of off-target effects (Rao et al. 2009). Moreover, the lack of a reporter gene does not allow discrimination between

transfected and untransfected cells. Conversely, shRNA effects are longer as the shRNA oligo is continuously synthesized in the nucleus of the host cell, and its expression can be tracked by fluorescent tags. Therefore, although siRNA is a convenient way to study the global impact of transient suppression of gene expression, an enriched GFP-tagged shRNA cell population was employed to perform more durable and sensitive studies based on single-cell evaluations of PAK4 depletion.

GFP-tagged shControl and shPAK4 cells were injected in the yolk sac of zebrafish embryos using the same protocol that proved to be successful with primary adenocarcinoma cell lines. Despite the decreased invadopodia activity *in-vitro*, it was found that zebrafish injected with PAK4 knockdown cells did not show any reduction in tumour cell invasion (Figure 4.5). This finding is in contrast with previous studies on melanoma cells employing the same technique (Nicholas et al. 2016), possibly due to cell-type specific differences. It is possible that in prostate cancer PAK4 plays a crucial role in invadopodia regulation but might be dispensable for navigating the tissue architecture in the zebrafish model of invasion. Compared to zebrafish model of invasion, the invadopodia assay allows the visual determination of the cell ability to make invadopodia, whereas the mode of migration employed by metastatic cells in zebrafish cannot be established by simple embryos imaging. Moreover, invadopodia assay represents a more sensitive measurement of the cell activity, qualitatively and quantitatively (Emma T Bowden, Coopman, and Mueller 2001). Hence, they represent two distinct models for studying cells invasive potential. Our findings indicate that It is possible that dissemination *in-vivo* can be achieved by an alternative PAK4-independent pathway, which does not rely on metalloproteases activity. Prostate carcinoma cells are reported to be capable of amoeboid cell migration activity (Morley et al. 2014; Taddei et al. 2011). In amoeboid migration the physical matrix resistance is bypassed by squeezing of the cell body through the ECM preformed gaps, finding a path of invasion by the adoption of an amoeboid shape with no obvious polarity rather than generating one by proteolysis (Wolf et al. 2003). This mode of migration is characterised by increased contractility induced by the Rho-pathway (Sanz-Moreno et al. 2008), and previous reports indicates that PAK4 inhibition enhances RhoA activity (Callow et al. 2005; Wells et al. 2010; Nicholas et al. 2016). If this is the case, PAK4 depletion might lead to a hyperactivation of the RhoA pathway in our prostate cancer cells that could infer a selective advantage to shPAK4 cells, again inducing an amoeboid pattern of invasion. The relationship between PAK4 and RhoA will be explored further in Chapter 5 of this thesis.

It is thought that these two distinguished modes of tumour cell migration are interconvertible and are influenced by the microenvironments of nearby tissues (A. G. Clark and Vignjevic 2015). In particular, it has been shown that variation in the parameters of the ECM such as density and stiffness can trigger the transition between the amoeboid and mesenchymal migration modes (Friedl and Alexander 2011; Taddei et al. 2013). Therefore, it is likely that differences in the properties of the zebrafish yolk sac, which is composed in large part by lipids (Fraher et al. 2016), and gelatin, which is mainly constituted by denatured collagen I, favours an adaptation response towards the amoeboid phenotype that facilitates tumour invasion even in shPAK4 cells. Moreover, additional studies demonstrated that inhibition of proteases in mesenchymal HT-1080 fibrosarcoma and MDA-MB-231 carcinoma cell lines resulted in amoeboid conversion (Wolf et al. 2003; Carragher et al. 2006). Therefore, altering the PAK4 intracellular molecular pathways that are involved in proteolytic-dependant invasion might have led to the adoption of the amoeboid type of invasion independently of the characteristics of the surrounding environment. Indeed it was noted that 1542 cells which have a low level of invadopodia activity perform equally well in the zebrafish invasion assay.

Nevertheless, results presented here reveal that PAK4 is important in invadopodia activity in prostate cancer cells, and the specific requirements of PAK4 was validated in the rescue experiments (Figure 4.17). Given the complexity of the experiment, it is not surprising that a complete rescue to control population level of invadopodia was not seen. Perhaps a better way of proceeding would be the establishment of a stable re-expression of rescue PAK4, to limit the manipulation stress the cells would be subjected to and improve their experimental performance, which was not possible due to the time constraints of the project. To dissect the potential role that each PAK4 functional domain plays in invadopodia regulation, three additional rescue constructs carrying inactivating mutations in different domains were tested alongside the wild-type PAK4. PAK4-H19,22L mirrored the rescue phenotype exhibited by the whole length PAK4, indicating that the N-terminal CRIB domain necessary for the Cdc42/Rac (Abo et al. 1998) was not a key effector for invadopodia regulation. It is already established that PAK4 binding with Cdc42 may not impact on PAK4 kinase activity, suggesting a different regulatory route for Goup II PAKs that varies from that of Group I (Abo et al. 1998). Similarly, depletion of the proline-rich sequences region in PAK4, rescued invadopodia formation and gelatin degradation in invadopodia assay. This sequence has

been reported to interact with the PI3K regulatory subunit p85α (King et al. 2017) but while PAK4 can be activated through PI3K downstream of HGF signalling in epithelial cells (Wells, Abo, and Ridley 2002) recent evidences indicate that in prostate PI3K does not seem to induce PAK4 activation (M.-H. Park et al. 2013). Moreover, PAK4-deltaPxxP comprises the depletion of the GEF interacting domain (GID), which resides in position 298-323, and mediates the inactivating phosphorylation of GEF-H1 (Wells et al. 2010) We can therefore speculate that neither Cdc42, nor PI3K or GID interactions are key mediators of PAK4 activity in invadopodia. In contrast, kinase dead PAK4-K350,351M failed to rescue PAK4 depletion, as these cells did not display a significant increase in invadopodia activity (Figure 4.14). Thus, in our study, PAK4 promotes invadopodia activity via a kinase-dependent mechanism that does not require Cdc42 interaction. Recent findings have demonstrated a direct interaction between the PAK4 GBD domain and RhoU, which is retained even in PAK4-H19,22L mutant protein and cooperates with PAK4 in regulating adhesion turnover (Dart et al. 2015). RhoU, also known as Wrch1, has been implicated in migration and invasion in prostate cancer (Alinezhad et al. 2016). In osteoclasts and c-Src-expressing cells, RhoU localises to podosome and regulates cells motility (Ory, Brazier, and Blangy 2007). Given the close structural and functional association between podosome and invadopodia, it is possible that RhoU plays a role in promoting invadopodia activity. We speculate that RhoU might be involved in PAK4 activation and could participate in the modulation of invadopodia activity by PAK4 in prostate cancer. However, there are currently no reports in the literature that associate RhoU specifically to invadopodia.

Reduction of PAK4 did not reduce the percentage of cells with actin puncta in melanoma, suggesting that PAK4 acts in later stages of invadopodia lifecycle, operating predominantly on matrix degradation (Nicholas et al. 2017). In our study, in contrast, reduction of PAK4 levels also affected puncta formation (Figure 4.10 and 4.11) and invadopodia size (Figure 4.14). These findings could lead to two hypothesis. Either PAK4 only mediates puncta formation, with a loss of formation in prostate cancer cells resulting in reduced matrix degradation. Alternatively, in prostate cells PAK4 functions separately both at the formation stage and at the matrix degradation stage, potentially joining with two different regulatory pathways.

If PAK4 has a specific function in matrix degradation, it might be speculated that PAK4 depletion affects the expression or activity of metalloproteases. Invadopodia ultimately rely on the secretion of metalloproteases (MMPs) to degrade the extracellular matrix, and several PAKs isoforms have been implicated in the regulation of MMPs activity. PAK1 phosphorylation in the invasive breast cancer TMX2–28 cell line stimulates the expression of MMP1 and MMP3 (Rider, Oladimeji, and Diakonova 2013). In contrast, PAK1 activation down-regulated MMP-2 (Rider, Oladimeji, and Diakonova 2013). Pharmacological inhibition of PAK4 using the Compound 31 (C31), led to reduction of MMP2 expression (Figure 4.17), in line with previous report (Hao et al. 2018) and consistent with PAK4 knockdown studies in ovarian cancer (Siu et al. 2010). Soluble MMP2 activity is tightly regulated at both transcriptional and protein level (Yan and Boyd 2007; Sawicki 2013), but the machinery governing MMP2 production and its specific delivery to the invadopodia front remains unclear. MMP2 has been reported to be functionally associated with PAK4 in glioma, where MMP2 is thought to directly interacts with PAK4 through PAK4 kinase domain (Kesanakurti et al. 2012), which might explain why the use of kinase-dead PAK4 mutant was not able to rescue the invadopodia phenotype to the levels of the control population (Figure 4.17). Nevertheless, transmembrane MT1-MMP is known to cleave and activate pro-MMP2 (Strongin et al. 1995). Therefore, it is likely that PAK4 regulation of MMP2 could be achieved via MT1-MMP. Analysis of MT1-MMP level and immunostaining experiments suggest an intracellular accumulation of MT1-MMP in the perinuclear region of PAK4 depleted cells (Figure 4.19). For invadopodia functioning it is essential that MT1-MMP is continuously internalized from the plasma membrane to the endocytic compartment via clathrin and/or caveolar mediated pathways (Remacle, Murphy, and Roghi 2003). Internalized MT1-MMP can be recycled back to the plasma membrane of newly-formed invadopodia through late endosome/lysosomes (Castro-Castro et al. 2016; Remacle, Murphy, and Roghi 2003). Inhibition of MT1-MMP recycling and sequestering of MT1-MMP within intracellular endosomal negatively affects the ability of cells to invade the matrix (Williams and Coppolino 2011; Linklater, Jewett, and Prekeris 2018). The localized accumulation of MT1-MMP observed by immunostaining in shPAK4 cells might be preventing the delivery of the active enzyme at the invadopodium surface, limiting the degradative ability of PAK4 depleted cells. It is possible that PAK4 is involved in the trafficking of the intracellular vesicles containing MMPs for matrix degradation at invadopodia.

The data presented in this chapter indicate that PAK4 drives invadopodia in prostate cancer. Moreover, it was shown that PAK4 regulation of invadopodia dynamics might occur during the early phases of invadopodia lifecycle, by controlling the localized actin polymerisation. Therefore, PAK4 function in invadopodia could be restricted to a specific phase of invadopodia dynamics, or it could play a dual role, by also enhancing matrix degradation via general regulation of metalloproteases activity.

4.4. Future work

This chapter identified PAK4 as a potential invadopodia driver in prostate cancer. Moreover, data suggests that a different mode of invasion could be employed by the primary prostate adenocarcinoma cell lines tested according to the environmental conditions. The contribution of PAK4 to invasion could be further investigated by employing alternative assays such as 3D-spheroids invasion assay, which allows the study of cell invasion in a more physiological, 3D environment compared to 2D studies (Rodrigues et al. 2018). The study of multicellular organoids such as spheroids would permit the acquisition of important sets of data through the analysis of parameters such as spheroids size, compactness, distance of invasion in response to PAK4 pharmacological inhibition or PAK4 depletion. Unfortunately, our attempt to induce spheroids formation in CT-1532 shControl and shPAK4 cell line was unsuccessful, possibly due to an inadequate response of the cells towards the collagen concentration and/or acidic environment. Due to the time constraints of this project, it was not possible to optimize the protocol available in the Wells lab to adapt it to the cell line of interest. It might be noteworthy to assess whether molecular pathways involved in amoeboid migration are overexpressed and compensating for the lack of PAK4 activity in zebrafish invasion assay, by performing knock-down experiments on the ROCK signalling. Additionally, shPAK4 cell behaviour could be further explored in zebrafish using live imaging techniques in this organism, which would allow more detailed comparative studies with melanoma PAK4 depleted cells to be performed. For example, fluorescent transgenic zebrafish lines in which the reporter transgene is specifically expressed in the vascular endothelial cells could be exploited to evaluate the impact of PAK4 depletion on cellular intravasation and extravasation abilities. A thorough investigation into the actin puncta downsizing as a consequence of PAK4 depletion could be carried out through high resolution confocal imaging, which would allow to assess the real puncta size.

Chapter 5

Exploring the PAK4:PDZ-RhoGEF:RhoA interaction

Chapter 5. Exploring the PAK4:DZ-RhoGEF:RhoA interaction.

5.1. Introduction

Previous chapters have demonstrated for the first time that PAK4 is required for invadopodia activity in prostate cancer cell lines. PAK4 has been localised to podosome, degrading protrusions belonging to the cells of the monocytic lineage (Gringel et al. 2006; Wells and Jones 2010; Foxall et al. 2019) and invadopodia in melanoma cells (Nicholas et al. 2016). PAK4 was reported to regulate podosome number and size in primary human macrophage, by altering the cellular actin dynamics (Gringel et al. 2006). Moreover, pharmacological inhibition of PAK4 resulted in a reduction of podosome formation, which was recovered following removal of the inhibitor (Foxall et al. 2019). Also PAK1, a different member of the PAK family and belonging to group I of PAKs (Arias-Romero and Chernoff 2008), has been involved in invadopodia dynamics. In rat mammary adenocarcinoma cells MTLn3 cells PAK1 was localised at mature invadopodia protrusions, together with Cortactin (Moshfegh et al. 2014). Recent studies have pinpointed PAK1 and PAK4 functioning during specific stages of invadopodia lifecycle, highlighting how protein kinases activities in invadopodia can be spatiotemporally restricted to defined phase (Foxall et al. 2016). In A-375M2 melanoma cell line, PAK4 activity was reported to be restricted to the later maturation stages. PAK4 reduction led to decreased matrix degradation but no change was observed in the ability to initiate actin puncta, indicators of nascent invadopodia (Nicholas et al. 2016). In the same study, PAK1 was required for invadopodia formation, rather than maturation, as PAK1 depleted cells were not able to form actin puncta (Nicholas et al. 2016). However, this study has found PAK4 depletion leads to a loss of actin puncta. Differential results across PAK studies have previously been reported. PAK1 phosphorylation of Cortactin at Serine 113, led to contradictory results depending on the cell type tested. In A375MM melanoma cell line cortactin phosphorylation on Ser113 by PAK1 enhanced invadopodia formation (I. Ayala et al. 2008). Oppositely, a more recent study conducted in MTLn3and MDA-MB-231 breast cancer cell lines indicated that PAK1-mediated phosphorylation of Cortactin downstream of Rac1 induces invadopodia disassembly and turnover (Moshfegh et al. 2014). Given the therapeutic interest of developing PAK pharmacological inhibitors, a better understanding of the cell-specificity of PAK activity and the downstream effectors which regulate invadopodia dynamic is crucial.

A designated GEF Interacting Domain (GID) has been identified in group II PAKs, which is highly conserved between PAK4, PAK5 and PAK6 (Callow et al. 2005). Through this domain, PAK4 is reported to interact with GEF-H1 to control localisation and function. (Callow et al. 2005). It has been suggested that PAK4-mediated phosphorylation on Ser-885 of GEF-H1 inhibits its GEF activity, resulting in reduced Rho activation (Callow et al. 2005). In prostate cancer PAK4 has been previously reported to inhibit RhoA exchange activity via GEF-H1 (Wells et al. 2010). Additionally, PAK4 is also reported to interact with another RhoA GEF; PDZ-RhoGEF (Barac et al. 2004). This interaction is thought to drive invadopodia maturation in melanoma cells via inhibiting RhoA activity, as PAK4 depletion led to a remarkable increase in prominent actin stress fibres (Nicholas et al. 2016, 2017).

Studies focusing on the role of RhoA in tumour cell invasion have led to opposite results, with RhoA expression associated with either increased or decreased tumour invasion, depending on the cell type investigated and the experimental technique. RhoA has been shown to enhance cell invasion by promoting invadopodia, amoeboid migration, and influencing tumour cells plasticity and migratory properties (Struckhoff, Rana, and Worthylake 2011).

Overexpression of RhoA increased peritoneal dissemination in rat MM1 hepatoma cells (Yoshioka, Nakamori, and Itoh 1999), and leptin-induced activation of the RhoA/ROCK pathway in OVCAR3 and SKOV3 ovarian cancer cells resulted in enhanced Matrigel invasion (Ghasemi et al. 2017). Knockdown of RhoA expression via siRNA in MDA-MB-231 breast cancer cells inhibited cell proliferation and invasion through Matrigel, and negatively affected tumour growth and angiogenesis *in-vivo* (Pillé et al. 2005). These studies support the hypothesis of a pro-invasive role for RhoA. Conversely, MDA-MB-231 cells depleted of RhoA expression exhibited elongated cellular protrusions enriched in Cortactin and efficiently invaded in a 3D invasion assay in Matrigel (Vega et al. 2011). Similar results were observed in PC3 prostate cancer cell line (Vega et al. 2011) and SUM-159 and MCF-7 breast cancer cell lines (Simpson, Dugan, and Mercurio 2004). Moreover, mice implanted with breast cancer 4T1 cells depleted of RhoA expression exhibited enhanced metastatic dissemination in the lung (Kalpana et al. 2019).

The mechanisms by which RhoA can have opposite effects on cancer cell invasion are not clear. It is possible that different RhoA substrates and downstream effectors are activted according to the experimental assay and the length or level of RhoA depletion.

This chapter investigates the involvement of RhoA in invadopodia in prostate cancer as potential downstream effector of PAK4, and examine whether the PAK4 regulates RhoA activity by acting on specific RhoA GEFs.

5.2. Results

5.2.1. CT-1532 cells do not exhibit an increase in stress fibre formation in response to RhoA activation or PAK4 depletion

Actin stress fibres are contractile actomyosin bundles involved in cell adhesion and morphogenesis, and their assembly has been correlated to increased cell rigidity and reduced cell motility (Friedl and Wolf 2003). Stress fibres formation is predominantly induced by the small GTPases RhoA via its effectors: Rho-associated protein kinase (ROCK) and the formin mDia1 (Ridley and Hall 1992; Leung et al. 1996; Watanabe et al. 1997). Recent studies suggested a correlation between PAK4 activity and actin stress fibres formation: in epithelial cells, activated PAK4 causes a decrease in stress fibres (Wells, Abo, and Ridley 2002), whereas in prostate cancer DU-145 cells PAK4 knockdown induced an increase in RhoA activity which, in turn, increased the number of prominent stress fibres (Wells et al. 2010). This induction of actin stress fibres formation was also observed in melanoma cells depleted of PAK4 expression concomitant with increased levels of active RhoA (Nicholas et al. 2016). It was therefore hypothesised that PAK4 depletion in prostate CT-1532 cells would increase stress fibres formation in response to hyper-activation of RhoA. However, analysis of cell phenotype on glass and gelatin revealed that shPAK4 cells do not have prominent actin stress fibres, and no apparent changes were observed between shControl and shPAK4 cell lines (Figure 5.1).

The highly metastatic prostate cancer cell line PC3 has been reported to have very few stress fibres under basal growth conditions, and filaments assembly was not detected following reduced PAK4 expression (Ahmed et al. 2008). It is therefore possible that the lack of stress fibres observed in shPAK4 cells is due to the inability of CT-1532 cell line to undergo significant stress fibres formation following RhoA activation. To test this hypothesis, parental CT-1532 cells were stimulated with Lysophosphatidic acid (LPA) to induce RhoA activation (Kranenburg et al. 1999). 10µM of LPA for 1 hour was established as an optimal concentration and duration of treatment based on the literature (Guo et al. 2006) and previous experiments conducted in the Wells lab. The non tumorigenic mouse fibroblast NIH/3T3 cell line served as positive control (Kuo et al. 2003).

NIH/3T3 cells treated with LPA showed numerous well-organized actin stress fibres, which increased by 78% compared to untreated cells (Figure 5.2). In contrast, LPA stimulated CT-

1532 cells were indistinguishable from the control, and both cell populations had only 7% of cells exhibiting prominent actin stress fibres (Figure 5.2)

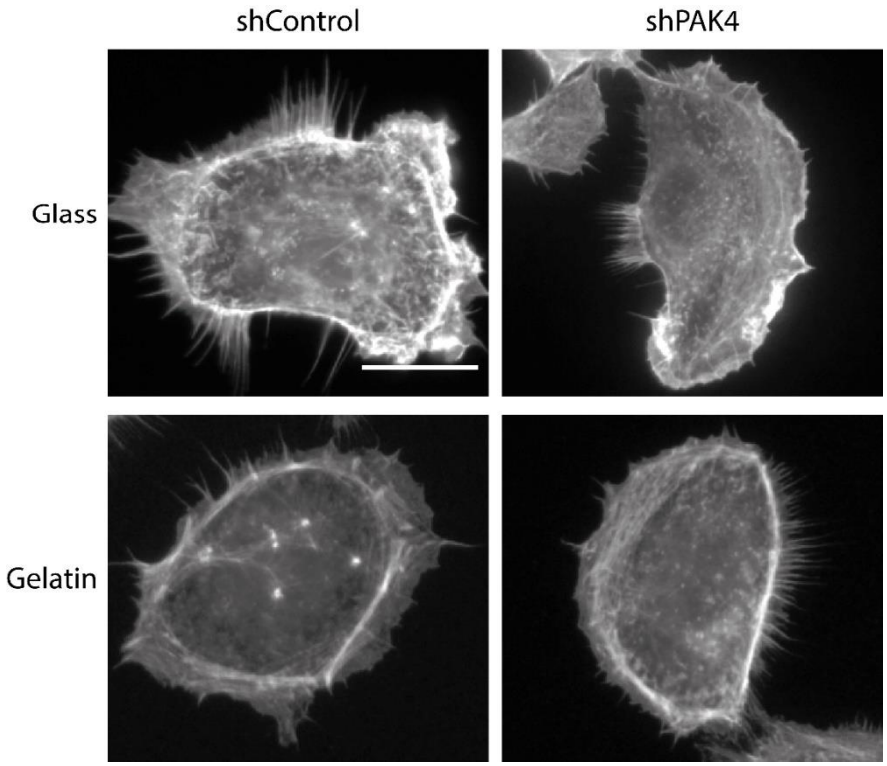

Figure 5. 1: Representative images of PAK4 depleted CT-1532 cells seeded on glass and gelatin.
Cells were seeded on Cy3-conjugated gelatin or glass coverslips for 24 hrs and stained for F-actin to visualize the presence of actin stress fibres in PAK4 depleted cells compared to control. Scale bar = 10µm

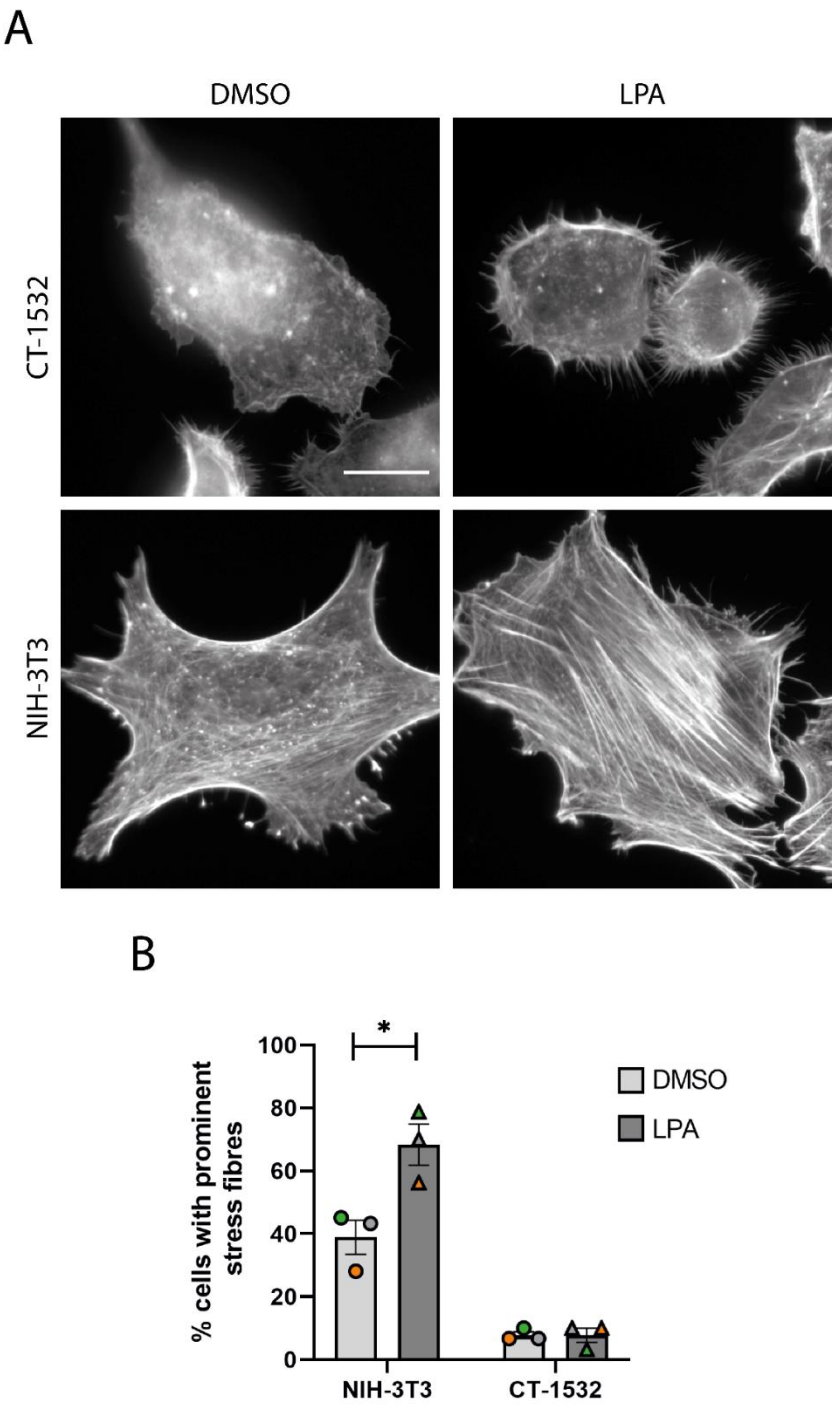

Figure 5. 2: Analysis of actin stress fibres formation in PAK4 depleted cells an NIH/3T3 cells after LPA treatment.

Representative images of CT-1532 and NIH/3T3 cells after treatment with 10µM of LPA. After 1 hour incubation, cells were fixed and stained or F-actin in order to allow the visualization of actin stress fibres formation (A). Graphical representation of the percentage of cells exhibiting prominent stress fibres in LPA treated cells compared to control cells (B). Significance was calculated with student's t-test across the single cell lines. *p<0.05. Data are presented as mean values ± S.E.M. Scale bar = 10µm.

5.2.2. CT-1532 cells increase cell roundness in response to RhoA activation or PAK4 depletion

Analysis of cytoskeletal actin fibres conducted in this study found that no assembly of prominent stress fibres existed in prostate CT-1532 cells, not even in case of direct RhoA activation by LPA treatment. Therefore, it was not possible to understand whether PAK4 depletion in prostate cancer cells is able to induce the activation of RhoA solely on the base of actin filaments assembly in our shPAK4 cells. Following these observations, cell shape was examined to check for alternative morphological phenotypes that have been linked to RhoA activation. Activation of RhoA is known to promote a more rounded cell shape with less processes (Ridley and Hall 1992; Kranenburg et al. 1999; Tseliou et al. 2016), whereas RhoA inhibition by siRNA or C3 transferase induced cell elongation in PC3 cells (Vega et al. 2011). Hence, the cell roundness was measured in CT-1532 cells in which RhoA was activated by LPA treatment to identify any morphological change that might indicate an activation of RhoA signalling. Morphological analysis revealed a significant rounding of the cell body in response to LPA in CT-1532 cells compared to unstimulated cells (Figure 5.3), in agreement with previous studies (Kranenburg et al. 1999). Likewise, PAK4 depleted cells were significantly rounder compared to control cells (Figure 5.4). These findings suggest that the rounder cell morphology in shPAK4 is indicative of an activation of the RhoA-GTP signalling pathway in the absence of stress fibres induction.

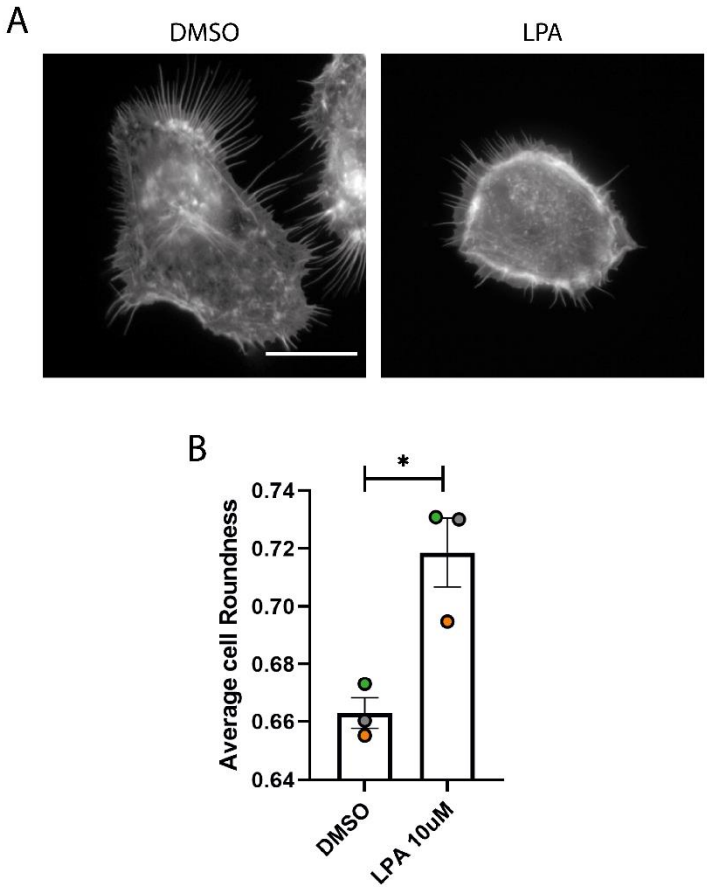

Figure 5. 3: Cell shape analysis of CT-1532 cells after LPA treatment.
Representative images of CT-1532 cells after treatment with 10µM of LPA. After 1 hour incubation, cells were fixed and stained or F-actin (A). Graphical representation of the average cell roundness in LPA treated cells compared to control cells (B). Significance was calculated with student's t-test. *p<0.05. Data are presented as mean values ± S.E.M. Scale bar = 10µm.

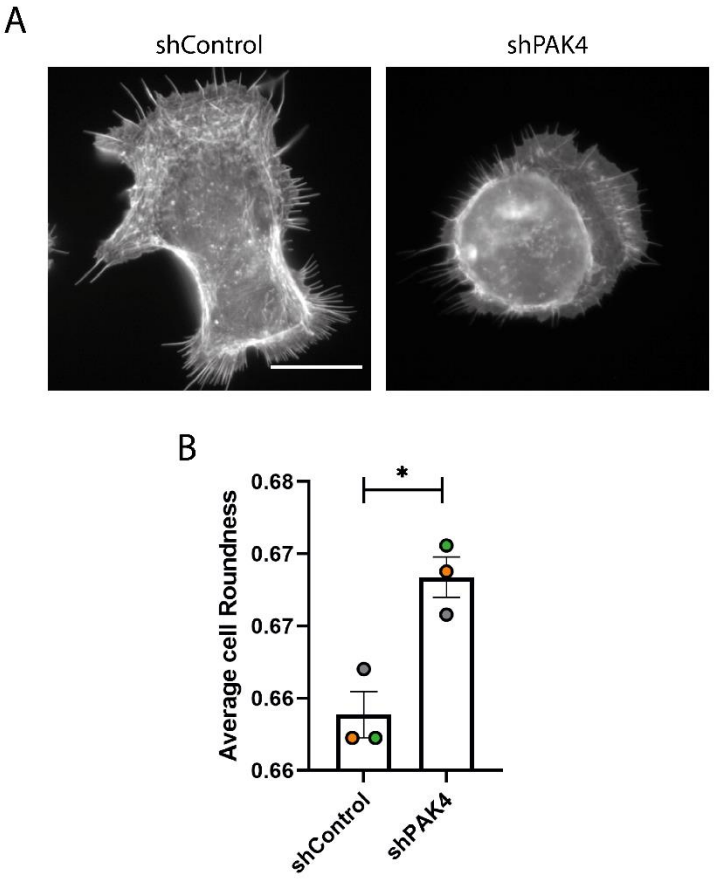

Figure 5. 4: Cell shape analysis of PAK4 depleted CT-1532 cells.
Representative images of PAK4 depleted CT-1532 cells fixed and stained or F-actin for the analysis of cell morphology (A). Graphical representation of the average cell roundness in PAK4 depleted cells compared to control cells (B). Significance was calculated with student's t-test. *p<0.05. Data are presented as mean values ± S.E.M. Scale bar = 10µm

5.2.3. PAK4 depletion increases RhoA-GTP levels

To directly determine whether PAK4 depletion impacts on RhoA activation, RhoA-GTP levels were evaluated via a pull down assay using GST-Rhotekin-RBD beads. The Rho binding domain (RBD) of the human Rhotekin protein specifically recognises and binds to GTP-bound and not GDP-bound, Rho proteins. Consistent with our hypothesis, and with studies conducted on melanoma (Nicholas et al. 2016), PAK4 knockdown significantly increased the amount of RhoA-GTP levels by approximately 75% compared to the control population (Figure 5.5).

RhoC, another member of the Rho-GTPases family has been linked to invadopodia activity. Despite the sequence similarity between RhoA and RhoC, these two proteins are thought to play differential roles in cancer invasion (Vega et al. 2011). RhoC knockdown significantly decreased invasion and led to shorter and less efficient invadopodial protrusion (Bravo-Cordero et al. 2011). Bravo-Cordero et al. demonstrated that RhoC activation is subjected to a fine spatiotemporal regulation during invadopodium formation and RhoC-GTP is confined to a ring-shaped area around the invadopodium actin core (Bravo-Cordero et al. 2011). To test whether the invadopodia phenotype observed in shPAK4 cells could be associated to altered levels of RhoC-GTP, shPAK4 cell lysates subjected to Rho pulldown were additionally probed for RhoC. No differences were detected in RhoC-GTP levels in shPAK4 cells compared to the shControl cells (Figure 5.6), suggesting that PAK4 specifically regulates RhoA activity.

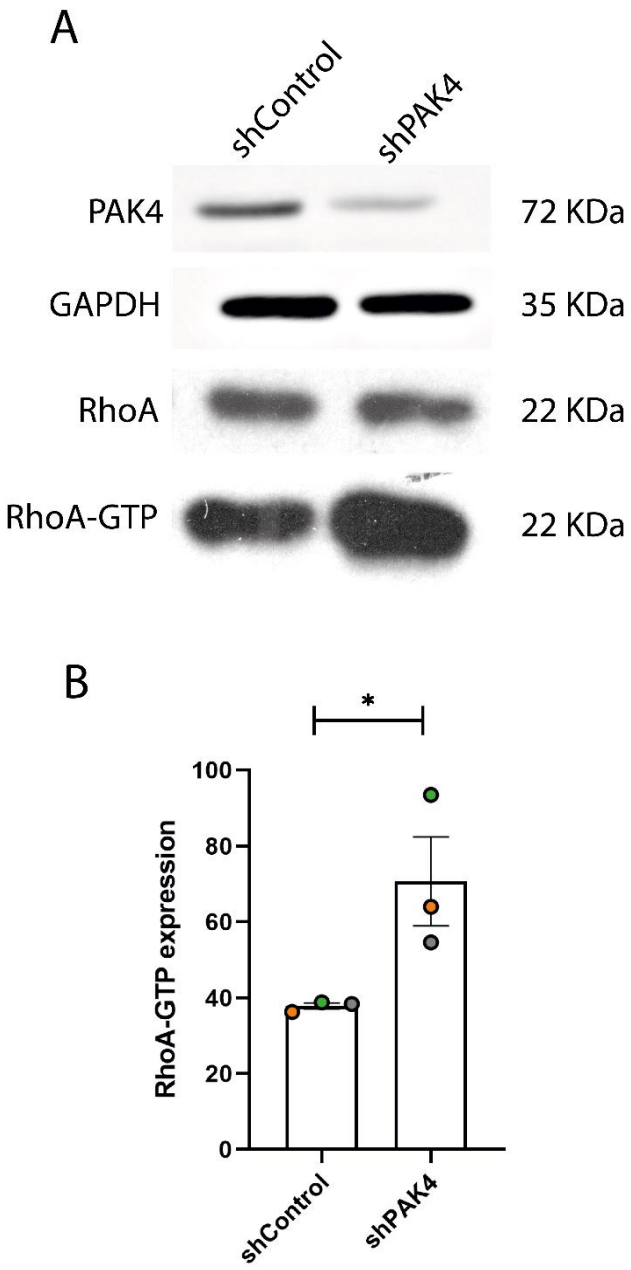

Figure 5. 5: Analysis of RhoA-GTP levels in PAK4 depleted CT-1532 cells.
Western blot analysis of the levels of active RhoA in PAK4 depleted CT-1532 cells. Cells lysates were incubated with Rhotekin-RBD beads and Rho-conjugated beads were precipitated by centrifugation and probed for RhoA, PAK4 and GAPDH (A). Protein levels were analysed by densitometric analysis. Intensity of bands related to RhoA-GTP were corrected for the expression level of total RhoA and plotted as mean±SEM (B). Experiment was repeated with three independent cell lysates (n=3). Statistical significance was calculated between shControl and and shPAK4 cancer cell with Student's t-test, *p<0.05.

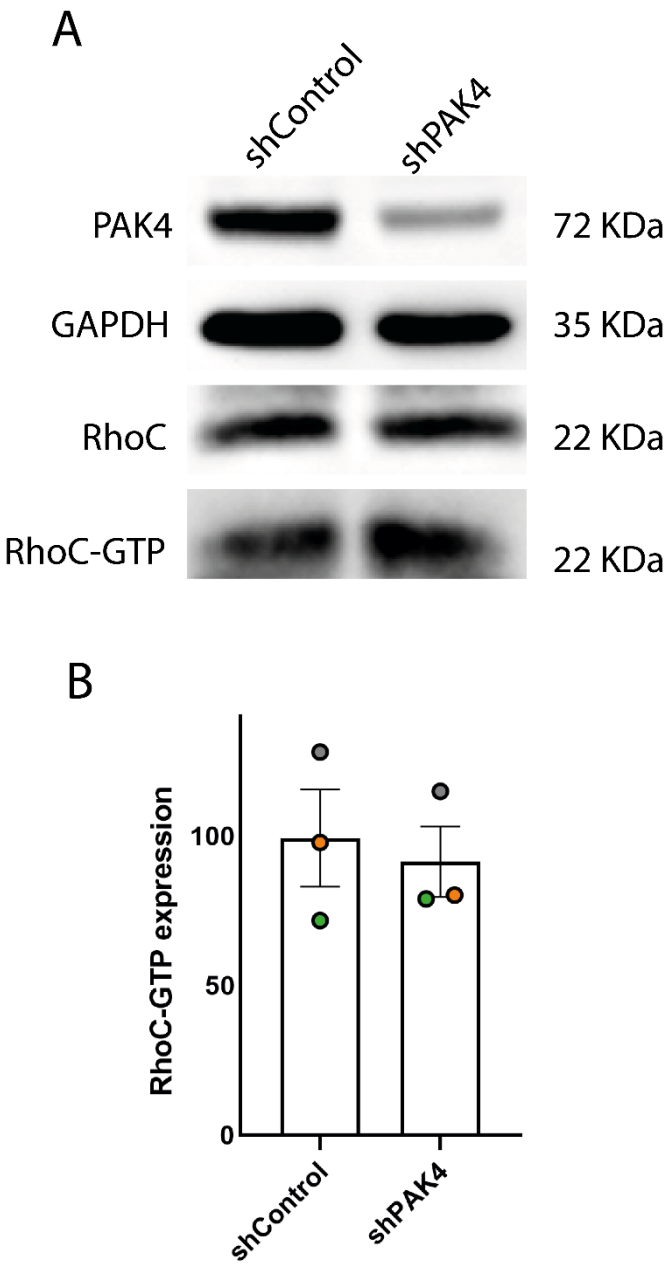

Figure 5. 6: Analysis of RhoC-GTP levels in PAK4 depleted CT-1532 cells
Western blot analysis of the levels of active RhoC in PAK4 depleted CT-1532 cells. Cells lysates were incubated with Rhotekin-RBD beads and Rho-conjugated beads were precipitated by centrifugation and probed for RhoC, PAK4 and GAPDH (A). Protein levels were analysed by densitometric analysis. Intensity of bands related to RhoC-GTP were corrected for the expression level of total RhoC and plotted as mean±SEM (B). Experiment was repeated with three independent cell lysates (n=3). Statistical significance was calculated between shControl and and shPAK4 cancer cell with Student's t-test.

5.2.4. Inhibition of RhoA activity by C3 transferase reduces matrix degradation

The findings presented so far indicate a link between PAK4 and RhoA activity in prostate cancer cells. RhoA is a well-known orchestrator of invadosome dynamics (Spuul et al. 2014), but there are contradictory data regarding its precise role in invadopodium function. Mounting evidence indicates that RhoA might be specifically important for invadopodium maturation, as RhoA reduction led to a drastic reduction of matrix degradation (Sakurai-Yageta et al. 2008; Bravo-Cordero et al. 2011). Moreover, constitutive activation of the RhoA signalling pathway resulted in increased formation of invadopodia, facilitating tumour intravasation (Roh-Johnson et al. 2014). Having observed that the PAK4 reduction significantly induces RhoA-GTP activity in prostate cancer cells in concomitance with decrease of invadopodia formation and activity, we sought to determine the specific effect of RhoA inhibition on invadopodia function in prostate cancer cells.

RhoA activity was pharmacologically inhibited via C3 Transferase, a bacterial enzyme that blocks RhoA function by ADP ribosylation on Asparagine 41, rendering the protein biologically inactive (Wilde and Aktories 2001). C3 Transferase is known to exert its major influence on RhoA activity, while having little effect on the other members of the Rho family RhoB and RhoC (Wilde and Aktories 2001). C3 treatment of Src-transformed NIH/3T3 cells has been reported to disrupt both invadosome structure and the associated ECM degrading activity(Berdeaux et al. 2004). CT-1532 cells treated with 0.5 µg/ml of C3 Transferase exhibited a remarkable decrease of matrix degradation when compared to the control population (Figure 5.7A-B) (Berdeaux et al. 2004). A similar trend towards a lower number of cells forming invadopodia, positive for overlapping of actin puncta and matrix degradation, was observed upon C3 treatment, although not statistically significant (Figure 5.7C).

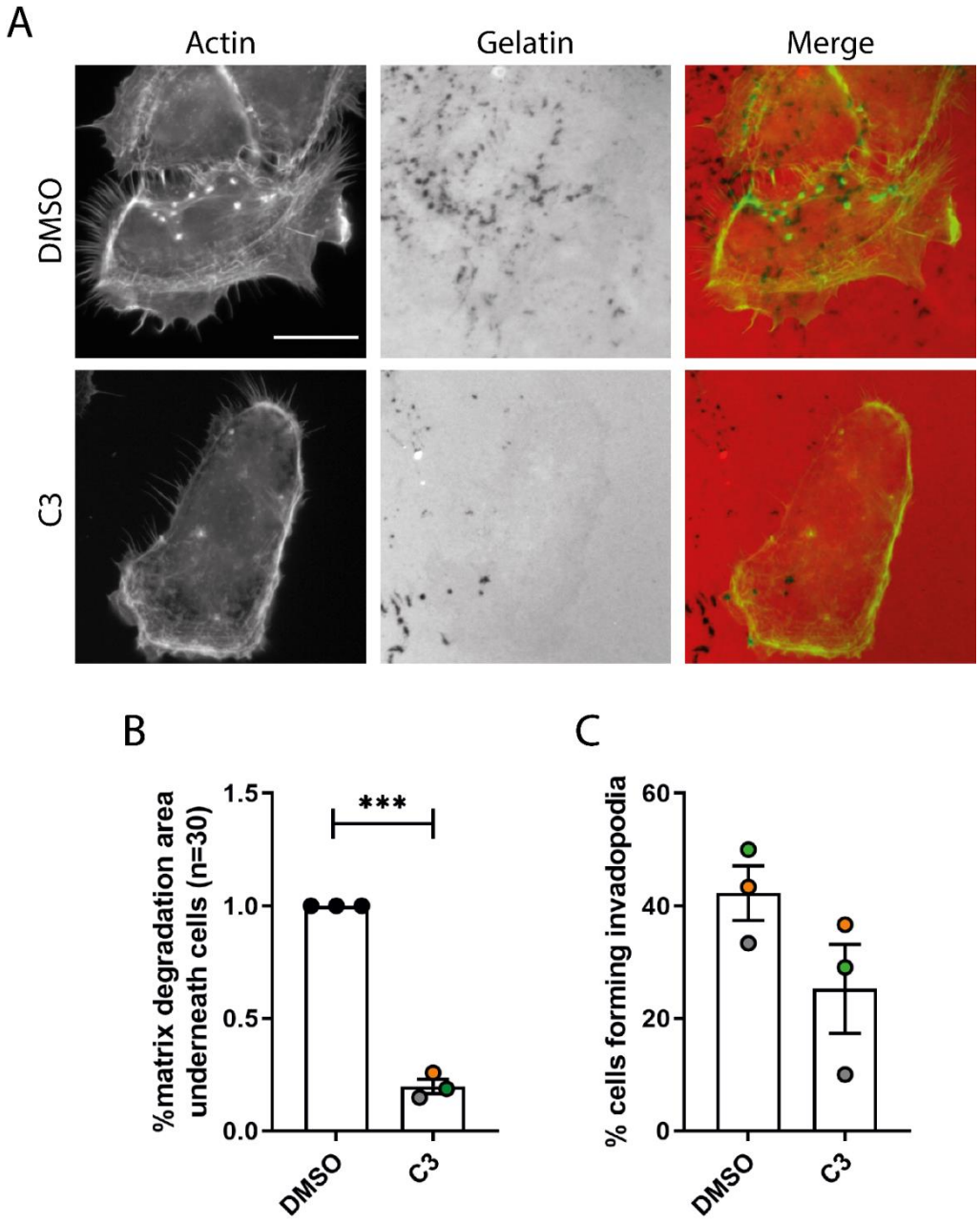

Figure 5. 7: Invadopodia assay of CT-1532 after C3 Transferase treatment.
Representative invadopodia assay images of CT-1532 cell line treated with 0.5 µg/ml of C3 Transferase to inhibit Rho activity. Cells were seeded on Cy3-conjugated gelatin for 24 hrs and stained for F-actin (A). Graphical representation of the percentage of degraded area underneath cells surface (B) and the percentage of cells making invadopodia (C). Significance was calculated with student's t-test. ***p<0.001. Data are presented as mean values ± S.E.M. Scale bar = 10µm.

5.2.5. Transient RhoA depletion reduces matrix degradation and invadopodia formation in CT-1532 cell line

The C3 Transferase experiment indicate a role for Rho family proteins in invadopodia in prostate cancer. To ensure that the invadopodia phenotype observed was specific to RhoA inhibition, RhoA expression was depleted in CT-1532 cells via siRNA technology prior to the invadopodia assay. Transient RhoA knockdown in CT-1532 cell line was achieved using two different siRhoA oligos. RhoA expression was successfully reduced by 65% in case of oligo 1 (Figure 5.8A-B), and 70% in case of oligo 2 compared to the siControl population (Figure 5.8C-D) at 96 hours (4 days) post transfection, which corresponds to the time frame required for performing knockdown experiment and the subsequent invadopodia assay.

Having established two siRNA sequences that can effectively diminish RhoA expression, the effect of RhoA depletion on the ability of CT-1532 cells to form invadopodia was examined. RhoA knockdown using oligo 1 dramatically decreased matrix degradation, as well as the number of invadopodia-forming cells (Figure 5.9), in agreement with previous reports (Bravo-Cordero et al. 2011). These data were validated by the use of a second oligo, which impaired ECM degradation, but did not show a significant effect on the number of cells forming invadopodia (Figure 5.10). These findings further validate the importance of RhoA in matrix degradation.

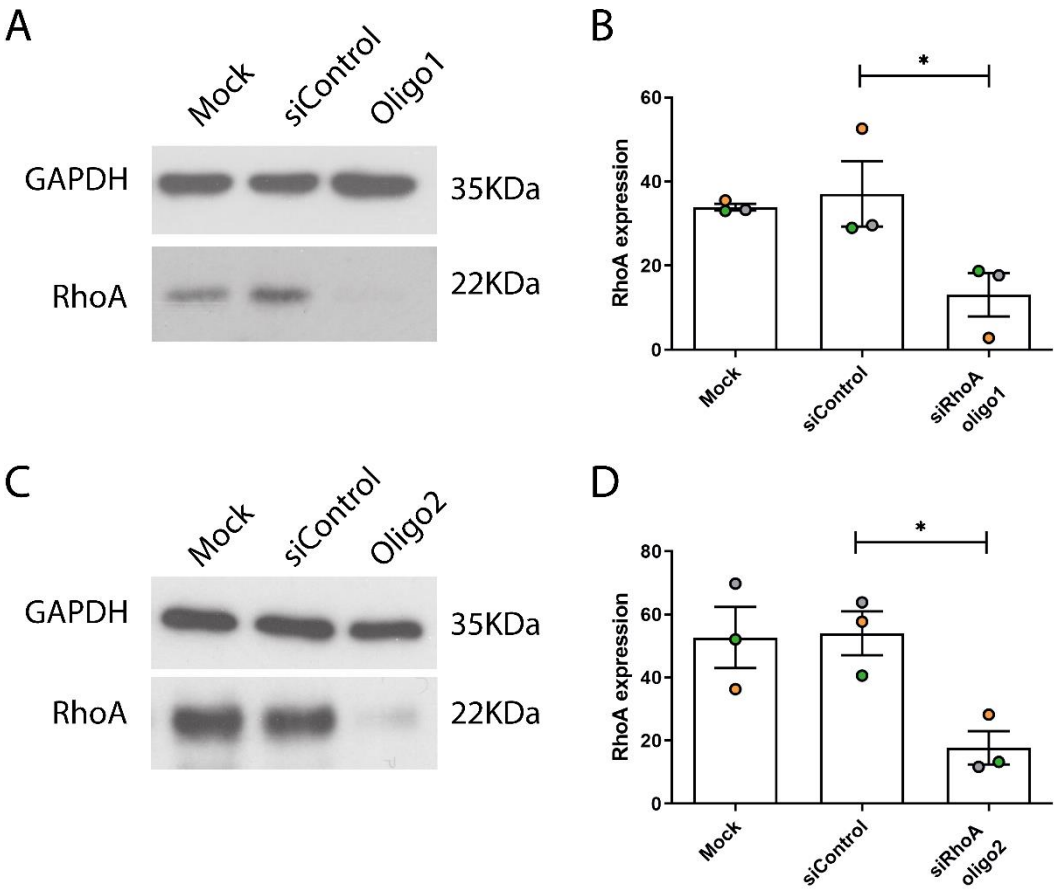

Figure 5. 8: Transient reduction of RhoA expression in CT-1532 cell line by siRNA.
Western blot analysis of the expression levels of RhoA in CT-1532 following transient transfection with two different PAK4 siRNA ooligonucleotides and RNAiMAX transfection reagent. Control cells were transfected with a control siRNA (siControl) or treated with transfection reagents in absence of oligos (Mock). RhoA expression levels were analysed by Western blot 72 hours post-transfection with siRhoA oligo 1 (A). Protein levels were analysed by densitometric analysis. Intensity of bands related to the protein of interest were corrected for the loading control (GAPDH) and plotted as relative ratio mean±SEM for oligo 1 (B). Western blot analysis of the expression levels of RhoA in CT-1532 following transient transfection with siRhoA oligo 2 (C) and the protein levels analysed by densitometric analysis for SiRhoA oligo 2 (D). Experiment was repeated with three independent cell lysates (n=3). Statistical significance was calculated against the siControl cell lines with One-way Anova followed by Tukey's multiple cmparison test, *p<0.05.

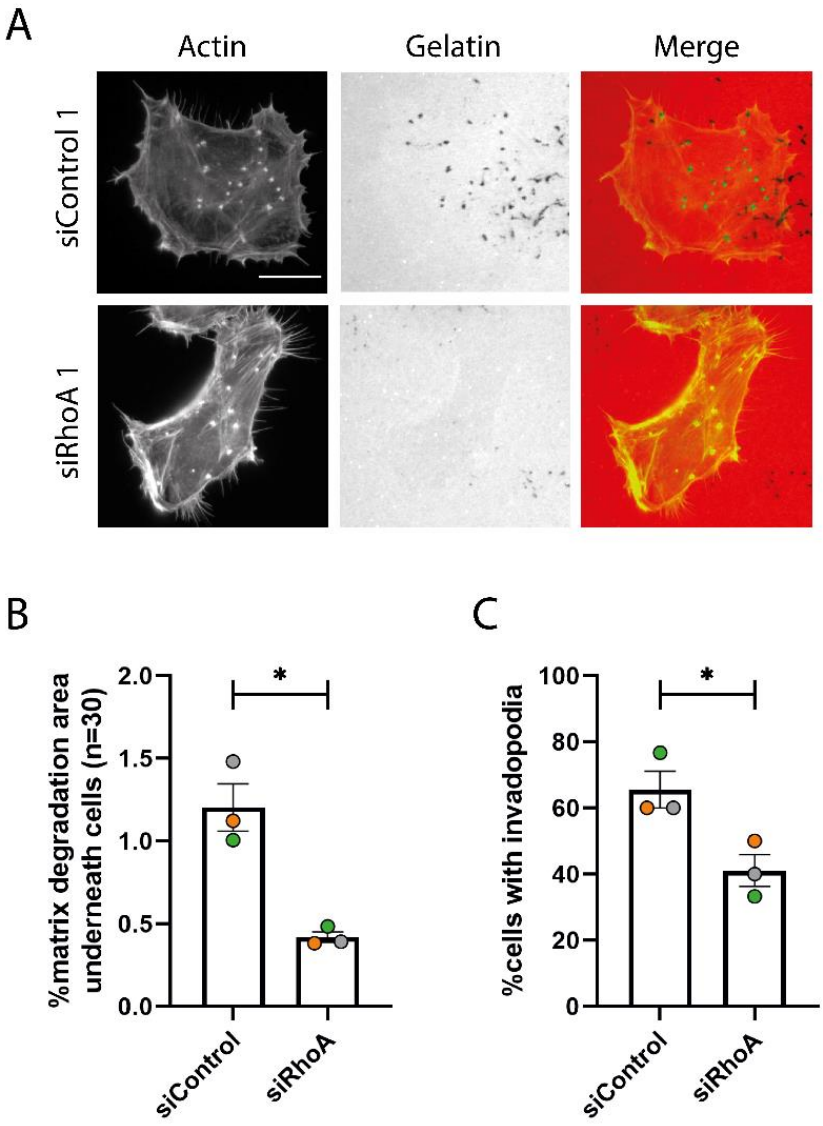

Figure 5. 9: Invadopodia assay of CT-1532 siRhoA oligo 1 cells.
Representative invadopodia assay images of RhoA depleted CT-1532 cells with siRhoA oligo 1. Cells were seeded on Cy3-conjugated gelatin for 24 hrs and stained for F-actin (A). Graphical representation of the measurement of the degraded area underneath cells surface (B) and the percentage of cells forming invadopodia (C). Significance was calculated against the siControl population with Student's t-test. *p<0.05. Data are presented as mean values ± S.E.M. Scale bar = 10µm.

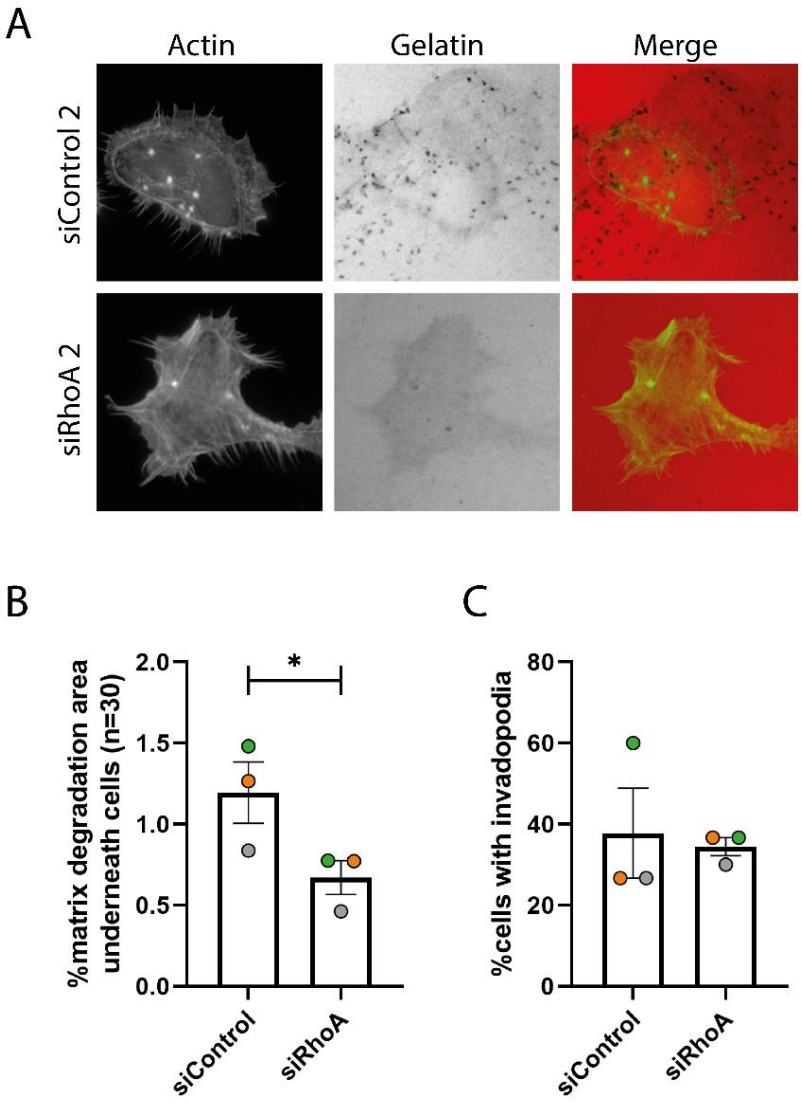

Figure 5. 10: Invadopodia assay of CT-1532 siRhoA oligo 2 cells.
Representative invadopodia assay images of RhoA depleted CT-1532 cells with siRhoA oligo 2. Cells were seeded on Cy3-conjugated gelatin for 24 hrs and stained for F-actin (A). Graphical representation of the measurement of the degraded area underneath cells surface (B) and the percentage of cells forming invadopodia (C). Significance was calculated against the siControl population with Student's t-test. *p<0.05. Data are presented as mean values ± S.E.M. Scale bar = 10µm.

5.2.6. RhoA inhibition does not affect actin puncta formation

Results presented in Chapter 3 revealed that PAK4 depletion negatively affects actin puncta formation, which are considered to be invadopodia precursors. Interestingly, while RhoA has been reported to be essential for invadopodia degradation in rat mammary adenocarcinoma, it was dispensable for invadopodia precursor formation (Bravo-Cordero et al. 2011).

To investigate if RhoA functions in invadopodium precursor core initiation or stabilization in prostate cancer cells, the percentage of cells with actin puncta when plated on gelatin was calculated in siRhoA and C3 treated cells. RhoA reduction with either siRNA oligo #1 or #2 had no effect on the percentage of cells with actin puncta when compared to the control population (Figure 5.11). Similarly, no significant differences were observed in cells following treatment with C3 Transferase (Figure 5.12). These findings suggest that RhoA activation is likely required at later stage during the maturation of the protrusion rather than formation, and possibly RhoA is inactive during the early phase of precursor formation.

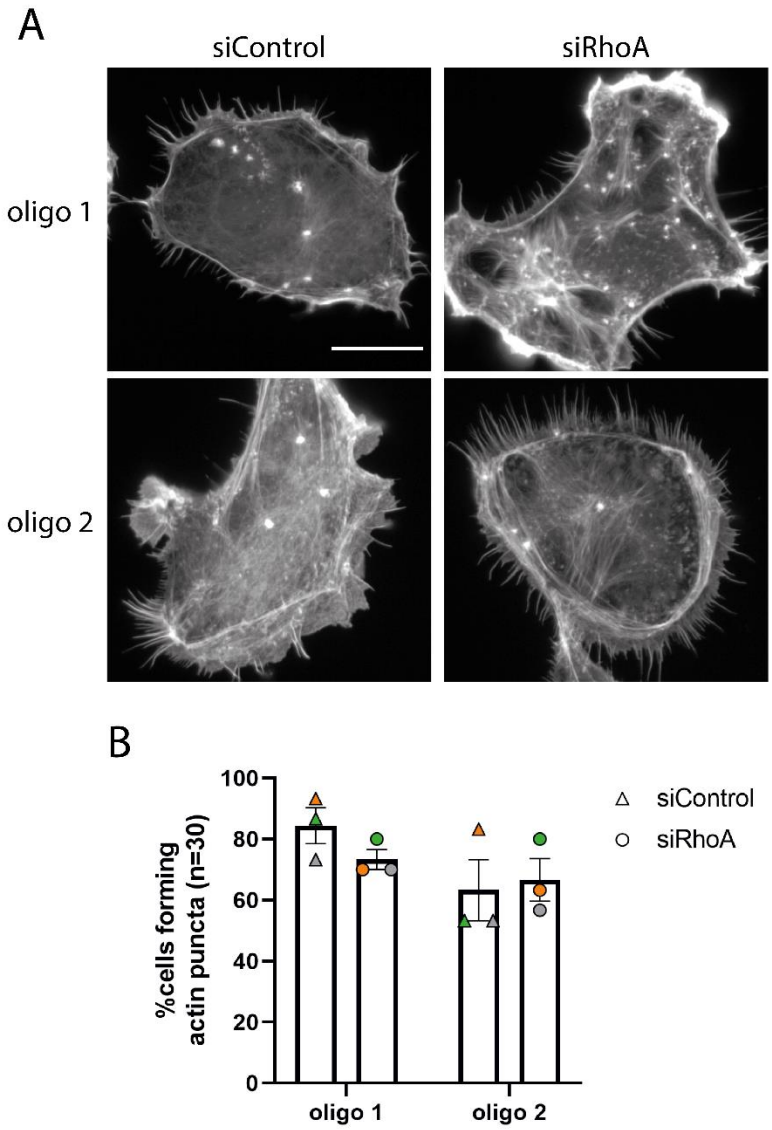

Figure 5. 11: Analysis of actin puncta formation in CT-1532 siRhoA cell lines.
Representative images of CT-1532 cells with reduced RhoA expression via siRNA oligo 1 or oligo 2. Cells were seeded on Cy3-conjugated gelatin for 24 hrs and stained for F-actin (A). Graphical representation of percentage of cells forming prominent actin puncta in CT-1532 siRhoA cells (B). Significance was calculated against the respective siControl population with Student's t-test. Data are presented as mean values ± S.E.M. Scale bar=10µm

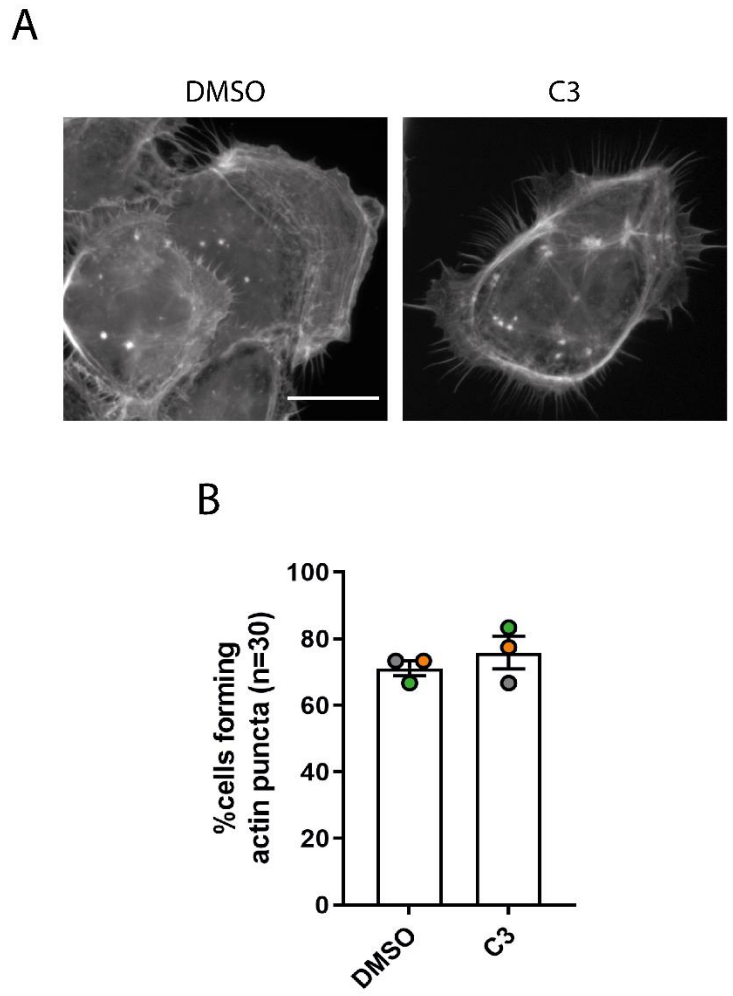

Figure 5. 12: Analysis of actin puncta formation in CT-1532 after treatment with C3 Transferase.
Representative images of CT-1532 cells treated with 0.5 µg/ml of C3 Transferase to inhibit Rho activity. Cells were seeded on Cy3-conjugated gelatin for 24 hrs and stained for F-actin (A). Graphical representation of percentage of cells forming prominent actin puncta in CT-1532 cells upon C3 Transferase treatment (B). Significance was calculated against the respective siControl population with Student's t-test. Data are presented as mean values ± S.E.M. Scale bar=10µm

5.2.7. C3 treatment in shPAK4 cells restores puncta formation but not matrix degradation

PAK4 depleted cells exhibited increased levels of RhoA-GTP (Figure 5.5), indicating a negative regulation of RhoA activity by PAK4. Additionally, cells with reduced level of RhoA were not able to degrade the matrix while still forming actin puncta. If PAK4 negatively regulates RhoA during invadopodia formation, inhibition of RhoA activity in PAK4 depleted cells, which lack of both puncta assembly and matrix degradation, may restore formation the of invadopodia precursor.

Thus, PAK4 depleted cell lines were subjected to C3 Transferase treatment followed by invadopodia assay (Figure 5.13A). Interestingly, the number of cells forming actin puncta increased in the shPAK4 cells upon C3 Transferase treatment to a level similar to the control population, and remarkably increased when compared to the untreated shPAK4 cells (Figure 5.13C). Therefore, inactivation of RhoA by C3 Transferase in PAK4 depleted cells was able to rescue the actin puncta formation, indicators of nascent invadopodia.

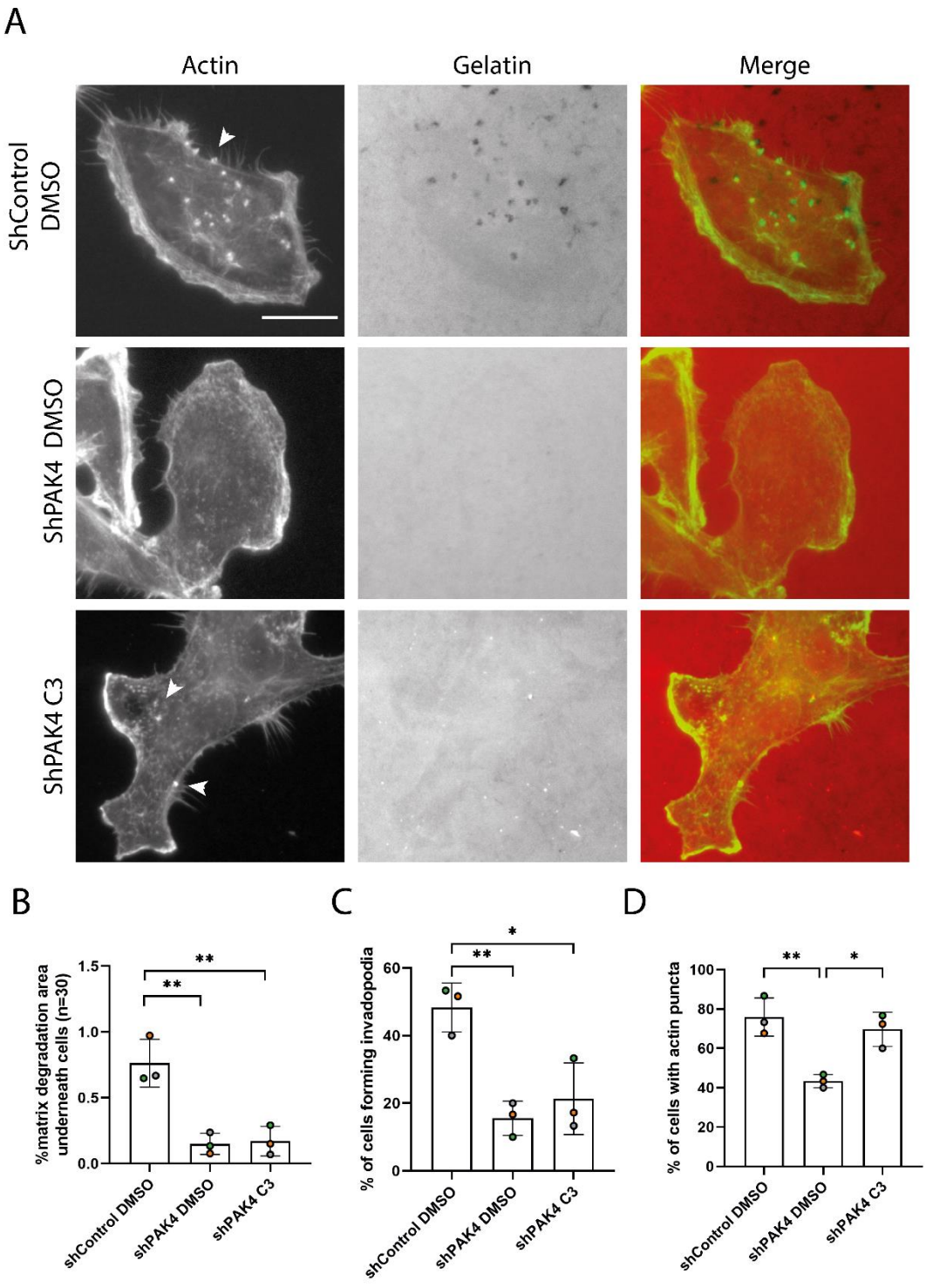

Figure 5. 13: Invadopodia assay of PAK4 depleted cells CT-1532 after C3 Transferase treatment.
Representative invadopodia assay images of shPAK4 CT-1532 cell line treated with 0.5 µg/ml of C3 Transferase to inhibit Rho activity. Cells were seeded on Cy3-conjugated gelatin for 24 hrs and stained for F-actin (A). Graphical representation of the percentage of degraded area underneath cells surface (B), the percentage of cells making invadopodia (C) and the percentage of cells with prominent actin puncta (D). Significance was calculated with One-way Anova followed by Tukey's multiple comparison test against the shControl population or the shPAK4 cell line, *p<0.05, **p<0.01. Data are presented as mean values ± S.E.M. Scale bar = 10µm.

5.2.8. RhoA-GTP biosensor localises around invadopodia

Bravo-Cordero et al. previously identified a spatiotemporal patterns of RhoC activation around invadopodia using an inducible RhoC FLARE biosensor, which was expressed in rat mammary adenocarcinoma cell lines (Bravo-Cordero et al. 2011). The same methodology applied to RhoA did not reveal a well-defined patterns of RhoA activity during invadopodia development, but rather a casual fluctuation in between the core and the outside region of invadopodia structure (Bravo-Cordero et al. 2011). However, stable expression of RhoA biosensor might results in saturation of RhoA signal. Therefore, expression of exogenous RhoA might not properly mirror the endogenous pattern of RhoA activation and might not allow to discriminate between small variation of RhoA activation within subcellular structures such as invadopodia. Indeed, RhoA function and regulation in invadopodia is likely highly complex and probably dependant on the cell-type and experimental technique adopted (Spuul et al. 2014). Having established a specific significance for RhoA in invadopodia in prostate cancer, we sought to determine the distribution of endogenous RhoA-GTP in the invadopodia context. The AHPH-GFP RhoA biosensor developed by Piekny and Glotzer (Piekny and Glotzer 2008) was chosen to directly visualized active RhoA-GTP. The biosensor was derived from the C-terminal domain of Anillin, which is composed of AHD and PH (Pleckstrin homology) domains and it's structurally related to the RhoA binding protein Rhotekin (Piekny and Glotzer 2008). Several studies have proven the validity of using GFP-AHPH to track RhoA-GTP expression (Priya et al. 2015; H. H. Yu et al. 2016; Liang et al. 2017), although there are no reports regarding the use of this biosensor in the invadopodia context.

Crystalization and biochemical studies has demonstrated the direct binding of the AH domain of anillin contained in the GFP-AHPH biosensor with RhoA (Piekny and Glotzer 2008; Sun et al. 2015). However, there are no reports in the literature specifically analysing the ability of GFP-AHPH biosensor to bind other members of the Rho family. Therefore, before proceeding with immunostaining analysis, the selective binding of the biosensor to RhoA and not RhoC was tested by co-immunoprecipitation in HEK293 cells. Cells were co-transfected with AHPH-GFP and Myc-RhoC, or AHPH-GFP and FLAG-RhoA before GFP pulldown. Western blot analysis of the pulldown lysates revealed that FLAG-RhoA, but not

Myc-RhoC, precipitated together with GFP-AHPH (Figure 5.14), confirming the specific binding of the biosensor to RhoA protein.

Following AHPH-GFP binding validation, CT-1532 cells were transfected with the RhoA-GTP biosensor and seeded onto gelatin-coated coverslips. Interestingly, a distinctive localisation of RhoA-GTP surrounding the invadopodial structure was repeatedly observed (Figure 5.1A). Analysis of the fluorescence intensity along the invadopodia surface area and along an arbitrary line crossing the invadopodial structure identified a GFP-positive ring extending around the actin core and not overlapping with the actin puncta nor matrix degradation (Figure 5.15B-C), similarly to what has been reported for RhoC by FRET biosensor (Bravo-Cordero et al. 2011). Encouragingly, quantification of the AHPH-positive cells forming invadopodia revealed that more than 10% of the cells exhibited at least one invadopodia characterised by this RhoA-GTP expression pattern (Figure 5.15D). Occasionally the GFP signal colocalised with actin puncta. These findings possibly indicate a spatial organization of RhoA-GTP activity that influences invadopodia dynamics.

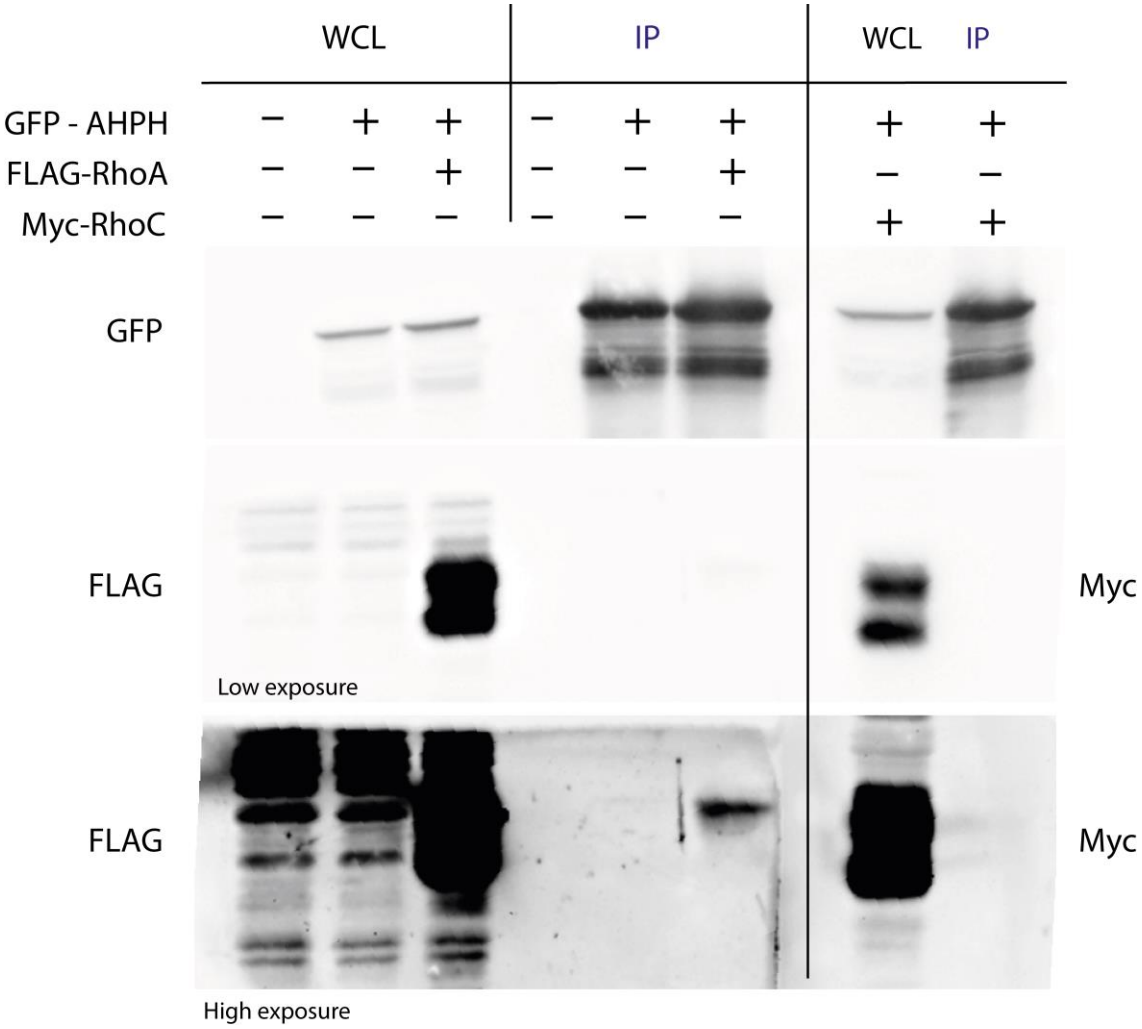

Figure 5. 14: Co-immunoprecipitation of AHPH with RhoA in HEK293 cells.
AHPH-GFP was transfected in HEK293 cells with or without FLAG-RhoA and Myc-RhoC. Cells were lysed and samples were subjected to the GFP-trap immunoprecipitation assay followed by Western blot analysis of the precipitated complexes. AHPH-GFP overexpressing cells were used as technical positive control while untrasfected cells were used as negative control. FLAG-RhoA, but not Myc-RhoC, was found to immunoprecipitated with GFP-AHPH.

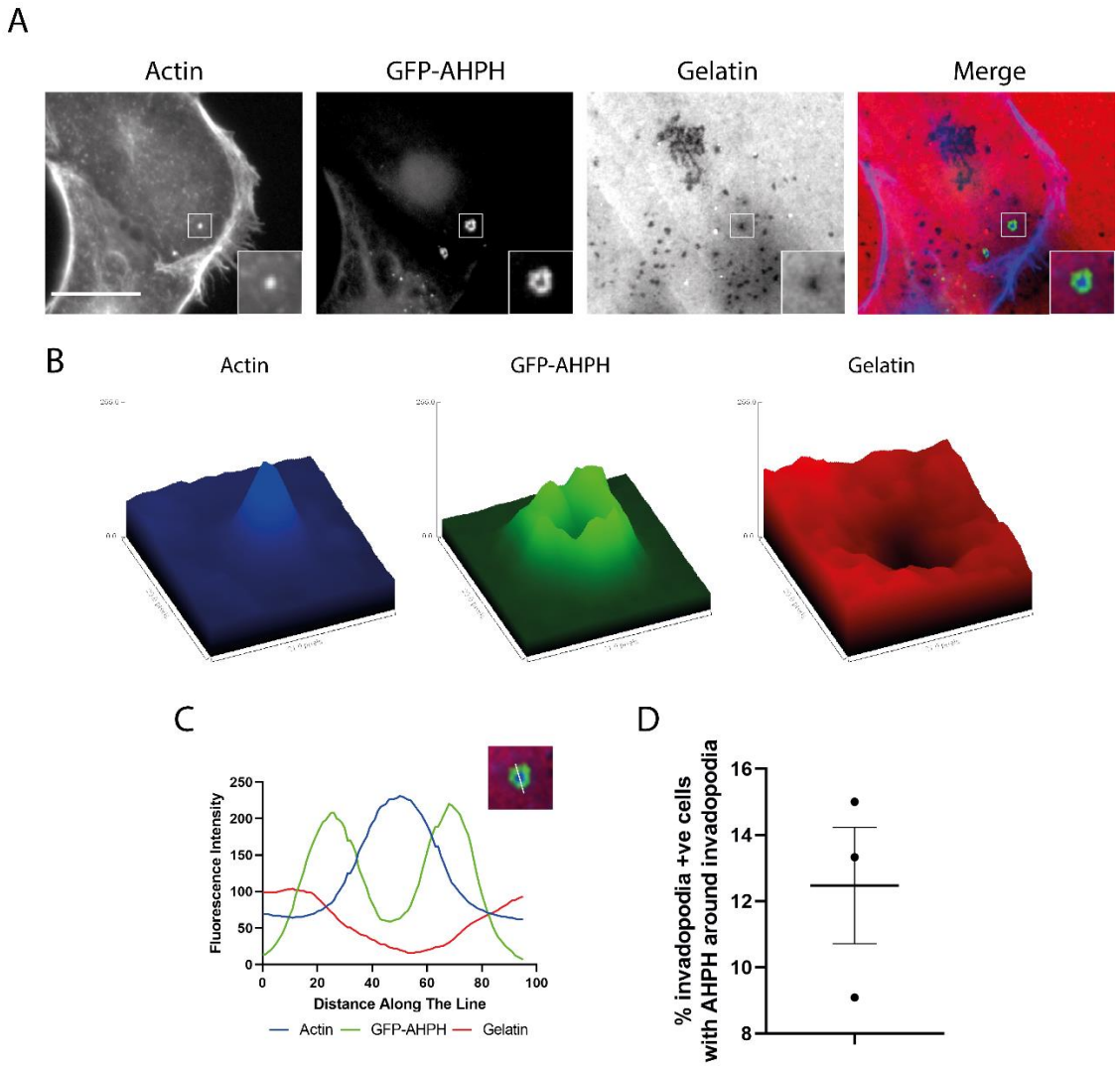

Figure 5. 15. Analysis of RhoA-GTP localisation by immunofluorescence.
Representative images of a CT-1532 cell plated on cy3-conjugated gelatin and stained for F-actin, expressing GFP-labelled RhoA-GTP biosensor around the invadopodial core (A). Representative 3D surface intensity plot showing local variation of fluorescence intensity for Actin, Cy3-gelatin and AHPH-GFP measured from the selected area in A (B). Representative line scan plot showing local variation of fluorescence intensity for Actin, Cy3-gelatin and AHPH-GFP measured by drawing an arbitrary line crossing through the invadopodia structure (C). Graphical representation of the percentage of invadopodia-forming cells expressing GFP-AHPH in which RhoA-GTP activity was detected around the invadopodia structure. A total of 45 cells over three independent experiments were analysed (D). Data are presented as mean values ± S.E.M. Scale bar = 10µm.

5.2.9. PAK4 co-immunoprecipitates with PDZ-RhoGEF in CT-1532 cell line

Taken together, these results suggest that PAK4 may signals in invadopodia via modulating RhoA activity. Positive regulation of RhoA is primarily achieved via multiple GEFs, that promotes dissociation of GDP and binding of GTP, which activates RhoA (Schmidt and Hall 2002). PDZ-RhoGEF is known to almost exclusively activate RhoA, with preferential binding over RhoB and RhoC, and no activity towards the other Rho family members, such as Rac1 and Cdc42 (Jaiswal et al. 2011). Interestingly, studies on yeast and HEK293 cells revealed that exogenous PDZ-RhoGEF interacts with PAK4, and PDZ-RhoGEF ability to mediate RhoA-GTP accumulation is abolished upon binding to PAK4 (Barac et al. 2004; Rosenfeldt et al. 2006). Moreover, exogenous PDZ-RhoGEF was found to co-localise with PAK4 to invadopodia in melanoma (Nicholas et al. 2016), and it has been suggested that PAK4 inhibits PDZ-RhoGEF to drive invadopodia maturation (Nicholas et al. 2016). Therefore, it was hypothesized that PAK4 signalling to RhoA could occur via PDZ-RhoGEF in prostate cancer. To investigate a potential interaction between PDZ-RhoGEF and PAK4, immunoprecipitation experiments were carried out in the CT-1532 cell line. Endogenous PAK4 was pulled down and samples were subjected to Western blotting and probed for PDZ-RhoGEF to assess the presence of PAK4:PDZ-RhoGEF complexes. The results of the immunoprecipitation experiments confirmed the binding between endogenous PAK4 and endogenous PDZ-RhoGEF, the first time this endogenous interaction has been observed (Figure 5.17).

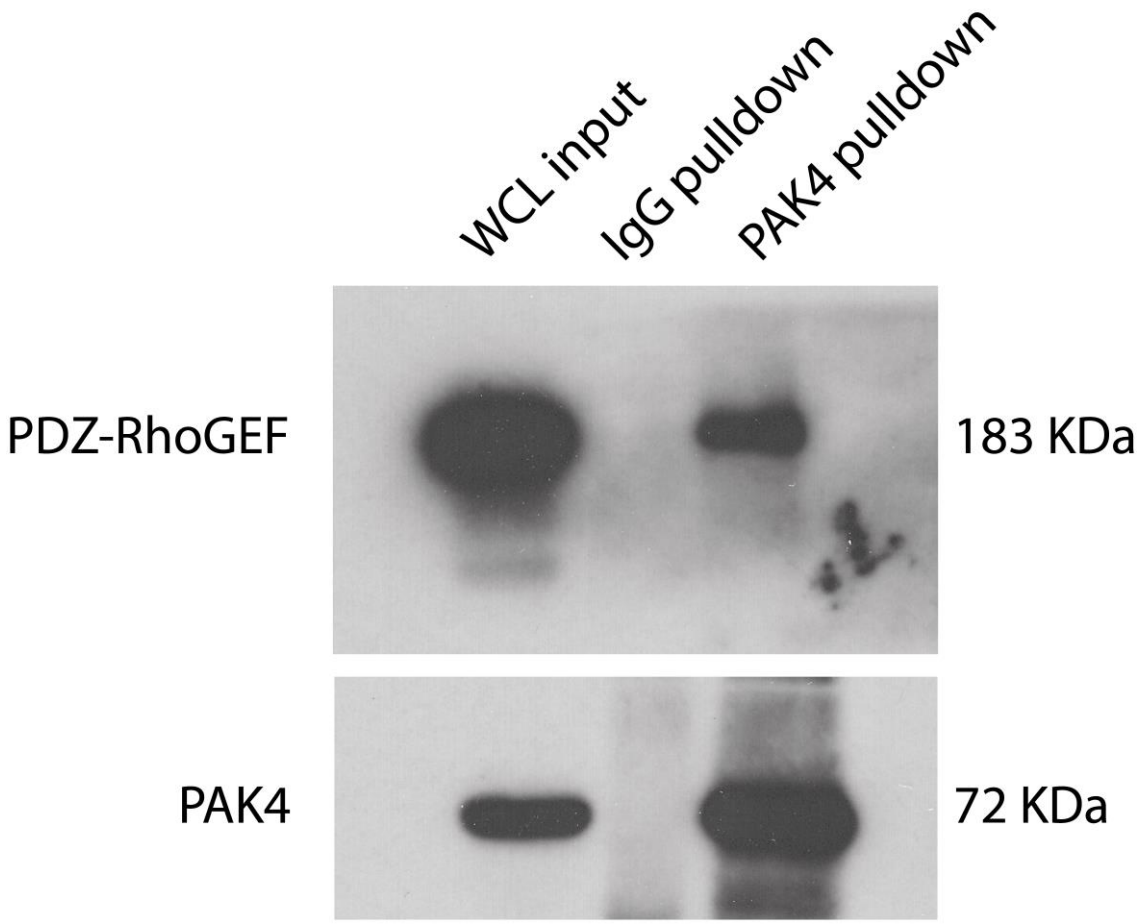

Figure 5. 16: Endogenous co-immunoprecipitation of PAK4 with PDZ-RhoGEF.
Direct interaction between PAK4 and PDZ-RhoGEF was evaluated by endogenous co-immunoprecipitation in CT-1532 cells. Protein complexes were resolved by Western blot for detection of PAK4 and PDZ-RhoGEF and compared to whole cell lysates (input). Results clearly highlights the existence of a complex between PAK4 and PDZ-RhoGEF, as a clear band appears uniquely in the lane corresponding to PAK4 pulldown.

5.2.10. Identification of PDZ-RhoGEF residues phosphorylated by PAK4

The establishment of the endogenous binding between PAK4 and PDZ-RhoGEF prompted the question of what structural domains are involved in this protein interaction. Barac et al. showed that PAK4 can bind specifically to the C-terminus of PDZ-RhoGEF, constituted by the last 451 residues outside the PH domain (Barac et al. 2004). Moreover, both the C-terminal portion and the full length of PDZ-RhoGEF were characterized by a strong increase in serine-threonine phosphorylation upon incubation with active PAK4 (Barac et al. 2004). These results indicate that the C-terminal domain of PDZ-RhoGEF is a direct target for PAK4 and it serves as phosphorylation substrate.

To further validate the C-terminal region of PDZ-RhoGEF as substrate for PAK4 kinase activity, and to map more precisely the putative PAK4 phosphorylation sites, a peptide array covering the amino acidic sequence of C-terminal PDZ-RhoGEF was designed. A total of 33 immobilized peptides were analysed, each harbouring serine residues. Three peptides on the array contained sequences that are reported to be phosphorylated by PAK4 and served as positive control: β-5 integrin on Ser-759 and Ser-762 (peptide #34), Paxillin on Ser-272 (peptide #35) and β-catenin on Ser-675 (peptide #36) (Dart and Wells 2013). A peptide containing only Alanine residues served as negative control (peptide #37). The array was incubated with purified, recombinant PAK4 and [γ^{32}P]ATP, in an *in-vivo* kinase assay followed by autoradiography. Amongst the peptides analysed, three PDZ-RhoGEF peptides showed a strong signal positive for *in-vitro* phosphorylation by PAK4, corresponding to peptide #12 (Ser-1295), peptide #18 (Ser-1364 and Ser-1367), peptide #31 (Ser-1505) (Figure5.18). Notably, Ser-1364 was identified as candidate PAK4 phosphorylation site also by the phosphorylation site prediction software GSP 5.0, which utilises specific protein kinases consensus motifs (C. Wang et al. 2020). Two of the positive controls were verified as PAK4 phosphorylation targets, however, Paxillin Ser-272 exhibited lack of signal. This is possibly due to a lower affinity for phosphorylation compared to the adjacent sequences, which might be preferentially targeted by PAK4, or due to the absence of PAK4 downstream targets that drives PAK4-mediated phosphorylation on paxillin S272 (Dart et al. 2015) .

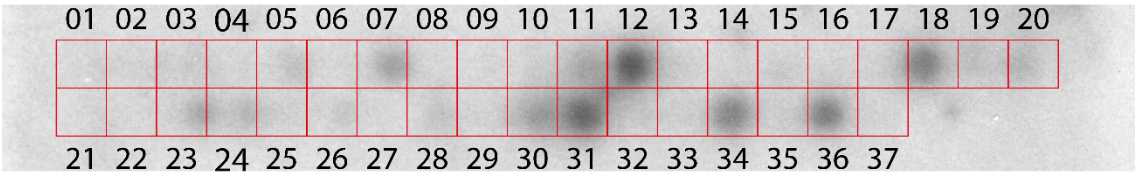

1	QGPTPSRVELD	20	TDHSEAPM
2	VELDDSDVFHG	21	EAPMSPPQPD
3	PGGTGSQQRVQ	22	PPQPDSLPAG
4	PEQEGSAEEEE	23	PRRPSRSPPSL
5	VLPCPSTSLDGEN	24	RSPPSLALRD
6	EGLADSALEDV	25	PPSLALRDVG
7	HLILWSLLPGH	26	RELLKSLGGE
8	LTPTPSVISVT	27	LGGESSGGTT
9	VISVTSHPWD	28	WTDGSLSPPAK
10	WDPGSPGQAP	29	EPLASDSRN
11	DMGLCSLEHLP	30	DSRNSHELGPC
12	PRTRNSGIWE	31	CPEDGSDAPLE
13	GIWESPELDR	32	PLEDSTADAA
14	LAEDASSTEAA	33	TADAAASPGP
15	EVAGSKVVPA	34	AKFQSERSRARY
16	PALPESGQSEP	35	DELMASLSDFK
17	ESGQSEPGPPEV	36	KKRLSVELTS
18	NCFYVSMPSGP	37	AAAAAAAAA
19	GPPDSSTDHS		

Figure 5. 17: Analysis of candidate PAK4-mediated phosphorylation targets on the C-terminal domain of PDZ-RhoGEF.

Analysis of the 33 peptides representing all serine residues in the C-terminal sequence of PDZ-RhoGEF immobilized on a membrane and incubated with PAK4 kinase and γ-32P-ATP. Incorporation of ATP was detected by autoradiography. Peptides in blue represents PDZ-RhoGEF residues phosphorylated by PAK4, peptides in green represents known PAK4 substrates serving as positive control, peptide in red serves as negative control.

5.3. Discussion

This chapter focused on the identification of potential mechanisms and protein interactors by which PAK4 might be regulating invadopodia dynamics in prostate cancer. Previous research conducted on melanoma has demonstrated a link between PAK4 activity and RhoA in invadopodia, where reduction of PAK4 expression led to decreased matrix degradation together with the formation of prominent stress fibres (Nicholas et al. 2016, 2017), important phenotypic markers of RhoA activation (Ridley and Hall 1992). However, analysis of the morphological phenotype in CT-1532 PAK4 depleted cells revealed that these cells do not form stress fibres even when RhoA activity is exogenously induced by treatment with LPA. In order to mediated intracellular events, LPA binds and activate surface six different G-Protein Coupled Receptors (GPCRs), named LPA_{1-6}, which subsequently initiate a variety of downstream signalling pathways involved in several biological functions (Lin, Huang, and Lee 2015). LPA receptors are differently expressed in prostate cancer cell lines, with levels that vary depending on the receptor type and cell line considered. There is a great body of evidence demonstrating the relevance of LPA receptors in the prostate setting, and notably, LPA receptors activation has been associated with increased Matrigel invasion via RhoA and cell rounding in PC3 cell line (Lin, Huang, and Lee 2015). Consistently with these reports, increase in RhoA activity in CT-1532 cells by LPA manifested in a more rounded cell shape, which was mirrored by CT-1532 shPAK4 cells, indicating an hyperactivation of the RhoA pathway in these cells. This observation represents a further deviation from melanoma cells that were reported to exhibit an unchanged elongation degree upon PAK4 reduction (personal communication by N. Nicholas). The phenotypic differences observed between prostate and melanoma arising in response to the same molecular event could be due to the different tissue type of origin, and highlights how, although RhoA has similar role in regulating cytoskeletal dynamics globally, RhoA may have differential functions in morphology and invadopodia according to the cell line considered. Indeed, similar discrepancies have been observed even across prostate cancer cell lines, where stable PAK4 knockdown led to an increased prominence of actin fibres in DU-145 but not in PC-3 cells (Wells et al. 2010; Ahmed et al. 2008).

Nevertheless, the ability of PAK4 to influence levels of active RhoA was confirmed by RhoA-GTP pulldown in PAK4 depleted cells, confirming previous reports that indicate PAK4 as negative regulator of RhoA (Callow et al. 2005; Wells et al. 2010; Nicholas et al. 2016).

The importance of RhoA in invadopodia has been largely described, but its precise role is yet not fully understood, and studies focused on RhoA function within invadosome have yielded conflicting results. Previous data in the literature showed that decreased expression of RhoA in human breast cancer MDA-MB-231 and rat mammary carcinoma MTLn3 cells dramatically reduced matrix degradation as well as the number of invadopodia per cell (Sakurai-Yageta et al. 2008; Bravo-Cordero et al. 2011). Breast cancer cells expressing a constitutively active RhoA mutant formed more invadopodia than WT (Roh-Johnson et al. 2014). With regards to prostate cancer, increased RhoA activity stimulates ECM degradation and invadopodia formation in PC3 cells, and was severely impaired in cells expressing dominant-negative RhoA mutant or C3 Transferase (Hwang et al. 2016). Conversely, expression of a dominant negative RhoA in RPMI7951 human melanoma cells did not affect the matrix degradation by invadopodia (Nakahara et al. 2003). Interestingly, Berdeaux et al. showed that both expression of constitutively active RhoA and dominant negative RhoA diminished Src-induced podosome and gelatin degradation (Berdeaux et al. 2004). Later studies confirmed that activation of RhoA via LPA or via expression of a constitutively active RhoA mutant inhibited podosome formation and function (Schramp et al. 2008; C. Yu et al. 2013). These findings denote a complex role for RhoA in cell invasion, which may differ according to the cell type and the assay employed.

The siRNA experiments presented in this chapter are partially aligned with such findings, as reduction of RhoA levels resulted in a remarkable decrease of invadopodia-mediated matrix degradation in our primary prostate adenocarcinoma cell line (Figure 5.9 and 5.10). However, in this study, increased RhoA activation resulting from lack of the negative regulation by PAK4 did not enhance invadopodia formation and matrix degradation in shPAK4 cells, but rather supressed it. Thus, our data suggest that constitutive activation of RhoA in prostate cancer might hinder invadopodia activity, possibly by favouring alternative modes of cell invasion.

It is possible that high RhoA signalling in prostate cancer cells leads to a predominant activation of downstream pathways associated with utilization of amoeboid motility, which

perhaps exerts a negative feedback on other invadopodia regulators. Indeed tumour cells are able to switch between the mesenchymal mode of migration, accompanied by invadopodia formation, and amoeboid invasion, which is degradation-independent and its catalysed by activation of the RhoA-ROCK-MLC2 pathway (Sanz-Moreno et al. 2008). Given that these two mechanisms of invasion are distinguished and interconvertible (A. G. Clark and Vignjevic 2015), it is reasonable to hypothesise the existence of an inhibitory cross-talk between these two signalling pathways. For example, it has been reported that inhibition of ROCK can enhance invadopodia formation (Sedgwick et al. 2015), and activation of the RhoA-ROCK axis via stimulation with Prostaglandin E in dendritic cells caused the dissolution of podosomes (van Helden et al. 2008). This hypothesis might explain why PAK4 depleted cells lacked invadopodia but were still able to disseminate *in-vivo* in Zebrafis, as outlined in chapter 4. Likewise, activation of RhoA in PC3 cells stimulated tumorigenesis and bone dissemination *in-vivo* (Hwang et al. 2016). The opposite observation was made in melanoma cells (Nicholas et al. 2016). It is possible that here constitutive activation of RhoA following PAK4 depletion is not inducing an amoeboid-related signalling and RhoA functions differently in this cell type (Nicholas et al. 2016). Indeed, it has already been established that the same signalling modulated by Rho- GTPases can elicit different cell type-specific effects (L. Wang and Zheng 2007).

If constitutive RhoA activation promotes amoeboid-like mode of invasion, a finer control of RhoA activity may be, instead, important for invadosome function. It has been suggested that a coordinated cycling of RhoA between the active, GTP-bound and the inactive, GDP-bound states, plays an essential role in regulating many aspects of podosome dynamics (Spuul et al. 2014). Melanoma studies suggest that RhoA activation is likely required at early stages during invadopodia lifecycle, while it needs to be suppressed later on in order to allow invadopodia maturation (Nicholas et al. 2017). Interestingly, CT-1532 with reduced expression or activation of RhoA were unable to degrade the matrix but retained their ability to form actin puncta (Figure 5.11 and 5.12). This finding suggests that in these cells RhoA function might be crucial for the later phases of invadopodia lifecycle, consisting in the protrusion maturation and matrix degradation, but it's dispensable for invadopodia precursor, in agreement with previous reports (Bravo-Cordero et al. 2011). According to our data, RhoA is negatively regulated by PAK4, but differently from RhoA, reduction of PAK4 expression decreased both nascent invadopodia and gelatin degradation. Thus, we

speculate that RhoA is maintained inactive by PAK4 during the early phase in the lifecycle of invadopodia, when the stabilization and elongation of the actin precursor occur, and it's subsequently released from inhibition in order to allow efficient invadopodia maturation and gelatin degradation. This hypothesis is further supported by the fact that limiting RhoA activation in shPAK4 cells by C3 Transferase restores puncta (nascent invadopodia) formation but does not rescue the degradation phenotype to the control levels (Figure 5.13). Consistent with this finding, RhoA was reported to cooperate with Cdc42 to promote the delivery of MT1-MMP to invadopodia (Sakurai-Yageta et al. 2008). RhoA stimulates the association of the exocyst complex with the IQ-GTPase activating protein 1 (IQGAP1), aiding the fusion of the vesicle at the invadopodial plasma membrane and therefore inducing local matrix degradation (Sakurai-Yageta et al. 2008).

Additional information on the spatiotemporal regulation of Rho-GTPases can be provided throughout using specific biosensors, which offer useful insights into the activity kinetic of these molecules intracellularly. FRET-based biosensors showed low RhoA activity outside and inside the core of invadopodia structures (Bravo-Cordero et al. 2011). On the contrary, RhoC activity was restricted to the area surrounding the protrusion, thanks to a tight regulation operated by localised variation in p190RhoGEF and p190RhoGAP activity (Bravo-Cordero et al. 2011). Excitingly, the reported RhoC distribution pattern resembles what we have observed with the fluorescent AHPH-based biosensor for RhoA-GTP (Figure 5.15), hinting that RhoA could be subjected to a similar spatiotemporal coordination. The discrepancy between our finding and the diffuse distribution of RhoA-GTP reported by Bravo-Cordero et al. might be explained by the different nature of the biosensors employed. Stable integration of FRET-based biosensors which incorporates the target protein can cause over-expression artifacts (Haugh 2012). Amplification or saturation of the signal could amplify or negatively interfere with endogenous processes which are especially deleterious for proteins that are subjected to fine tuning of activity and/or localization, such as RhoA. Moreover, the subcellular localization is often influenced by multiple factors, such as interactions with other proteins or lipids, and the protein molecular recognition could be negatively affected by the biosensor construct (Haugh 2012). Hence, it is possible that the small nature of the AHPH-GFP biosensor, and the fact that it binds directly to endogenous RhoA without competing for common substrates, made it more suitable for subcellular studies that cannot be reproduced by the FRET biosensor. Of note, PAK4 was found to be

localized in a ring structure around the podosome core, and immunoprecipitated with other ring proteins such as paxillin and vinculin which are also present in invadopodia (Foxall et al. 2019). These data further support a role for PAK4 as RhoA regulator in invadopodia.

The localization pattern exhibited by RhoA around invadopodia suggests that RhoA-mediated fusion of the exocyst complex may occur at the membrane fraction that surrounds the protrusion core, where it participates in delivering MT1-MMP to the invadopodial membrane. Indeed, RhoA is known to interact and bind to lipid rafts, cholesterol-enriched lipidic domains that floats within the bilayer of plasma membranes, contributing to increase the membrane fluidity and protein trafficking (Moissoglu and Schwartz 2014). MT1-MMP was found to localise at lipid rafts, which represents key elements for the correct assembly and function of invadopodia (Yamaguchi et al. 2009). Perhaps MT1-MMP is incorporated to the lipidic bilayer through its transmembrane domain and subsequently mobilised towards the invadopodium edge via lipid rafts. Notably, RhoA-GTP was occasionally spotted to colocalise with the actin core of invadopodia structures, and invadopodia negative for RhoA-GTP signals were also detected. These findings suggest an even more complex and dynamic role for RhoA-GTP in invadopodia in prostate cancer, tightly regulated in a spatiotemporal manner.

A coordinated interplay between guanine exchange factors (GEFs) and GTPase activating proteins (GAPs) is required to achieve the strict spatiotemporal regulation of Rho GTPase activation at invadopodia. PAK4 has been reported to inhibit the activation of RhoA via phosphorylation of GEF-H1 in prostate cancer cells (Wells et al. 2010). However, in melanoma cells phosphorylation levels of GEF-H1 protein were not affected by PAK4 depletion (Nicholas et al. 2016). Rather, PDZ-RhoGEF, another RhoGEF which selectively binds and activates RhoA (Oleksy et al. 2006), was found to colocalise with PAK4 to invadopodia (Nicholas et al. 2016) and identified as PAK4 interactor (Barac et al. 2004). PAK4 is thought to bind and inhibit PDZ-RhoGEF by binding to its 341 amino acids C-terminus domain (Barac et al. 2004). Interestingly, this interaction was not detected in PAK1 and PAK2, possibly indicating a unique regulatory pathway for PAK4 (Barac et al. 2004; Rosenfeldt et al. 2006). Despite recent progresses, however, the role of the PAK4:PDZ-RhoGEF complex has not been extensively studied, and the molecular mechanisms at the base of this interaction remain to be elucidated. Our data confirm for the first time the

existence of a complex between PAK4 and PDZ-RhoGEF endogenously. Similarly, it's the first time that such interaction is described in the prostate cancer setting (Figure 5.17).

Phosphorylation levels of both C-terminus and whole length of PDZ-RhoGEF increased following incubation with constitutively active PAK4 (Barac et al. 2004). Additional experiments highlighted the requirement of an intact C-terminal region of PDZ-RhoGEF for binding to PAK4, as the interaction was abolished was abolished in case of deletion of the C-terminal portion of PDZ-RhoGEF (Barac et al. 2004). Studies into the regulatory mechanisms that control RhoGEFs activity indicate that phosphorylation could promote both activation or inhibition of the GEF function. Tyrosine phosphorylation of PDZ-RhoGEF and LARG, both RhoA regulators, on their C-terminal domain by FAK in HEK293T cells serves as positive modulator, enhancing their GEF activity (Chikumi, Fukuhara, and Gutkind 2002). GEF-H1 is reported to be positively regulated by threonine phosphorylation by extracellular signal-regulated kinase (ERK) on Thr-678 (Fujishiro et al. 2008), located on the PH domain Intriguingly, GEF-H1 can be inhibited by phosphorylation on the C-terminal residues Ser-959 and Ser-885 by ERK and PAK1, respectively (von Thun et al. 2013; Frank T Zenke et al. 2004). Another RhoA interactor, Net1, is phosphorylated by PAK1 on Ser-152, down-regulating Net1 GEF activity (Alberts et al. 2005). These studies provide important evidences that RhoGEF regulation by phosphorylation can have diverging effects on the protein functionality. The downstream mechanism by which phosphorylation controls RhoGEFs activity also vary: phosphorylation could directly regulate GEFs function, or mediate the recruitment of other RhoGEF binding interactors which act themselves as GEFs modulators. Alternatively, phosphorylation promotes a conformational change that allows or prevents GEF activity or access to secondary regulatory events. All these mechanisms have been reported in different RhoGEFs which participate to modulation of RhoA (Patel and Karginov 2014), and allow a defined tuning of of RhoA activation at specific subcellular locations. Interestingly, there are currently no direct evidence of phosphorylation occurring on the catalytic domain DH of RhoGEFs (Patel and Karginov 2014).

The details of PDZ-RhoGEF regulation mechanism by phosphorylation have not been identified yet. Current reports indicate that C-terminal domain of PDZ-RhoGEF is necessary and sufficient to mediate the protein homo- and hetero-dimerization leading to inhibitory effect (Chikumi et al. 2004). We speculate that PAK4 phosphorylation on the C-terminal

region of PDZ-RhoGEF could promote the formation of an autoinhibitory conformation on PDZ-RhoGEF, holding the protein in its inactive state. However, PAK4 target residues on PDZ-RhoGEF have not been mapped yet. In this study, four different serines residing on the C-terminal domain of PDZ-RhoGEF have been identified as potential candidates for PAK4 phosphorylation: Ser-1295, Ser-1364, Ser-1367 and Ser-1505. There is no reference yet in the literature as to whether these sites modulate PDZ-RhoGEF activity. Interestingly, Ser-1364, as also predicted as putative PAK4 substrate by GPS software, a computational predicting tool for the identification of kinase specific phosphorylation sites. Moreover, a protein sequence alignment analysis was conducted with BLAST Software to assess the potential homology of the C-Terminal region of PDZ-RhoGEF to other known RhoGEFs, which may provide some new insights into the relevance of these residues in PDZ-RhoGEF regulation. Unfortunately, protein alignment did not reveal any significant homology within the RhoGEFs family members for the sequence considered.

The data presented in this chapter identify RhoA as a signalling molecule in invadopodia in prostate cancer. Moreover, RhoA activity seems to be spatiotemporally regulated in invadopodia, possibly as downstream effector of a specific PAK4:PDZ-RhoGEF signalling pathway. PAK4 regulation of PDZ-RhoGEF is thought to be mediated by PAK4 phosphorylation activity, which further validates the importance of PAK4 kinase domain in invadopodia.

5.4. Future works

This chapter sought to identify the molecular pathway by which PAK4 elicits its functional response in invadopodia dynamics in prostate cancer. The use of more advanced ultra-resolution microscopy techniques, would allow to better dissect the spatial organization of RhoA-GTP within invadopodia structures. Moreover, stable expression of fluorescent actin combined with fluorescent biosensor in live cells would permit the tracking of live cells on gelatin, elucidating whether RhoA activity is specifically required during certain phases of invadopodia lifecycle. Analysis of metalloproteases secretion and activation by ELISA of conditioned media or gelatin zymography in siRhoA cells might provide some useful information about RhoA function in promoting matrix degradation, clarifying whether RhoA in prostate cancer invadopodia works mainly by acting on the regulation of actin dynamics or secretion of MMPs. In the latter case, it would be interesting to evaluate potential RhoA binding partners that are known to be associated with the exocyst complex, such as IQGAP1. Moreover, specific antibodies raised to the phosphorylated residues identified by our peptide array experiments could be utilised to better understand when PDZ-RhoGEF is phosphorylated at these sites during cell migration and in invadopodia assays.

Chapter 6

Concluding Remarks

Chapter 6. Concluding Remarks

Advanced prostate cancer (PCa) presenting with metastatic spread to distant lymph nodes or to other sites of the body is associated with an overall poor prognosis and survival rate. The first line of treatment for this type of disease is androgen deprivation therapy, which deprives the tumour cells of androgens necessary for cellular proliferation in the early phases of tumour development. However, many tumours eventually relapse and become castrate-resistant. In most of the cases, the tumour progress to more advanced stage characterised by metastatic dissemination leaving patients with a life expectancy of only few months, mainly due to the lack of efficient anti-metastatic drugs available on the market (Karantanos, Corn, and Thompson 2013). Therefore, understanding the molecular mechanisms underlying prostate cancer invasion is particularly important in order to develop novel therapeutic strategies.

One particular area of interest is the targeting of invadopodia. Invadopodia are plasma membrane protrusions that extend from the ventral surface of cancer cells and can degrade the extracellular matrix through the local secretion of metalloproteases, aiding cancer cell invasion through the surrounding tissues. Invadopodia have been observed *in-vitro* and *in-vivo* in a number of invasive cancer types (Yamaguchi 2012) and they have been directly linked to metastasis in rodent models (Eckert et al. 2011; Gligorijevic et al. 2012; Gligorijevic, Bergman, and Condeelis 2014) and ex-ovo chicken embryos models (Leong et al. 2014). Moreover, high-resolution multiphoton microscopy allowed the detection of invadopodia-like structures in primary breast carcinoma in mice (Gligorijevic, Bergman, and Condeelis 2014). Currently, there are not strong evidence associating invadopodia with prostate cancer progression in the literature, as the most studied cell lines (obtained from metastatic lesions) have not been reported to efficiently form invadopodia. Therefore, a key question posed was if evidence of invadopodia activity in prostate cancer could be established using alternative prostate cancer cell lines derived from primary adenocarcinoma could be employed for invadopodia and prostate cancer invasion studies. The cell lines examined were isolated from radical prostatectomy specimens and transformed with a recombinant retrovirus encoding E6 and E7 proteins of human papillomavirus 16 (HPV-16) (Bright et al. 1997), but they have never been extensively investigated. Therefore, it was first sought to establish whether these cell lines might constitute valid study models for prostate cancer,

paying particular attention to their proliferative ability and the expression of epithelial and cancer associated markers.

Interestingly, analysis of the cadherins markers associate with the epithelial to mesenchymal switch highlighted a partial loss of the epithelial phenotype and the acquisition of a hybrid EMT state which has been associated with increased metastatic potential and poorer survival outcome (George et al. 2017; Liao and Yang 2020) (Figure 3.3, 3.4 and 3.5). Excitedly, when subjected to *in-vitro* invadopodia assay, all prostate cancer cell lines tested efficiently formed invadopodia without any prior stimulation, as confirmed by positive cortactin staining (Figure 3.9). Moreover, they also performed optimally in Zebrafish invasion assay, where all cell lines were able to disseminate from the site of injection to the tail, suggesting that these cells lines hold a notable invasive potential (Figure 3.15). Thus, primary tumour-derived prostate cell lines might serve as a valid experimental tool to study invadopodia dynamics, and to expand our knowledge regarding the early phase of metastatic progression initiating from primary localized adenocarcinoma. The relevance of invadopodia in prostate cancer invasion was further highlighted by the discovery that circulating tumour cells (CTCs) isolated from the peripheral blood of 17 prostate cancer patients can spontaneously generate invadopodia-like protrusion in culture. These patient-derived cells were able to degrade the matrix and were positive for invadopodia-marker cortactin (Figure 3.18). Currently, there are no other reports linking invadopodia to prostate cancer CTCs, hence this study provides new important insights into the physiological relevance of invadopodia in a clinical setting, suggesting that these cells might utilise invadopodia protrusion to disseminate when inside the human body.

Having validated invadopodia as a potential mechanism of metastatic spread in the prostate setting, attention turned to the molecular mechanisms involved in invadopodia dynamics. P-21 activated kinases have been previously reported to be involved in driving invadopodia activity (I. Ayala et al. 2008; Moshfegh et al. 2014). Of the six PAKs family members, PAK4 is the most studied, and PAK4 has been reported to localise in podosomes (structures related to invadopodia) as well as in invadopodia in melanoma cell lines (Gringel et al. 2006; Nicholas et al. 2016; Foxall et al. 2019). PAK4 has also been implicated in promoting prostate cancer cell scattering and migration (Ahmed et al. 2008; Whale et al. 2013), and to drive prostate cancer adhesion turnover (Wells et al. 2010). However, the precise role of PAK4 in invadopodia is still unclear, and the relationship between PAK4 activity and invadopodia has never been investigated in prostate cancer. Depletion of PAK4 severely impaired the ability

of primary prostate cancer cells to form invadopodia and degrade the matrix, hence demonstrating that PAK4 is necessary for invadopodia activity (Figure 4.9). PAK4 capacity to regulate invadopodia was attributed to its kinase domain based on the observation that, differently from other PAK4 rescue mutants, kinase dead PAK4 was unable to restore invadopodia formation and invadopodia-mediated degradation in PAK4 depleted cells (Figure 4.17). Inactivating mutations in PAK4 domains responsible for the interaction between PAK4 and its established upstream regulators did not seem to affect the ability of PAK4 to rescue invadopodia.

In melanoma, the activity of PAK4 was focussed in later stages of invadopodia maturation, with PAK4 mainly affecting the ability of cells to degrade the extracellular matrix (Nicholas et al. 2016). However, in this study reduction of PAK4 expression led to a significant decrease of nascent invadopodia formation, pointing at an early role for PAK4 in prostate cancer (Figure 4.10 and 4.11). Indeed, the few active invadopodia detected in knockdown cells appeared to be reduced in size (Figure 4.14). These findings suggest two possibilities (Figure 6.1): either PAK4 acts solely as regulator of invadopodia formation through regulation of RhoA activity or PAK4 acts both at the invadopodia formation stage and the matruation stage. In this model, PAK4 inhibits RhoA during invadopodia formation, by directly interacting with PDZ-RhoGEF (Figure 5.16), a specific Rho activator which has not binding affinity for other Rho-GTPases such as Cdc42 or Rac1, and preferentially activates RhoA over the other Rho isoforms (Jaiswal et al. 2011). PAK4 phosphorylates PDZ-RhoGEF on its terminal domain (additional evidence of the importance of PAK4 kinase domain in invadopodia), negatively affecting its catalytic activity towards RhoA (Figure 5.17).

Alternatively, PAK4 could function later during invadopodia lifecycle at degradation level. In the latter case, RhoA activity is required for degradation and PAK4 inhibition of RhoA is prevented by the spatial confinement of PDZ-RhoGEF and RhoA around the invadopodial core. According to the model presented here, successful invadopodia function requires a regulated balance between RhoA activation and inactivation. A similar mechanism of transient activation has been observed in a different Rho-GTPase involved in invadopodia: Rac1 has been reported to be transitorily activated during invadopodia disassembly, while it remains inactive during invadopodia formation (Moshfegh et al. 2014). PAK4 could also promote matrix degradation via regulation of metalloproteases activity. Nevertheless, in this study, pharmacological inhibition of PAK4 decreased MMP2 levels (Figure 4.18),

complementing previous studies in which PAK4 was reported to enhance MMP2 expression (Siu et al. 2010; Kesanakurti et al. 2012).

However, based on the findings presented here it is not possible to rule out the possibility that PAK4 might play a dual role, being equally important in both invadopodia formation and degradation. This is not the first time an invadopodia regulator has been shown to be important in multiple phases of invadopodia lifecycle: Cdc42 has been reported to participate in both invadopodia precursor assembly (Razidlo et al. 2014) and MMPs delivery (Sakurai-Yageta et al. 2008). Moreover, the dual role of PAK4 could be facilitated by PAK4-mediated regulation of multiple pathways at a transcriptional level. For example, PAK4 has been shown to promote β-catenin stabilization and enhance its transcriptional activity (Dart and Wells 2013). Indeed, further studies are needed to elucidate the precise mechanisms by which this regulation might take place.

In conclusion, this thesis demonstrated for the first time that invadopodia might play a physiological role in prostate cancer invasion, highlighting their importance as therapeutic target for preventing metastatic dissemination. Moreover, it clearly illustrated the critical role played by PAK4 in regulating invadopodia dynamics, and proposed a potential downstream pathway that could as well hold interesting therapeutic potential.

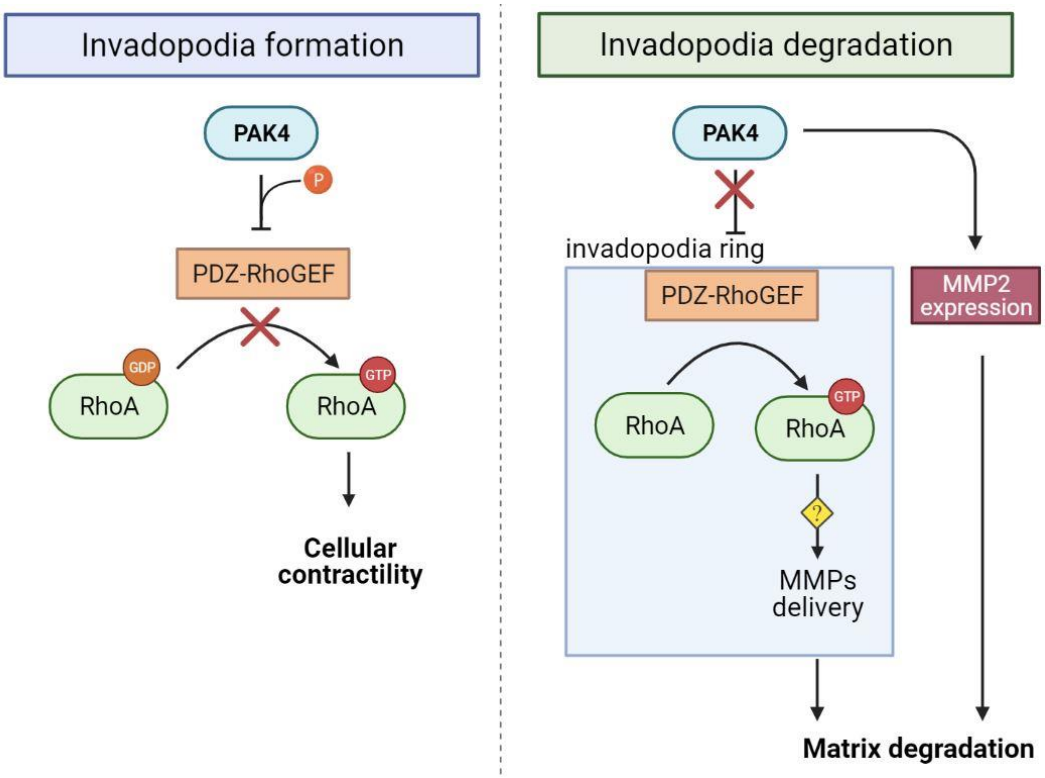

Figure 6. 1: Schematic diagram of the proposed model of PAK4 signalling pathway in invadopodia in prostate cancer.

PAK4 might play multiple roles in invadopodia in prostate cancer. During invadopodia formation (early phase) the inhibitory phosphorylation of PDZ-RhoGEF by PAK4 prevents the accumulation of RhoA-GTP, inhibiting RhoA-mediated cellular contractility and inducing PAK4-mediated invadopodia. During invadopodia maturation (later phase), RhoA-GTP localises around the invadopodia core in a ring-shaped area, where it might participate to the delivery of metalloproteases to the invadopodial membrane. PAK4 inhibitory effect on PDZ-RhoGEF ceases, possibly due to different subcellular localisation. PAK4 still contributes to promoting matrix degradation by stimulating the expression of metalloproteases.

Bibliography

Abo, A, J Qu, M S Cammarano, C Dan, A Fritsch, V Baud, B Belisle, and A Minden. 1998. "PAK4, a Novel Effector for Cdc42Hs, Is Implicated in the Reorganization of the Actin Cytoskeleton and in the Formation of Filopodia." *The EMBO Journal* 17 (22): 6527–40. doi:10.1093/emboj/17.22.6527.

Afshar, Mehran, Felicity Evison, Nicholas D James, and Prashant Patel. 2015. "Shifting Paradigms in the Estimation of Survival for Castration-Resistant Prostate Cancer: A Tertiary Academic Center Experience." *Urologic Oncology: Seminars and Original Investigations* 33 (8): 338.e1-338.e7. doi:https://doi.org/10.1016/j.urolonc.2015.05.003.

Ahmed, Tasneem, Kerry Shea, John R W Masters, Gareth E Jones, and Claire M Wells. 2008. "A PAK4-LIMK1 Pathway Drives Prostate Cancer Cell Migration Downstream of HGF." *Cellular Signalling* 20 (7). England: 1320–28. doi:10.1016/j.cellsig.2008.02.021.

Ahn, Hee Kyung, Jiryeon Jang, Jeeyun Lee, Park Se Hoon, Joon Oh Park, Young Suk Park, Ho Yeong Lim, Kyoung-Mee Kim, and Won Ki Kang. 2011. "P21-Activated Kinase 4 Overexpression in Metastatic Gastric Cancer Patients." *Translational Oncology* 4 (6). Division of Hematology-Oncology, Department of Medicine, Samsung Medical Center, Sungkyunkwan University School of Medicine, Seoul, South Korea.: 345–49. doi:10.1593/tlo.11145.

Alberts, Arthur S, Huajun Qin, Heather S Carr, and Jeffrey A Frost. 2005. "PAK1 Negatively Regulates the Activity of the Rho Exchange Factor NET1." *The Journal of Biological Chemistry* 280 (13). United States: 12152–61. doi:10.1074/jbc.M405073200.

Alinezhad, Saeid, Riina-Minna Väänänen, Jesse Mattsson, Yifeng Li, Terhi Tallgrén, Natalia Tong Ochoa, Anders Bjartell, et al. 2016. "Validation of Novel Biomarkers for Prostate Cancer Progression by the Combination of Bioinformatics, Clinical and Functional Studies." *PLOS ONE* 11 (5). Public Library of Science: e0155901.

Anjomshoaa, A, Y-H Lin, M A Black, J L McCall, B Humar, S Song, R Fukuzawa, et al. 2008. "Reduced Expression of a Gene Proliferation Signature Is Associated with Enhanced

Malignancy in Colon Cancer." *British Journal of Cancer* 99 (6). Nature Publishing Group: 966–73. doi:10.1038/sj.bjc.6604560.

Aoyama, A, and W T Chen. 1990. "A 170-KDa Membrane-Bound Protease Is Associated with the Expression of Invasiveness by Human Malignant Melanoma Cells." *Proceedings of the National Academy of Sciences of the United States of America* 87 (21): 8296–8300.

Arias-Romero, Luis E, and Jonathan Chernoff. 2008. "A Tale of Two Paks." *Biology of the Cell* 100 (2). England: 97–108. doi:10.1042/BC20070109.

Armstrong, Andrew J, Matthew S Marengo, Sebastian Oltean, Gabor Kemeny, Rhonda L Bitting, James D Turnbull, Christina I Herold, Paul K Marcom, Daniel J George, and Mariano A Garcia-Blanco. 2011. "Circulating Tumor Cells from Patients with Advanced Prostate and Breast Cancer Display Both Epithelial and Mesenchymal Markers." *Molecular Cancer Research : MCR* 9 (8): 997–1007. doi:10.1158/1541-7786.MCR-10-0490.

Artym, Vira V, Kazue Matsumoto, Susette C Mueller, and Kenneth M Yamada. 2011. "Dynamic Membrane Remodeling at Invadopodia Differentiates Invadopodia from Podosomes." *European Journal of Cell Biology* 90 (2–3). Germany: 172–80. doi:10.1016/j.ejcb.2010.06.006.

Artym, Vira V, Kenneth M Yamada, and Susette C Mueller. 2009. "ECM Degradation Assays for Analyzing Local Cell Invasion." *Methods in Molecular Biology (Clifton, N.J.)* 522. United States: 211–19. doi:10.1007/978-1-59745-413-1_15.

Ayala, Alberto G, and Jae Y Ro. 2007. "Prostatic Intraepithelial Neoplasia: Recent Advances." *Archives of Pathology & Laboratory Medicine* 131 (8). United States: 1257–66. doi:10.1043/1543-2165(2007)131[1257:PINRA]2.0.CO;2.

Ayala, Inmaculada, Massimiliano Baldassarre, Giada Giacchetti, Giusi Caldieri, Stefano Tetè, Alberto Luini, and Roberto Buccione. 2008. "Multiple Regulatory Inputs Converge on Cortactin to Control Invadopodia Biogenesis and Extracellular Matrix Degradation." *Journal of Cell Science* 121 (3): 369 LP – 378. doi:10.1242/jcs.008037.

Ayala, Inmaculada, Giada Giacchetti, Giusi Caldieri, Francesca Attanasio, Stefania Mariggiò, Stefano Tetè, Roman Polishchuk, Vincent Castronovo, and Roberto Buccione. 2009. "Faciogenital Dysplasia Protein Fgd1 Regulates Invadopodia

Biogenesis and Extracellular Matrix Degradation and Is Up-Regulated in Prostate and Breast Cancer." *Cancer Research* 69 (3). United States: 747–52. doi:10.1158/0008-5472.CAN-08-1980.

Balasenthil, Seetharaman, Aysegul A Sahin, Christopher J Barnes, Rui-An Wang, Richard G Pestell, Ratna K Vadlamudi, and Rakesh Kumar. 2004. "P21-Activated Kinase-1 Signaling Mediates Cyclin D1 Expression in Mammary Epithelial and Cancer Cells." *Journal of Biological Chemistry* 279 (2): 1422–28. doi:10.1074/jbc.M309937200.

Barac, Ana, John Basile, Jose Vazquez-Prado, Yuan Gao, Yi Zheng, and J Silvio Gutkind. 2004. "Direct Interaction of P21-Activated Kinase 4 with PDZ-RhoGEF, a G Protein-Linked Rho Guanine Exchange Factor." *The Journal of Biological Chemistry* 279 (7). United States: 6182–89. doi:10.1074/jbc.M309579200.

Baskaran, Yohendran, Yuen-Wai Ng, Widyawilis Selamat, Felicia Tay Pei Ling, and Ed Manser. 2012. "Group I and II Mammalian PAKs Have Different Modes of Activation by Cdc42." *EMBO Reports* 13 (7). England: 653–59. doi:10.1038/embor.2012.75.

Beaty, Brian T, and John Condeelis. 2014. "Digging a Little Deeper: The Stages of Invadopodium Formation and Maturation." *European Journal of Cell Biology* 93 (10–12): 438–44. doi:10.1016/j.ejcb.2014.07.003.

Begum, Asma, Issei Imoto, Ken-ichi Kozaki, Hitoshi Tsuda, Emina Suzuki, Teruo Amagasa, and Johji Inazawa. 2009. "Identification of PAK4 as a Putative Target Gene for Amplification within 19q13.12-Q13.2 in Oral Squamous-Cell Carcinoma." *Cancer Science* 100 (10). England: 1908–16. doi:10.1111/j.1349-7006.2009.01252.x.

Bello, D, M M Webber, H K Kleinman, D D Wartinger, and J S Rhim. 1997. "Androgen Responsive Adult Human Prostatic Epithelial Cell Lines Immortalized by Human Papillomavirus 18." *Carcinogenesis* 18 (6). England: 1215–23. doi:10.1093/carcin/18.6.1215.

Berdeaux, Rebecca L, Begona Diaz, Lomi Kim, and G Steven Martin. 2004. "Active Rho Is Localized to Podosomes Induced by Oncogenic Src and Is Required for Their Assembly and Function." *The Journal of Cell Biology* 166 (3). United States: 317–23. doi:10.1083/jcb.200312168.

Berges, R R, J Vukanovic, J I Epstein, M CarMichel, L Cisek, D E Johnson, R W Veltri, P C Walsh, and J T Isaacs. 1995. "Implication of Cell Kinetic Changes during the

Progression of Human Prostatic Cancer." *Clinical Cancer Research : An Official Journal of the American Association for Cancer Research* 1 (5): 473–80.

Bhavsar, Anil, and Sadhna Verma. 2014. "Anatomic Imaging of the Prostate." *BioMed Research International* 2014: 728539. doi:10.1155/2014/728539.

Bokoch, Gary M. 2003. "Biology of the P21-Activated Kinases." *Annual Review of Biochemistry* 72. United States: 743–81. doi:10.1146/annurev.biochem.72.121801.161742.

Bonkhoff, H, U Stein, and K Remberger. 1994. "The Proliferative Function of Basal Cells in the Normal and Hyperplastic Human Prostate." *The Prostate* 24 (3). United States: 114–18. doi:10.1002/pros.2990240303.

———. 1995. "Endocrine-Paracrine Cell Types in the Prostate and Prostatic Adenocarcinoma Are Postmitotic Cells." *Human Pathology* 26 (2). United States: 167–70. doi:10.1016/0046-8177(95)90033-0.

Bono, Johann S de, Howard I Scher, R Bruce Montgomery, Christopher Parker, M Craig Miller, Henk Tissing, Gerald V Doyle, Leon W W M Terstappen, Kenneth J Pienta, and Derek Raghavan. 2008. "Circulating Tumor Cells Predict Survival Benefit from Treatment in Metastatic Castration-Resistant Prostate Cancer." *Clinical Cancer Research : An Official Journal of the American Association for Cancer Research* 14 (19). United States: 6302–9. doi:10.1158/1078-0432.CCR-08-0872.

Bos, Johannes L, Holger Rehmann, and Alfred Wittinghofer. 2007. "GEFs and GAPs: Critical Elements in the Control of Small G Proteins." *Cell* 129 (5). United States: 865–77. doi:10.1016/j.cell.2007.05.018.

Bostwick, David G, Harry B Burke, Daniel Djakiew, Susan Euling, Shuk-mei Ho, Joseph Landolph, Howard Morrison, et al. 2004. "Human Prostate Cancer Risk Factors." *Cancer* 101 (10 Suppl). United States: 2371–2490. doi:10.1002/cncr.20408.

Bostwick, David G, Anna Pacelli, and Antonio Lopez-Beltran. 1996. "Molecular Biology of Prostatic Intraepithelial Neoplasia." *The Prostate* 29 (2). John Wiley & Sons, Ltd: 117–34. doi:https://doi.org/10.1002/(SICI)1097-0045(199608)29:2<117::AID-PROS7>3.0.CO;2-C.

Bowden, E T, M Barth, D Thomas, R I Glazer, and S C Mueller. 1999. "An Invasion-Related Complex of Cortactin, Paxillin and PKCmu Associates with Invadopodia at Sites of

Extracellular Matrix Degradation." *Oncogene* 18 (31). England: 4440–49. doi:10.1038/sj.onc.1202827.

Bowden, Emma T, Peter J Coopman, and Susette C B T - Methods in Cell Biology Mueller. 2001. "Chapter 29 Invadopodia: Unique Methods for Measurement of Extracellular Matrix Degradation in Vitro." In *Cytometry*, 63:613–27. Academic Press. doi:https://doi.org/10.1016/S0091-679X(01)63033-4.

Brandt, B, R Junker, C Griwatz, S Heidl, O Brinkmann, A Semjonow, G Assmann, and K S Zänker. 1996. "Isolation of Prostate-Derived Single Cells and Cell Clusters from Human Peripheral Blood." *Cancer Research* 56 (20). United States: 4556–61.

Bravo-Cordero, Jose Javier, Matthew Oser, Xiaoming Chen, Robert Eddy, Louis Hodgson, and John Condeelis. 2011. "A Novel Spatiotemporal RhoC Activation Pathway Locally Regulates Cofilin Activity at Invadopodia." *Current Biology : CB* 21 (8): 635–44. doi:10.1016/j.cub.2011.03.039.

Bright, Robert K., Cathy D. Vocke, Michael R. Emmert-Buck, Paul H. Duray, Diane Solomon, Patricia Fetsch, Johng S. Rhim, W. Marston Linehan, and Suzanne L. Topalian. 1997. "Generation and Genetic Characterization of Immortal Human Prostate Epithelial Cell Lines Derived from Primary Cancer Specimens." *Cancer Research* 57 (5): 995–1002.

Buccione, Roberto, Giusi Caldieri, and Inmaculada Ayala. 2009. "Invadopodia: Specialized Tumor Cell Structures for the Focal Degradation of the Extracellular Matrix." *Cancer Metastasis Reviews* 28 (1–2). Netherlands: 137–49. doi:10.1007/s10555-008-9176-1.

Buehring, G C, and R R Williams. 1976. "Growth Rates of Normal and Abnormal Human Mammary Epithelia in Cell Culture." *Cancer Research* 36 (10). United States: 3742–47.

Bussemakers, M J, A Van Bokhoven, K Tomita, C F Jansen, and J A Schalken. 2000. "Complex Cadherin Expression in Human Prostate Cancer Cells." *International Journal of Cancer* 85 (3). United States: 446–50.

Cai, Songwang, Zhiqiang Ye, Xiaohong Wang, Yuhang Pan, Yimin Weng, Sen Lao, Hongbo Wei, and Lian Li. 2015. "Overexpression of P21-Activated Kinase 4 Is Associated with Poor Prognosis in Non-Small Cell Lung Cancer and Promotes Migration and

Invasion." *Journal of Experimental & Clinical Cancer Research : CR* 34 (1): 48. doi:10.1186/s13046-015-0165-2.

Callow, Marinella G, Felix Clairvoyant, Shirley Zhu, Brian Schryver, David B Whyte, James R Bischoff, Bahija Jallal, and Tod Smeal. 2001. "Requirement for PAK4 in the Anchorage-Independent Growth of Human Cancer Cell Lines." *Journal of Biological Chemistry* , October. doi:10.1074/jbc.M105732200.

Callow, Marinella G, Sergey Zozulya, Mikhail L Gishizky, Bahija Jallal, and Tod Smeal. 2005. "PAK4 Mediates Morphological Changes through the Regulation of GEF-H1." *Journal of Cell Science* 118 (Pt 9). England: 1861–72. doi:10.1242/jcs.02313.

Carragher, N O, S M Walker, L A Scott Carragher, F Harris, T K Sawyer, V G Brunton, B W Ozanne, and M C Frame. 2006. "Calpain 2 and Src Dependence Distinguishes Mesenchymal and Amoeboid Modes of Tumour Cell Invasion: A Link to Integrin Function." *Oncogene* 25 (42): 5726–40. doi:10.1038/sj.onc.1209582.

Carter, Julia H, Larry E Douglass, James A Deddens, Bruce M Colligan, Tejal R Bhatt, Jackson O Pemberton, Susan Konicek, Joanne Hom, Mark Marshall, and Jeremy R Graff. 2004. "Pak-1 Expression Increases with Progression of Colorectal Carcinomas to Metastasis." *Clinical Cancer Research* 10 (10): 3448 LP – 3456.

Castro-Castro, Antonio, Valentina Marchesin, Pedro Monteiro, Catalina Lodillinsky, Carine Rossé, and Philippe Chavrier. 2016. "Cellular and Molecular Mechanisms of MT1-MMP-Dependent Cancer Cell Invasion." *Annual Review of Cell and Developmental Biology* 32 (October). United States: 555–76. doi:10.1146/annurev-cellbio-111315-125227.

Chan, Amanda Y, Salvatore J Coniglio, Ya-yu Chuang, David Michaelson, Ulla G Knaus, Mark R Philips, and Marc Symons. 2005. "Roles of the Rac1 and Rac3 GTPases in Human Tumor Cell Invasion." *Oncogene* 24 (53): 7821–29. doi:10.1038/sj.onc.1208909.

Chang, R T M, Roger Kirby, and B J Challacombe. 2012. "Is There a Link between BPH and Prostate Cancer?" *The Practitioner* 256 (1750). England: 2,13-16.

Chao, Yvonne, Qian Wu, Marie Acquafondata, Rajiv Dhir, and Alan Wells. 2012. "Partial Mesenchymal to Epithelial Reverting Transition in Breast and Prostate Cancer Metastases." *Cancer Microenvironment : Official Journal of the International*

Cancer Microenvironment Society 5 (1): 19–28. doi:10.1007/s12307-011-0085-4.

Chen, Ni, and Qiao Zhou. 2016. “The Evolving Gleason Grading System.” *Chinese Journal of Cancer Research = Chung-Kuo Yen Cheng Yen Chiu* 28 (1): 58–64. doi:10.3978/j.issn.1000-9604.2016.02.04.

Chen, Shuaili, Theresa Auletta, Ostap Dovirak, Christina Hutter, Karen Kuntz, Samira El-ftesi, Jude Kendall, et al. 2008. “Copy Number Alterations in Pancreatic Cancer Identify Recurrent PAK4 Amplification.” *Cancer Biology & Therapy* 7 (11). Cold Spring Harbor Laboratory, Cold Spring Harbor, New York, New York, USA.: 1793–1802. doi:10.4161/cbt.7.11.6840.

Chen, W T. 1989. “Proteolytic Activity of Specialized Surface Protrusions Formed at Rosette Contact Sites of Transformed Cells.” *The Journal of Experimental Zoology* 251 (2). United States: 167–85. doi:10.1002/jez.1402510206.

Chen, W T, C C Lee, L Goldstein, S Bernier, C H Liu, C Y Lin, Y Yeh, W L Monsky, T Kelly, and M Dai. 1994. “Membrane Proteases as Potential Diagnostic and Therapeutic Targets for Breast Malignancy.” *Breast Cancer Research and Treatment* 31 (2–3). Netherlands: 217–26. doi:10.1007/BF00666155.

Cheng, Liang, Rodolfo Montironi, David G Bostwick, Antonio Lopez-Beltran, and Daniel M Berney. 2012. “Staging of Prostate Cancer.” *Histopathology* 60 (1). England: 87–117. doi:10.1111/j.1365-2559.2011.04025.x.

Chikumi, Hiroki, Ana Barac, Babak Behbahani, Yuan Gao, Hidemi Teramoto, Yi Zheng, and J Silvio Gutkind. 2004. “Homo- and Hetero-Oligomerization of PDZ-RhoGEF, LARG and P115RhoGEF by Their C-Terminal Region Regulates Their in Vivo Rho GEF Activity and Transforming Potential.” *Oncogene* 23 (1): 233–40. doi:10.1038/sj.onc.1207012.

Chikumi, Hiroki, Shigetomo Fukuhara, and J Silvio Gutkind. 2002. “Regulation of G Protein-Linked Guanine Nucleotide Exchange Factors for Rho, PDZ-RhoGEF, and LARG by Tyrosine Phosphorylation: Evidence of a Role for Focal Adhesion Kinase.” *The Journal of Biological Chemistry* 277 (14). United States: 12463–73. doi:10.1074/jbc.M108504200.

Ching, Yick-Pang, Veronica Y L Leong, Man-Fong Lee, Hai-Tao Xu, Dong-Yan Jin, and Irene Oi-Lin Ng. 2007. “P21-Activated Protein Kinase Is Overexpressed in Hepatocellular

Carcinoma and Enhances Cancer Metastasis Involving c-Jun NH₂-Terminal Kinase Activation and Paxillin Phosphorylation." *Cancer Research* 67 (8): 3601 LP – 3608.

Christiansen, Jason J, and Ayyappan K Rajasekaran. 2006. "Reassessing Epithelial to Mesenchymal Transition as a Prerequisite for Carcinoma Invasion and Metastasis." *Cancer Research* 66 (17). United States: 8319–26. doi:10.1158/0008-5472.CAN-06-0410.

Chuang, Ya-yu, Nhan L Tran, Nicole Rusk, Mitsutoshi Nakada, Michael E Berens, and Marc Symons. 2004. "Role of Synaptojanin 2 in Glioma Cell Migration and Invasion." *Cancer Research* 64 (22): 8271 LP – 8275. doi:10.1158/0008-5472.CAN-04-2097.

Clainche, Christophe Le, and Marie-France Carlier. 2008. "Regulation of Actin Assembly Associated With Protrusion and Adhesion in Cell Migration." *Physiological Reviews* 88 (2). American Physiological Society: 489–513. doi:10.1152/physrev.00021.2007.

Clark, Andrew G, and Danijela Matic Vignjevic. 2015. "Modes of Cancer Cell Invasion and the Role of the Microenvironment." *Current Opinion in Cell Biology* 36: 13–22. doi:https://doi.org/10.1016/j.ceb.2015.06.004.

Clark, Emily S, Amy S Whigham, Wendell G Yarbrough, and Alissa M Weaver. 2007. "Cortactin Is an Essential Regulator of Matrix Metalloproteinase Secretion and Extracellular Matrix Degradation in Invadopodia." *Cancer Research* 67 (9): 4227 LP – 4235.

Combeau, Gaëlle, Patricia Kreis, Florence Domenichini, Muriel Amar, Philippe Fossier, Véronique Rousseau, and Jean-Vianney Barnier. 2012. "The P21-Activated Kinase PAK3 Forms Heterodimers with PAK1 in Brain Implementing Trans-Regulation of PAK3 Activity." *The Journal of Biological Chemistry* 287 (36): 30084–96. doi:10.1074/jbc.M112.355073.

Cook, D R, K L Rossman, and C J Der. 2014. "Rho Guanine Nucleotide Exchange Factors: Regulators of Rho GTPase Activity in Development and Disease." *Oncogene* 33 (31): 4021–35. doi:10.1038/onc.2013.362.

Coopman, P J, M T Do, E W Thompson, and S C Mueller. 1998. "Phagocytosis of Cross-Linked Gelatin Matrix by Human Breast Carcinoma Cells Correlates with Their Invasive Capacity." *Clinical Cancer Research : An Official Journal of the American*

Association for Cancer Research 4 (2). United States: 507–15.

Cotteret, Sophie, Zahara M Jaffer, Alexander Beeser, and Jonathan Chernoff. 2003. "P21-Activated Kinase 5 (Pak5) Localizes to Mitochondria and Inhibits Apoptosis by Phosphorylating BAD." *Molecular and Cellular Biology* 23 (16). American Society for Microbiology: 5526–39. doi:10.1128/MCB.23.16.5526-5539.2003.

Cui, Yuanyuan, and Soichiro Yamada. 2013. "N-Cadherin Dependent Collective Cell Invasion of Prostate Cancer Cells Is Regulated by the N-Terminus of α-Catenin." *PloS One* 8 (1): e55069. doi:10.1371/journal.pone.0055069.

Dan, Chuntao, April Kelly, Ora Bernard, and Audrey Minden. 2001. "Cytoskeletal Changes Regulated by the PAK4 Serine/Threonine Kinase Are Mediated by LIM Kinase 1 and Cofilin." *Journal of Biological Chemistry* 276 (34): 32115–21. doi:10.1074/jbc.M100871200.

Dart, Anna E, Gary M Box, William Court, Madeline E Gale, John P Brown, Sarah E Pinder, Suzanne A Eccles, and Claire M Wells. 2015. "PAK4 Promotes Kinase-Independent Stabilization of RhoU to Modulate Cell Adhesion." *The Journal of Cell Biology* 211 (4). The Rockefeller University Press: 863–79. doi:10.1083/jcb.201501072.

Dart, Anna E, and Claire M Wells. 2013. "P21-Activated Kinase 4 – Not Just One of the PAK." *European Journal of Cell Biology* 92 (4): 129–38. doi:http://dx.doi.org/10.1016/j.ejcb.2013.03.002.

Davis, Sally J, Karen E Sheppard, Richard B Pearson, Ian G Campbell, Kylie L Gorringe, and Kaylene J Simpson. 2013. "Functional Analysis of Genes in Regions Commonly Amplified in High-Grade Serous and Endometrioid Ovarian Cancer." *Clinical Cancer Research* 19 (6): 1411 LP – 1421. doi:10.1158/1078-0432.CCR-12-3433.

Deer, Emily L, Jessica González-Hernández, Jill D Coursen, Jill E Shea, Josephat Ngatia, Courtney L Scaife, Matthew A Firpo, and Sean J Mulvihill. 2010. "Phenotype and Genotype of Pancreatic Cancer Cell Lines." *Pancreas* 39 (4): 425–35. doi:10.1097/MPA.0b013e3181c15963.

Desai, Bhavik, Tao Ma, and Meenakshi A Chellaiah. 2008. "Invadopodia and Matrix Degradation, a New Property of Prostate Cancer Cells during Migration and Invasion." *Journal of Biological Chemistry* 283 (20): 13856–66. doi:10.1074/jbc.M709401200.

Díaz, Begoña, Angela Yuen, Shinji Iizuka, Shigeki Higashiyama, and Sara A Courtneidge. 2013. “Notch Increases the Shedding of HB-EGF by ADAM12 to Potentiate Invadopodia Formation in Hypoxia.” *Journal of Cell Biology* 201 (2): 279–92. doi:10.1083/jcb.201209151.

Eckert, Mark A, Thinzar M Lwin, Andrew T Chang, Jihoon Kim, Etienne Danis, Lucila Ohno-Machado, and Jing Yang. 2011. “Twist1-Induced Invadopodia Formation Promotes Tumor Metastasis.” *Cancer Cell* 19 (3): 372–86. doi:10.1016/j.ccr.2011.01.036.

Emmert-Buck, Michael R, Cathy D Vocke, Rudy O Pozzatti, Paul H Duray, Scott B Jennings, Charles D Florence, Zhengping Zhuang, David G Bostwick, Lance A Liotta, and W Marston Linehan. 1995. “Allelic Loss on Chromosome 8p12–21 in Microdissected Prostatic Intraepithelial Neoplasia.” *Cancer Research* 55 (14): 2959 LP – 2962.

Enderling, Heiko, Nelson R Alexander, Emily S Clark, Kevin M Branch, Lourdes Estrada, Cornelia Crooke, Jérôme Jourquin, et al. 2017. “Dependence of Invadopodia Function on Collagen Fiber Spacing and Cross-Linking: Computational Modeling and Experimental Evidence.” *Biophysical Journal* 95 (5). Elsevier: 2203–18. doi:10.1529/biophysj.108.133199.

Fidler, Isaiah J. 1970. “Metastasis: Quantitative Analysis of Distribution and Fate of Tumor Emboli Labeled With 125I-5-Iodo-2’ -Deoxyuridine23.” *JNCI: Journal of the National Cancer Institute* 45 (4): 773–82. doi:10.1093/jnci/45.4.773.

Flynn, Daniel C, Youngjin Cho, Deanne Vincent, and Jess M Cunnick. 2008. “Podosomes and Invadopodia: Related Structures with Common Protein Components That May Promote Breast Cancer Cellular Invasion.” *Breast Cancer : Basic and Clinical Research* 2. Libertas Academica: 17–29. doi:10.4137/bcbcr.s789.

Foxall, Elizabeth, Aikaterini Pipili, Gareth E Jones, and Claire M Wells. 2016. “Significance of Kinase Activity in the Dynamic Invadosome.” *European Journal of Cell Biology* 95 (11). Germany: 483–92. doi:10.1016/j.ejcb.2016.07.002.

Foxall, Elizabeth, Adela Staszowska, Liisa M Hirvonen, Mirella Georgouli, Mariacristina Ciccioli, Alexander Rimmer, Lynn Williams, et al. 2019. “PAK4 Kinase Activity Plays a Crucial Role in the Podosome Ring of Myeloid Cells.” *Cell Reports* 29 (11): 3385-3393.e6. doi:https://doi.org/10.1016/j.celrep.2019.11.016.

Fraher, Daniel, Andrew Sanigorski, Natalie A Mellett, Peter J Meikle, Andrew J Sinclair, and Yann Gibert. 2016. “Zebrafish Embryonic Lipidomic Analysis Reveals That the Yolk Cell Is Metabolically Active in Processing Lipid.” *Cell Reports* 14 (6). United States: 1317–29. doi:10.1016/j.celrep.2016.01.016.

Fram, Sally, Helen King, David B Sacks, and Claire M Wells. 2014. “A PAK6-IQGAP1 Complex Promotes Disassembly of Cell-Cell Adhesions.” *Cellular and Molecular Life Sciences : CMLS* 71 (14): 2759–73. doi:10.1007/s00018-013-1528-5.

Franovic, Aleksandra, Kathryn C Elliott, Laetitia Seguin, M Fernanda Camargo, Sara M Weis, and David A Cheresh. 2015. “Glioblastomas Require Integrin Avβ3/PAK4 Signaling to Escape Senescence.” *Cancer Research* 75 (21): 4466–73. doi:10.1158/0008-5472.CAN-15-0988.

Friedl, Peter, and Stephanie Alexander. 2011. “Cancer Invasion and the Microenvironment: Plasticity and Reciprocity.” *Cell* 147 (5). Elsevier: 992–1009. doi:10.1016/j.cell.2011.11.016.

Friedl, Peter, and Katarina Wolf. 2003. “Tumour-Cell Invasion and Migration: Diversity and Escape Mechanisms.” *Nature Reviews Cancer* 3 (5): 362–74. doi:10.1038/nrc1075.

Fujishiro, Shuh-Hei, Susumu Tanimura, Shogo Mure, Yuji Kashimoto, Kazushi Watanabe, and Michiaki Kohno. 2008. “ERK1/2 Phosphorylate GEF-H1 to Enhance Its Guanine Nucleotide Exchange Activity toward RhoA.” *Biochemical and Biophysical Research Communications* 368 (1). United States: 162–67. doi:10.1016/j.bbrc.2008.01.066.

George, Jason T, Mohit Kumar Jolly, Shengnan Xu, Jason A Somarelli, and Herbert Levine. 2017. “Survival Outcomes in Cancer Patients Predicted by a Partial EMT Gene Expression Scoring Metric.” *Cancer Research* 77 (22): 6415–28. doi:10.1158/0008-5472.CAN-16-3521.

Georgess, Dan, Irma Machuca-Gayet, Anne Blangy, and Pierre Jurdic. 2014. “Podosome Organization Drives Osteoclast-Mediated Bone Resorption.” *Cell Adhesion & Migration* 8 (3): 191–204. doi:10.4161/cam.27840.

Ghasemi, Ahmad, Seyed Isaac Hashemy, Mahmoud Aghaei, and Mojtaba Panjehpour. 2017. “RhoA/ROCK Pathway Mediates Leptin-Induced UPA Expression to Promote Cell Invasion in Ovarian Cancer Cells.” *Cellular Signalling* 32: 104–14.

doi:https://doi.org/10.1016/j.cellsig.2017.01.020.

Giancotti, Filippo G. 2013. “Mechanisms Governing Metastatic Dormancy and Reactivation.” *Cell* 155 (4): 750–64. doi:https://doi.org/10.1016/j.cell.2013.10.029.

Gligorijevic, Bojana, Aviv Bergman, and John Condeelis. 2014. “Multiparametric Classification Links Tumor Microenvironments with Tumor Cell Phenotype.” *PLOS Biology* 12 (11). Public Library of Science: e1001995.

Gligorijevic, Bojana, Jeffrey Wyckoff, Hideki Yamaguchi, Yarong Wang, Evanthia T Roussos, and John Condeelis. 2012. “N-WASP-Mediated Invadopodium Formation Is Involved in Intravasation and Lung Metastasis of Mammary Tumors.” *Journal of Cell Science* 125 (Pt 3). England: 724–34. doi:10.1242/jcs.092726.

Gnesutta, Nerina, and Audrey Minden. 2003. “Death Receptor-Induced Activation of Initiator Caspase 8 Is Antagonized by Serine/Threonine Kinase PAK4.” *Molecular and Cellular Biology* 23 (21). American Society for Microbiology: 7838–48. doi:10.1128/MCB.23.21.7838-7848.2003.

Gnesutta, Nerina, Jian Qu, and Audrey Minden. 2001. “The Serine/Threonine Kinase PAK4 Prevents Caspase Activation and Protects Cells from Apoptosis.” *Journal of Biological Chemistry* 276 (17): 14414–19. doi:10.1074/jbc.M011046200.

Goc, Anna, Ahmad Al-Azayzih, Maha Abdalla, Belal Al-Husein, Sravankumar Kavuri, Jeffrey Lee, Kelvin Moses, and Payaningal R Somanath. 2013. “P21 Activated Kinase-1 (Pak1) Promotes Prostate Tumor Growth and Microinvasion via Inhibition of Transforming Growth Factor β Expression and Enhanced Matrix Metalloproteinase 9 Secretion.” *The Journal of Biological Chemistry* 288 (5). American Society for Biochemistry and Molecular Biology: 3025–35. doi:10.1074/jbc.M112.424770.

Goicoechea, Silvia M, Sahezeel Awadia, and Rafael Garcia-Mata. 2014. “I’m Coming to GEF You: Regulation of RhoGEFs during Cell Migration.” *Cell Adhesion & Migration* 8 (6): 535–49. doi:10.4161/cam.28721.

Gringel, Alexandra, Daniel Walz, Georg Rosenberger, Audrey Minden, Kerstin Kutsche, Petra Kopp, and Stefan Linder. 2006. “PAK4 and AlphaPIX Determine Podosome Size and Number in Macrophages through Localized Actin Regulation.” *Journal of Cellular Physiology* 209 (2). United States: 568–79. doi:10.1002/jcp.20777.

Guan, Xiaoying, Xiaoli Guan, Chi Dong, and Zuoyi Jiao. 2020. “Rho GTPases and Related Signaling Complexes in Cell Migration and Invasion.” *Experimental Cell Research* 388 (1). United States: 111824. doi:10.1016/j.yexcr.2020.111824.

Guérin, Olivier, Jean Louis Fischel, Jean-Marc Ferrero, Alexandre Bozec, and Gerard Milano. 2010. “EGFR Targeting in Hormone-Refractory Prostate Cancer: Current Appraisal and Prospects for Treatment.” *Pharmaceuticals (Basel, Switzerland)* 3 (7). MDPI: 2238–47. doi:10.3390/ph3072238.

Guo, Rishu, Elizabeth A Kasbohm, Puneeta Arora, Christopher J Sample, Babak Baban, Neetu Sud, Perumal Sivashanmugam, Nader H Moniri, and Yehia Daaka. 2006. “Expression and Function of Lysophosphatidic Acid LPA1 Receptor in Prostate Cancer Cells.” *Endocrinology* 147 (10). United States: 4883–92. doi:10.1210/en.2005-1635.

Ha, Byung Hak, Matthew J Davis, Catherine Chen, Hua Jane Lou, Jia Gao, Rong Zhang, Michael Krauthammer, et al. 2012. “Type II P21-Activated Kinases (PAKs) Are Regulated by an Autoinhibitory Pseudosubstrate.” *Proceedings of the National Academy of Sciences of the United States of America* 109 (40). United States: 16107–12. doi:10.1073/pnas.1214447109.

Hagedorn, Elliott J, Joshua W Ziel, Meghan A Morrissey, Lara M Linden, Zheng Wang, Qiuyi Chi, Sam A Johnson, and David R Sherwood. 2013. “The Netrin Receptor DCC Focuses Invadopodia-Driven Basement Membrane Transmigration in Vivo.” *The Journal of Cell Biology* 201 (6): 903 LP – 913.

Hall, Alan. 2012. “Rho Family GTPases.” *Biochemical Society Transactions* 40 (6): 1378–82. doi:10.1042/BST20120103.

Hammerich, Kai, Gustavo Ayala, and Thomas Wheeler. 2008. *Anatomy of the Prostate Gland and Surgical Pathology of Prostate Cancer*. *Prostate Cancer*. doi:10.1017/CBO9780511551994.003.

Hanahan, D, and R A Weinberg. 2011. “Hallmarks of Cancer: The next Generation.” *Cell* 144. doi:10.1016/j.cell.2011.02.013.

Hao, Chenzhou, Fan Zhao, Hongyan Song, Jing Guo, Xiaodong Li, Xiaolin Jiang, Ran Huan, et al. 2018. “Structure-Based Design of 6-Chloro-4-Aminoquinazoline-2-Carboxamide Derivatives as Potent and Selective P21-Activated Kinase 4 (PAK4)

Inhibitors." *Journal of Medicinal Chemistry* 61 (1). United States: 265–85. doi:10.1021/acs.jmedchem.7b01342.

Harnden, Patricia, Mike D Shelley, Bernadette Coles, John Staffurth, and Malcom D Mason. 2007. "Should the Gleason Grading System for Prostate Cancer Be Modified to Account for High-Grade Tertiary Components? A Systematic Review and Meta-Analysis." *The Lancet Oncology* 8 (5). Elsevier: 411–19. doi:10.1016/S1470-2045(07)70136-5.

Harris, William P, Elahe A Mostaghel, Peter S Nelson, and Bruce Montgomery. 2009. "Androgen Deprivation Therapy: Progress in Understanding Mechanisms of Resistance and Optimizing Androgen Depletion." *Nature Clinical Practice. Urology* 6 (2): 76–85. doi:10.1038/ncpuro1296.

Haugh, Jason M. 2012. "Live-Cell Fluorescence Microscopy with Molecular Biosensors: What Are We Really Measuring?" *Biophysical Journal* 102 (9): 2003–11. doi:10.1016/j.bpj.2012.03.055.

Hazan, Rachel B, Greg R Phillips, Rui Fang Qiao, Larry Norton, and Stuart A Aaronson. 2000. "Exogenous Expression of N-Cadherin in Breast Cancer Cells Induces Cell Migration, Invasion, and Metastasis." *The Journal of Cell Biology* 148 (4): 779 LP – 790.

Hazan, Rachel B, Rui Qiao, Rinat Keren, Ines Badano, and Kimita Suyama. 2004. "Cadherin Switch in Tumor Progression." *Annals of the New York Academy of Sciences* 1014 (April). United States: 155–63.

He, Li-Fang, Hong-Wu Xu, Min Chen, Zhi-Rong Xian, Xiao-Fen Wen, Min-Na Chen, Cai-Wen Du, Wen-He Huang, Jun-Dong Wu, and Guo-Jun Zhang. 2017. "Activated-PAK4 Predicts Worse Prognosis in Breast Cancer and Promotes Tumorigenesis through Activation of PI3K/AKT Signaling." *Oncotarget* 8 (11): 17573–85. doi:10.18632/oncotarget.7466.

Heerboth, Sarah, Genevieve Housman, Meghan Leary, Mckenna Longacre, Shannon Byler, Karolina Lapinska, Amber Willbanks, and Sibaji Sarkar. 2015. "EMT and Tumor Metastasis." *Clinical and Translational Medicine* 4: 6. doi:10.1186/s40169-015-0048-3.

Heinlein, Cynthia A, and Chawnshang Chang. 2004. "Androgen Receptor in Prostate

Cancer.” *Endocrine Reviews* 25 (2): 276–308. doi:10.1210/er.2002-0032.

Helden, Suzanne F G van, Machteld M Oud, Ben Joosten, Niels Peterse, Carl G Figdor, and Frank N van Leeuwen. 2008. “PGE-2-Mediated Podosome Loss in Dendritic Cells Is Dependent on Actomyosin Contraction Downstream of the RhoA–Rho-Kinase Axis.” *Journal of Cell Science* 121 (7): 1096 LP – 1106. doi:10.1242/jcs.020289.

Hill, David, Lanpeng Chen, Ewe Snaar-Jagalska, and Bill Chaudhry. 2018. “Embryonic Zebrafish Xenograft Assay of Human Cancer Metastasis.” *F1000Research* 7 (October). F1000 Research Limited: 1682. doi:10.12688/f1000research.16659.2.

Holm, Caroline, Suresh Rayala, Karin Jirström, Olle Stål, Rakesh Kumar, and Göran Landberg. 2006. “Association Between Pak1 Expression and Subcellular Localization and Tamoxifen Resistance in Breast Cancer Patients.” *JNCI: Journal of the National Cancer Institute* 98 (10): 671–80.

Hoshino, Daisuke, Kevin M Branch, and Alissa M Weaver. 2013. “Signaling Inputs to Invadopodia and Podosomes.” *Journal of Cell Science* 126 (14): 2979 LP – 2989. doi:10.1242/jcs.079475.

Hotary, K, E Allen, A Punturieri, I Yana, and S J Weiss. 2000. “Regulation of Cell Invasion and Morphogenesis in a Three-Dimensional Type I Collagen Matrix by Membrane-Type Matrix Metalloproteinases 1, 2, and 3.” *The Journal of Cell Biology* 149 (6). United States: 1309–23.

Huibregtse, J M, and S L Beaudenon. 1996. “Mechanism of HPV E6 Proteins in Cellular Transformation.” *Seminars in Cancer Biology* 7 (6). England: 317–26. doi:10.1006/scbi.1996.0041.

Humphrey, P A, X Zhu, R Zarnegar, P E Swanson, T L Ratliff, R T Vollmer, and M L Day. 1995. “Hepatocyte Growth Factor and Its Receptor (c-MET) in Prostatic Carcinoma.” *The American Journal of Pathology* 147 (2): 386–96.

Humphrey, Peter A. 2004. “Gleason Grading and Prognostic Factors in Carcinoma of the Prostate.” *Modern Pathology* 17 (3): 292–306. doi:10.1038/modpathol.3800054.

Huttenlocher, Anna, and Alan Rick Horwitz. 2011. “Integrins in Cell Migration.” *Cold Spring Harbor Perspectives in Biology* 3 (9): a005074. doi:10.1101/cshperspect.a005074.

Hwang, Young Sun, Jongsung Lee, Xianglan Zhang, and Paul F Lindholm. 2016. “Lysophosphatidic Acid Activates the RhoA and NF-KB through Akt/IκBα Signaling and Promotes Prostate Cancer Invasion and Progression by Enhancing Functional Invadopodia Formation.” *Tumor Biology* 37 (5): 6775–85. doi:10.1007/s13277-015-4549-x.

Jacob, Abitha, and Rytis Prekeris. 2015. “The Regulation of MMP Targeting to Invadopodia during Cancer Metastasis .” *Frontiers in Cell and Developmental Biology* .

Jaiswal, Mamta, Lothar Gremer, Radovan Dvorsky, Lars Christian Haeusler, Ion C Cirstea, Katharina Uhlenbrock, and Mohammad Reza Ahmadian. 2011. “Mechanistic Insights into Specificity, Activity, and Regulatory Elements of the Regulator of G-Protein Signaling (RGS)-Containing Rho-Specific Guanine Nucleotide Exchange Factors (GEFs) P115, PDZ-RhoGEF (PRG), and Leukemia-Associated RhoGEF (LARG).” *The Journal of Biological Chemistry* 286 (20): 18202–12. doi:10.1074/jbc.M111.226431.

Jin, Shenghao, Ya Zhuo, Weining Guo, and Jeffrey Field. 2005. “P21-Activated Kinase 1 (Pak1)-Dependent Phosphorylation of Raf-1 Regulates Its Mitochondrial Localization, Phosphorylation of BAD, and Bcl-2 Association.” *Journal of Biological Chemistry* 280 (26): 24698–705. doi:10.1074/jbc.M413374200.

Jolly, Mohit Kumar, Marcelo Boareto, Bin Huang, Dongya Jia, Mingyang Lu, Eshel Ben-Jacob, José N Onuchic, and Herbert Levine. 2015. “Implications of the Hybrid Epithelial/Mesenchymal Phenotype in Metastasis.” *Frontiers in Oncology* 5 (July). Frontiers Media S.A.: 155. doi:10.3389/fonc.2015.00155.

Jones, D L, D A Thompson, and K Munger. 1997. “Destabilization of the RB Tumor Suppressor Protein and Stabilization of P53 Contribute to HPV Type 16 E7-Induced Apoptosis.” *Virology* 239 (1). United States: 97–107. doi:10.1006/viro.1997.8851.

Jun, Gu, Li Keqiang, Li Maolan, Wu Xiangsong, Zhang Lin, Ding Qichen, Wu Wenguang, et al. 2012. “A Role for P21-Activated Kinase 7 in the Development of Gastric Cancer.” *The FEBS Journal* 280 (1). Wiley/Blackwell (10.1111): 46–55. doi:10.1111/febs.12048.

Kalpana, Gardiyawasam, Christopher Figy, Miranda Yeung, and Kam C Yeung. 2019.

"Reduced RhoA Expression Enhances Breast Cancer Metastasis with a Concomitant Increase in CCR5 and CXCR4 Chemokines Signaling." *Scientific Reports* 9 (1): 16351. doi:10.1038/s41598-019-52746-w.

Kang, M K, and N H Park. 2001. "Conversion of Normal to Malignant Phenotype: Telomere Shortening, Telomerase Activation, and Genomic Instability during Immortalization of Human Oral Keratinocytes." *Critical Reviews in Oral Biology and Medicine : An Official Publication of the American Association of Oral Biologists* 12 (1). United States: 38–54.

Karantanos, T, P G Corn, and T C Thompson. 2013. "Prostate Cancer Progression after Androgen Deprivation Therapy: Mechanisms of Castrate Resistance and Novel Therapeutic Approaches." *Oncogene* 32 (49): 5501–11. doi:10.1038/onc.2013.206.

Kasai, Shinji, Kazunobu Sugimura, Kunio Matsumoto, Nozomu Nishi, Taketoshi Kishimoto, and Tosikazu Nakamura. 1996. "Hepatocyte Growth Factor Is a Paracrine Regulator of Rat Prostate Epithelial Growth." *Biochemical and Biophysical Research Communications* 228 (2): 646–52. doi:https://doi.org/10.1006/bbrc.1996.1710.

Kelly, Mollie L, and Jonathan Chernoff. 2012. "Mouse Models of PAK Function." *Cellular Logistics* 2 (2): 84–88. doi:10.4161/cl.21381.

Kesanakurti, D, C Chetty, D Rajasekhar Maddirela, M Gujrati, and J S Rao. 2012. "Functional Cooperativity by Direct Interaction between PAK4 and MMP-2 in the Regulation of Anoikis Resistance, Migration and Invasion in Glioma." *Cell Death & Disease* 3 (12): e445–e445. doi:10.1038/cddis.2012.182.

Khan, Mohammad Imran, Abid Hamid, Vaqar Mustafa Adhami, Rahul K Lall, and Hasan Mukhtar. 2015. "Role of Epithelial Mesenchymal Transition in Prostate Tumorigenesis." *Current Pharmaceutical Design* 21 (10): 1240–48. doi:10.2174/1381612821666141211120326.

Kim, Ji Hyang, Han Na Kim, Kyu Taek Lee, Jong Kyun Lee, Seong-Ho Choi, Seung Woon Paik, Jong Chul Rhee, and Anson W Lowe. 2008. "Gene Expression Profiles in Gallbladder Cancer: The Close Genetic Similarity Seen for Early and Advanced Gallbladder Cancers May Explain the Poor Prognosis." *Tumour Biology : The Journal of the International Society for Oncodevelopmental Biology and Medicine* 29 (1).

Netherlands: 41–49. doi:10.1159/000132570.

Kimmelman, Alec C, Aram F Hezel, Andrew J Aguirre, Hongwu Zheng, Ji-hye Paik, Haoqiang Ying, Gerald C Chu, et al. 2008. “Genomic Alterations Link Rho Family of GTPases to the Highly Invasive Phenotype of Pancreas Cancer.” *Proceedings of the National Academy of Sciences* 105 (49): 19372 LP – 19377. doi:10.1073/pnas.0809966105.

King, Helen, Nicole S Nicholas, and Claire M Wells. 2014. “Role of P-21-Activated Kinases in Cancer Progression.” *International Review of Cell and Molecular Biology* 309: 347–87. doi:http://dx.doi.org/10.1016/B978-0-12-800255-1.00007-7.

King, Helen, Kiruthikah Thillai, Andrew Whale, Prabhu Arumugam, Hesham Eldaly, Hemant M Kocher, and Claire M Wells. 2017. “PAK4 Interacts with P85 Alpha: Implications for Pancreatic Cancer Cell Migration.” *Scientific Reports* 7 (1): 42575. doi:10.1038/srep42575.

Klezovitch, Olga, and Valeri Vasioukhin. 2015. “Cadherin Signaling: Keeping Cells in Touch.” *F1000Research* 4 (F1000 Faculty Rev). F1000Research: 550. doi:10.12688/f1000research.6445.1.

Knapp, Stefan. 2013. “8 - 3D Structure and Physiological Regulation of PAKs.” In , edited by Hiroshi B T - Paks Maruta Rac/Cdc42 (p21)-activated Kinases, 137–48. Oxford: Elsevier. doi:https://doi.org/10.1016/B978-0-12-407198-8.00008-4.

Knudsen, Beatrice S, Glenn A Gmyrek, Jennifer Inra, Douglas S Scherr, E Darracott Vaughan, David M Nanus, Michael W Kattan, William L Gerald, and George F Vande Woude. 2002. “High Expression of the Met Receptor in Prostate Cancer Metastasis to Bone.” *Urology* 60 (6). United States: 1113–17. doi:10.1016/s0090-4295(02)01954-4.

Kohrman, Abraham Q, and David Q Matus. 2017. “Divide or Conquer: Cell Cycle Regulation of Invasive Behavior.” *Trends in Cell Biology* 27 (1). England: 12–25. doi:10.1016/j.tcb.2016.08.003.

Krakhmal, N V, M V Zavyalova, E V Denisov, S V Vtorushin, and V M Perelmuter. 2015. “Cancer Invasion: Patterns and Mechanisms.” *Acta Naturae* 7 (2). A.I. Gordeyev: 17–28.

Kranenburg, O, M Poland, F P van Horck, D Drechsel, A Hall, and W H Moolenaar. 1999.

"Activation of RhoA by Lysophosphatidic Acid and Galpha12/13 Subunits in Neuronal Cells: Induction of Neurite Retraction." *Molecular Biology of the Cell* 10 (6). The American Society for Cell Biology: 1851–57. doi:10.1091/mbc.10.6.1851.

Kreis, Patricia, Véronique Rousseau, Emmanuel Thévenot, Gaëlle Combeau, and Jean-Vianney Barnier. 2008. "The Four Mammalian Splice Variants Encoded by the P21-Activated Kinase 3 Gene Have Different Biological Properties." *Journal of Neurochemistry* 106 (3). John Wiley & Sons, Ltd: 1184–97. doi:https://doi.org/10.1111/j.1471-4159.2008.05474.x.

Kuo, Jean-Cheng, Jia-Ren Lin, James M Staddon, Hiroshi Hosoya, and Ruey-Hwa Chen. 2003. "Uncoordinated Regulation of Stress Fibers and Focal Adhesions by DAP Kinase." *Journal of Cell Science* 116 (23): 4777 LP – 4790. doi:10.1242/jcs.00794.

Kuroiwa, Miho, Chitose Oneyama, Shigeyuki Nada, and Masato Okada. 2011. "The Guanine Nucleotide Exchange Factor Arhgef5 Plays Crucial Roles in Src-Induced Podosome Formation." *Journal of Cell Science* 124 (10): 1726 LP – 1738. doi:10.1242/jcs.080291.

Lei, Ming, Wange Lu, Wuyi Meng, Maria-Carla Parrini, Michael J Eck, Bruce J Mayer, and Stephen C Harrison. 2000. "Structure of PAK1 in an Autoinhibited Conformation Reveals a Multistage Activation Switch." *Cell* 102 (3): 387–97. doi:https://doi.org/10.1016/S0092-8674(00)00043-X.

Leonard, D, M J Hart, J V Platko, A Eva, W Henzel, T Evans, and R A Cerione. 1992. "The Identification and Characterization of a GDP-Dissociation Inhibitor (GDI) for the CDC42Hs Protein." *The Journal of Biological Chemistry* 267 (32). United States: 22860–68.

Leong, Hon S, Amy E Robertson, Konstantin Stoletov, Sean J Leith, Curtis A Chin, Andrew E Chien, M Nicole Hague, et al. 2014. "Invadopodia Are Required for Cancer Cell Extravasation and Are a Therapeutic Target for Metastasis." *Cell Reports* 8 (5). United States: 1558–70. doi:10.1016/j.celrep.2014.07.050.

Leung, T, X Q Chen, E Manser, and L Lim. 1996. "The P160 RhoA-Binding Kinase ROK Alpha Is a Member of a Kinase Family and Is Involved in the Reorganization of the Cytoskeleton." *Molecular and Cellular Biology* 16 (10): 5313 LP – 5327. doi:10.1128/MCB.16.10.5313.

Li, Ang, John C Dawson, Manuel Forero-Vargas, Heather J Spence, Xinzi Yu, Ireen König, Kurt Anderson, and Laura M Machesky. 2010. “The Actin-Bundling Protein Fascin Stabilizes Actin in Invadopodia and Potentiates Protrusive Invasion.” *Current Biology : CB* 20 (4): 339–45. doi:10.1016/j.cub.2009.12.035.

Li, Xiang, Weihong Wen, Kangdong Liu, Feng Zhu, Margarita Malakhova, Cong Peng, Tingting Li, et al. 2011. “Phosphorylation of Caspase-7 by P21-Activated Protein Kinase (PAK) 2 Inhibits Chemotherapeutic Drug-Induced Apoptosis of Breast Cancer Cell Lines.” *Journal of Biological Chemistry* 286 (25): 22291–99. doi:10.1074/jbc.M111.236596.

Li, Xiaodong, Qiang Ke, Yanshu Li, Funan Liu, Ge Zhu, and Feng Li. 2010. “DGCR6L, a Novel PAK4 Interaction Protein, Regulates PAK4-Mediated Migration of Human Gastric Cancer Cell via LIMK1.” *The International Journal of Biochemistry & Cell Biology* 42 (1). Netherlands: 70–79. doi:10.1016/j.biocel.2009.09.008.

Li, Zhilun, Hongquan Zhang, Lars Lundin, Minna Thullberg, Yajuan Liu, Yunling Wang, Lena Claesson-Welsh, and Staffan Strömblad. 2010. “P21-Activated Kinase 4 Phosphorylation of Integrin B5 Ser-759 and Ser-762 Regulates Cell Migration.” *Journal of Biological Chemistry* 285 (31): 23699–710. doi:10.1074/jbc.M110.123497.

Liang, Xuan, Srikanth Budnar, Shafali Gupta, Suzie Verma, Siew-Ping Han, Michelle M Hill, Roger J Daly, et al. 2017. “Tyrosine Dephosphorylated Cortactin Downregulates Contractility at the Epithelial Zonula Adherens through SRGAP1.” *Nature Communications* 8 (1). Nature Publishing Group UK: 790. doi:10.1038/s41467-017-00797-w.

Liao, Tsai-Tsen, and Muh-Hwa Yang. 2020. “Hybrid Epithelial/Mesenchymal State in Cancer Metastasis: Clinical Significance and Regulatory Mechanisms.” *Cells* 9 (3). doi:10.3390/cells9030623.

Lin, Yueh-Chien, Yuan-Li Huang, and Hsinyu Lee. 2015. “Lysophosphatidic Acid in Prostate Cancer Progression.” *Translational Cancer Research; Vol 4, No 5 (October 2015): Translational Cancer Research (Lysophospholipids on Immunity and Cancer)*.

Linder, Stefan. 2007. “The Matrix Corroded: Podosomes and Invadopodia in Extracellular Matrix Degradation.” *Trends in Cell Biology* 17 (3). England: 107–17.

doi:10.1016/j.tcb.2007.01.002.

Linder, Stefan, Christiane Wiesner, and Mirko Himmel. 2011. “Degrading Devices: Invadosomes in Proteolytic Cell Invasion.” *Annual Review of Cell and Developmental Biology* 27 (1). Annual Reviews: 185–211. doi:10.1146/annurev-cellbio-092910-154216.

Linklater, Erik, Cayla E Jewett, and Rytis Prekeris. 2018. “Chapter 5 - Polarized Membrane Trafficking in Development and Disease: From Epithelia Polarization to Cancer Cell Invasion.” In *Perspectives in Translational Cell Biology*, edited by P B T - Cell Polarity in Development and Disease Michael Conn, 121–46. Boston: Academic Press. doi:https://doi.org/10.1016/B978-0-12-802438-6.00005-X.

Liu, Y, N Chen, X Cui, X Zheng, L Deng, S Price, V Karantza, and A Minden. 2010. “The Protein Kinase Pak4 Disrupts Mammary Acinar Architecture and Promotes Mammary Tumorigenesis.” *Oncogene* 29 (44): 5883–94. doi:10.1038/onc.2010.329.

Liu, Yingying, Hang Xiao, Yanmei Tian, Tanya Nekrasova, Xingpei Hao, Hong Jin Lee, Nanjoo Suh, Chung S Yang, and Audrey Minden. 2008. “The Pak4 Protein Kinase Plays a Key Role in Cell Survival and Tumorigenesis in Athymic Mice.” *Molecular Cancer Research* 6 (7): 1215 LP – 1224. doi:10.1158/1541-7786.MCR-08-0087.

Lonergan, Peter E, and Donald J Tindall. 2011. “Androgen Receptor Signaling in Prostate Cancer Development and Progression.” *Journal of Carcinogenesis* 10: 20. doi:10.4103/1477-3163.83937.

Lorenz, Mike, Hideki Yamaguchi, Yarong Wang, Robert H Singer, and John Condeelis. 2004. “Imaging Sites of N-WASP Activity in Lamellipodia and Invadopodia of Carcinoma Cells.” *Current Biology* 14 (8). Elsevier: 697–703. doi:10.1016/j.cub.2004.04.008.

Lu, W, Y H Xia, J J Qu, Y Y He, B L Li, C Lu, X Luo, and X P Wan. 2013. “P21-Activated Kinase 4 Regulation of Endometrial Cancer Cell Migration and Invasion Involves the ERK1/2 Pathway Mediated MMP-2 Secretion.” *Neoplasma* 60 (5). Slovakia: 493–503. doi:10.4149/neo_2013_064.

Lu, Wange, and Bruce J Mayer. 1999. “Mechanism of Activation of Pak1 Kinase by Membrane Localization.” *Oncogene* 18 (3): 797–806. doi:10.1038/sj.onc.1202361.

Ma, Peng-de, Bin Sheng, Y Fan, E Du, Z Zhang, Y Liu, Y Xu, and Kuo Yang. 2016. “Increased Expression of Cortactin Is Associated with Prostate Cancer Progression / Invasiveness and Metastasis.” In .

Machesky, L M, and R H Insall. 1998. “Scar1 and the Related Wiskott-Aldrich Syndrome Protein, WASP, Regulate the Actin Cytoskeleton through the Arp2/3 Complex.” *Current Biology : CB* 8 (25). England: 1347–56. doi:10.1016/s0960-9822(98)00015-3.

Mahlamäki, Eija H, Päivikki Kauraniemi, Outi Monni, Maija Wolf, Sampsa Hautaniemi, and Anne Kallioniemi. 2004. “High-Resolution Genomic and Expression Profiling Reveals 105 Putative Amplification Target Genes in Pancreatic Cancer.” *Neoplasia (New York, N.Y.)* 6 (5): 432–39. doi:10.1593/neo.04130.

Maitland, Norman J. 2008. “Pathobiology of the Human Prostate.” *Trends in Urology, Gynaecology & Sexual Health* 13 (4). John Wiley & Sons, Ltd: 12–19. doi:https://doi.org/10.1002/tre.74.

Mandal, Shyamali, Keith R Johnson, and Margaret J Wheelock. 2008. “TGF-Beta Induces Formation of F-Actin Cores and Matrix Degradation in Human Breast Cancer Cells via Distinct Signaling Pathways.” *Experimental Cell Research* 314 (19). United States: 3478–93. doi:10.1016/j.yexcr.2008.09.013.

Marzo, Angelo M De, Elizabeth A Platz, Siobhan Sutcliffe, Jianfeng Xu, Henrik Gronberg, Charles G Drake, Yasutomo Nakai, William B Isaacs, and William G Nelson. 2007. “Inflammation in Prostate Carcinogenesis.” *Nature Reviews. Cancer* 7 (4). England: 256–69. doi:10.1038/nrc2090.

Mattila, Pieta K, and Pekka Lappalainen. 2008. “Filopodia: Molecular Architecture and Cellular Functions.” *Nature Reviews. Molecular Cell Biology* 9 (6). England: 446–54. doi:10.1038/nrm2406.

McNeal, J E, A Villers, E A Redwine, F S Freiha, and T A Stamey. 1991. “Microcarcinoma in the Prostate: Its Association with Duct-Acinar Dysplasia.” *Human Pathology* 22 (7). United States: 644–52. doi:10.1016/0046-8177(91)90286-x.

Md Hashim, Nur Fariesha, Nicole S Nicholas, Anna E Dart, Serafim Kiriakidis, Ewa Paleolog, and Claire M Wells. 2013. “Hypoxia-Induced Invadopodia Formation: A Role for β-PIX.” *Open Biology* 3 (6): 120159. doi:10.1098/rsob.120159.

Miki, H, S Suetsugu, and T Takenawa. 1998. “WAVE, a Novel WASP-Family Protein Involved in Actin Reorganization Induced by Rac.” *The EMBO Journal* 17 (23): 6932–41. doi:10.1093/emboj/17.23.6932.

Moissoglu, Konstadinos, and Martin Alexander Schwartz. 2014. “Spatial and Temporal Control of Rho GTPase Functions.” *Cellular Logistics* 4 (2). Taylor & Francis: e943618–e943618. doi:10.4161/21592780.2014.943618.

Morley, Samantha, Martin H Hager, Sara G Pollan, Beatrice Knudsen, Dolores Di Vizio, and Michael R Freeman. 2014. “Trading in Your Spindles for Blebs: The Amoeboid Tumor Cell Phenotype in Prostate Cancer.” *Asian Journal of Andrology* 16 (4). Medknow Publications & Media Pvt Ltd: 530–35. doi:10.4103/1008-682X.122877.

Moshfegh, Yasmin, Jose Javier Bravo-Cordero, Veronika Miskolci, John Condeelis, and Louis Hodgson. 2014. “A Trio–Rac1–Pak1 Signalling Axis Drives Invadopodia Disassembly.” *Nature Cell Biology* 16 (6): 571–83. doi:10.1038/ncb2972.

Mueller, S C, G Ghersi, S K Akiyama, Q X Sang, L Howard, M Pineiro-Sanchez, H Nakahara, Y Yeh, and W T Chen. 1999. “A Novel Protease-Docking Function of Integrin at Invadopodia.” *The Journal of Biological Chemistry* 274 (35). United States: 24947–52. doi:10.1074/jbc.274.35.24947.

Murphy, Danielle A, and Sara A Courtneidge. 2011. “The ‘ins’ and ‘Outs’ of Podosomes and Invadopodia: Characteristics, Formation and Function.” *Nature Reviews. Molecular Cell Biology* 12 (7). England: 413–26. doi:10.1038/nrm3141.

Nakahara, Hirokazu, Tomohiro Otani, Takuya Sasaki, Yasuhiro Miura, Yoshimi Takai, and Mikihiko Kogo. 2003. “Involvement of Cdc42 and Rac Small G Proteins in Invadopodia Formation of RPMI7951 Cells.” *Genes to Cells* 8 (12). John Wiley & Sons, Ltd: 1019–27. doi:https://doi.org/10.1111/j.1365-2443.2003.00695.x.

Nakai, Yasutomo, and Norio Nonomura. 2013. “Inflammation and Prostate Carcinogenesis.” *International Journal of Urology : Official Journal of the Japanese Urological Association* 20 (2). Australia: 150–60. doi:10.1111/j.1442-2042.2012.03101.x.

Nauseef, Jones T, and Michael D Henry. 2011. “Epithelial-to-Mesenchymal Transition in Prostate Cancer: Paradigm or Puzzle?” *Nature Reviews. Urology* 8 (8). England:

428–39. doi:10.1038/nrurol.2011.85.

Nicholas, Nicole S, Aikaterini Pipili, Michaela S Lesjak, Simon M Ameer-Beg, Jenny L C Geh, Ciaran Healy, Alistair D MacKenzie Ross, et al. 2016. “PAK4 Suppresses PDZ-RhoGEF Activity to Drive Invadopodia Maturation in Melanoma Cells.” *Oncotarget* 7 (43). United States: 70881–97. doi:10.18632/oncotarget.12282.

Nicholas, Nicole S, Aikaterini Pipili, Michaela S Lesjak, and Claire M Wells. 2017. “Differential Role for PAK1 and PAK4 during the Invadopodia Lifecycle.” *Small GTPases*, March. United States, 1–7. doi:10.1080/21541248.2017.1295830.

Nieman, Marvin T, Ryan S Prudoff, Keith R Johnson, and Margaret J Wheelock. 1999. “N-Cadherin Promotes Motility in Human Breast Cancer Cells Regardless of Their E-Cadherin Expression.” *The Journal of Cell Biology* 147 (3): 631 LP – 644.

Nieto, M. Angela, Ruby Yun-Ju Huang, Rebecca A. Jackson, and Jean Paul Thiery. 2016. “EMT: 2016.” *Cell* 166 (1): 21–45. doi:https://doi.org/10.1016/j.cell.2016.06.028.

Nieto, M Angela, and Amparo Cano. 2012. “The Epithelial-Mesenchymal Transition under Control: Global Programs to Regulate Epithelial Plasticity.” *Seminars in Cancer Biology* 22 (5–6). England: 361–68. doi:10.1016/j.semcancer.2012.05.003.

Nobes, C D, and A Hall. 1995. “Rho, Rac, and Cdc42 GTPases Regulate the Assembly of Multimolecular Focal Complexes Associated with Actin Stress Fibers, Lamellipodia, and Filopodia.” *Cell* 81 (1). United States: 53–62. doi:10.1016/0092-8674(95)90370-4.

Oleksy, Arkadiusz, Łukasz Opaliński, Urszula Derewenda, Zygmunt S Derewenda, and Jacek Otlewski. 2006. “The Molecular Basis of RhoA Specificity in the Guanine Nucleotide Exchange Factor PDZ-RhoGEF.” *The Journal of Biological Chemistry* 281 (43). United States: 32891–97. doi:10.1074/jbc.M606220200.

Olson, Adam, Vien Le, Joseph Aldahl, Eun-Jeong Yu, Erika Hooker, Yongfeng He, Dong-Hong Lee, et al. 2019. “The Comprehensive Role of E-Cadherin in Maintaining Prostatic Epithelial Integrity during Oncogenic Transformation and Tumor Progression.” *PLOS Genetics* 15 (10). Public Library of Science: e1008451.

Ong, Christy C, Adrian M Jubb, Peter M Haverty, Wei Zhou, Victoria Tran, Tom Truong, Helen Turley, et al. 2011. “Targeting P21-Activated Kinase 1 (PAK1) to Induce Apoptosis of Tumor Cells.” *Proceedings of the National Academy of Sciences of the*

United States of America 108 (17). National Academy of Sciences: 7177–82. doi:10.1073/pnas.1103350108.

Ong, Christy C, Adrian M Jubb, Diana Jakubiak, Wei Zhou, Joachim Rudolph, Peter M Haverty, Marcin Kowanetz, et al. 2013. "P21-Activated Kinase 1 (PAK1) as a Therapeutic Target in BRAF Wild-Type Melanoma." *JNCI: Journal of the National Cancer Institute* 105 (9): 606–7.

Ory, Stéphane, Hélène Brazier, and Anne Blangy. 2007. "Identification of a Bipartite Focal Adhesion Localization Signal in RhoU/Wrch-1, a Rho Family GTPase That Regulates Cell Adhesion and Migration." *Biology of the Cell* 99 (12). England: 701–16. doi:10.1042/BC20070058.

Oser, Matthew, Hideki Yamaguchi, Christopher C Mader, J J Bravo-Cordero, Marianela Arias, Xiaoming Chen, Vera Desmarais, Jacco van Rheenen, Anthony J Koleske, and John Condeelis. 2009. "Cortactin Regulates Cofilin and N-WASp Activities to Control the Stages of Invadopodium Assembly and Maturation." *The Journal of Cell Biology* 186 (4): 571–87. doi:10.1083/jcb.200812176.

Padmanaban, Veena, Ilona Krol, Yasir Suhail, Barbara M Szczerba, Nicola Aceto, Joel S Bader, and Andrew J Ewald. 2019. "E-Cadherin Is Required for Metastasis in Multiple Models of Breast Cancer." *Nature* 573 (7774): 439–44. doi:10.1038/s41586-019-1526-3.

Pandya, Pahini, Jose L Orgaz, and Victoria Sanz-Moreno. 2017. "Modes of Invasion during Tumour Dissemination." *Molecular Oncology* 11 (1). John Wiley and Sons Inc.: 5–27. doi:10.1002/1878-0261.12019.

Pantel, Klaus, Claudia Hille, and Howard I Scher. 2019. "Circulating Tumor Cells in Prostate Cancer: From Discovery to Clinical Utility." *Clinical Chemistry* 65 (1): 87–99. doi:10.1373/clinchem.2018.287102.

Park, Jung-Jin, Mee-Hee Park, Eun Hye Oh, Nak-Kyun Soung, Soo Jae Lee, Jae-Kyung Jung, Ok-Jun Lee, et al. 2018. "The P21-Activated Kinase 4-Slug Transcription Factor Axis Promotes Epithelial−mesenchymal Transition and Worsens Prognosis in Prostate Cancer." *Oncogene* 37 (38): 5147–59. doi:10.1038/s41388-018-0327-8.

Park, M-H, H-S Lee, C-S Lee, S T You, D-J Kim, B-H Park, M J Kang, et al. 2013. "P21-Activated Kinase 4 Promotes Prostate Cancer Progression through CREB."

Oncogene 32 (19). England: 2475–82. doi:10.1038/onc.2012.255.

Parrini, Maria Carla, Ming Lei, Stephen C Harrison, and Bruce J Mayer. 2002. "Pak1 Kinase Homodimers Are Autoinhibited in Trans and Dissociated upon Activation by Cdc42 and Rac1." *Molecular Cell* 9 (1). United States: 73–83. doi:10.1016/s1097-2765(01)00428-2.

Parsons, D Williams, Tian-Li Wang, Yardena Samuels, Alberto Bardelli, Jordan M Cummins, Laura DeLong, Natalie Silliman, et al. 2005. "Colorectal Cancer: Mutations in a Signalling Pathway." *Nature* 436 (7052). England: 792. doi:10.1038/436792a.

Patel, Maulik, and Andrei V Karginov. 2014. "Phosphorylation-Mediated Regulation of GEFs for RhoA." *Cell Adhesion & Migration* 8 (1). Landes Bioscience: 11–18. doi:10.4161/cam.28058.

Paz, Helicia, Navneeta Pathak, and Jing Yang. 2014. "Invading One Step at a Time: The Role of Invadopodia in Tumor Metastasis." *Oncogene* 33 (33): 4193–4202. doi:10.1038/onc.2013.393.

Pertz, Olivier, Louis Hodgson, Richard L Klemke, and Klaus M Hahn. 2006. "Spatiotemporal Dynamics of RhoA Activity in Migrating Cells." *Nature* 440 (7087): 1069–72. doi:10.1038/nature04665.

Phuyal, Santosh, and Hesso Farhan. 2019. "Multifaceted Rho GTPase Signaling at the Endomembranes ." *Frontiers in Cell and Developmental Biology* .

Piano, Mario De, Valeria Manuelli, Giorgia Zadra, Jonathan Otte, Per-Henrik D Edqvist, Fredrik Pontén, Salpie Nowinski, et al. 2020. "Lipogenic Signalling Modulates Prostate Cancer Cell Adhesion and Migration via Modification of Rho GTPases." *Oncogene* 39 (18): 3666–79. doi:10.1038/s41388-020-1243-2.

Pichot, Christina S, Constadina Arvanitis, Sean M Hartig, Samuel A Jensen, John Bechill, Saad Marzouk, Jindan Yu, Jeffrey A Frost, and Seth J Corey. 2010. "Cdc42-Interacting Protein 4 Promotes Breast Cancer Cell Invasion and Formation of Invadopodia through Activation of N-WASp." *Cancer Research* 70 (21): 8347–56. doi:10.1158/0008-5472.CAN-09-4149.

Piekny, Alisa J, and Michael Glotzer. 2008. "Anillin Is a Scaffold Protein That Links RhoA, Actin, and Myosin during Cytokinesis." *Current Biology : CB* 18 (1). England: 30–36.

doi:10.1016/j.cub.2007.11.068.

Pignatelli, Jeanine, David A Tumbarello, Ronald P Schmidt, and Christopher E Turner. 2012. “Hic-5 Promotes Invadopodia Formation and Invasion during TGF-β–Induced Epithelial–Mesenchymal Transition.” *Journal of Cell Biology* 197 (3): 421–37. doi:10.1083/jcb.201108143.

Pillé, J.-Y., C Denoyelle, J Varet, J.-R. Bertrand, J Soria, P Opolon, H Lu, et al. 2005. “Anti-RhoA and Anti-RhoC SiRNAs Inhibit the Proliferation and Invasiveness of MDA-MB-231 Breast Cancer Cells in Vitro</Em> and in Vivo</Em>.” *Molecular Therapy* 11 (2). Elsevier: 267–74. doi:10.1016/j.ymthe.2004.08.029.

Poincloux, Renaud, Floria Lizárraga, and Philippe Chavrier. 2009. “Matrix Invasion by Tumour Cells: A Focus on MT1-MMP Trafficking to Invadopodia.” *Journal of Cell Science* 122 (17): 3015 LP – 3024. doi:10.1242/jcs.034561.

Priya, Rashmi, Guillermo A Gomez, Srikanth Budnar, Suzie Verma, Hayley L Cox, Nicholas A Hamilton, and Alpha S Yap. 2015. “Feedback Regulation through Myosin II Confers Robustness on RhoA Signalling at E-Cadherin Junctions.” *Nature Cell Biology* 17 (10). England: 1282–93. doi:10.1038/ncb3239.

“Prostate Cancer UK.” n.d. https://prostatecanceruk.org/prostate-information/prostate-tests.

Puhr, Martin, Julia Hoefer, Georg Schäfer, Holger H H Erb, Su Jung Oh, Helmut Klocker, Isabel Heidegger, Hannes Neuwirt, and Zoran Culig. 2012. “Epithelial-to-Mesenchymal Transition Leads to Docetaxel Resistance in Prostate Cancer and Is Mediated by Reduced Expression of MiR-200c and MiR-205.” *The American Journal of Pathology* 181 (6). United States: 2188–2201. doi:10.1016/j.ajpath.2012.08.011.

Putzi, M J, and A M De Marzo. 2000. “Morphologic Transitions between Proliferative Inflammatory Atrophy and High-Grade Prostatic Intraepithelial Neoplasia.” *Urology* 56 (5). United States: 828–32. doi:10.1016/s0090-4295(00)00776-7.

Qu, J, M S Cammarano, Q Shi, K C Ha, P de Lanerolle, and A Minden. 2001. “Activated PAK4 Regulates Cell Adhesion and Anchorage-Independent Growth.” *Molecular and Cellular Biology* 21 (10): 3523–33. doi:10.1128/MCB.21.10.3523-3533.2001.

Qu, Jian, Xiaofan Li, Bennet G Novitch, Ye Zheng, Matthew Kohn, Jian-Ming Xie, Spencer Kozinn, Roderick Bronson, Amer A Beg, and Audrey Minden. 2003. “PAK4 Kinase Is

Essential for Embryonic Viability and for Proper Neuronal Development." *Molecular and Cellular Biology* 23 (20): 7122–33. doi:10.1128/mcb.23.20.7122-7133.2003.

Rajadurai, Charles V, Serhiy Havrylov, Kossay Zaoui, Richard Vaillancourt, Matthew Stuible, Monica Naujokas, Dongmei Zuo, Michel L Tremblay, and Morag Park. 2012. "Met Receptor Tyrosine Kinase Signals through a Cortactin–Gab1 Scaffold Complex, to Mediate Invadopodia." *Journal of Cell Science* 125 (12): 2940 LP – 2953. doi:10.1242/jcs.100834.

Rao, Donald D, John S Vorhies, Neil Senzer, and John Nemunaitis. 2009. "SiRNA vs. ShRNA: Similarities and Differences." *Advanced Drug Delivery Reviews* 61 (9): 746–59. doi:https://doi.org/10.1016/j.addr.2009.04.004.

Razidlo, Gina L, Barbara Schroeder, Jing Chen, Daniel D Billadeau, and Mark A McNiven. 2014. "Vav1 as a Central Regulator of Invadopodia Assembly." *Current Biology : CB* 24 (1): 86–93. doi:10.1016/j.cub.2013.11.013.

Remacle, Albert, Gillian Murphy, and Christian Roghi. 2003. "Membrane Type I-Matrix Metalloproteinase (MT1-MMP) Is Internalised by Two Different Pathways and Is Recycled to the Cell Surface." *Journal of Cell Science* 116 (19): 3905 LP – 3916. doi:10.1242/jcs.00710.

Rider, Leah, Peter Oladimeji, and Maria Diakonova. 2013. "PAK1 Regulates Breast Cancer Cell Invasion through Secretion of Matrix Metalloproteinases in Response to Prolactin and Three-Dimensional Collagen IV." *Molecular Endocrinology (Baltimore, Md.)* 27 (7): 1048–64. doi:10.1210/me.2012-1322.

Ridley, A J. 2001. "Rho GTPases and Cell Migration." *Journal of Cell Science* 114 (Pt 15). England: 2713–22.

Ridley, A J, and A Hall. 1992. "The Small GTP-Binding Protein Rho Regulates the Assembly of Focal Adhesions and Actin Stress Fibers in Response to Growth Factors." *Cell* 70 (3). United States: 389–99. doi:10.1016/0092-8674(92)90163-7.

Rodrigues, Tânia, Banani Kundu, Joana Silva-Correia, S C Kundu, Joaquim M Oliveira, Rui L Reis, and Vitor M Correlo. 2018. "Emerging Tumor Spheroids Technologies for 3D in Vitro Cancer Modeling." *Pharmacology & Therapeutics* 184: 201–11. doi:https://doi.org/10.1016/j.pharmthera.2017.10.018.

Roh-Johnson, M, J J Bravo-Cordero, A Patsialou, V P Sharma, P Guo, H Liu, L Hodgson, and J Condeelis. 2014. “Macrophage Contact Induces RhoA GTPase Signaling to Trigger Tumor Cell Intravasation.” *Oncogene* 33 (33): 4203–12. doi:10.1038/onc.2013.377.

Rosenfeldt, Hans, Maria Domenica Castellone, Paul A Randazzo, and J Silvio Gutkind. 2006. “Rac Inhibits Thrombin-Induced Rho Activation: Evidence of a Pak-Dependent GTPase Crosstalk.” *Journal of Molecular Signaling* 1 (December). BioMed Central: 8. doi:10.1186/1750-2187-1-8.

Rottner, K, A Hall, and J V Small. 1999. “Interplay between Rac and Rho in the Control of Substrate Contact Dynamics.” *Current Biology : CB* 9 (12). England: 640–48. doi:10.1016/s0960-9822(99)80286-3.

Sahai, Erik, and Christopher J Marshall. 2003. “Differing Modes of Tumour Cell Invasion Have Distinct Requirements for Rho/ROCK Signalling and Extracellular Proteolysis.” *Nature Cell Biology* 5 (8). England: 711–19. doi:10.1038/ncb1019.

Sakurai-Yageta, Mika, Chiara Recchi, Gaëlle Le Dez, Jean-Baptiste Sibarita, Laurent Daviet, Jacques Camonis, Crislyn D’Souza-Schorey, and Philippe Chavrier. 2008. “The Interaction of IQGAP1 with the Exocyst Complex Is Required for Tumor Cell Invasion Downstream of Cdc42 and RhoA.” *The Journal of Cell Biology* 181 (6). The Rockefeller University Press: 985–98. doi:10.1083/jcb.200709076.

Sander, E E, J P ten Klooster, S van Delft, R A van der Kammen, and J G Collard. 1999. “Rac Downregulates Rho Activity: Reciprocal Balance between Both GTPases Determines Cellular Morphology and Migratory Behavior.” *The Journal of Cell Biology* 147 (5). The Rockefeller University Press: 1009–22. doi:10.1083/jcb.147.5.1009.

Sanz-Moreno, Victoria, Gilles Gadea, Jessica Ahn, Hugh Paterson, Pierfrancesco Marra, Sophie Pinner, Erik Sahai, and Christopher J Marshall. 2008. “Rac Activation and Inactivation Control Plasticity of Tumor Cell Movement.” *Cell* 135 (3): 510–23. doi:https://doi.org/10.1016/j.cell.2008.09.043.

Sanz-Moreno, Victoria, and Christopher J Marshall. 2010. “The Plasticity of Cytoskeletal Dynamics Underlying Neoplastic Cell Migration.” *Current Opinion in Cell Biology* 22 (5): 690–96. doi:https://doi.org/10.1016/j.ceb.2010.08.020.

Sawicki, Grzegorz. 2013. “Intracellular Regulation of Matrix Metalloproteinase-2 Activity: New Strategies in Treatment and Protection of Heart Subjected to Oxidative Stress.” Edited by C F Sier and L Xi. *Scientifica* 2013. Hindawi Publishing Corporation: 130451. doi:10.1155/2013/130451.

Schenk, Jeannette M, Alan R Kristal, Kathryn B Arnold, Catherine M Tangen, Marian L Neuhouser, Daniel W Lin, Emily White, and Ian M Thompson. 2011. “Association of Symptomatic Benign Prostatic Hyperplasia and Prostate Cancer: Results from the Prostate Cancer Prevention Trial.” *American Journal of Epidemiology* 173 (12): 1419–28. doi:10.1093/aje/kwq493.

Schlomm, Thorsten, Patrick Kirstein, Liv Iwers, Birte Daniel, Thomas Steuber, Jochen Walz, Felix H K Chun, et al. 2007. “Clinical Significance of Epidermal Growth Factor Receptor Protein Overexpression and Gene Copy Number Gains in Prostate Cancer.” *Clinical Cancer Research : An Official Journal of the American Association for Cancer Research* 13 (22 Pt 1). United States: 6579–84. doi:10.1158/1078-0432.CCR-07-1257.

Schmid, H P, J E McNeal, and T A Stamey. 1993. “Observations on the Doubling Time of Prostate Cancer. The Use of Serial Prostate-Specific Antigen in Patients with Untreated Disease as a Measure of Increasing Cancer Volume.” *Cancer* 71 (6). United States: 2031–40. doi:10.1002/1097-0142(19930315)71:6<2031::aid-cncr2820710618>3.0.co;2-q.

Schmidt, Anja, and Alan Hall. 2002. “Guanine Nucleotide Exchange Factors for Rho GTPases: Turning on the Switch.” *Genes & Development* 16 (13). United States: 1587–1609. doi:10.1101/gad.1003302.

Schoumacher, Marie, Robert D Goldman, Daniel Louvard, and Danijela M Vignjevic. 2010. “Actin, Microtubules, and Vimentin Intermediate Filaments Cooperate for Elongation of Invadopodia.” *The Journal of Cell Biology* 189 (3). United States: 541–56. doi:10.1083/jcb.200909113.

Schramp, Mark, Olivia Ying, Tai Young Kim, and G Steven Martin. 2008. “ERK5 Promotes Src-Induced Podosome Formation by Limiting Rho Activation.” *The Journal of Cell Biology* 181 (7). The Rockefeller University Press: 1195–1210. doi:10.1083/jcb.200801078.

Sedgwick, Alanna E, James W Clancy, M Olivia Balmert, and Crislyn D'Souza-Schorey. 2015. "Extracellular Microvesicles and Invadopodia Mediate Non-Overlapping Modes of Tumor Cell Invasion." *Scientific Reports* 5 (October). England: 14748. doi:10.1038/srep14748.

Seiler, Christoph, Gangarao Davuluri, Joshua Abrams, Fitzroy J Byfield, Paul A Janmey, and Michael Pack. 2012. "Smooth Muscle Tension Induces Invasive Remodeling of the Zebrafish Intestine." *PLoS Biology* 10 (9). United States: e1001386. doi:10.1371/journal.pbio.1001386.

Sells, Mary Ann, Ulla G Knaus, Shubha Bagrodia, Diane M Ambrose, Gary M Bokoch, and Jonathan Chernoff. 1997. "Human P21-Activated Kinase (Pak1) Regulates Actin Organization in Mammalian Cells." *Current Biology* 7 (3): 202–10. doi:https://doi.org/10.1016/S0960-9822(97)70091-5.

Simpson, Kaylene J, Aisling S Dugan, and Arthur M Mercurio. 2004. "Functional Analysis of the Contribution of RhoA and RhoC GTPases to Invasive Breast Carcinoma." *Cancer Research* 64 (23): 8694 LP – 8701. doi:10.1158/0008-5472.CAN-04-2247.

Singer, K H, R M Scearce, D T Tuck, L P Whichard, S M Denning, and B F Haynes. 1989. "Removal of Fibroblasts from Human Epithelial Cell Cultures with Use of a Complement Fixing Monoclonal Antibody Reactive with Human Fibroblasts and Monocytes/Macrophages." *The Journal of Investigative Dermatology* 92 (2). United States: 166–70. doi:10.1111/1523-1747.ep12276685.

Siu, Michelle K Y, Hoi Yan Chan, Daniel S H Kong, Esther S Y Wong, Oscar G W Wong, Hextan Y S Ngan, Kar Fai Tam, et al. 2010. "P21-Activated Kinase 4 Regulates Ovarian Cancer Cell Proliferation, Migration, and Invasion and Contributes to Poor Prognosis in Patients." *Proceedings of the National Academy of Sciences* 107 (43): 18622 LP – 18627.

Soosairajah, Juliana, Sankar Maiti, O'neil Wiggan, Patrick Sarmiere, Nathalie Moussi, Boris Sarcevic, Rashmi Sampath, James R Bamburg, and Ora Bernard. 2005. "Interplay between Components of a Novel LIM Kinase-Slingshot Phosphatase Complex Regulates Cofilin." *The EMBO Journal* 24 (3). England: 473–86. doi:10.1038/sj.emboj.7600543.

Spratley, Samantha J, Ligia I Bastea, Heike Döppler, Kensaku Mizuno, and Peter Storz.

2011. “Protein Kinase D Regulates Cofilin Activity through P21-Activated Kinase 4.” *The Journal of Biological Chemistry* 286 (39): 34254–61. doi:10.1074/jbc.M111.259424.

Spuul, Pirjo, Paolo Ciufici, Véronique Veillat, Anne Leclercq, Thomas Daubon, IJsbrand Kramer, and Elisabeth Génot. 2014. “Importance of RhoGTPases in Formation, Characteristics, and Functions of Invadosomes.” *Small GTPases* 5. Landes Bioscience: e28195–e28195. doi:10.4161/sgtp.28713.

Steenbergen, R D, J M Walboomers, C J Meijer, E M van der Raaij-Helmer, J N Parker, L T Chow, T R Broker, and P J Snijders. 1996. “Transition of Human Papillomavirus Type 16 and 18 Transfected Human Foreskin Keratinocytes towards Immortality: Activation of Telomerase and Allele Losses at 3p, 10p, 11q and/or 18q.” *Oncogene* 13 (6). England: 1249–57.

Stockert, Juan C, Richard W Horobin, Lucas L Colombo, and Alfonso Blázquez-Castro. 2018. “Tetrazolium Salts and Formazan Products in Cell Biology: Viability Assessment, Fluorescence Imaging, and Labeling Perspectives.” *Acta Histochemica* 120 (3). Germany: 159–67. doi:10.1016/j.acthis.2018.02.005.

Strongin, A Y, I Collier, G Bannikov, B L Marmer, G A Grant, and G I Goldberg. 1995. “Mechanism of Cell Surface Activation of 72-KDa Type IV Collagenase. Isolation of the Activated Form of the Membrane Metalloprotease.” *The Journal of Biological Chemistry* 270 (10). United States: 5331–38. doi:10.1074/jbc.270.10.5331.

Struckhoff, Amanda P, Manish K Rana, and Rebecca A Worthylake. 2011. “RhoA Can Lead the Way in Tumor Cell Invasion and Metastasis.” *Frontiers in Bioscience (Landmark Edition)* 16 (January). United States: 1915–26. doi:10.2741/3830.

Sun, Lingfei, Ruifang Guan, I-Ju Lee, Yajun Liu, Mengran Chen, Jiawei Wang, Jian-Qiu Wu, and Zhucheng Chen. 2015. “Mechanistic Insights into the Anchorage of the Contractile Ring by Anillin and Mid1.” *Developmental Cell* 33 (4): 413–26. doi:10.1016/j.devcel.2015.03.003.

Taddei, Maria Letizia, Elisa Giannoni, Giuseppina Comito, and Paola Chiarugi. 2013. “Microenvironment and Tumor Cell Plasticity: An Easy Way Out.” *Cancer Letters* 341 (1): 80–96. doi:https://doi.org/10.1016/j.canlet.2013.01.042.

Taddei, Maria Letizia, Matteo Parri, Adriano Angelucci, Francesca Bianchini, Chiara

Marconi, Elisa Giannoni, Giovanni Raugei, Mauro Bologna, Lido Calorini, and Paola Chiarugi. 2011. “EphA2 Induces Metastatic Growth Regulating Amoeboid Motility and Clonogenic Potential in Prostate Carcinoma Cells.” *Molecular Cancer Research* 9 (2): 149 LP – 160. doi:10.1158/1541-7786.MCR-10-0298.

Takkunen, Minna, Mika Hukkanen, Mikko Liljestrom, Reidar Grenman, and Ismo Virtanen. 2010. “Podosome-like Structures of Non-Invasive Carcinoma Cells Are Replaced in Epithelial-Mesenchymal Transition by Actin Comet-Embedded Invadopodia.” *Journal of Cellular and Molecular Medicine* 14 (6B). England: 1569–93. doi:10.1111/j.1582-4934.2009.00868.x.

Tanya, Nekrasova, and Minden Audrey. 2011. “PAK4 Is Required for Regulation of the Cell-Cycle Regulatory Protein P21, and for Control of Cell-Cycle Progression.” *Journal of Cellular Biochemistry* 112 (7). Wiley-Blackwell: 1795–1806. doi:10.1002/jcb.23092.

Teng, Yong, Xiayang Xie, Steven Walker, David T White, Jeff S Mumm, and John K Cowell. 2013. “Evaluating Human Cancer Cell Metastasis in Zebrafish.” *BMC Cancer* 13 (October). England: 453. doi:10.1186/1471-2407-13-453.

Thiery, Jean Paul. 2002. “Epithelial-Mesenchymal Transitions in Tumour Progression.” *Nature Reviews. Cancer* 2 (6). England: 442–54. doi:10.1038/nrc822.

Thun, Anne von, Christian Preisinger, Oliver Rath, Juliane P Schwarz, Chris Ward, Naser Monsefi, Javier Rodríguez, et al. 2013. “Extracellular Signal-Regulated Kinase Regulates RhoA Activation and Tumor Cell Plasticity by Inhibiting Guanine Exchange Factor H1 Activity.” *Molecular and Cellular Biology* 33 (22): 4526–37. doi:10.1128/MCB.00585-13.

Tolde, Ondrej, Daniel Rosel, Pavel Vesely, Petr Folk, and Jan Brabek. 2010. “The Structure of Invadopodia in a Complex 3D Environment.” *European Journal of Cell Biology* 89 (9). Germany: 674–80. doi:10.1016/j.ejcb.2010.04.003.

Tolias, K F, J H Hartwig, H Ishihara, Y Shibasaki, L C Cantley, and C L Carpenter. 2000. “Type Ialpha Phosphatidylinositol-4-Phosphate 5-Kinase Mediates Rac-Dependent Actin Assembly.” *Current Biology : CB* 10 (3). England: 153–56. doi:10.1016/s0960-9822(00)00315-8.

Tomita, Kyoichi, Adrie van Bokhoven, Geert J L H van Leenders, Emiel T G Ruijter,

Cornelius F J Jansen, Marion J G Bussemakers, and Jack A Schalken. 2000. “Cadherin Switching in Human Prostate Cancer Progression.” *Cancer Research* 60 (13): 3650 LP – 3654.

Tseliou, M, A Al-Qahtani, S Alarifi, S H Alkahtani, C Stournaras, and G Sourvinos. 2016. “The Role of RhoA, RhoB and RhoC GTPases in Cell Morphology, Proliferation and Migration in Human Cytomegalovirus (HCMV) Infected Glioblastoma Cells.” *Cellular Physiology and Biochemistry* 38 (1): 94–109. doi:10.1159/000438612.

Vadlamudi, Ratna K, Liana Adam, Rui-An Wang, Mahitosh Mandal, Diep Nguyen, Aysegul Sahin, Jonathan Chernoff, Mien-Chie Hung, and Rakesh Kumar. 2000. “Regulatable Expression of P21-Activated Kinase-1 Promotes Anchorage-Independent Growth and Abnormal Organization of Mitotic Spindles in Human Epithelial Breast Cancer Cells.” *Journal of Biological Chemistry* 275 (46): 36238–44. doi:10.1074/jbc.M002138200.

Valastyan, S, and R A Weinberg. 2011. “Tumor Metastasis: Molecular Insights and Evolving Paradigms.” *Cell* 147. doi:10.1016/j.cell.2011.09.024.

Vega, Francisco M, Gilbert Fruhwirth, Tony Ng, and Anne J Ridley. 2011. “RhoA and RhoC Have Distinct Roles in Migration and Invasion by Acting through Different Targets.” *The Journal of Cell Biology* 193 (4): 655–65. doi:10.1083/jcb.201011038.

Vega, Francisco M, and Anne J Ridley. 2008. “Rho GTPases in Cancer Cell Biology.” *FEBS Letters* 582 (14). England: 2093–2101. doi:10.1016/j.febslet.2008.04.039.

Wang, Chenwei, Haodong Xu, Shaofeng Lin, Wankun Deng, Jiaqi Zhou, Ying Zhang, Ying Shi, Di Peng, and Yu Xue. 2020. “GPS 5.0: An Update on the Prediction of Kinase-Specific Phosphorylation Sites in Proteins.” *Genomics, Proteomics & Bioinformatics* 18 (1): 72–80. doi:https://doi.org/10.1016/j.gpb.2020.01.001.

Wang, Lei, and Yi Zheng. 2007. “Cell Type-Specific Functions of Rho GTPases Revealed by Gene Targeting in Mice.” *Trends in Cell Biology* 17 (2). Elsevier: 58–64. doi:10.1016/j.tcb.2006.11.009.

Wang, R-A, H Zhang, S Balasenthil, D Medina, and R Kumar. 2006. “PAK1 Hyperactivation Is Sufficient for Mammary Gland Tumor Formation.” *Oncogene* 25 (20): 2931–36. doi:10.1038/sj.onc.1209309.

Wang, Wei, Liangzhong Lim, Yohendran Baskaran, Ed Manser, and Jianxing Song. 2013.

"NMR Binding and Crystal Structure Reveal That Intrinsically-Unstructured Regulatory Domain Auto-Inhibits PAK4 by a Mechanism Different from That of PAK1." *Biochemical and Biophysical Research Communications* 438 (1): 169–74. doi:https://doi.org/10.1016/j.bbrc.2013.07.047.

Wang, Xiao-Xia, Qian Cheng, Shang-Nuan Zhang, He-ya Qian, Jin-Xia Wu, Hui Tian, Dong-Sheng Pei, and Jun-Nian Zheng. 2013. "PAK5-Egr1-MMP2 Signaling Controls the Migration and Invasion in Breast Cancer Cell." *Tumour Biology : The Journal of the International Society for Oncodevelopmental Biology and Medicine* 34 (5). United States: 2721–29. doi:10.1007/s13277-013-0824-x.

Watanabe, Naoki, Pascal Madaule, Tim Reid, Toshimasa Ishizaki, Go Watanabe, Akira Kakizuka, Yuji Saito, Kazuwa Nakao, Brigitte M Jockusch, and Shuh Narumiya. 1997. "P140mDia, a Mammalian Homolog of Drosophila Diaphanous,Is a Target Protein for Rho Small GTPase and Is a Ligand for Profilin." *The EMBO Journal* 16 (11). John Wiley & Sons, Ltd: 3044–56. doi:https://doi.org/10.1093/emboj/16.11.3044.

Wells, Claire M., and Gareth E. Jones. 2010. "The Emerging Importance of Group II PAKs." *Biochemical Journal* 425 (3): 465–73. doi:10.1042/BJ20091173.

Wells, Claire M, Arie Abo, and Anne J Ridley. 2002. "PAK4 Is Activated via PI3K in HGF-Stimulated Epithelial Cells." *Journal of Cell Science* 115 (20): 3947 LP – 3956.

Wells, Claire M, Andrew D Whale, Maddy Parsons, John R W Masters, and Gareth E Jones. 2010. "PAK4: A Pluripotent Kinase That Regulates Prostate Cancer Cell Adhesion." *Journal of Cell Science* 123 (Pt 10). England: 1663–73. doi:10.1242/jcs.055707.

Wen, Xingqiao, Xiaojuan Li, Bing Liao, Yong Liu, Jieying Wu, Xiaoxu Yuan, Bin Ouyang, Qipeng Sun, and Xin Gao. 2009. "Knockdown of P21-Activated Kinase 6 Inhibits Prostate Cancer Growth and Enhances Chemosensitivity to Docetaxel." *Urology* 73 (6). United States: 1407–11. doi:10.1016/j.urology.2008.09.041.

Wever, Olivier De, Wendy Westbroek, An Verloes, Nele Bloemen, Marc Bracke, Christian Gespach, Erik Bruyneel, and Marc Mareel. 2004. "Critical Role of N-Cadherin in Myofibroblast Invasion and Migration in Vitro Stimulated by Colon-Cancer-Cell-Derived TGF-β or Wounding." *Journal of Cell Science* 117 (20): 4691 LP – 4703.

Whale, A D, A Dart, M Holt, G E Jones, and C M Wells. 2013. "PAK4 Kinase Activity and

Somatic Mutation Promote Carcinoma Cell Motility and Influence Inhibitor Sensitivity." *Oncogene* 32 (16). England: 2114–20. doi:10.1038/onc.2012.233.

Wilde, Christian, and Klaus Aktories. 2001. "The Rho-ADP-Ribosylating C3 Exoenzyme from Clostridium Botulinum and Related C3-like Transferases." *Toxicon* 39 (11): 1647–60. doi:https://doi.org/10.1016/S0041-0101(01)00152-0.

Williams, Karla C, and Marc G Coppolino. 2011. "Phosphorylation of Membrane Type 1-Matrix Metalloproteinase (MT1-MMP) and Its Vesicle-Associated Membrane Protein 7 (VAMP7)-Dependent Trafficking Facilitate Cell Invasion and Migration." *The Journal of Biological Chemistry* 286 (50). American Society for Biochemistry and Molecular Biology: 43405–16. doi:10.1074/jbc.M111.297069.

Wilt, Timothy J, and Hashim U Ahmed. 2013. "Prostate Cancer Screening and the Management of Clinically Localized Disease." *BMJ (Clinical Research Ed.)* 346 (January). England: f325.

Wisdom, Katrina M, Kolade Adebowale, Julie Chang, Joanna Y Lee, Sungmin Nam, Rajiv Desai, Ninna Struck Rossen, et al. 2018. "Matrix Mechanical Plasticity Regulates Cancer Cell Migration through Confining Microenvironments." *Nature Communications* 9 (1): 4144. doi:10.1038/s41467-018-06641-z.

Wolf, Katarina, and Peter Friedl. 2009. "Mapping Proteolytic Cancer Cell-Extracellular Matrix Interfaces." *Clinical & Experimental Metastasis* 26 (4): 289–98. doi:10.1007/s10585-008-9190-2.

Wolf, Katarina, Irina Mazo, Harry Leung, Katharina Engelke, Ulrich H von Andrian, Elena I Deryugina, Alex Y Strongin, Eva-B. Bröcker, and Peter Friedl. 2003. "Compensation Mechanism in Tumor Cell Migration : Mesenchymal–Amoeboid Transition after Blocking of Pericellular Proteolysis ." *Journal of Cell Biology* 160 (2): 267–77. doi:10.1083/jcb.200209006.

Wong, L E, N Chen, V Karantza, and A Minden. 2013. "The Pak4 Protein Kinase Is Required for Oncogenic Transformation of MDA-MB-231 Breast Cancer Cells." *Oncogenesis* 2 (6): e50–e50. doi:10.1038/oncsis.2013.13.

Wu, Xiaochong, Heather S Carr, Ippeita Dan, Peter P Ruvolo, and Jeffrey A Frost. 2008. "P21 Activated Kinase 5 Activates Raf-1 and Targets It to Mitochondria." *Journal of Cellular Biochemistry* 105 (1): 167–75. doi:10.1002/jcb.21809.

Yamaguchi, Hideki. 2012. “Pathological Roles of Invadopodia in Cancer Invasion and Metastasis.” *European Journal of Cell Biology* 91 (11–12). Germany: 902–7. doi:10.1016/j.ejcb.2012.04.005.

Yamaguchi, Hideki, Mike Lorenz, Stephan Kempiak, Corina Sarmiento, Salvatore Coniglio, Marc Symons, Jeffrey Segall, et al. 2005a. “Molecular Mechanisms of Invadopodium Formation : The Role of the N-WASP–Arp2/3 Complex Pathway and Cofilin .” *Journal of Cell Biology* 168 (3): 441–52. doi:10.1083/jcb.200407076.

———. 2005b. “Molecular Mechanisms of Invadopodium Formation.” *The Journal of Cell Biology* 168 (3): 441 LP – 452.

Yamaguchi, Hideki, Yukiko Takeo, Shuhei Yoshida, Zen Kouchi, Yoshikazu Nakamura, and Kiyoko Fukami. 2009. “Lipid Rafts and Caveolin-1 Are Required for Invadopodia Formation and Extracellular Matrix Degradation by Human Breast Cancer Cells.” *Cancer Research* 69 (22): 8594 LP – 8602. doi:10.1158/0008-5472.CAN-09-2305.

Yamamoto, Hayato, Mihoko Sutoh, Shingo Hatakeyama, Yasuhiro Hashimoto, Takahiro Yoneyama, Takuya Koie, Hisao Saitoh, et al. 2011. “Requirement for FBP17 in Invadopodia Formation by Invasive Bladder Tumor Cells.” *The Journal of Urology* 185 (5). United States: 1930–38. doi:10.1016/j.juro.2010.12.027.

Yan, Chunhong, and Douglas D Boyd. 2007. “Regulation of Matrix Metalloproteinase Gene Expression.” *Journal of Cellular Physiology* 211 (1). United States: 19–26. doi:10.1002/jcp.20948.

Yana, I, and S J Weiss. 2000. “Regulation of Membrane Type-1 Matrix Metalloproteinase Activation by Proprotein Convertases.” *Molecular Biology of the Cell* 11 (7). The American Society for Cell Biology: 2387–2401. doi:10.1091/mbc.11.7.2387.

Yoshioka, Kiyoko, Shoji Nakamori, and Kazuyuki Itoh. 1999. “Overexpression of Small GTP-Binding Protein RhoA Promotes Invasion of Tumor Cells.” *Cancer Research* 59 (8): 2004 LP – 2010.

Yu, Cheng-han, Nisha Bte Mohd Rafiq, Anitha Krishnasamy, Kevin L Hartman, Gareth E Jones, Alexander D Bershadsky, and Michael P Sheetz. 2013. “Integrin-Matrix Clusters Form Podosome-like Adhesions in the Absence of Traction Forces.” *Cell Reports* 5 (5): 1456–68. doi:10.1016/j.celrep.2013.10.040.

Yu, Huapeng H, Michael R Dohn, Nicholas O Markham, Robert J Coffey, and Albert B

Reynolds. 2016. “P120-Catenin Controls Contractility along the Vertical Axis of Epithelial Lateral Membranes.” *Journal of Cell Science* 129 (1): 80–94. doi:10.1242/jcs.177550.

Yu, Wayne, Yasmine Kanaan, Young Kyung Bae, and Edward Gabrielson. 2009. “Chromosomal Changes in Aggressive Breast Cancers with Basal-like Features.” *Cancer Genetics and Cytogenetics* 193 (1): 29–37. doi:10.1016/j.cancergencyto.2009.03.017.

Zenke, F T, C C King, B P Bohl, and G M Bokoch. 1999. “Identification of a Central Phosphorylation Site in P21-Activated Kinase Regulating Autoinhibition and Kinase Activity.” *The Journal of Biological Chemistry* 274 (46). United States: 32565–73. doi:10.1074/jbc.274.46.32565.

Zenke, Frank T, Mira Krendel, Celine DerMardirossian, Charles C King, Benjamin P Bohl, and Gary M Bokoch. 2004. “P21-Activated Kinase 1 Phosphorylates and Regulates 14-3-3 Binding to GEF-H1, a Microtubule-Localized Rho Exchange Factor.” *The Journal of Biological Chemistry* 279 (18). United States: 18392–400. doi:10.1074/jbc.M400084200.

Zhang, Dingxiao, Shuhong Zhao, Xinyun Li, Jason S Kirk, and Dean G Tang. 2018. “Prostate Luminal Progenitor Cells in Development and Cancer.” *Trends in Cancer* 4 (11): 769–83. doi:10.1016/j.trecan.2018.09.003.

Zhang, Hongquan, Zhilun Li, Eva-Karin Viklund, and Staffan Strömblad. 2002. “P21-Activated Kinase 4 Interacts with Integrin Alpha v Beta 5 and Regulates Alpha v Beta 5-Mediated Cell Migration.” *The Journal of Cell Biology* 158 (7): 1287–97. doi:10.1083/jcb.200207008.

Zhang, Hui-Juan, Michelle K Y Siu, Matthew C W Yeung, Li-Li Jiang, Victor C Y Mak, Hextan Y S Ngan, Oscar G W Wong, Hong-Quan Zhang, and Annie N Y Cheung. 2011. “Overexpressed PAK4 Promotes Proliferation, Migration and Invasion of Choriocarcinoma.” *Carcinogenesis* 32 (5). England: 765–71. doi:10.1093/carcin/bgr033.

Zhang, Jian, Jian Wang, Qiqiang Guo, Yu Wang, Ying Zhou, Huizhi Peng, Maosheng Cheng, Dongmei Zhao, and Feng Li. 2012. “LCH-7749944, a Novel and Potent P21-Activated Kinase 4 Inhibitor, Suppresses Proliferation and Invasion in Human

Gastric Cancer Cells.” *Cancer Letters* 317 (1). Ireland: 24–32. doi:10.1016/j.canlet.2011.11.007.